VNIVERSITAT DE VALÈNCIA

Facultad de Medicina y Odontología

Department of Physiology

Doctoral Program in Physiology

Interhippocampal demyelination in the early onset of Alzheimer's disease

Doctoral Thesis

Artemis Ftara

Supervised by: **Ana Lloret Alcañiz**

Valencia, July 2024

VNIVERSITAT DE VALÈNCIA

Facultad de Medicina y Odontología

Department of Physiology

Doctoral Program in Physiology

Interhippocampal demyelination in the early onset of Alzheimer's disease

Doctoral Thesis

Artemis Ftara

Supervised by: Ana Lloret Alcañiz

Valencia, July 2024

Prof. Dña. Ana Lloret Alcañiz, Catedrática del Dpto. de Fisiología de la Facultad de Medicina y Odontología de la Universitat de Valencia.

CERTIFICA:

Que la presente memoria, titulada "Interhippocampal demyelination in the early onset of Alzheimer's disease", corresponde al trabajo realizado bajo su dirección por Dña. Artemis Ftara, para su presentación como Tesis Doctoral en el Programa de Doctorado en Fisiología de la Universitat de Valencia.

Y para que conste firma el presente certificado en Valencia, a

ANA ISABEL
LLORET ALCAÑIZ
- NIF:20162077R

Firmado digitalmente por
ANA ISABEL LLORET
ALCAÑIZ - NIF:20162077R
Fecha: 2024.07.23 12:12:29
+02'00'

Fdo. Dña. Ana Lloret Alcañiz

Acknowledgements

This thesis is a reflection of the unwavering support and boundless love I received from my family during this challenging academic pursuit. I owe an immense debt of gratitude to my parents, Giorgos and Eleni, who nurtured my curiosity and supported my educational ambitions from the very beginning. This endeavor would not have been possible without the financial support from my parents and their moral guidance. Words cannot express my gratitude to my sister, Fillio, for her endless patience and understanding, especially during the most demanding phases of this research. She has been my anchor and my safe space, throughout these years.

I would like to specially thank my supervisor Dra. Ana Lloret for her dedicated support and guidance. Ana continuously provided encouragement and was always willing and enthusiastic to assist in any way she could throughout the research project. I would also like to thank Dra. Sara Xapelli, the host supervisor during my international internship, who generously provided me with knowledge and expertise.

I am also grateful to my colleagues from both UV and iMM, whose presence and insights have been pivotal in navigating the complexities of my research topic. A special mention to Dra. Rita Soares, whose mentorship extended beyond the academic realm into personal guidance, providing comfort and motivation during tough times.

Lastly, I would be remiss in not mentioning my friends, who provided both distractions when needed and encouragement when it seemed impossible to continue. More specifically, a heartfelt thank you to my partner Álvaro, and my friends Élena, Xema, Despoina and Katerina. Their belief in me has kept my spirits and motivation high during this process.

Index

Abbreviation list

3xTg: triple transgenic mice with APP695, M146V PSEN1 and P301L transgenes

5XFAD: transgenic mice with five familial Alzheimer's disease mutations

Aβ/ Abeta: beta amyloid

ACH: amyloid cascade hypothesis

AD: Alzheimer’s disease

aMCI: amnesic Mild Cognitive Impairment

AMPA: a-amino-3-hydroxy-5-methyl-4-isoxazole propionic acid

AMPAr: a-amino-3-hydroxy-5-methyl-4-isoxazole propionic acid receptor

APC/C-Cdh1: Anaphase-Promoting Complex/Cyclosome

APOE: Apolipoprotein E

APP: Amyloid Precursor Protein

APP/PS1: double transgenic mice APPswe/ PSEN1dE9

ATP: adenosine triphosphate

bFGF: basic fibroblast growth factor

BSA: bovine albumin serum

CA1: cornu ammonis 1 of the hippocampus

CA3: cornu ammonis 3 of the hippocampus

CC: corpus callosum

CNP: 2’,3’-Cyclic-nucleotide 3'-phosphodiesterase

CNS: central nervous system

CSF: cerebrospinal fluid

CTR: control group

DIV: day *in vitro*

df: dorsal fornix

DL-TBOA: DL-Threo-Beta-Benzyloxyaspartate

DMEM: Dulbecco's modified eagle medium

DTI: diffusion tensor imaging

E: embryonic day

EAA: excitatory amino acid

EAAT: excitatory amino acid transporter

EGF: epidermal growth factor

EM: electron microscopy

EOAD: early onset of Alzheimer’s disease

EPSP: excitatory postsynaptic potential

FA: fractional anisotropy

FAD: Familial Alzheimer’s disease

FDA: Food and Drug Administration

FEOAD: Familial early onset of Alzheimer’s disease

FLOAD: Familial late onset of Alzheimer’s disease

GM: grey matter

GS: glutamine synthetase

HBSS: Hanks' balanced saline solution

LOAD: late onset of Alzheimer’s disease

MAG: myelin associated protein

MBP: myelin basic protein

MCI: Mild Cognitive Impairment

MD: mean diffusivity

MOG: myelin oligodendrocyte glycoprotein

MRI: Magnetic Resonance Imaging

Nfl: Neurofilament light chain

NG2: nerve/glial-antigen 2

NMDA: N-methyl-D-aspartate acid

NMDAr: N-methyl-D-aspartate acid receptor

NR: nodes of Ranvier

NSA: neurosphere assay

NSPCs: neural stem progenitor cells

NSCs: neural stem cells

O1: Oligodendrocyte Marker O1

O4: Oligodendrocyte Marker O4

Olig2: Oligodendrocyte Transcription Factor 2

OLs: oligodendrocytes

OPCs: oligodendrocyte progenitor cells

PDGFRα: platelet derived growth factor receptor alpha

PDL: Poly-D-Lysine

PET: positron emission tomography

PFA: paraformaldehyde

PLP: protolipid protein

PSEN1: presenilin 1

PSEN2: presenilin 2

QNZ46: 4-[6-Methoxy-2-[(1E)-2-(3-nitrophenyl) ethenyl]-4-oxo-3(4H)quinazolinyl]benzoic acid

RD: radial diffusivity

rTg4510: transgenic mice carrying the P301L mutation

SAD: sporadic Alzheimer's disease

SFM: serum-free medium

SEOAD: sporadic early onset of Alzheimer's disease

SLOAD: sporadic late onset of Alzheimer's disease

SVZ: subventricular zone

V3: third ventricle

vhc: ventral hippocampal commissure

WM: white matter

WT: wild-type

Abstract

Alzheimer's disease (AD) is a neurodegenerative condition that hinders thinking, memory and behavior. Two of the main brain abnormalities linked to AD are the buildup of beta-amyloid (Aβ) into aggregates outside of neurons and the accumulation of an aberrant form of the protein tau inside of neurons. In addition, myelin degeneration has also been widely documented in AD patients and experimental animal models. Demyelination is an early event that emerges before tau and Aβ pathologies and even before atrophy of white and gray matter, and has also been observed in the fornix. Fornix is a thin, C-shaped bundle of white matter consisting of myelinated fibers, implicated in episodic memory. What is more, in the initial stages of AD, oligodendrocytes (OLs) abnormalities were found to undergo significant alterations linked to cognitive decline. Another trait observed during AD pathology, is the excessive release of glutamate into the extracellular space by pre-synaptic nerve terminals that causes excitotoxicity by overstimulating particularly NMDA receptors and impaired glutamate uptake by EAAT. Furthermore, functional NMDA receptors are expressed on the myelin sheath, that could partially provoke paranodal myelin damage in response to elevated glutamate levels.

This work aims to address the fact that demyelination and alterations in oligodendrocyte lineage cells occur specifically at the dorsal fornix, in young transgenic mice, before the development of cognitive impairment. Another goal of this study, is to demonstrate that the rise in glutamate is due to amyloid increase in cultured neurons. Glutamate could leak out of axons and bind to NMDA glutamate receptors and EAAT, causing myelin damage.

The obtained results demonstrated a significant decrease in the levels of myelin components in the dorsal fornix of APP/PS1 mice compared to controls, while the levels of neuraxon marker were unchanged. Additionally, it was observed an increase in the levels of oligodendrocyte progenitor cells, and at the same time, a significant

decrease of mature myelinating OLs. Simultaneously, these alterations were not detected in their hippocampi. In neurosphere cultures, treatment with Aβ resulted in a significant decrease of myelin levels. Co-treatment with DL-TBOA, a competitive blocker of EAAT, reversed efficiently this decline. There were no appreciable changes in myelin levels in the combined treatment of Aβ with QNZ46, a non-competitive NMDA antagonist, when compared to Aβ-treated group. Additionally, the population of neurons was unaffected by Aβ treatment, and no notable differences were seen under any circumstances.

In conclusion, APP/PS1 mice exhibit demyelination of the dorsal fornix accompanied by changes in oligodendrocyte lineage cells. In neurosphere cultures, Aβ-treated cells also undergo demyelination, which was reverted after DL-TBOA treatment. This implies that Aβ-induced glutamate excitotoxicity may be a potential mechanism of myelin degeneration.

INTRODUCTION

“Ασφάλεια εστί το προνοείν και προλαμβάνειν. Το δε προνοείν και προλαμβάνειν κρείττον εστί του θεραπεύειν.”

Ιπποκράτης

“It is safe to foresee and prevent. Foresight and prevention is better than cure.”

Hippocrates

Introduction

Alzheimer's disease

Overview

Alzheimer's disease (AD) is a neurodegenerative condition that hinders thinking, memory and behavior, and in the long run, the capacity to perform even simple everyday activities (Guo et al., 2020). This condition bears the name of the German physician Alois Alzheimer, who at the turn of the 20th century, developed an interest in the case of Auguste Deter (Figure 1), a 51-year-old female patient with distinct symptoms from those of typical dementia patients (Small & Cappai, 2006). In a 1907 paper titled " Über eine eigenartige Erkrankung der Hirnrinde'" (On certain peculiar disease of the cerebral cortex), Dr. Alzheimer listed her symptoms, which included mental confusion, difficulties sleeping, and memory impairment (Alzheimer, 1907; Ramirez-Bermudez, 2012).

Figure 1. Alois Alzheimer and Auguste Deter (Dahm, 2006; Ciurea et al., 2023).

Upon postmortem examination, the brain was found to be uniformly atrophic and had prominent neurofibrillary pathology. Using silver staining, one of the most modern techniques available at the time, Alzheimer also reported the presence of peculiar deposits in the cortex (Figure 2). The histological analysis identified two types of lesions that had not been seen before: small oval-shaped fibrils and plaques of an undetermined matter known as miliary foci, which are now known as amyloid plaques (Ciurea et al., 2023).

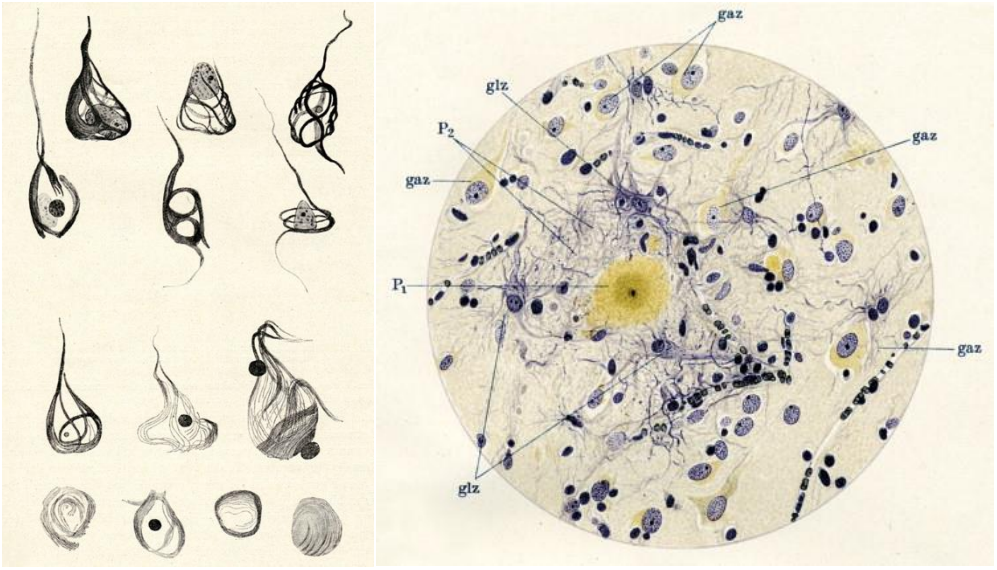

Figure 2. Alzheimer's drawings of amyloid plaques and neurofibrillary tangles (Alzheimer, 1911; Dahm, 2006).

Brain changes in Alzheimer's disease

Over time, scientists have discovered numerous alterations in the brain that could disrupt chemical communication and cause cognitive, learning, and daily functioning issues associated with Alzheimer's disease. Two of the main brain abnormalities linked to Alzheimer's disease are the buildup of the protein fragment beta-amyloid (Aβ) into aggregates (beta-amyloid plaques) outside of neurons, and the accumulation of an aberrant form of the protein tau (tau tangles) inside of neurons (Figure 3) (Yiannopoulou & Papageorgiou, 2020). Smaller beta-amyloid formations and plaques can harm neurons by obstructing synaptic transmission between neurons. Within the neurons, tau tangles impede the passage of nutrients and other chemicals necessary for the survival and regular operation of neurons. Following these modifications, AD is characterized by neurodegeneration, which causes brain atrophy, as

well as microglia activation that results in chronic inflammation (Alzheimer's facts and figures, 2024).

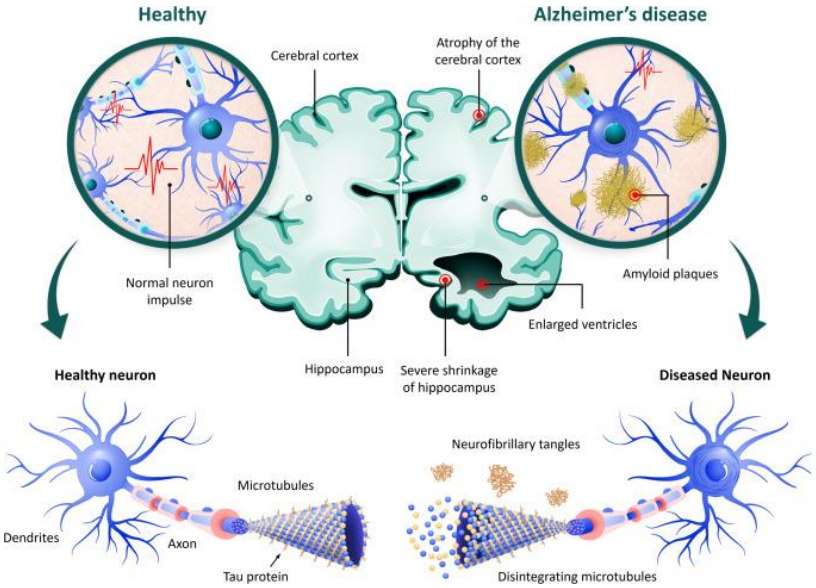

Figure 3. Histologically, senile plaques and neurofibrillary tangles are the main lesions presented in the patients' brains (Gao et al., 2019).

Signs and symptoms

Typically, mild memory impairments are the initial indication of Alzheimer's. Forgetting the names of places and things, as well as recent conversations or events, are a few examples of this. Moreover, poor judgment or reasoning might indicate Alzheimer's disease in its very early stages (Figure 4). As the illness progresses, memory worsens and other symptoms could appear as well, such as: disorientation and confusion, trouble organizing or making decisions, issues with speech and language, struggles in performing self-care tasks, personality changes, such as turning hostile and wary of others, having hallucinations and delusions, mood swings or anxiety (Teixeira, Rocha & Gatchel, 2023; Barage & Sonawane, 2015).

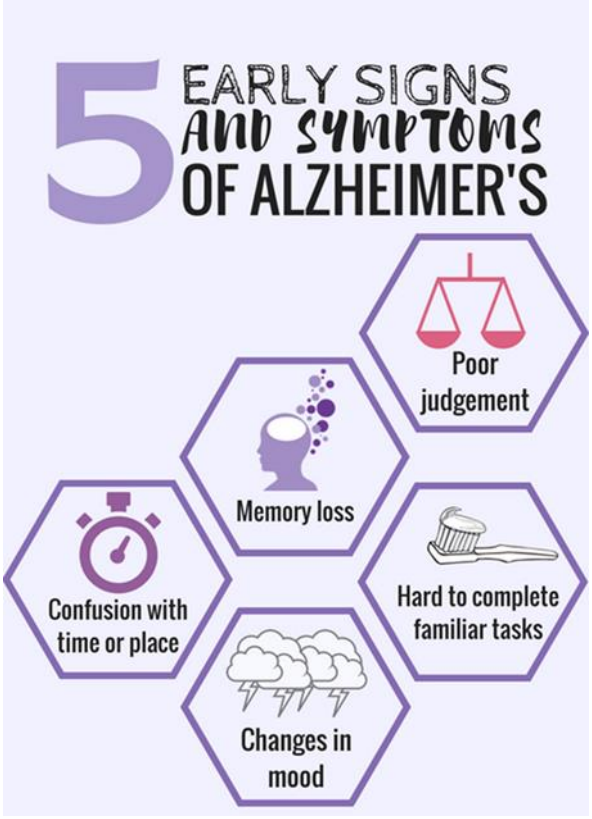

Figure 4. The most common early symptoms of Alzheimer's disease (alz.org).

Stages and AD continuum

The Alzheimer's disease continuum refers to the gradual progression of the disease from brain abnormalities that are imperceptible by the affected person, to brain abnormalities that lead to impaired memory and subsequently physical disability. The three main stages of this continuum are: the preclinical Alzheimer's disease stage, the mild cognitive impairment (MCI) brought on by Alzheimer's disease stage, and the Alzheimer's dementia stage. Mild, moderate, and severe dementia are further classifications for the Alzheimer's dementia stage (Figure 5). The length of each stage on the continuum of Alzheimer's disease varies according to a number of factors, including age, genetics, and biological sex (Alty et al., 2024; Parnetti et al., 2019). Early identification of patients most at risk of developing MCI from AD is made possible thanks to biomarkers reflecting the underlying pathology of AD. Imaging techniques such as magnetic resonance imaging (MRI) and positron emission tomography (PET) can provide biomarker information by visualizing structural and molecular changes in the brain. Fluid biomarker testing, like cerebrospinal fluid (CSF), can also detect aggregated tau and Aβ presence. Clinical research demonstrates that these biomarkers provide crucial information for diagnosis in the early stages of the disease. Extending test ranges is a subject of ongoing research, encompassing blood-based biomarkers for the identification of AD risk and the tracking of disease progression (Porsteinsson et al., 2021).

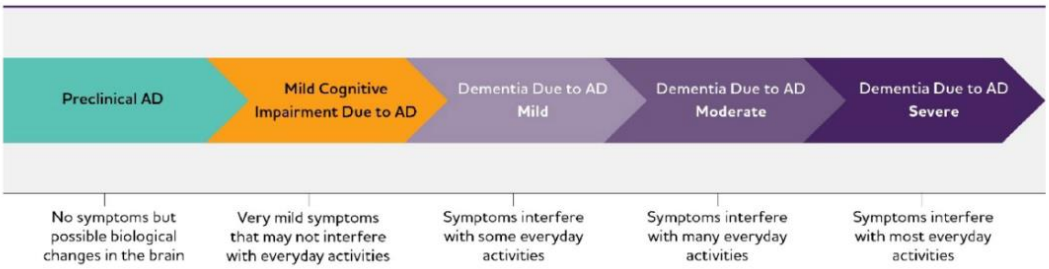

Figure 5. The Alzheimer's disease (AD) continuum and its representative stages (Alzheimer's Association Report, 2023).

Causes and risk factors

The foremost risk factors for Alzheimer's dementia are advanced age, genetics (in particular the e4 allele of the apolipoprotein E - APOE gene, trisomy in Down syndrome and genetic mutations), and a family history of the disease (Silva et al., 2019; Schworer et al., 2024). Moreover, the likelihood of developing AD is increased by several acquired factors (Figure 6). Less education, high blood pressure, hearing loss, smoking, obesity, depression, lack of physical activity, diabetes, low social interaction, insufficient sleep, excessive alcohol intake, traumatic brain injury, and air pollution are among these factors (Livingston et al., 2020; Sabia et al., 2021).

Figure 6. The twelve most important modifiable dementia risk factors (World Alzheimer Report, 2023).

Epidemiology and prevalence

Nowadays, over 55 million individuals globally suffer from dementia, with more than 60% residing in low- and middle-income nations. Almost ten million new cases are reported annually. It is projected that by 2050, there will be 139 million dementia patients worldwide. Alzheimer's disease, the most prevalent type of dementia, accounts for 60–70% of cases. In 2019, dementia resulted in $1.3 trillion dollars cost to economies worldwide; by 2030, that amount is predicted to have more than doubled to $2.8 trillion dollars (World Alzheimer Report, 2023; “Dementia,” World Health Organization, accessed May 30, 2024).

Drug treatments

Alzheimer's disease pathophysiology is complicated, and its etiology is still unknown. Thus the development of therapeutic treatments for AD is still an ongoing research endeavor. In order to slow the progression of AD, early treatment is important. Clinical trials focusing on anti-Aβ amyloid medications are currently in progress; however, the majority of these trials have been discontinued due to unfavorable side effects and ineffectiveness. For instance, a clinical trial involving aducanumab, donanemab, lecanemab, and other anti-Aβ drugs, found a strong correlation between the incidence of amyloid-related imaging abnormalities and Aβ plaque clearance. Donanemab was found to slower tau accumulation in clinical studies. Future research approaches should investigate the relationship between lower Aβ plaques and tau levels. Acanumab's accelerated Food and Drug Administration (FDA) approval gave hope for the development of AD drugs, and expectations of more affordable and efficient therapies for AD patients (Peng et al., 2023; FDA, 2021; FDA, 2023).

Physiopathology of Alzheimer’s disease

Alzheimer’s disease cases can be classified based on the age at which the disease first manifests as well as whether or not there is a family history of the condition. AD is classified as early onset (EOAD) or late onset (LOAD). Cases of AD that appear before the age of 65 are referred to as EOAD, while cases of AD that occur at or after the age of 65 are referred to as LOAD. Familial AD (FAD) implies a positive family history, whereas sporadic AD (SAD) denotes no familial history of the disease. When family history is absent or insufficient, it can be challenging to distinguish between familial and sporadic

cases, particularly in large cohorts. Nevertheless, LOAD accounts for 90–99% of all AD cases, making it by far the most common form of the disease (Figure 7). Approximately 60% of all LOAD cases are sporadic LOAD (SLOAD), and the remaining 40% are familial LOAD (FLOAD). Conversely, EOAD accounts for only 1–10% of all AD cases (Figure 7). Of these, up to 60% are cases of familial EOAD (FEOAD), and the remaining 40% are cases of sporadic EOAD (SEOAD) (Reitz, Rogaeva & Beecham, 2020; Nardini, Hogan, Flamier & Bernier, 2021). It is important to note that this classic division is unduly restrictive because, on the one hand, there are examples of EOAD without any proof of Mendelian inheritance, and, on the other hand, LOAD is often associated with a strong familial clustering that occasionally resembles a Mendelian pattern. The genetics of LOAD is more intricate than that of FEOAD, which is caused by low frequency and highly penetrant mutations in three genes, APP, PSEN1 and PSEN2 (Bertram, Lill & Tanzi, 2010).

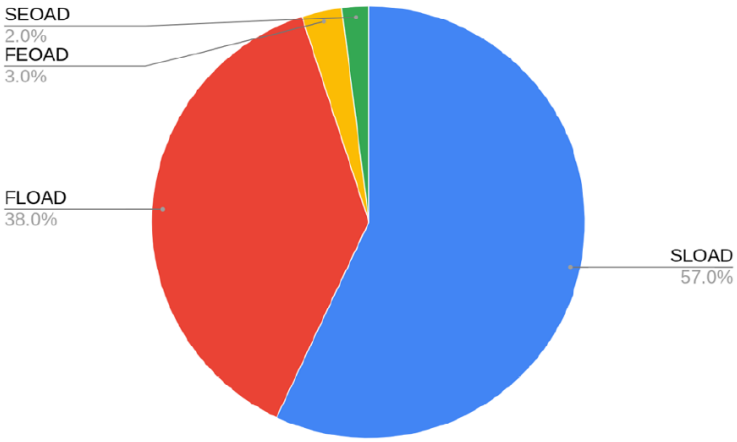

Figure 7. Approximate distribution of AD cases (Nardini et al., 2021)

Genetics of Alzheimer's disease

Complex in nature, AD is influenced by both genetic and environmental factors. Currently, more than 100 variants on at least 34 genes have been found to be pathogenic or risk modifying in AD. APP, PSEN1, or PSEN2 mutations account for the majority of AD cases, while the APOE ε4 variant carries risk as well (Nystuen et al., 2024). These genes will be discussed in further detail below.

Amyloid Precursor Protein (APP)

Amyloid precursor protein (APP) is classified as a type I membrane protein (Orobets & Karamyshev, 2023). In humans, the APP gene is located on chromosome 21q21.3 (Barber, 2012). Different APP isoforms are produced by alternative splicing and differential processing (Orobets & Karamyshev, 2023). Normally, α-secretase cleaves APP proteolytically, forming soluble APPα. Nevertheless, under pathological conditions, APP is firstly cleaved by β-secretase, and subsequently by γ-secretase, forming insoluble Aβ monomers

that oligomerize and result in Aβ plaques as shown in Figure 8 (Nystuen et al., 2024).

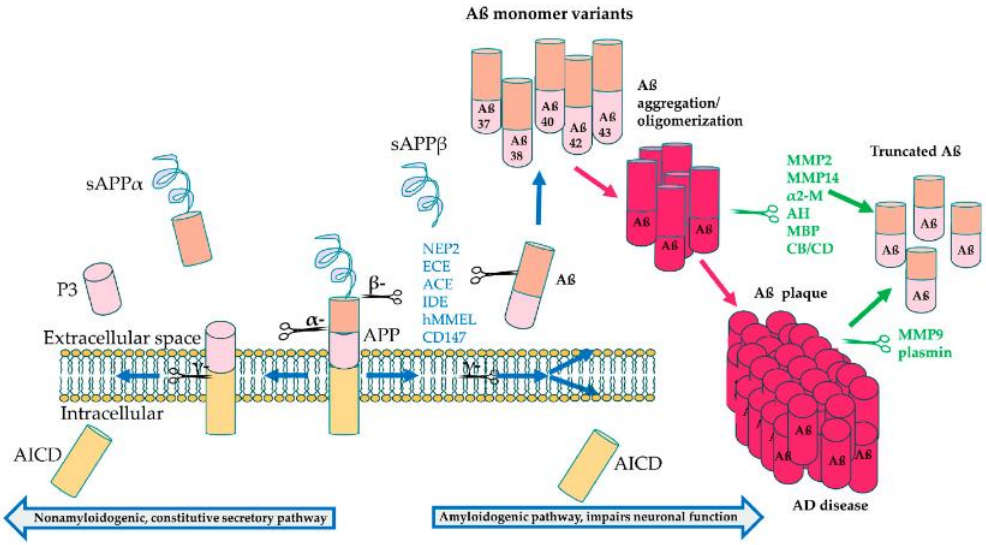

Figure 8. APP processing and cleavage (Nystuen et al., 2024).

Presenilin genes

The polytopic transmembrane protein presenilin is encoded by the homologous genes PSEN1 and PSEN2 (Sun et al., 2024). The presenilin proteins encoded by these genes have 66% sequence homology (Bagaria, Bagyinszky & An, 2022). PSEN1 is found on chromosome 14 (14q24.2), whereas PSEN2 is found on chromosome 1 (1q42.13) (Kabir et al., 2020). Over 300 mutations in PSEN1 and 87 mutations in PSEN2 have been documented thus far (Bagaria, Bagyinszky & An, 2022). As of right now, variations in PSEN1 are the most common cause of AD, whereas variants in PSEN2 are comparatively infrequent (Figure 9) (Xiao et al., 2021). The γ-secretase complex's regular processing of APP is disrupted by mutant presenilin proteins, particularly PSEN1 mutants, which promote the production of Aβ42 over Aβ40 (Yang, Bagyinskzky & An,

2023). The shift in the Aβ42/Aβ40 ratio is especially noteworthy because Aβ42 is more likely to accumulate into toxic oligomers and fibrils, which causes the development of amyloid plaques (Sun et al., 2024).

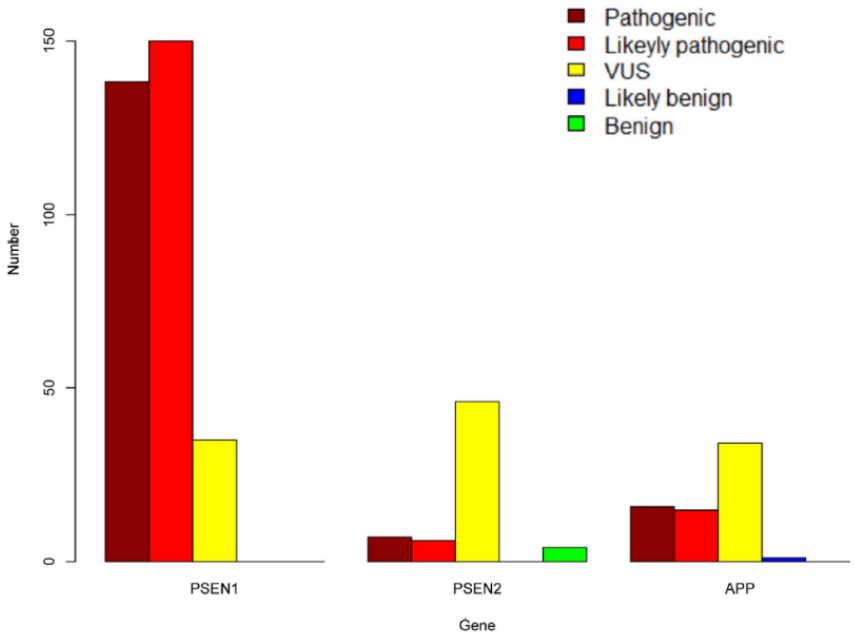

Figure 9. The number of PSEN1, PSEN2 and APP variants (Xiao et al., 2021). VUS= variants of uncertain significance.

Hypotheses related to AD etiology

The precise pathogenesis of AD is still unknown at this time due to its complexity. As a result, numerous theories regarding AD have been established, each corresponding to a different cause. A few of these theories are the following (Figure 10): The Amyloid Cascade Hypothesis, the Tau Protein Hyperphosphorylation Hypothesis, the Mitochondrial Cascade Hypothesis, the Cholinergic Hypothesis, the Neuroinflammation Hypothesis, the 5-HT6 Receptor Hypothesis, the Dendritic Hypothesis, the Calcium homeostasis and NMDA hypotheses, the Neurovascular hypothesis, the Metal ion hypothesis, the Lymphatic system hypothesis, the virus hypothesis and others (Liu et al., 2019; Agarwal, et al., 2021; Cáceres, et al., 2023). We have chosen the amyloid cascade as the primary hypothesis to be explored in this thesis due to its clinical significance and the abundance of experimental data supporting it.

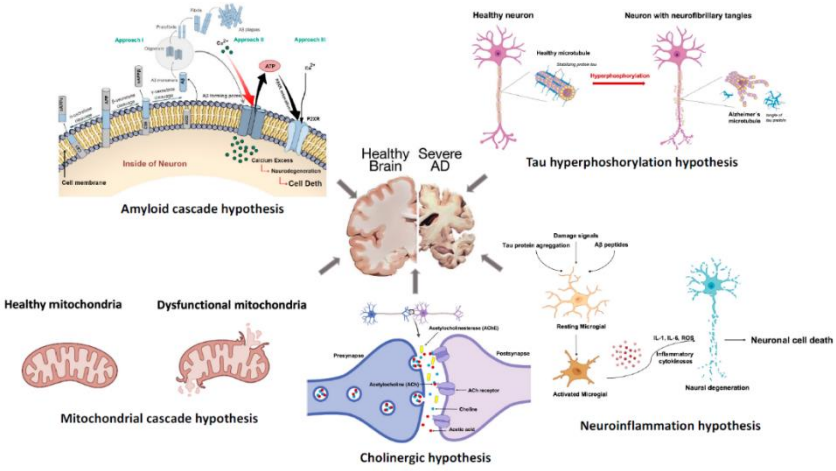

Figure 10. The different hypotheses regarding AD (Cáceres et al., 2023).

Amyloid cascade hypothesis

Researchers almost entirely concentrated on the toxic qualities of Aβ peptide, after identifying it as the peptide monomer responsible for the insoluble senile plaques found in the brains of Alzheimer's patients (Fedele, 2023). This perspective led to the development of the initial amyloid cascade hypothesis (ACH) by Hardy and Higgins in 1992 (Figure 11). According to this hypothesis, the build-up of Aβ is the primary cause of a chain of molecular events that promote the formation of hyperphosphorylated tau aggregates, the stimulation of neuronal death mechanisms, and ultimately dementia (Hardy & Higgins, 1992; Granzotto & Sensi, 2024). Numerous empirical findings and research investigations contradict the hypothesis. Amyloid cannot be causally associated with AD because the natural history of AD progression is inconsistent with brain amyloid formation (Kurkinen et al., 2023). As a result, the ACH has been revised, and the current theory suggests that the upstream pathogenic process for AD, which takes place years before clinical onset, is the accumulation of soluble Aβ oligomers. However, different mechanisms appear to be involved in the accumulation of Aβ, primarily due to increased production in the familial form or decreased clearance in the sporadic form (Fedele, 2023).

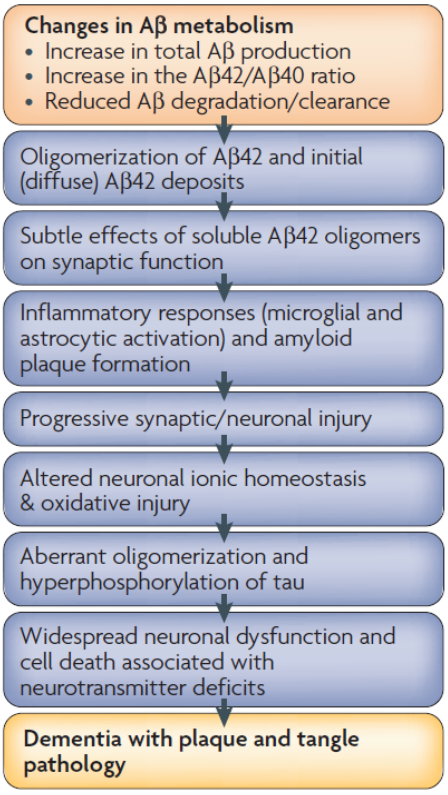

Figure 11. The amyloid cascade hypothesis (Haas & Selkoe, 2007).

Oligodendrocyte lineage and Alzheimer's disease

Overview

Apart from microglia and astroglia, oligodendrocytes (OLs) are one of the main glial cell types found in the central nervous system (Kuhn, Gritti, Crooks & Dombrowski, 2019; Verkhratsky et al., 2019). In the 1800s, first Virchow, and then Deiters and Golgi, provided the first descriptions of oligodendrocytes (Virchow, 1856; Deiters, 1865; Golgi, 1885). Virchow coined the term "Nervenkitt," which translates to "nerve glue," after studying the intricate structure of the brain and noting the emergence of cells between nerves (Virchow, 1858). They were initially believed to serve only as connective tissue. William Ford Robertson, a Scottish pathologist, was the first to illustrate an unidentified group of brain cells (Figure 12) at the end of the 19th century (Robertson, 1899 & 1900a). He subsequently named these cells "mesoglia," a term that refers to a type of immune cell that is present in the brain (Robertson, 1900b). Using more sophisticated staining methods, such as silver carbonate, Pio del Rio-Hortega eventually distinguished microglia from oligodendroglia. Moreover, he determined four types of oligodendroglia and identified their myelinating function (Del Río-Hortega, 1920; 1921; 1933).

The four types of oligodendroglia, also known as oligodendrocytes, are the following (Verkhratsky & Butt, 2013):

i) Type I oligodendrocytes, which are more abundant in the cortex and the grey matter, and myelinate small diameter axons.

ii) Type II oligodendrocytes, that are more prevalent in white matter, like the corpus callosum, optic nerve, cerebellum and spinal cord.

iii) Type III oligodendrocytes, that are found in the cerebral and cerebellar peduncles, the medulla oblongata, and the spinal cord funiculi and myelinate less but bigger in diameter axons.

iv) Type IV oligodendrocytes, that resemble Schwann cells are only found in tracts close to the central nervous system (CNS) entrance and exit points of nerve roots and myelinate large diameter axons.

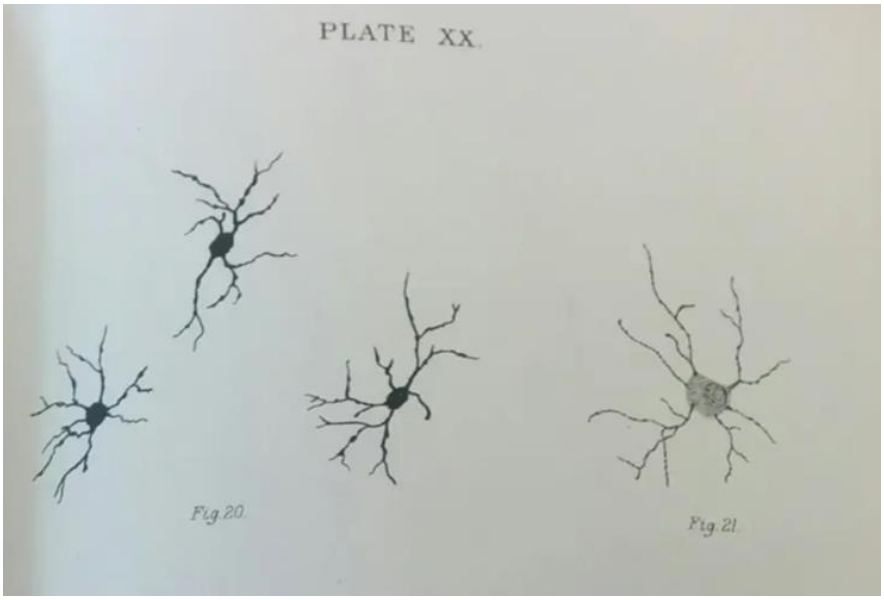

Figure 12. Robertson's drawings of oligodendrocytes from his textbook (Robertson, 1900b).

Oligodendrocyte differentiation and migration

Oligodendrocyte progenitor cells (OPCs), a type of bipolar precursor cells, are the source of oligodendrocytes (Hardy & Reynolds, 1991). William Stallcup and colleagues identified this type of neuroglia in the 1980s, after developing an antibody against a chondroitin sulphate proteoglycan known as NG2 (Stallcup, 1981). Around embryonic day 12.5 (E12.5), OPCs initially emerge from radial glial cells of the ventral ventricular zone and the dorsal spinal cord (Ra,

Miller & Noble, 1983; Pringle & Richardson, 1993; Timsit et al., 1995; Warf, Fok-Seang & Miller, 1991; Vallstedt, Klos & Ericson, 1991; Fogarty, Richardson & Kessaris, 2005). There are three distinct temporal waves of OPC development (Timsit et al.,1995). The first wave occurs in the forebrain and is followed by a smaller second wave in the dorsal ventricular zone and by a third postnatal wave originating in the cortex (Kessaris et al.,2006). Myelinating OLs are produced when OPCs differentiate as they migrate toward the CNS (Richardson, Kessaris & Pringle, 2006).

Developmental Markers of OPCs and OLs

The most potent markers for OPCs are the platelet-derived growth factor receptor α (PDGFRα) and the proteoglycan NG2 (Emery & Dugas, 2013; Nishiyama et al., 1996; Pringle et al., 1992). Pre-OLs start to express CNPase, O4 and O1 (Jakovcevski et al., 2009). For the identification of mature OLs, Olig2, a specific cell lineage marker is widely used (Figure 13) (López-Muguruza & Matute, 2023).

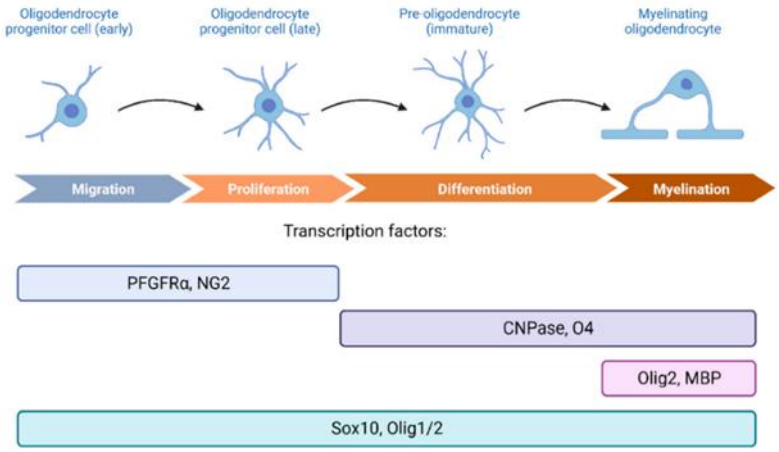

Figure 13. Stages of OL differentiation and their specific markers (López-Muguruza & Matute, 2023).

Distribution of OPC and OLs within the CNS

OPCs constitute the majority of dividing cells in the CNS (Geha et al., 2010), accounting for 2-9% of all CNS cells (Dawson et al., 2003; Nishiyama, 2007; Nishiyama et al., 2009; Richardson et al., 2011; Nishiyama et al., 2016). Grey matter (GM) and white matter (WM) have equal distributions of OPCs, with GM having slightly less (Dawson et al., 2003). OLs constitute 45–75% of all glial cells making them the most common glial cell population (Pelvig et al., 2008; von Bartheld et al., 2016).

Main functions of OLs and OPCs

OLs' primary function is to produce myelin that is coiled around axons (Raine, 1984). OLs have been linked to several other functions besides myelination. For example, OLs maintain ionic homeostasis in the central nervous system by buffering increased extracellular potassium that is evoked by neuronal excitation (Menichella, 2006). Moreover, oligodendroglia contributes to immunomodulation (Kirby & Castelo-Branco, 2021) and guarantee the long-term stability of axons by providing trophic and metabolic support (Nave, 2010; Lee et al., 2012; Beirowski, 2013; Narine & Colognato, 2022).

Throughout lifetime, OPCs maintain the capacity to proliferate, migrate and differentiate into mature OLs. After demyelination, OPCs undergo differentiation and maturation that finally result in remyelination (Franklin & Ffrench-Constant, 2008; Smith, Blakemore & McDonald, 1979; Groves et al., 1993; Rivers et al., 2008; Gibson et al.,2014). Remarkably, OPCs support CNS plasticity in addition to serving as an endogenous source of OLs (Young, 2013). OPCs also have immunomodulatory properties (Baerwald, & Popko, 1998; Arnett et al., 2001; Bonora et al., 2014) and can migrate to injury sites in reacting to inflammatory stimuli, similar to microglia (Hughes et al., 2013; Kang et al., 2013).

Dysfunctions of OLs and OPCs in AD pathology

In the initial stages of AD, oligodendrocyte abnormalities were found to undergo significant alterations linked to cognitive decline (Bartzokis, 2004; Destrooper & Karran, 2016; Nasrabady et al., 2018; Zhang et al., 2019). Despite the fact that AD is thought to be related to GM changes, postmortem AD brains distinctly exhibit WM damage (Scheltens et al., 1995; Gouw et al., 2008; Nasrabady et al., 2018). Moreover, WM aberrations can be found in AD patients at least ten years before clinical symptoms appear (Mortamais et al., 2013; Lee et al., 2016; Araque Caballero et al., 2018). Interestingly, WM pathology in AD primarily affects the areas of the CNS that were the last to be myelinated during development, a process known as neuropathologic retrogenesis (Braak & Braak, 1996; Reisberg et al., 2002), implying a possible link between late myelination and AD. Several proteins associated with the oligodendrocyte lineage have been found to be substantially decreased in the WM of postmortem AD brains (Roher, 2002). For instance, in the brains of AD patients, there are fewer Olig2-positive cells (Behrendt et al., 2013). On the other hand, it was observed a rise in PDGFR positive cells within WM on postmortem human AD brains, suggesting that an OPC response is linked to WM lesions, possibly by actively trying to remyelinate the lesion area (Simpson, 2007).

Animal models for AD additionally demonstrated abnormalities in oligodendrocyte lineage cells. According to some studies, WM alterations are a precocious clinical indicator of APP/PS1 mice (Chao et al., 2018; Dong et al., 2018). A study conducted by Desai and colleagues (2010) revealed an increase in mature nonmyelinating cells, while the number of immature oligodendrocytes remained steady (Desai, 2010). In addition, Lorenzini et al. (2020) noticed that Tg2576 had lower levels of Olig2 expression, a mature oligodendrocyte marker, at all ages when compared to wild-type (WT) (Lorenzini et al., 2020). Additionally, Behrendt et al. (2013) reported that APP/PS1 mice at 6–8 months of age had a higher

number of OPCs (Behrendt et al., 2013), and Dong and colleagues (2018) found evidence of a higher number of NG2 cells, a specific OPC marker, in the temporal lobe of 6 month-old APP/PS1 mice (Dong et al., 2018). Lorenzini et al. (2020) have noted a significant increase in the expression of OPC marker PDGFR gene in Tg2576 mice at 5 months of age (Lorenzini et al., 2020). These evidence streams lend credence to the idea that OLs induce AD in addition to reacting to pathology. It is interesting to note that Zhang and colleagues (2019) discovered OPCs with a phenotype resembling senescence in the Aβ plaque environments of AD patients' brains and APP/PS1 mice's brains. Additionally, they demonstrated that giving senolytic medications to APP/PS1 mice eliminated senescent OPCs from the brain, stopped plaque development, and enhanced cognitive function (Zhang et al., 2019). Although the precise mechanisms by which senescent OPCs contribute to the pathogenesis of AD are still unknown, it is possible that the secretory profiles of these cells have an impact on the activation or exacerbation of local inflammation, demyelination, and/or neuronal dysfunction (Han et al., 2022).

Myelin and Alzheimer's disease

Overview

Myelinated fibers were first discovered by Van Leeuwenhoek in 1717 (Kister & Kister, 2023). Rudolf Virchow first used the term "myelin" in 1854 to refer to a structure that is especially prevalent in the brain's core. The word comes from the Greek word "myelos", which means "marrow" (Boullerne, 2016). Ranvier discovered in 1878 that axon myelin coverage is not continuous but is instead sporadically disrupted by non-myelinated segments, which are now referred to as "nodes of Ranvier". The molecular mechanism underlying the nodes of Ranvier assembly has been thoroughly explained recently (Rasband & Peles, 2021). Histological stainings conducted in the 20th century by Pio Del Rio Hortega and Wilder Penfield revealed that oligodendrocytes, rather than neurons, are the source of myelin (Stadelmann et al., 2019).

Myelin structure

Myelin is a multilayered structure of equally dense membrane, as demonstrated by electron microscopy. It consists of two distinct alternating layers: the major dense line and the intraperiod line, which reflect the electron-dense and light layers, respectively (Figure 14) (Hartline, 2008; Aggarwal, Yurlova & Simons, 2011; Salzer & Zalc, 2016). The major dense line depicts the closely condensed cytoplasmic surfaces, while the interperiod line represents the tightly apposed outer membranes (Aggarwal, Yurlova & Simons, 2011). The myelin internode is composed of two types of myelin, which are different morphologically: compact myelin, that composes the majority of the internode (myelin segment on the axon), and noncompact myelin, which mainly comprises the

internode's edges (Soldan & Pirko, 2012). Short segments of exposed axolemma, known as the Ranvier nodes, segregate the internodes along individual myelinated axons. The high density of sodium channels found in Ranvier nobes, enables saltatory propagation of action potentials in an energy-efficient manner (Aggarwal, Yurlova & Simons, 2011).

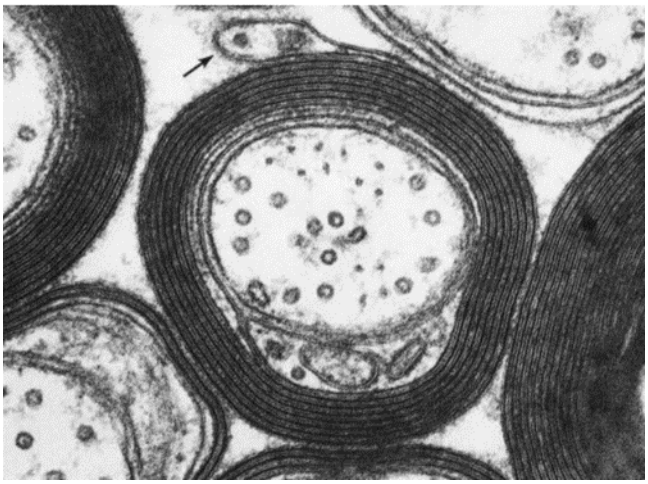

Figure 14. A CNS myelinated fiber (Morell & Quarles, 1999).

Myelin composition

Like all cell membranes, the myelin sheath consists of up of three main components: protein molecules, lipids, and water. However, the proportions of these components differs in myelin. The typical cell membrane has a roughly equal ratio of proteins to lipids, whereas the dry myelin sheath has a high lipid proportion (70%–85%) and a low protein proportion (15%) (Figure 15) (Poitelon et al., 2020). Cholesterol, phospholipids, and glycosphingolipids are found in myelin, with cholesterol and glycosphingolipids being the major lipid components of myelin, consisting around 27% and 31% of total myelin lipids, respectively (Jackman, Ishii & Bansal, 2009). Due to its

high lipid content, myelin is an effective electrical insulator and less ion-permeable. This feature also has an impact on the physical characteristics of the membrane, including its deformation and stiffness (Harayama & Riezman, 2018). Myelin basic protein (MBP) and protolipid protein (PLP) comprise almost 80% of the total protein content of myelin (30% and 50%, respectively). MBP is synthesized inside myelin at the location of myelin compaction and can be found at the cytoplasmic surface of compact myelin membranes (Zeller et al., 1984; Privat et al., 1979). Two other structural myelin proteins are the 2'3'-cyclic-nucleotide-3'phosphodiesterase (CNP) and the myelin associated protein (MAG) (Lappe-Siefke et al., 2003), and the latter is specifically found in the myelin sheaths of oligodendroglial membranes (Quarles, 2006). The myelin oligodendrocyte glycoprotein (MOG) is an another glycoprotein linked to white matter and myelin. This transmembrane glycoprotein is found on the surface of oligodendrocytes and myelin sheaths. The surface location of this protein may serve as a means of conveying extracellular information to the interior of oligodendrocytes. It has also been linked to autoimmune aspects of demyelinating diseases of the CNS (Gardinier et al., 1992; Morell & Quarles, 1999).

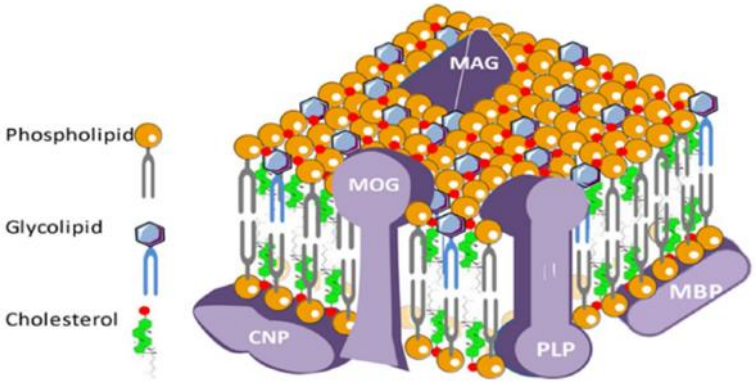

Figure 15. Myelin composition (Maitre et al., 2023).

Myelin functions

For many years, the general consensus has been that myelin serves only as an insulation membrane allowing maximum conduction velocity and reducing axonal energy consumption (Huxley & Stämpfli, 1949). Moreover, myelination impacts axon maturation, survival, and regeneration through signaling molecules and trophic support (Lee et al., 2012). Through changes in the axonal cytoskeleton, myelination, for instance, allows an axon to reach its maximum diameter (Windebank et al., 1985; Sánchez et al., 1996). It has also been suggested that myelin provides chemical energy (ATP) to the axon (Morelli, Ravera & Panfoli, 2011). Lipid composition of myelin is particularly important to cellular communication. Activation of different receptors and signaling molecules influences the maturation of oligodendrocytes, coordinated production of myelin, control of axonal development, and maintenance of axonal integrity (Baron et al., 2003; Bryant, et al., 2009; Krämer et al., 1999).

Myelin damage in AD pathology

Myelin and oligodendrocytes are susceptible to a number of pathological situations, such as ischemia, hypoxia, and brain injuries (Skoff et al., 2011; Gregersen et al., 2001; Mierzwa et al., 2015). Myelin degeneration has also been widely documented in AD patients and experimental animal models. Myelin and various lipids necessary for preserving myelin integrity are considerably reduced in the brain tissue of AD patients, according to studies about myelin pathology (Brun & Englund, 1986; Wallin et al., 1989). Another study that revealed a notable reduction in the levels of MBP in the postmortem brains of AD patients confirmed these findings (Roher et al., 2002). Remarkably, lower cholesterol was also noticed, along with higher Aβ peptide levels (Roher et al., 2002). Zhan and colleagues (2014) examined myelin reduction and deterioration in

AD in another research (Zhan et al., 2014). The findings suggested that the brains of AD patients had a significantly higher degree of myelin degradation along with decreased myelin integrity than the brains of age-matched healthy individuals (Zhan et al., 2014). The aforementioned data also align with the findings of biochemical studies that demonstrate elevated antibody levels against various glial-derived antigens (anti-MOG, anti-MAG, anti-MBP, and anti-PLP) in the serum of AD patients compared to healthy control participants (Papuć et al., 2015).

Recent developments in complex brain imaging methods have improved our ability to evaluate myelin alterations in AD. When compared to controls, patients with AD and MCI displayed significantly lower myelin content in their parietal and temporal cortices on T2-weighted MRI (Kavroulakis et al., 2018). Additionally, patients with AD showed a greater reduction in myelin content than patients with MCI (Kavroulakis et al., 2018). Further investigation into myelination appears to be possible with the development of q-Space Myelin Map Imaging, an MRI technique. This method offers a more sensitive way to assess the density and distribution of myelin in various brain regions by determining the diffusion of water molecules within myelin (Ota et al., 2019). Particularly, the hippocampus (Figure 16) and other brain regions exhibited reduced myelin density in AD patients (Ota et al., 2019). It was discovered that cognitive decline in these AD patients was correlated with changes in myelin organization. These findings have been reinforced by additional clinical research (Tse et al., 2018; Bouhrara et al., 2018). According to a recent study, brain tissues from AD patients additionally displayed decreased MBP expression in the cortex and hippocampus, two areas essential for memory and cognition (Chen et al., 2021).

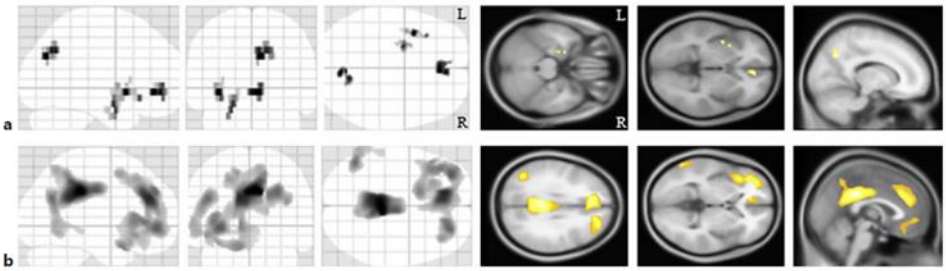

Figure 16. Morphological changes in the brain of an AD patient compared to a healthy subject (Ota et al., 2019).

Additionally, a number of preclinical animal investigations offer new perspectives on the myelin pathology linked to AD (Desai et al., 2010; Dong et al., 2018; Kaya et al., 2020). Most importantly, it has been documented that APP/PS1 mice exhibit early myelin degeneration (3-6 months of age), which predates the notable cognitive decline (at 6 months of age) (Dong et al., 2018). Additional study in a murine model of AD confirms that myelin loss (at 12 months of age) appears before amyloid pathology (at 13–14 months of age), indicating that it may be involved in the pathophysiology of AD (Tse et al., 2018). Another study conducted on APP/PS1 mice revealed that the hippocampal tissues of 2 month-old APP/PS1 mice exhibited different myelin morphology when compared to age-matched WT mice (Wu et al., 2017). Moreover, a research demonstrated that a focal myelin injury clearly develops in the core of Aβ plaque in both transgenic mouse models and AD patients (Mitew et al., 2010).

In the early stages of AD, a number of signaling pathways involved in myelin restoration are also disrupted (Hirschfeld et al., 2022). These results demonstrate the possible link between AD pathophysiology and myelin dysfunction.

Glutamate and Alzheimer's disease

Overview

Glutamate is the main fast excitatory neurotransmitter in the nervous system, and it plays an essential role in many various brain functions including memory, long-term potentiation, and synaptic plasticity (Alix & Domingues, 2011; Fairman & Amara, 1999). Additionally, glutamate may be a strong neurotoxin. In fact, the pathophysiology of numerous serious neurological conditions in humans, including epilepsy, amyotrophic lateral sclerosis, and stroke, has been linked to glutamate excitotoxicity (Smith, 2000). The transmitter role of glutamate was not recognized until the early 1980s (Fonnum, 1984), despite the fact that it has been known to have an excitatory effect (Hayashi, 1954; Curtis et al., 1959; 1960), play a central metabolic role in the brain (Krebs, 1935), and have very high glutamate uptake activity in brain cells (Stern et al., 1949).

Molecular cloning allowed for the identification of several families of glutamate receptor proteins (Niswender & Conn, 2010; Traynelis et al., 2010; Nicoletti et al., 2011). The receptors are divided into two categories: ionotropic receptors and metabotropic receptors (Gregory et al., 2013; Zhou & Danbolt, 2014). The ionotropic receptors are further categorized as N-methyl-D-aspartate (NMDA) receptors (NMDAr) (Gonda, 2012; Bonaccorso et al., 2011; Santangelo et al., 2012), AMPA (a-amino-3-hydroxy-5-methyl-4-isoxazole propionic acid) receptors (AMPAr) (Rogawski, 2013) and kainate receptors (Lerma & Marques, 2013). At least one type of glutamate receptor is expressed by the majority, if not all, of the nervous system's cells (Steinhauser & Gallo, 1996; Vernadakis, 1996; Forsythe & Barnes-Davies, 1997; Wenthold & Roche, 1998; Petralia et al., 1999; Conti et al., 1999; Shelton & McCarthy, 1999; Bergles et al., 2000).

Ionotropic (ligand-gated ion channels) receptors are the primary target of glutamate's post-synaptic action (Meldrum, 2000; Tapiero

et al., 2002). These receptors are ion channels that are permeable to cations, though the relative permeability to Na^{+} and Ca^{+2} varies depending on the family and subunit composition of the receptor (Attwell, 2000; Meldrum, 2000).

Numerous studies have been conducted on the NMDA receptor, particularly since it was found that many forms of synaptic plasticity are caused by activation of this excitatory amino acid (EAA) receptor (Dingledine et al., 1999). It appears that the NMDAr has two agonist-binding sites (Qian & Johnson, 2002; Tzschentke, 2002), and among the agonists are glutamate, N-methyl-D-aspartate, and several other EAAs (Qian & Johnson, 2002).

Excitatory amino acid transporters (EAAT) were discovered through a number of studies. There are five distinct EAATs, denoted as EAAT1 (Storck et al., 1992), EAAT2 (Pines et al., 1992), EAAT3 (Kanai & Hediger, 1992), EAAT4 (Fairman et al., 1995), and EAAT5 (Arriza et al., 1997). EAAT3 appears to be the most efficient glutamate transporter, with EAAT1 and EAAT2 following behind (Grewer et al., 2000; Wadiche & Kavanaugh, 1998; Wadiche et al., 1995), while EAAT4 and EAAT5 have extremely low rates of turnover (Mim et al., 2005; Gameiro et al., 2011).

EAAT exhibit unique patterns of localization with respect to expression in various brain areas and cell types. Whereas EAAT3, EAAT4, and EAAT5 are primarily found in neurons (Dehnes et al., 1998; Holmseth et al., 2012; Pow & Barnett, 2000), EAAT1 and EAAT2 are mostly expressed in astrocytes (Chaudhry et al., 1995; Danbolt, Storm-Mathisen & Kanner, 1992; Lehre et al., 1995). Interestingly, EAAT2 and EAAT3 are widely distributed in many different brain regions, including the striatum, cortex, and the hippocampus (Lehre et al., 1995; Holmseth et al., 2012). Subtype-specific subcellular localizations are also displayed by EAATs. EAAT1 and 2 therefore exhibit a strong perisynaptic distribution (Chaudhry et al., 1995; Schreiner et al., 2014). Additionally, research revealed that EAATs are also present in neurons, and more precisely in presynaptic axon terminals (Danbolt, Furness & Zhou, 2016; Furness et al., 2008). EAAT5 is located pre-synaptically (Wersinger et al.,

2006), while EAAT3 and EAAT4 are located post-synaptically. EAAT3 is primarily found in cell soma and dendrites (Holmseth et al., 2012), while EAAT4 is found in dendrites and dendritic spines (Nagao, Kwak & Kanazawa, 1997; Yamada et al., 1996).

Glutamate-glutamine cycle

When glutamate is absorbed by cells, it can be utilized again as a transmitter or for metabolic processes like protein synthesis, energy metabolism, and ammonia fixation (Danbolt, 2001). Glutamate reuse as a transmitter in nerve terminals is simple. A vesicular glutamate transporter carries glutamate into synaptic vesicles, where it is released by exocytosis (Südhof, 1995; Augustine et al., 1996; Ludger & Galli, 1998; Cousin & Robinson, 1999). Birnbaumer et al. (1994) reported that a Ca^{+2}-dependent mechanism involving N- and P/Q-type voltage-dependent Ca^{+2} channels, which seem to be closely associated with vesicle docking sites, releases glutamate from vesicles in presynaptic terminals (Birnbaumer et al., 1994). The excitatory postsynaptic potential (EPSP), which is mainly related to AMPA receptor activation, is produced when a single vesicle is released. The glutamate concentration within the vesicle is estimated to be 100 mmol/L. The glutamate transporters can also function in reverse to "release" glutamate. This would happen when cerebral ischemia decreases the Na^+ and K^+ gradient across the membrane (Levy et al., 1998, Obrenovitch & Urenjak, 1997).

Glutamate that is absorbed by EAATs in astrocytes from the extracellular fluid is converted into glutamine, which is then released into the extracellular fluid, absorbed by neurons, and converted back into glutamate (Figure 17). This trafficking of glutamate and glutamine between astrocytes and neurons has been suggested to be a key mechanism for the recycling of transmitter glutamate and is widely known as the glutamine-glutamate cycle (Hertz, 1979).

The idea that glutamate is divided into two pools was first proposed in the early 1970s (Van den Berg & Garfinkel, 1971). Few years later, glutamine synthetase (GS) was demonstrated to be a glial enzyme through immunocytochemical analysis, supporting the idea that glutamine is synthesised predominantly by glial cells (Martinez-Hernandez et al., 1977; Erecinska & Silver, 1990; Westergaard et al., 1995; Ottersen et al., 1996).

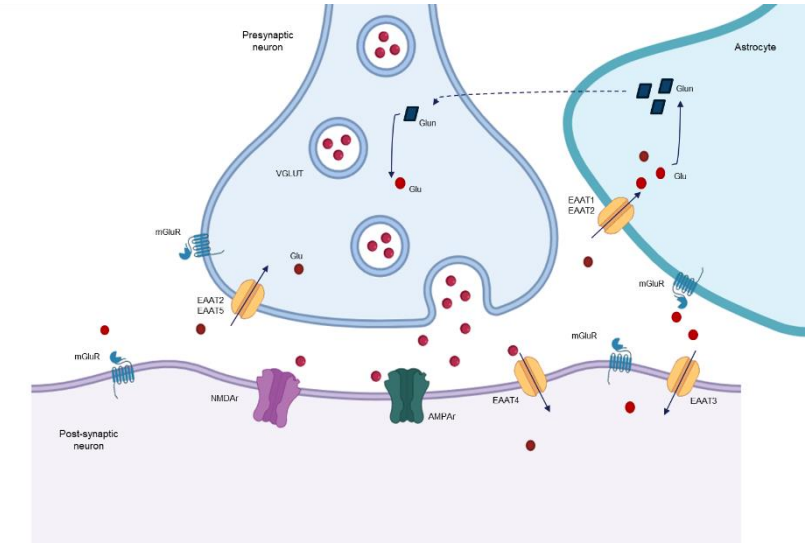

Figure 17. The glutamate-glutamine cycle. Designed with BioRender. Glu: glutamate; Gln: glutamine; EAAT: excitatory amino acid transporter; VGLUT: vesicular glutamate transporter; NMDAr: N-methyl-D-aspartate acid receptors; AMPAr: a-amino-3-hydroxy-5-methyl-4-isoxazole propionic acid receptor; mGluR: metabotropic receptor.

Glutamate excitotoxicity

In vivo, the concentration of glutamate is approximately 0.6 µM, when the synaptic cleft is at rest (Bouvier et al., 1992). The process of synaptic transmission involves a rapid (1–2 ms) and spatially localized increase in extracellular glutamate to levels higher than 10 µM (Clements et al., 1992). A high-affinity uptake system on pre- and post-synaptic neuronal cell membranes as well as the membranes of nearby glial cells mediates the termination of glutamate's excitatory action (Danbolt, 2001). The excessive release of glutamate into the extracellular space by astrocytes and pre-synaptic nerve terminals causes excitotoxicity by overstimulating glutamate receptors, particularly NMDA receptors (Gagliardi, 2000; Koh & Choi, 1987) in a positive feedback loop (Rodriguez-Rodriguez, Almeida & Bolaños, 2013; Norris et al., 2006). Overstimulation of NMDA receptors causes excessive Ca^{+2} and Na^{+} influx through glutamate receptor-gated ion channels and passive movements of Cl^{-} and water (Mody & MacDonald, 1995). Glutamate's ability to be both extremely toxic and vital for neurotransmission creates a delicate balance between pathology and plasticity. Glutamate excitotoxicity has been linked to several neurological conditions, such as Alzheimer's disease, amyotropic lateral sclerosis, Huntington's disease, trauma, ischemia and epilepsy (Rothstein, 1996; Won et al., 2002; Hynd et al., 2004; Tannenberg et al., 2004; Fujikawa, 2005; Rego & de Almeida, 2005; Yi & Hazell, 2006).

Glutamate dysregulation in Alzheimer's disease

Dysregulation of the glutamatergic system all through the tripartite synapse has been demonstrated by a variety of imaging methods and postmortem tissue analyses. These alterations are primarily influenced by protein accumulation and aggregation status and present at different stages of the cognitive impairment in AD continuum. Glutamatergic excitotoxicity is primarily caused by

either Aβ (Fuchsberger et al., 2016), or hyperphosphorylated tau, which increases neuronal excitability and induces overexcitation (Huijbers et al., 2019; 2015). It is believed that morphological alterations in neuronal structure as well as hyperactivity are precursors to AD pathology and cognitive impairment (Ghatak et al., 2019). Constant NMDAr overactivation impairs physiological signal recognition, which impacts memory retention and recollection (Danysz & Parsons, 2012). In later stages of AD, glutamate levels are noticeably lower and hyperactivity is discrepant. This is ascribed to the loss of neurons resulting from exposure to an excitotoxic surroundings or from hyperphosphorylated tau microtubule disruption. Abnormal glutamate signaling exhibiting biphasic changes throughout the AD spectrum is caused by a variety of receptors and transporters. AMPAr and NMDAr subunits are modified postsynaptically throughout the AD spectrum, with upregulation observed early in the course of the disease and downregulation in later stages (Findley et al., 2019). Previous research indicated that AD is also associated with impaired glutamate uptake (Walton & Dodd, 2006). The notion that EAAT2 activity shields the brain from AD-related dysfunctions is supported by studies conducted in rodents. For instance, cognitive impairment in AD mice developed faster when one allele of the EAAT2 gene was absent (Mookherjee et al., 2011).

It has been demonstrated that in APP/PS1 mice, hippocampal basal and stimulus-evoked glutamate signaling becomes hyperactive in a subregion-specific way before cognitive decline begins (Hascup & Hascup, 2015). The CA1 exhibits the first alterations, with stimulus-evoked glutamate release being noticeably higher by three months of age. Basal glutamate levels are raised all over the hippocampal region starting at six months of age, coinciding with the onset of hippocampal plaque accumulation. At this age, glutamate release also rises in the dentate gyrus and remains high throughout the course of the disease. Up until the age of 12 months, when plaque accumulation becomes more noticeable, CA3-evoked glutamate release is not elevated (Hascup et al., 2020a). Furthermore, anatomically aligned but temporally delayed plaque deposition was

noted, along with hyperactive glutamate signaling (Hascup et al., 2020b). These findings provide additional evidence that the glutamatergic system could serve as an early biomarker and therapeutic target.

Several other AD animal models have documented similar alterations in glutamate signaling as the disease progresses. Human tau with the P301L mutation is expressed in rTg4510 AD mouse model. Age-dependent cognitive decline, neuronal degeneration, and neurofibrillary tangle development are observed in this model. These mice also showed increased hippocampal glutamate by six months, which corresponded with acquisition errors on the behavioral task of the Barnes maze (Hunsberger et al., 2014; Hunsberger et al., 2015). In addition, the PS19 tauopathy AD model exhibits higher hippocampal glutamate concentrations at three months of age. Glutamate levels in these mice decrease as they get older due to fewer synapses and neurons in them. Early-life elevated glutamate levels combined with later-life neuronal loss indicate an excitotoxic mechanism (Crescenzi et al., 2017). By applying electrophysiological methods, persistent hyperactive glutamatergic synapses in the entorhinal cortex were identified in the 3xTg AD at three months of age (Arsenault et al., 2011). Whole-cell patch clamp recordings of CA1 pyramidal neurons in 5xFAD mice are observed to exhibit higher spontaneous excitatory post-synaptic currents at 2 and 4 months of age (Li et al., 2021). Overall, these studies demonstrate that excessive glutamatergic signaling occurs either prior to or concurrently with the build-up of tau and/or amyloid.

It has also been demonstrated that excitotoxic mechanisms (Mark et al., 2001) cause oligodendrocyte (Matute et al., 1997; McDonald et al., 1998) and neuron (Choi, Maulucci-Gedde & Kriegstein, 1987; Epstein, Lipton & Rosenberg, 1994) loss in response to elevated extracellular glutamate levels. When exposed to glutamate at concentrations of 1 mM or 0.1 mM, paranodal myelin appeared to be highly vulnerable. Axo-glial junction collapse paranodal myelin disruption, and juxtaparanodal K^+ channel exposure and redistribution were linked to the damage. According to findings of

Fu and colleagues (2009), one of the main mechanisms underlying the functional loss in the WM injury is the disruption of paranodal myelin brought on by glutamate (Fu et al., 2009). Several investigations have demonstrated that functional NMDA receptors are expressed on the myelin sheath in the WM of developing and adult central nervous system tissues, such as rat cerebellum and corpus callosum (Káradóttir et al., 2005), and the mouse and rat optic nerve (Salter & Fern, 2005; Micu et al., 2006; Baltan et al., 2008). This suggests that the presence of NMDA receptors is a characteristic shared by all myelin sheaths, regardless of their stage of maturation (Matute, 2006). Remarkably, it has been observed that during chemical ischemia, NMDA receptors on myelin mediate Ca^{+2} accumulation (Micu et al., 2006) and induce myelin loss (Salter & Fern, 2005). It was also reported that damage to the myelin sheath was avoided by blocking NMDA receptors (Salter & Fern, 2005). It has been shown that in vivo administration of CNS 1102, a NMDA receptor antagonist, after temporary focal ischemia, protects the cerebral white matter's myelin sheath from ischemic injury (Schäbitz, Li & Fisher, 2000). Fu et al. (2009) also discovered that in isolated ventral spinal cord WM from adult guinea pigs, NMDA and kainite could partially provoke paranodal myelin damage (Fu et al., 2009). This finding implies that the NMDA and kainate receptors on the paranodal myelin may mediate the paranodal myelin damage caused by glutamate (Brand-Schieber & Werner, 2003). Moreover, according to Doyle et al. (2018), acute ischemic myelin injury occurs due to vesicular glutamate release from axons, resulting in cytotoxic over-activation of GluN2C/D-containing myelinic NMDA GluRs (Doyle et al., 2018).

Limbic system and Alzheimer's disease

Anatomy and functions of the limbic system

An assembly of brain regions commonly found above the brainstem, below the cerebral cortex, and lateral to the thalamus is known as the limbic system (Mori & Aggarwal, 2014). The term "grand lobe limbique" (derived from the Latin word "limbus," which means "border") was originally employed by Paul Broca in the late 1800s to refer to this general area of the brain, which includes the cingulate and the parahippocampal gyri (Broca, 1890). Nonetheless, the American physician James Papez expounded on its presumed function in emotion in the landmark 1937 paper entitled "A proposed mechanism of emotion". This structure is known as the Papez circuit (Papez, 1937). Paul D. MacLean first used the term "limbic system" in 1952 to refer to the Broca's limbic lobe and the associated subcortical nuclei as the neural substrate of emotion (Nakano, 1998). Since then, other researchers have further investigated and elaborated on the limbic system notion (Nauta, 1958; Heimer & Van Hoesen, 2006).

The limbic system's constituent structures have undergone numerous definitions as a result of advancements in neuroscience. Visual, auditory, and somatosensory inputs processed in the area constitute the mesencephalic components. The anterior thalamic nuclei, the habenular commissure, and the hypothalamus make up the diencephalic components. The cortical and subcortical regions of the telencephalic components involve the olfactory bulbs, hippocampus, parahippocampal gyrus, fornix, columns of the fornix, mammillary body, septum pellucidum, amygdala, cingulate gyrus, and entorhinal cortex (Catani et al., 2013). Contemporary MRI methods, especially diffusion MRI, have provided important new understandings of the structure of the limbic system in the human brain (Smith et al., 1999; Callen et al., 2001). Compared to other

mammalian species, the human brain has comparatively smaller limbic tracts.

Though it was once thought that the limbic system was the only neurological system responsible for controlling emotion, this is no longer the case. The limbic system is only one area of the brain that controls visceral, autonomic processes. Generally speaking, the limbic system supports a number of cognitive functions, such as spatial memory, learning, motivation, emotional and social processing (Hariri, Bookheimer & Mazziotta, 2000; Patestas & Gartner, 2006).

Fornix anatomy

The hippocampus and other limbic regions are connected by a white matter bundle called the fornix. It was first recorded in a historical work by Andreas Vesalius called “De Humani Corporis Fabrica” in 1543 (Swanson, 2014). Situated in the mesial aspect of the cerebral hemispheres, the fornix is a thin, C-shaped bundle of white matter consisting of myelinated association, projection, and commissural fibers. There are roughly 1.2–2.7 million fibers in each hemisphere of the human fornix (Lang, 1992; Ozdogmus et al., 2009) and occupies an area between 1000 and 1800 cubic millimeters overall (Tsivilis et al., 2008; Bozoki et al., 2012). Located longitudinally from the mesial temporal lobe to the diencephalon and basal forebrain, the fornix is a major structure that outputs from the hippocampus. Hippocampal fibers gather into a thin layer called the alveus that is located medially to the floor of the temporal horn of the lateral ventricle. As the alveus runs posteromedially, fibers from the

subiculum connect with it and bundle into the fornix's fimbria. As more fibers are gathered by the fimbria, they expand in cross-sectional area and are referred to as the fornix's crura. The thin triangular forniceal commissure, also referred to as the psalterum or dorsal hippocampal commissure, enables the crura to project contralaterally and arch supero-anteriorly beneath the splenium of the corpus callosum. The forniceal body, which curves over the thalamus and under the septum pellucidum, is formed by the paracentral run of the crura. The left and right columns of the fornix body divided off rostrally and extend to the basal forebrain, anterior to the interventricular foramina. The anterior commissure is where the fornix columns divide; the pre-commissural fornix is formed by fibers that travel anteriorly, and the post-commissural fornix is made up of fibers that curve posteriorly (Senova et al., 2020).

Primate and rodent fornices differ significantly from one another, partly because of the different spatial arrangements of their respective hippocampi (Figure 18). The rodent hippocampus surrounds the hippocampal formation with a sheet of fimbria and alveus fibers and is shifted more rostrodorsally (Paxinos & Watson, 2013). Its dorsal and ventral components are rotated by 90 degrees (Szabo & Hennerici, 2014). Rodents feature a more developed commissural system compared to primates. Their dorsal commissure extends nearly the whole length of the fornix's longitudinal axis. Furthermore, in non-human primates and rodents, a thin transverse lamina called the ventral hippocampal commissure (vhc) is located just ventral to the columns at the level of the

subfornical organ (Strange et al., 2014; Kerever et al., 2015). The vhc consists of crossing dentate gyrus fibers and is likely absent in humans (Demeter, Rosene & van Hoesen, 1985). The fibers of the dorsal fornix (df), which is the murine counterpart of the human fornix body (Gloor et al., 1993), originate from the temporal hippocampal pole and extend medial to the septal hippocampus along the inferior aspect of the corpus callosum (Wyss, Swanson & Cowan, 1980). At the anterior commissure, where the rodent fimbria-fornix fibers split to reach their terminal nuclei, the narrow dorsal fornix finally disappears (Rosene & Hoesen, 1987).

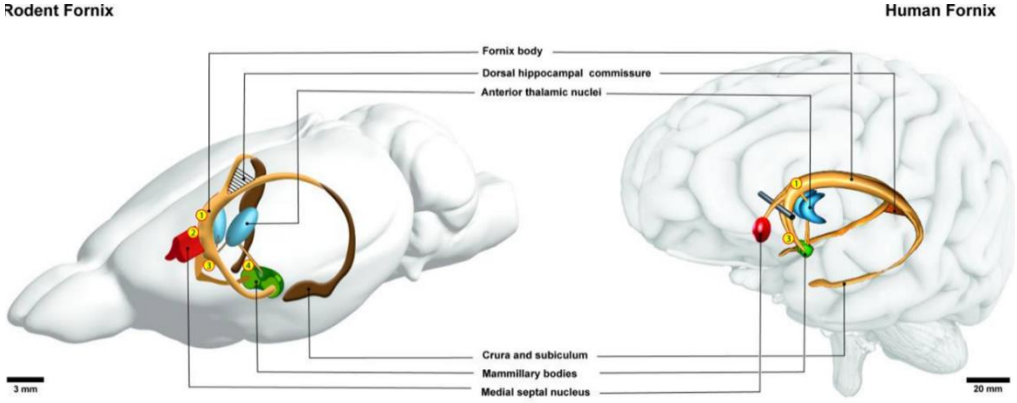

Figure 18. Anatomy of rodent and human fornix (Senova et al., 2020).

Fornix functions and its implication to memory

Based on clinical and experimental evidence, the fornical fibers may be distributed according to their function. Visuospatial memory information is primarily carried by the right fornix, whereas verbal memory information is primarily performed by the left. It is assumed that the rostral hippocampus, that manages interoceptive signals for

emotional and motivational learning and memory, sends projections to the lateral aspect of the fornix (Cameron & Archibald, 1981; Hodges & Carpenter, 1991; McMackin et al., 1996 Saunders & Aggleton, 2007; Tucker et al., 1988).

An important function of the fornix is in episodic memory, which deteriorates with normal aging (Head et al., 2008) and is usually the first cognitive domain to be affected in AD (Salmon & Butters, 1992). Studies using diffusion tensor imaging (DTI) reveal a relationship between episodic memory and fornix WM microstructure in elderly individuals who are cognitively normal (Metzler-Baddeley et al., 2011) and those at risk for AD (Mielke et al., 2012). Significantly, presymptomatic carriers of familial AD mutations exhibit fornix microstructural alterations years before they experience cognitive impairment and while their gray matter volume is still preserved (Ringman et al., 2007), implying that fornix integrity may be helpful in predicting memory decline.

Fornix degeneration in AD pathology

Several studies have repeatedly demonstrated that patients with fornix damage exhibit deficits in a variety of cognitive functions, particularly in episodic memory (Gaffan et al., 1991; Squire & Zola-Morgan, 1991; Aggleton et al., 2000). Furthermore, fornix degeneration, as a limbic system component, could predict progression to cognitive impairment more accurately than hippocampal atrophy and may occur before hippocampal atrophy (Fletcher et al., 2013).

Patients with AD (Teipel et al., 2013), and many with MCI (Pihlajamaki et al., 2009) have been reported to exhibit hippocampal and entorhinal cortical atrophy as measured by MRI. Additionally, compared to healthy controls, MCI and AD patients exhibit atrophied fornices (Callen et al., 2001; Copenhaver et al., 2006; Ringman et al., 2007; Hattori et al., 2012), as validated by a longitudinal follow-up study (Douaud et al., 2013).

As decreased franctional anisotropy (FA) occurred more than two years before the progression from MCI to AD, decreased FA of the fornix on DTI was found to be more sensitive than decreases in volume and/or area on structural MRI (Douaud et al., 2013). When comparing AD patients to healthy controls, as well as when comparing MCI and/or early onset AD patients (Mielke et al., 2009; Zhuang et al., 2010; Liu et al., 2011b; Oishi et al., 2012; Canu et al., 2013; Douaud et al., 2013; Nowrangi et al., 2013), fornix measurements revealed lower FA (Liu et al., 2011b; Metzler-Baddeley et al., 2012) and higher mean diffusivity (MD) and radial diffusivity (RD) in AD patients (Mielke et al., 2009; Stricker et al., 2009; Liu et al., 2011b; Hattori et al., 2012; Huang et al., 2012; Oishi et al., 2012; Nowrangi et al., 2013; Zhuang et al., 2013). Patients with genetically inherited dementias also exhibited an equivalent pattern of lower FA in the fornix, when compared to healthy controls (Ringman et al., 2007). Additionally, poorer performance on short- and long-term memory tasks as well as clinical dementia assessments in AD and MCI patients were linked to lower FA and higher diffusivity metrics in the fornix (Ringman et al., 2007; Mielke et al., 2009; 2012; Kantarci et al., 2011; Zhuang et al., 2013).

Decreased myelin content has been identified in the fornix. According to Nabizadeh et al. (2022), there is a strong correlation between altered WM microstructure throughout the brain and plasma Nfl levels (Nabizadeh et al., 2022). In the fornix, corpus callosum, and other brain regions, plasma Nfl has a negative correlation with FA. In other brain areas, including the corpus callosum, hippocampal cingulum and the fornix, there is a positive correlation with RD and MD values and plasma Nfl levels. In WM, demyelination and degeneration are correlated with lower FA and higher RD and MD values. This is further supported by the findings of Bangen and colleagues (2021), who aimed to quantify fornix myelin water fraction in nondemented older adults. Their results suggested that lower fornix myelin water fraction is significantly associated with poorer episodic memory performance (Bangen et al., 2021). Interestingly, forniceal WM alterations have also been documented as a biomarker of the transition from cognitively

normal to amnesic MCI (aMCI) subjects. Early aMCI subjects exhibited impaired WM in the fornix and absence of hippocampal atrophy, even when their cognitive function was normal, according to a cross-sectional study by Zhuang and colleagues (Zhuang et al., 2013). These results, along with those of other researches, imply that the fornix is related to memory function regardless of hippocampal volume, indicating that fornix myelin could be a useful biomarker for early medial temporal lobe age-related and AD risk-related changes (Fletcher et al., 2013; Gold et al., 2010; Ringman et al., 2007).

Furthermore, fornix demyelination in early AD is associated with elevated Aβ burden. DTI and ex vivo histopathology were combined in early research to examine the interaction among WM and amyloid burden. In mouse models, Song et al. (2004) and Sun et al. (2005) discovered that amyloid deposition and WM abnormalities, a sign of increased myelin degeneration, were positively correlated (Song et al., 2004; Sun et al., 2005). Another study examined older adults with and without MCI and included multiple vascular risk factors. The results suggest a correlation between amyloid burden and decreased FA in the fornix and corpus callosum (Chao et al., 2013). Rabin and colleagues (2019) examined the potential synergistic relationship between potential cognitive decline and continuous levels of Aβ burden and core fornix FA. Their findings demonstrated that core fornix FA and Aβ burden acted in concert to preferentially accelerate the longitudinal decline in episodic memory over time (Rabin et al., 2019). Further evidence suggested that this effect was unique to the fornix because interactions between Aβ burden and other white matter tracts did not correlate with cognitive decline (Rabin et al., 2018).

OBJECTIVES

Objectives

The general objective of this thesis is to determine white matter anomalies in the dorsal fornix as an early event in the progression of AD using the APP/PS1 mice model.

On the one hand, myelin loss in the hippocampal region has been specifically observed and is linked to the early onset of Alzheimer's disease. Consequently, the process of AD onset may be dependent on the demyelination of the dorsal fornix, which is the connection of the two hippocampi in the middle line. The premise of this hypothesis is that memory processing and inter-hippocampal connectivity are compromised in young transgenic APP/PS1 mice (4 and 6 months old) due to demyelination of the dorsal fornix. Furthermore, remyelination is hampered due to alterations in oligodendrocyte lineage cells at the dorsal fornix.

On the other hand, another important objective of this study is to clarify the mechanisms underlying the demyelination that has already been seen in AD. Therefore, our hypothesis includes that axonal vesicular glutamate releases into the periaxonal space beneath the myelin sheath, resulting in myelin loss. This myelin damage is caused through activation of NMDA glutamate receptors and disruption of EAATs. Aβ increases glutamate levels through the induction of glutaminase accumulation, which catalyzes the synthesis of glutamate from glutamine inside neurons. AD pathophysiology is enhanced when elevated glutamate levels increase Aβ levels in a positive feedback loop. More precisely, an increase in glutamate may trigger the release of glutamate from axons, which in turn may activate NMDA receptors and disrupt EAATs, and cause demyelination.

The specific objectives of this study are:

1. To elucidate the demyelination of the dorsal fornix in young APP/PS1 mice.

2. To detect alterations in oligodendrocyte lineage cells in the dorsal fornix of young APP/PS1 mice.

3. To determine whether the hippocampus of young transgenic mice exhibit demyelination or other OLs abnormalities.

4. To investigate whether Aβ-induced glutamate excitotoxicity activates NMDA receptors and disrupts EAATs, and subsequently cause demyelination in neurosphere cultures.

MATERIAL AND METHODS

Material and methods

Experimental animals

The double transgenic mice APPswe/ PSEN1dE9 (APP/PS1), which have been described by different groups as a model of Alzheimer's disease (Shen et al., 2018; Sasaguri et al., 2017; Viana da Silva et al., 2016; Lok et al., 2013), were used in this project. The APP gene mutation and the modified presenilin 1 (PSEN1) gene are the two coding vectors that are used to characterize this strain genetically. The inserted APP sequence, on the one hand, presents the corresponding Swedish mutations required for the alteration and encodes a mouse/human chimeric APP protein (Mo/HuAPP695swe) that has been humanized by modifying three amino acids. The PSEN1 sequence, on the other hand, encodes human presenilin, yet it lacks exon 9, which is linked to the onset of Alzheimer's disease. In both cases, a particular promoter is used to restrict their expression to the central nervous system. These mice can be distinguished at the phenotypic level by the formation of Aβ deposits at six months of age, which lead to an abundance of amyloid plaques in the cerebral cortex and hippocampal regions by nine months of age.

The C57BL/6J strain was used as a control group or wild-type (WT), which corresponds to the same genetic background as the transgenic strain used. Both strains were obtained from the Jackson laboratories in the United States and were established at the

University de Valencia's Faculty of Medicine's Central Research Unit (*Unitat Central d'Investigació de la Facultat de Medicina de la Universitat de València)*. In this service, hemizygous double transgenic offspring are obtained through crosses between the two strains and are maintained under conditions of 23±1°C temperature, a relative humidity of 60%, light-dark cycles of 12-12 hours and a food and water *ad libitum*.

Over the course of the project, 40 mice in total were used, half of them for immunofluorescence assays and the other half for immunoblotting. It should be noted that, all procedures that require the use of mice were approved by the Vicerectorate of Research at the University of Valencia's Commission on Ethics in Experimental Research (Comisión de Ética en la Investigación Experimental del Vicerrectorado de Investigación de la Universidad de Valencia; ref: 2022 VSC PEA 0123), and they were carried out in accordance with the guidelines set forth in Royal Decree 53/2013 (Real Decreto 53/2013), which establishes the fundamental standards applicable to the protection of animals used in research and other scientific purposes, including teaching.

Reagents and media

- **Lowry Reagent:** *Lowry Reagent Powder* dissolved in 40ml of double-distilled water (L3540-25VL, *Merck*).
- **Folin:** *Folin & Ciocalteu's phenol reagent* diluted to 22.5% in double-distilled water (F9252-500ML, *Sigma-Aldrich*).

- **Luminol:** *Immobilon Classico Western HRP substrate* (WBLUC0500, *Millipore*).
- **Restore™ Western blot Stripping Buffer** (21059, *Thermo Fisher Scientific*).
- **Pentobarbital sódico (Eutanax)** (100 mg/kg) (Dolethal Vetoquinol, Madrid, España).
- **Phosphate buffered saline (PBS):** pH 7.2-7.6, 1 tablet dissolved in 200ml of double-distilled water (P4417-50TAB, *Sigma-Aldrich*).
- **DMEM/F-12, GlutaMAX™ supplement** (31331028, *Gibco™*).
- **B-27™ Supplement (50X), serum free** (17504044, *Gibco™*).
- **HBSS, no calcium, no magnesium, no phenol red** (14175053, *Gibco™*).
- **Trypsin-EDTA (0.05%), phenol red** (25300054, *Gibco™*).
- **Penicillin-Streptomycin (10000 U/mL)** (15140122, *Gibco™*).
- **Beta-Amyloid (1-42)** (AS-20276, *AnaSpec*).
- **QNZ 46** (4801, *Tocris Bioscience™*).
- **DL-TBOA (DL-Threo-Beta-Benzyloxyaspartate)** (12-231-0, *Tocris Bioscience™*).
- **Fluoromount Aqueous Mounting Medium** (F4680-25ML, *Sigma-Aldrich*).
- **Goat serum** (G9023-10ML, *Sigma-Aldrich*).
- **Hoechst 33342 Solution (20 mM)** (62249, *Thermo Fisher Scientific*).
- **PageRuler™ Plus Prestained Protein Ladder, 10 to 250 kDa** (26619, *Thermo Scientific™*).

Buffers and solutions

- **TBS 10X:** 80g of NaCl and 24.2g of Trizma are added in 1 liter of double-distilled water. Once both compounds are dissolved, the solution's pH is adjusted to 7.6.
- **TBS-t:** 100ml of TBS 10X are disolved in 900ml of double-distilled water. Upon dissolution, 1 ml of Tween 20 is added and dissolved.
- **PBS-t:** Triton 100X is added to 0.5% in PBS and stirred until completely dissolved.
- **Electrophoresis buffer 10X [25 mM Trizma, 190 mM Glycine, 0,1% (w/v) SDS]:** In 1 liter of distilled water, 3 g of Trizma, 14.37 g of Glycine and 1 g of SDS are dissolved.
- **Transfer buffer [25 mM Trizma, 192 mM Glycine, 20% (v/v) methanol]:** Firstly, 14.4 g of Glycine and 3.03 g of Trizma are dissolved in 800 ml of distilled water. After dissolving the solid components, it should be refrigerated at 4ºC and only just before use 200 ml of methanol are added to the solution and it is stirred to homogenize all the components.
- **Tris HCl [1M], pH 6.8:** 60.55 g of Trizma are dissolved in 500 ml of distilled water and the solution's pH is adjusted to 6.8 with a HCl solution.
- **Tris HCl [1.5M], pH 8.8:** 90.83 g of Trizma are dissolved in 500 ml of distilled water and the solution's pH is adjusted to 8.8 with a HCl solution.

- **Lysis buffer:** 0.927 g of Trizma are diluted in 100 ml of distilled water and the solution is adjusted to a pH of 6.7. In 87 ml of this solution, 10 ml of glycerol and 2 g of SDS are added. Just before using this buffer, 40 µl of sodium orthovanadate [200mM] (phosphatase inhibitor) and 40 µl of the protease inhibitor cocktail are added to 3,766 ml of the solution obtained.
- **Loading buffer 2X [50 mM Tris HCl pH 6.8, 3% SDS, 10% glycerol, 0,005% bromophenol blue, 5% 2-mercaptoethanol]:** To 0.6 ml of Tris HCl pH 6.8, 1.5 ml 20% SDS, 1 ml of glycerol and 50 µl of 1% bromophenol blue are added. Afterwards, 9.6 ml of distilled water and 500 µl of mercaptoethanol are added.
- **Blocking solution for Immunohistochemistry:** Dilution 1:10. In 270µl of PBS-t, 30µl of goat serum are added.
- **Blocking solution (5% BSA) for Western blot:** 5 g of BSA are disolved in 100 ml of TBS-t.
- **Eutanax solution (15%):** In 1.5 ml of Eutanax, 0.5 ml of ethanol absolute are added, which will serve as an adjuvant. Finally, in this dilution, saline is added up to 10 ml.
- **Sodium Citrate Buffer (10mM Sodium Citrate, 0.05% Tween 20, pH 6.0):** 1.07055 g of sodium citrate are dissolved in approximately 400 ml of distilled water. Then 250µl of Tween-20 are added and the pH is adjusted to 6.0 with 1.0 N HCl. The volume is then brought to 500 ml and the solution is stored at room temperature for 3 months.

Antibodies

Primary antibodies

- **Rabbit anti-Neurofilament/Nfl antibody,** 1:1000 (ab207176, *abcam*)
- **Mouse anti-Neurofilament/Nfl antibody,** 1:1000 (ab7255, *abcam*)
- **Rabbit anti-PDGFRα,** 1:500 (ab203491, *abcam*)
- **Rat anti-CD140a(PDGFRα),** 1:200 (558774, *BD Pharmingen*)
- **Rabbit anti-Myelin oligodendrocyte glycoprotein/MOG antibody,** 1:1000 (ab233549, *abcam*)
- **Rabbit anti-Myelin Basic Protein/ MBP antibody,** 1:500 (ab40390, *abcam*)
- **Mouse anti-Myelin Basic Protein/ MBP antibody,** 1:500 (sc-71546, *Santa Cruz*)
- **Rat anti-Myelin Basic Protein/ MBP antibody,** 1:200 (MCA409S, *BioRad*)
- **Rabbit anti-Oligodendrocyte Transcription Factor 2/Olig2 antibody,** 1:1000 (GTX132732, *GeneTex*)
- **Mouse anti-beta Tubulin Loading Control Monoclonal antibody,** 1:2000 (MA5-16308, *Invitrogen*)

Secondary antibodies

- **Goat anti-Mouse IgG (H+L), Superclonal™ Recombinant Secondary Antibody, Alexa Fluor™ 488,** 1:800 (A28175, *Invitrogen*)
- **Anti-mouse IgG (H+L), F(ab')2 Fragment Alexa Fluor® 647 Conjugate,** 1:800 (4410, *CellSignaling Tech*)
- **Goat Anti-Rabbit IgG H&L (Alexa Fluor® 647),** 1:800 (ab150079, *abcam*)

- **Goat Anti-Rabbit IgG H&L (Alexa Fluor® 488),** 1:800 (ab150077, *abcam*)
- **Goat anti-Rabbit IgG (H+L) Secondary Antibody, HRP,** 1:10.000 (31460, *Invitrogen*)
- **Goat Anti-Mouse IgG, H&L Chain Specific Peroxidase Conjugate,** 1:10.000 (401215-2ML, *Sigma-Aldrich*)
- **Donkey anti-Mouse IgG (H+L) Highly Cross-Adsorbed Secondary Antibody, Alexa Fluor™ 568,** 1:200 (A10037, *Invitrogen*)
- **Donkey anti-Rabbit IgG (H+L) Highly Cross-Adsorbed Secondary Antibody, Alexa Fluor™ 568,** 1:200 (A10042, *Invitrogen*)
- **Donkey anti-Rabbit IgG (H+L) Highly Cross-Adsorbed Secondary Antibody, Alexa Fluor™ 488,** 1:200 (A21206, *Invitrogen*)
- **Donkey anti-Rat IgG (H+L) Highly Cross-Adsorbed Secondary Antibody, Alexa Fluor™ 488,** 1:200 (A21208, *Invitrogen*)

Equipment

The research group directed by Dr. Ana Lloret Alcañiz has the facilities and laboratory equipment required to complete all the work presented in the thesis that follows. This group is located in the Department of Physiology of the Faculty of Medicine and Dentistry of the University of Valencia. Furthermore, it was required to make use of the equipment and various services provided by the University of Valencia's Central Medicine Research Unit (Unidad Central de Investigación de Medicina, UCIM) at the Faculty of Medicine and the Central Support Service for Experimental Research (Servicio Central de Apoyo a la Investigación Experimental, SCSIE), situated on the Burjassot campus. Moreover, in the context of the international internship in Lisbon, it was made use of the equipment

and facilities provided by the Institute of Molecular Medicine João Lobo Antunes (iMM), associated research institution of the University of Lisbon, in Lisbon, Portugal. The equipment used is listed below.

- Unrefrigerated microcentrifuge (1-14, 90616, *Sigma*)
- Telstar™ AV-30/70 Vertical Laminar Flow Bench (*Telstar*)
- Telstar BIO II A (*Telstar*)
- Scale (AHZ-600, *Gram*) Sensibility ±0.01 g.
- Precision balance (*Acculab, Sartorius*) Sensibility ±0,0001g.
- Advanced UV/Visible Spectrophotometer; 90 to 264 VAC (7315, *Jenway*)
- Cary 3500 Multicell UV-Vis Spectrophotometer (*Agilent*)
- Potter-Glass-Teflon Homogenizer (Rw20 DZM, *Janke & Kunkel*)
- Mini-PROTEAN Tetra Handcast Systems (*Bio-Rad*)
- Mini Trans-Blot® Electrophoretic Transfer Cell (1703930, *Bio-Rad*)
- Amersham™ Protran® Western blotting membranes, nitrocellulose (GE10600002, *GE Healthcare Life Science*)
- ImageQuant™ LAS 4000 biomolecular imager (*GE Healthcare Bio-Sciences*)
- Laboratory pH meter 50 (*VioLab*)
- Eppendorf ThermoMixer® C (*Eppendorf*)
- Duomax 1030 Platform shaker (*Heidolph*)
- Cruma Ductless Fume Hood 1100 GA (*Cruma*)
- MPW-352R refrigerated laboratory centrifuge (10352R, MPW, *Med. Instruments*)
- FV1000 confocal laser microscope® (*Olympus*)
- 15mL Centrifuge Tube (430791, *Corning*)
- 50 mL Centrifuge Tube (430829, *Corning*)
- Axiovert 200 wide field microscope (*ZEISS*)
- Cell culture CO2 incubator (CCL-170B-8, *ESCO*)
- Labculture Class II Biological Safety Cabinet (2012-65727, *ESCO*)

- McILWAIN Tissue Chopper (MTC/2, *The Mickle Laboratory Engineering CO. LTD.*)
- Olympus microscope SZ51 (*Olympus*)
- Perfusion pump and cannula
- Leica SM2000 R Sliding Microtome (*Leica*)

Sampling methods

Animal sacrifice, tissue extraction and homogenate preparation

For the Western blot analyses, a total of 20 mice were used, including 10 double transgenic mice from the APP/PS1 strain and 10 mice from the wild-type strain. Each animal was sacrificed by cervical dislocation at an age of between four and six months old. Following brain extraction, the amygdala, hippocampus, cerebellum, and cerebral cortex were separated from the rest of the brain using surgical materials so they could be studied further. All samples were immediately immersed in liquid nitrogen and preserved at -80°C.

After the tissue is collected, it must be homogenized to allow for the complete liberation of all the proteins within for further investigation. Both mechanical and chemical methods were applied to complete this process. A piece of tissue was obtained, weighed, and for each 100 mg of tissue, 1 mL of lysis buffer was added. Afterwards, the tissue with the lysis buffer was subjected to mechanical homogenization with the homogenizer for a few seconds. After the tissue was completely homogenized, it was once more preserved at -80°C for subsequent protein analysis.

Fixation and preparation of tissue for immunofluorescence

Twenty mice in total were required for protein analysis and immunofluorescence assays: twenty were wild-type mice and twenty were APP/PS1 mice. These animals were sacrificed under anesthesia at the age of between four and six months in order to collect the sample. Specifically, these animals received an intraperitoneal injection of 0.5 mL of the previously mentioned Eutanax solution. Transcardial perfusion was carried out after it was established that there was no foot or ocular reflex. First, about 100 mL of heparinized saline (0.1%, pH 7.4) were used until the animal was bled as much as possible. Next, approximately 100 mL of paraformaldehyde 4% in phosphate-buffered saline (0.1M, pH 7.4) were added in order to achieve tissue fixation. After that, the brain was removed and allowed to post-fix for 24 hours at 4°C in the same paraformaldehyde solution in order to achieve the maximum tissue fixation possible. After 24 hours, the brain was switched to a solution of 30% sucrose in PBS at 4ºC. The tissue was kept in this solution until it managed to completely subside, which happened about 48 hours later. This indicates that the tissue is cryoprotected and ready to be sliced.

Once the brain tissue is completely fixed, the cutting was carried out in a Leica cryotome. Coronal cuts of 40 µm thick were carried out in series to obtain in a total of five Eppendorf tubes. This way, practically all levels of the brain could be found in each Eppendorf tube. Once obtained, the cuts were stored in a 30% sucrose solution at -20°C for subsequent use in immunofluorescence assays.

Analytical methods

Protein determination: Lowry method

The Lowry method was used to determine the total protein concentration in our homogenized tissue samples (Lowry, et al., 1951).

Method principle

The Lambert-Beer law and oxidation-reduction reactions serve as the foundation for the Lowry method. The presence of copper ions in the Lowry reagent can affect the structure of proteins by generating binding complexes between the ions and nitrogen atoms of the peptide bonds. This process, called the Biuret reaction, causes the proteins to lose their three-dimensional structure and exposes the aromatic groups of tyrosine and tryptophan. These exposed aromatic groups cause the reduction of the Folin-Ciocalteau reactive, resulting in complexes with a strong blue color whose absorption at a specific wavelength (660 nm) varies according to the concentration of proteins in the sample. According to the Lambert-Beer Law, the absorption of a substance (A) is directly proportional to its concentration (c), the length of time light travels through a substance (l), and a constant known as the molar extinction coefficient (Ɛ) that is unique to each substance at a particular wavelength. In such a way that it can be expressed according to the following formula:

$$A = c \cdot l \cdot \varepsilon$$

Thus, the values of the formula can be found for specific conditions based on a standard at various concentrations. In the case of protein determination, bovine albumin serum (BSA) is used as a standard. In such way, we can easily interpolate the known values of Lambert

Beer's law to determine the protein concentration of samples that were subjected to the same procedure (Lowry's method) and under the same conditions.

Procedure

Setting up the standard curve is required in order to calculate the concentration of proteins using the Lowry method. For the standard curve, serial dilutions of BSA were created at the following concentrations: 12.5 mg/mL, 6.25 mg/mL, 3.12 mg/mL, 1.56 mg/mL, 0.78 mg/l, 0.39 mg/l, and 0.195 mg/l.

After the preparation of the serial dilutions, 5µl of each sample, both from each point of the standard curve and from the homogenized tissue samples, were diluted in 495µl double-distilled water. Furthermore, a sample containing just 500µl of double-distilled water must be prepared in order to serve as a blank for the spectrophotometer's absorbance measurements.

After that, 500µl of Lowry's reagent was added to each sample, including the blank, and they were all left to incubate in the dark for 20 minutes. After that, 250µL of the Folin reagent were added, and the samples were left to incubate in the dark for 30 minutes. The Lowry reaction results in protein complexes that have the ability to absorb light with a wavelength of 660 nm.

After the reaction was completed, the absorption of each sample was measured at 660 nm, starting with the serial dilutions of the standard curve and setting as 0 the blank sample, which is protein-free. The equation of the line that establishes the absorbance-concentration relationship was determined using the Lambert-Beer law, once the absorbance measurements were acquired along with the known concentrations of the standard line and their corresponding absorbances. This line equation was used to interpolate the absorption values of homogenized tissue samples and determine the corresponding protein concentration.

Western blotting

The Western Blotting technique was used to determine the levels of different proteins of interest in the obtained homogenized tissue.

Method principle

The Western Blotting technique is used to detect protein levels present in biological samples and it depends on the capacity of specific antibodies to recognize proteins of interest. This technique consists of three phases: the SDS-PAGE polyacrylamide gel electrophoresis, the electrotransfer and the immunoblot.

The objective of polyacrylamide gel electrophoresis is to separate the proteins in the sample according to their size. SDS and mercaptoethanol cause protein denaturation, meaning they lose their native structure and acquire a net negative charge, which makes it possible to separate the proteins solely based on their molecular weight on a polyacrylamide gel. Due to the vertical electric current passage through the gel, the proteins are separated along the gel based on their respective sizes. These gels are made up of two parts: the "stacking" or concentrator gel and the "resolving" gel. The "stacking" gel is small in size and has a small and constant percentage of polyacrylamide. This allows all the proteins in the sample to start separating by size from the same position. The "resolving" gel is larger in size and has a larger and more variable percentage of polyacrylamide. In this gel is where the size separation of the proteins in each sample occurs. The percentage of polyacrylamide in these gels varies depending on the size of the protein of interest, resulting in gels with more or less space in their framework. Thus, it is advised to use gels with small percentages for large molecular weight proteins and gels with a high percentage of polyacrylamide for small proteins.

The goal of electrotransfer is to transfer the proteins that were previously separated in the polyacrylamide gel to a PVDF or nitrocellulose membrane. This transfer happens as a result of horizontal electric current flow. Transferring the proteins to these membranes exposes them so that they can be further detected by particular antibodies.

Finally, by means of the immunoblot, the detection of specific proteins, present in the membranes and separated based on their molecular weight is achieved. In this phase, the membrane must be blocked using a blocking solution in order to prevent the antibody from binding non-specifically. The desired antibody will only bind to the desired protein when the membrane is incubated in this way. This connection can only be found by using a secondary antibody that can both identify the constant region of the primary antibody and be conjugated with luminol, a peroxidase (Horseradish Peroxidase, HRP) that produces a chemoluminescent reaction, when it reacts with a substrate. Thus, there is a directly proportional relationship between the levels of the target protein and the intensity of the signal produced by the peroxidase reaction in contact with luminol (Kurien & Scofield, 2015; Mahmood & Yang, 2012).

Procedure

As was previously mentioned, electrophoresis on SDS-PAGE polyacrylamide gels is the starting point of the Western Blot. Thus the preparation of such gels is needed. In the present study, resolving gels of 15%, 12.5% and 10% polyacrylamide were used. The following table presents the required volumes of each reagent for each gel type:

	Resolving Gel			**Stacking Gel**
	15%	***12.5%***	***10%***	
Distilled water (ml)	3.65	4.27	4.9	3.075
Tris HCl 1.5M pH 8.8 (ml)	2.5	2.5	2.5	-
Tris HCl 0.5M pH 6.8 (ml)	-	-	-	1.25
Acrylamide (ml)	3.75	3.13	2.5	0.625
SDS 10% (µl)	100	100	100	50
APS 10% (µl)	30	30	30	15
TEMED (µl)	15	15	15	7.5

In the meantime, the samples that would be loaded into the gels were prepared. 20 µg of protein were prepared from each homogenized tissue sample with the corresponding volume of 2X Loading Buffer. Afterwards, the samples were incubated at 95°C for 5 minutes. Each sample was then loaded into each well of the polyacrylamide gel, which was previously placed in the electrophoresis apparatus and covered with the electrophoresis buffer. For roughly 90 minutes, the gel was subjected to a continuous voltage of 100 volts until the samples nearly reached the gel's end. The gel was then carefully collected and the electrotransfer was prepared using the Mini Trans-Blot®Electrophoretic Transfer Cell material. This kit contains the "sandwich," which was assembled as follows, starting with the black side and then placing successively sponge, filter paper, nitrocellulose membrane, polyacrylamide gel, filter paper, sponge. Following preparation, the "sandwich" was put in the transfer bucket with the Transfer Buffer, and the power supply was set to operate at a constant 240 mA for 90 minutes (120 mA for each gel). The tank was kept cold at all times and the voltage was constantly monitored to ensure it did not exceed 100 volts.

After the transfer is complete, it's necessary to perform a series of procedures in order to detect the protein of interest using a particular antibody. The membrane was first incubated with the blocking solution for an hour at room temperature in agitation. Next the membrane was incubated with the specific primary antibody, diluted in the blocking solution, and at the dilution indicated on the datasheet by the commercial company. The incubation lasted overnight at 4°C and in agitation. The primary antibody was removed the following day, and three TBS-t washes were performed at room temperature for five, five, and ten minutes while stirring. Following the washings, the membrane was incubated with the matching secondary antibody, which depended on the host, which is the constant component of the primary antibody. This incubation was performed for one hour at room temperature with gentle rocking. Three additional TBS-t washes were then carried out in the same way as previous ones and the membrane was exposed for chemiluminescence detection. The membrane was developed using the ImageQuantTM LAS 4000, GE Healthcare Bio- Sciences and 1 mL of Luminol was added to its surface ensuring the most uniform distribution possible.

In order to normalize the levels of the protein of interest, the levels of β-tubulin were determined as well in each membrane which serve as a loading control. To accomplish this, the membrane containing the desired protein after been developed, was then incubated with the Stripping solution for 15 minutes at room temperature with gentle rocking. The membrane will be properly cleaned after this incubation, enabling it to be blocked again and then incubated with a different antibody. Following incubation, the membrane was rinsed three times using TBS-t, and the previously described procedure was carried out again.

At last, the images acquired from the membranes were analyzed using the ImageGauge V4.0 software, which enables the densitometry analysis of the corresponding bands of the proteins in each membrane. Following the acquisition of each sample's

densitometry value, the average and corresponding standard deviation for each group were calculated.

Immunofluorescence

Method principle

Similar to the Western Blot, the immunofluorescence technique relies on the use of particular antibodies to detect proteins of interest. Instead of using a homogenized sample, the fixed tissue is directly the subject of the detection in this situation. This way, it enables the direct ascertainment of the distribution of the target protein in the tissue, allowing to determine whether there is a greater or lesser accumulation of this protein in a particular brain area.

Akin to the Western Blot, an incubation with a blocking solution must be carried out to prevent non-specific binding. However, the blocking is applied directly to the fixed tissue. Furthermore, rather than using bovine albumin as the blocking solution, in this case, it is used goat serum diluted in PBS-t in 1:10 ratio.

Another key dissimilarity between the two techniques is the detection method. As the technique's name indicates, fluorescence is used in this instance for detection. More specifically, a secondary antibody is used, which binds to the constant portion of the primary antibody but is conjugated with a fluorochrome rather than HRP. This molecule has the ability to absorb energy at one wavelength and emit it at another. This feature permits more than protein of interest to be analyzed at a time. This becomes feasible provided that distinct secondary antibodies that recognize the primary antibodies, exhibit fluorochromes with the ability to be excited and emit light at different wavelengths. That establishes a direct correlation between the amount of the target protein and the fluorescence intensity. Furthermore, the ability to examine multiple

proteins at the same time enables to verify whether or not the proteins are co-localized.

Procedure

The Slide-Mounted Sections technique was applied throughout this thesis. This technique involves mounting the sections on the slide as the first step, and then treating the tissue with various compounds while using an indelible and waterproof marker to prevent the solutions from spreading throughout the slide. This technique makes it possible to choose the tissue's interesting regions from the beginning. For each animal, at least three sections were mounted upon slides. The detailed steps of the technique are outlined below.

First, the sodium citrate buffer was heated up to 95°C. This buffer is used for efficient antigen retrieval. Tissues fixed with formaldehyde create protein cross-links that often obstruct the antibody penetration. It has been demonstrated that applying sodium citrate buffer to formaldehyde-fixed sections enhances antibody penetration and can raise the intensity and degree of immunoreactivity and immunostaining. The sections were heated in sodium citrate buffer at 95°C for 10 minutes. Subsequently, the tissue underwent three 5-, 5-, and 10-minute PBS-t washes in order to remove any residual sucrose that might have interfered with the procedure. After that, the sections were incubated for an hour at room temperature with the blocking solution, composed of goat serum diluted 1:10 in PBS-t. The blocked tissue was then left to overnight incubation with the primary antibodies of interest at 4°C. The next day, following the primary antibody incubation, three PBS-t washes were carried out once more. After that, the tissue was incubated for two hours with the corresponding secondary antibodies at room temperature. Due to the fact that these antibodies are conjugated with fluorophores and therefore light-sensitive, this procedure, along with the ones that follow, must be carried out in the greatest darkness possible. Subsequently, three

more PBS-t washes for 5, 5, and 10 minutes were performed in order to eliminate of any excesses of the secondary antibodies. Following washing, the tissue was incubated for 30 minutes with the 1:1000 dilution of Hoechst in PBS at room temperature. Because of its fluorescence and its capacity to bind to DNA, the Hoechst compound is used to observe the nuclei of individual cells and thus enables to guide through the tissue. Finally, three more PBS washes were applied, and the slides were covered with coverslips with the aid of the mounting medium. The slides were then stored at 4°C in the dark for later examination under the confocal microscope (Magaki et al., 2019; Pandurangan et al., 2024; Jiao et al., 1999).

Neurosphere assay

Method principle

Since its first description in 1992, the neurosphere assay (NSA) has proven to be an unique and effective tool in the study of neural stem cells (NSCs) (Reynolds & Weiss, 1992).
It can be challenging to separate NSCs from the two primary neurogenic niches in the postnatal and adult brain, the subventricular zone (SVZ) and the subgranular zone of the hippocampal dentate gyrus (DG), because it is still unclear what is needed to keep these cells in a physiological state.

In the NSA, cells are cultured in a serum-free medium that is chemically defined and contains growth factors, such as basic fibroblast growth factor (bFGF) and epidermal growth factor (EGF). These mitogens are used to select neural precursor cells (stem cells and progenitors), since they respond to EGF and FGF and enter in an active proliferation phase while other cells, differentiated cells, perish.

Growing into neurospheres, neural precursor cells can be passaged to increase the number of these cells even further. Most

importantly, these neural stem progenitor cells (NSPCs) exhibit multipotency, enabling them to differentiate into the three main cell types of the CNS: oligodendrocytes, astrocytes, and neurons.

Neuronal and glial differentiation, as well as NSC proliferation and self-renewal, can all be studied in the context of both health and disease using the renewable source of undifferentiated CNS precursors that the NSA offers. Furthermore, by removing extrinsic cues related to the cells' normal environment, in vitro studies can be used to assess the level of intrinsic specification present in neural precursors during development as well as to investigate the full potential of the cells. Additionally, this assay can be used to test various drugs and compounds and to adjust the properties of NSCs through genetic manipulation.

Since the neurosphere model maintains the cells in a serum-free medium, the only environmental cues that the cells receive are from their surroundings, making it useful for assessing potential regulators. What is more, in the NSA, neurospheres' ability to be easily expanded in culture, the high cell density per area and their heterogeneous composition bear some resemblance to in vivo niches.

Procedure

This protocol involved the isolation of NSPCs from the SVZ, one of the main neurogenic ninches, the expansion of these cells as neurospheres and finally their differentiation into neurons, astrocytes and oligodendrocytes (Soares et al., 2020).

Firstly, on the dissection day, the adequate amount of serum-free medium (SFM) was prepared. This growth medium consists of Dulbecco's modified eagle medium [(DMEM)/F12 with L-glutamine] supplemented with 100 U/mL penicillin and 100 µg/mL streptomycin (pen/strep), 1% B27, with also 10 ng/mL EGF and 5 ng/mL bFGF. Additionally, the Hanks' balanced saline solution (HBSS)

dissection medium, free of calcium and magnesium, was prepared supplemented with 100 U/mL pen/strep for the microdissection of SVZ.

Mice pups (P1–3) were euthanized in accordance with the procedures and policies of the animal care facility. Decapitation was performed using sharp scissors, with a single incision at the base of the brainstem. A midline skin incision running across the entire length of the head, exposed the skull's surface. A longitudinal incision at the base of the skull was made, and then a cut along the sagittal suture. The skull was peeled to the sides and the brain was exposed and isolated. The brain was placed into a Petri dish containing cold supplemented HBSS solution and placed under a dissecting microscope at low magnification. The brain was positioned on its dorsal surface and the meninges were removed from the ventral side of the brain using fine forceps. The brain was rotated onto the ventral aspect and the rest of the meninges was peeled off. The cerebellum and the olfactory bulbs were discarded and the brain was placed onto a tissue chopper. The brain was chopped into 450 µm coronal sections and the sectioned brain was collected into a new Petri dish filled with cold supplemented HBSS.

The SVZ was dissected, separating coronal slices in an anterior-to-posterior fashion, under a dissecting microscope. The dissected tissue was collected into a sample tube with supplemented HBSS solution.

To dissociate the SVZ, Trypsin-EDTA 0.05% was added to have a final concentration of 5−10% of Trypsin-EDTA 0.05% in HBSS. It was then incubated for 15 minutes at 37 °C, until the tissue was clumped together. The tissue was washed from the trypsin by removing the media and adding 1 mL of new HBSS supplemented solution for 4 consecutive times. The HBSS was removed and the digested tissue was resuspended in 1 mL of SFM supplemented with 10 ng/mL EGF and 5 ng/mL bFGF, and mechanically dissociated until getting a homogenous cell solution.

For the expansion of postnatal neural stem cells as neurospheres, the SVZ cell suspension was diluted at a density of 2 x 10^4 cells/mL in SFM supplemented with 10 ng/mL EGF and 5 ng/mL bFGF. The SVZ cells were seeded in uncoated 60 mm Petri dishes with a final volume of 5 mL/Petri dish. The SVZ cells for 6 days to form primary neurospheres, at 37 °C with 5% CO_2.

Differentiation of neurosphere cultures occurred when neurospheres had a diameter of 150−200 µm. Approximately 25 µL of neurosphere suspension medium was collected and plated on 100 µg/mL PDL in 0.167 M borate buffer coated glass coverslips, in 24-well plates. The plates were incubated at 37 °C for 15 min for the efficient adhesion of the neurospheres to the substrate. Afterwards, 500 µL of SFM devoid of growth factors were added and the plates were again incubated at 37 °C. After 24 h, the medium was replaced with fresh SFM devoid of growth factors. The neurospheres were differentiated for a total of 14 days. On DIV7 half-medium replacement was performed in order to supply the cultures with new nutrients and eliminate metabolic waste products. Pharmacological treatments of 1µM Aβ combined with 10µM DL-TBOA (non-transportable competitive blocker of glutamate absorption) and 10µM QNZ46 (GluN2C/GluN2D NMDA antagonist) were applied on DIV13 for 24 hours at 37°C and 5% CO_2. These treatments were chosen in order to assess whether they could alleviate the degenerative effect of Aβ.

Cell fixation was performed on DIV14 with 4% PFA in x1 PBS. The SFM was removed and 500 µL of 4% PFA were added to each well for 20 min at room temperature, and then three washes with 1x PBS, for 5 min each time were performed. The coverslips were stored until use in 500 µL of 1x PBS at 4 °C. Subsequently, immunocytochemistry assay was performed following the same principles and procedure as the previously described Immunofluorescence assay.

Confocal microscopy

Method principle

A confocal microscope's main functions include producing a point source of light and rejecting out-of-focus light, allowing for high-resolution imaging deep into tissues and optical sectioning for 3D reconstructions of imaged samples. Confocal microscopy operates on the basis of the same diffraction-limited spot being focused by both the illumination and detection optics. This spot is moved over the sample in order to create the entire image on the detector. Confocal imaging provides optical sectioning and reduces the haze seen in standard light microscopy with thick and highly-scattering samples by illuminating the entire field of view while little light passes through the focal plane (Eliot, 2020).

Procedure

With the FV1000 confocal fluorescence microscope, the tissue sections were observed and photos of the regions of interest were captured. It is a confocal microscope mounted on a motorized inverted IX81 which includes four lenses (10x, 20x, 40x-oil, 60x-oil, 60x-water) from which the 10x, 20x and 40x-oil lenses were used for visualizing image capturing. Four photomultipliers compose the detection system of this equipment: one is used for scanning light-field images, and the other three are used for fluorescence. Additionally, it features a spectral detection system that enables to modify the wavelength range that the detector receives and create a sequence of images (also known as a "λ scan") that are detected at various wavelengths. The equipment's excitation lines are 405nm, 488nm, 515nm, 559nm, 595nm y 635nm from which the 405nm, 488nm and 635nm were used for this thesis. For each section, one

or two images were captured that were further analyzed following photo acquisition.

Image analysis

The *ImageJ* software was used to analyze the acquired images. With this software, it was possible to quantify the amount of the protein of interest as well as the intensity of the fluorescence that was emitted. In order to achieve this, a minimum of three images were analyzed for every animal, where the area of interest was determined and the fluorescence was calculated with regard to the background noise. After that, the mean for every animal was determined as well as the mean and standard deviation for each group were derived. Additionally, the colocalization percentages could be determined with the ImageJ Fiji *Colocalization Threshold* plug-in. In this case, each mouse was represented by at least three images, from which the average of each mouse, the mean of each group, and the corresponding standard deviation were determined.

Statistical analysis

The average of each group and the corresponding standard deviation were calculated in the results obtained from all the above mentioned methods. The statistical value was ascertained by comparing two values from parametric samples using the T-Student test whereas for more than two values from parametric samples, the ANOVA test was applied (Ali & Bhaskar, 2016). $p \leq 0.05$ was the threshold set for validating the hypothesis. This statistical value served as the basis for determining the significance or lack thereof of the results obtained. Additionally, Levene's test (Levene, 1961) was applied to determine whether the variances of k samples are equal. Homogeneity of variance is the state in which variances are equal among samples. Certain statistical tests, like the analysis of

variance, make the assumption that variances in samples or groups are all the same. That assumption can be confirmed using the Levene test.

RESULTS

Results

Study of the morphology and structure of the dorsal fornix

Initially, it was aimed to ascertain whether the dorsal fornix of WT and APP/PS1 transgenic mice differed structurally. This was accomplished by labeling coronal sections of mice from both strains with Hoechst fluorescent dye. As can be seen in the following representative images, these sections were placed under the confocal microscope and various images were obtained from each mouse, focusing on the dorsal fornix (Figure 19). As shown in the images (Figures 20 & 21), the Hoechst fluorescent dye labeling enables the acquisition of cellular images because the dye penetrates the cells and effectively stains both live and fixed cells. With the Allen Brain Atlas as reference, it was made possible to identify and determine the different brain areas present on each section, such as the corpus callosum (CC), the third ventricle (V3) and of course the dorsal fornix (df).

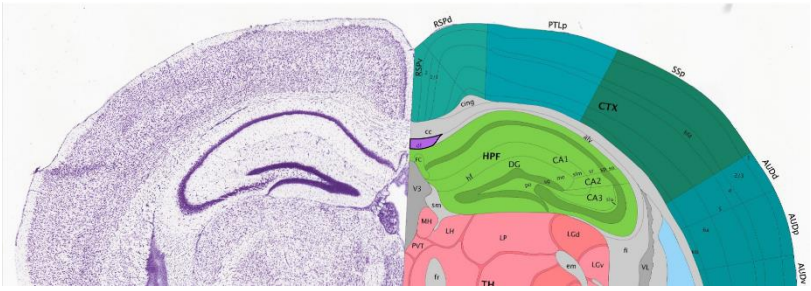

Figure 19. Allen Brain Atlas coronal section of adult mouse brain. Representative image of adult mouse brain in coronal planes of section used as anatomical reference in order to outline the dorsal fornix (df), the third ventricle (V3) and the corpus callosum (CC) on the confocal microscope images.

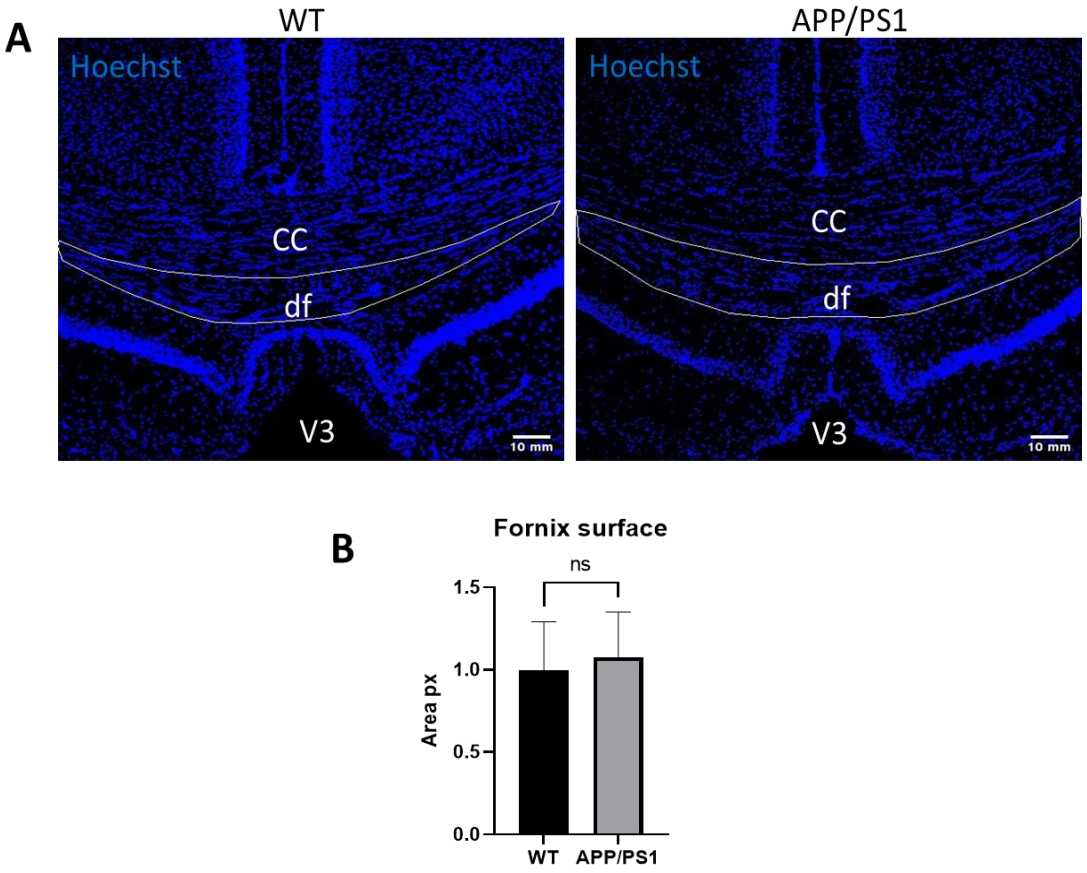

Figure 20. Area determination of the dorsal fornix in 4-month old mice. A. Representative immunofluorescence images of the dorsal fornix marking the nuclei with blue (Hoechst) in WT and APP/PS1 4 month-old mice. Scale=10mm. **B.** Area quantification of fornix in WT and APP/PS1 4 month-old mice. N=5. p>0,05 vs WT. df=dorsal fornix; CC= corpus callosum; V3= third ventricle.

The ImageJ software was used for demarcating the dorsal fornix area from these images. Consequently, the area definition led to the observation that there is no difference in the dorsal fornix area between WT and APP/PS1 mice in both age groups of 4 and 6 months old (Figures 20 & 21).

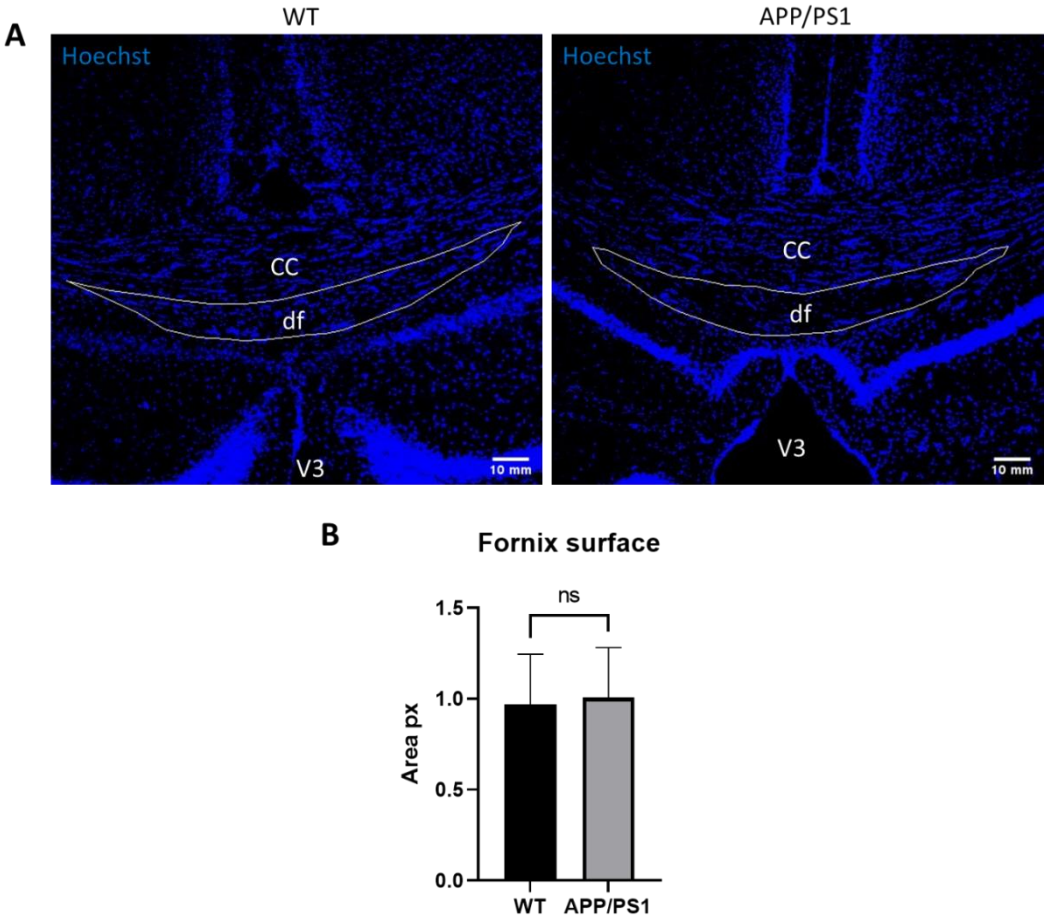

Figure 21. Area determination of the dorsal fornix in 6-month old mice. A. Representative immunofluorescence images of the dorsal fornix marking the nuclei with blue (Hoechst) in WT and APP/PS1 6-month old mice. Scale =10mm. **B.** Area quantification of fornix in WT and APP/PS1 6-month old mice. N=5. p>0,05 vs WT. df=dorsal fornix; CC=corpus callosum; V3= third ventricle.

Next, the total amount of neurons in the dorsal fornices of the WT and APP/PS1 transgenic mice was compared using the same mouse slices to see if there were any differences. To do so, the levels of the neuronal axonal protein Nfl were measured in the dorsal fornix of each group by immunofluorescence assay. The following result

shows that Nfl levels in the dorsal fornix of WT and APP/PS1 mice show no significant differences in both age groups of 4 and 6 months old (Figures 22 & 23).

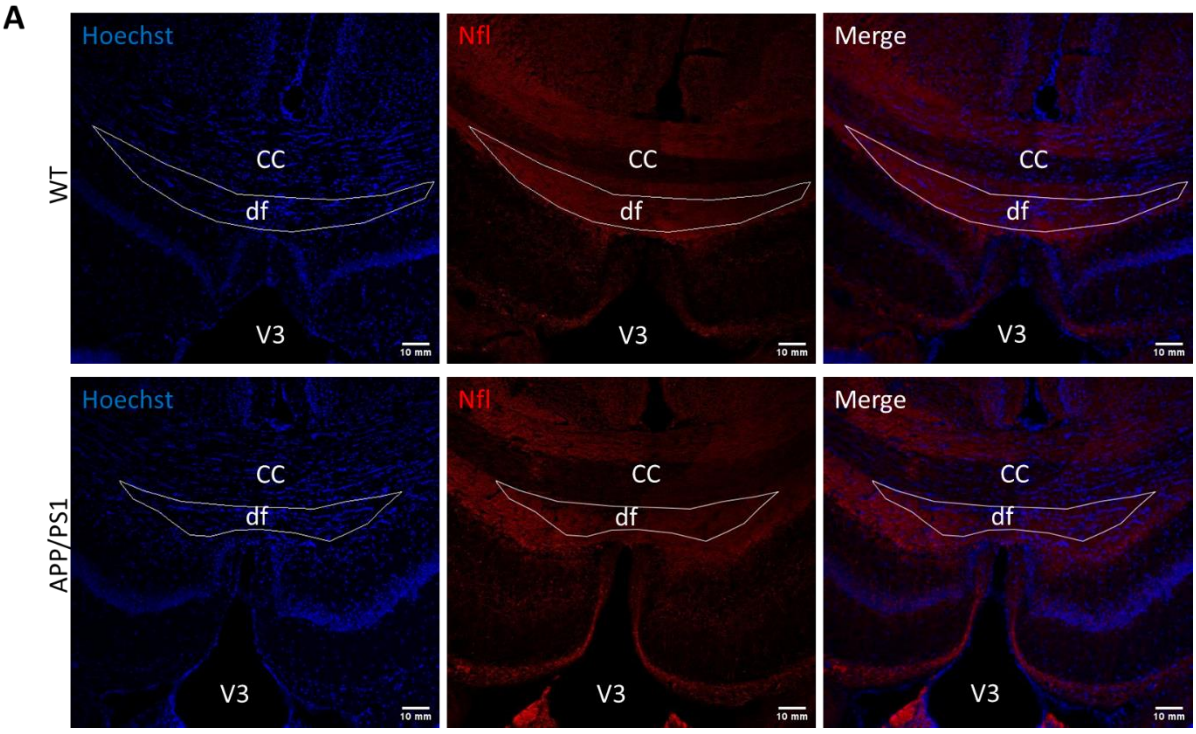

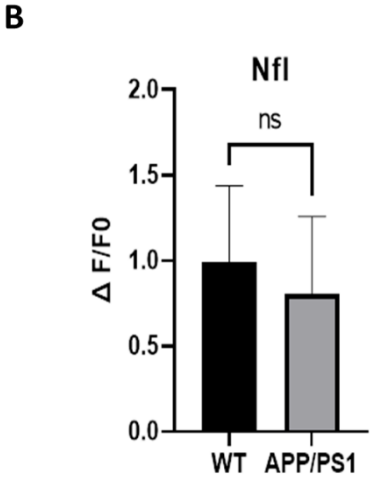

Figure 22. Immunofluorescence determination of Nfl levels in the dorsal fornix of 4 month-old mice. **A.** Representative immunofluorescence images of the dorsal fornix labeling the nuclei with blue (Hoechst) and Nfl with red in WT and APP/PS1 4 month-old mice. Scale =10mm. **B.** Quantification of the red fluorescence with respect to the corresponding to the levels of Nfl in WT and APP/PS1 4 month-old mice. N=5. p>0,05 vs WT. df=dorsal fornix; CC=corpus callosum; V3= third ventricle.

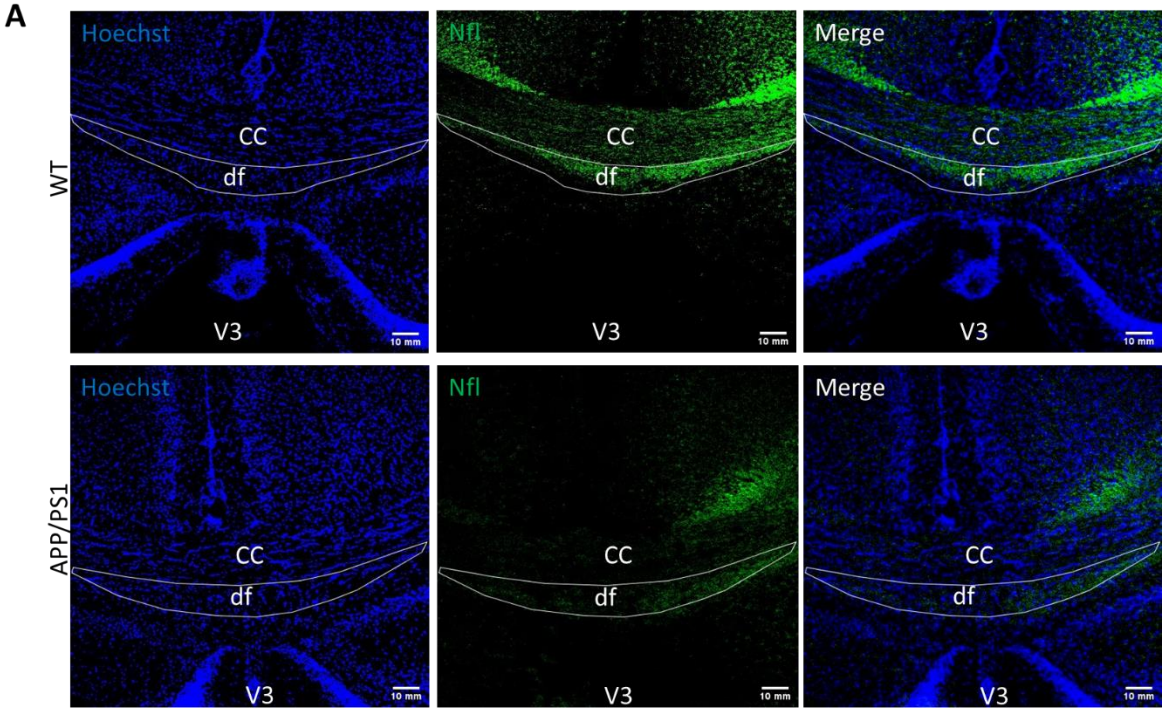

Figure 23. Immunofluorescence determination of Nfl levels in the dorsal fornix of 6 month-old mice. A. Representative immunofluorescence images of the dorsal fornix labeling the nuclei with blue (Hoechst) and Nfl with green in WT and APP/PS1 6 month-old mice. Scale =10mm. **B.** Quantification of the green fluorescence with respect to the background corresponding to the levels of Nfl in WT and APP/PS1 6 month-old mice. N=5. p>0,05 vs WT. df=dorsal fornix; CC=corpus callosum; V3= third ventricle.

Study of the main myelin components in the dorsal fornix of APP/PS1 and WT mice

The next objective was to determine whether the axonal myelin deposition was affected in the dorsal fornix of young, 4 month-old APP/PS1 mice. This was accomplished by studying two of the principal components of the myelin sheath, the myelin basic protein (MBP) and the myelin oligodendrocyte glycoprotein (MOG). Therefore, immunofluorescence assays were carried out to determine the levels of these myelin markers.

MBP levels in 4 month-old mice

The first myelin component to be studied was MBP. Immunofluorescence assay was carried out to detect the levels of MBP in the dorsal fornix of 4 month-old control and transgenic mice. For this purpose, coronal sections were used and the tissue was double-stained with anti-MBP antibody and anti-Nfl antibody. The Hoechst fluorescent dye was used to mark the cell nuclei and determine the different cerebral areas. As can be seen both in the representative images obtained and in the graph corresponding to the quantification of MBP levels, there is a noticeable decrease of MBP in the dorsal fornix of 4 month-old APP/PS1 mice compared to WT mice (Figure 24).

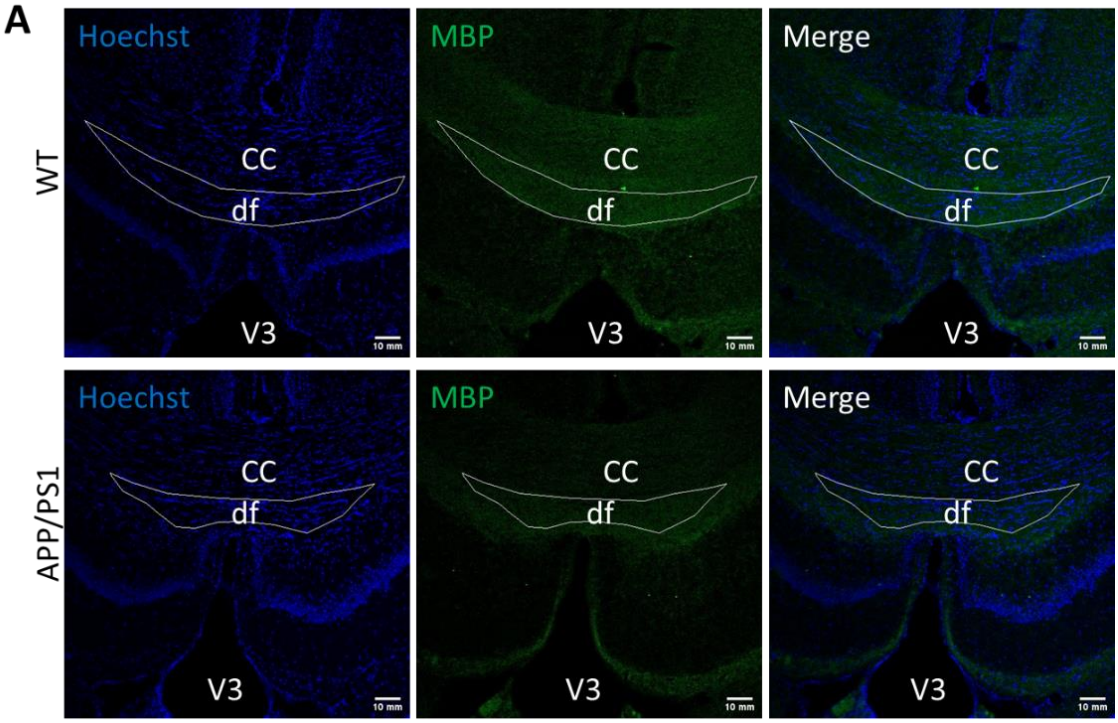

Figure 24. Immunofluorescence determination of MBP levels in the dorsal fornix of 4 month-old mice. A. Representative immunofluorescence images of the dorsal fornix labeling the nuclei with blue (Hoechst) and MBP with green in WT and APP/PS1 4 month-old mice. Scale =10mm. **B.** Quantification of the green fluorescence with respect to the background corresponding to the levels of MBP in WT and APP/PS1 4-month old mice. N=5. ***p<0,001 vs WT. df=dorsal fornix; CC=corpus callosum; V3= third ventricle.

Regarding the degree of colocalization between MBP and Nfl markers, the percentage of MBP and Nfl colocalization in the dorsal fornix of APP/PS1 mice was significantly decreased (Figure 25).

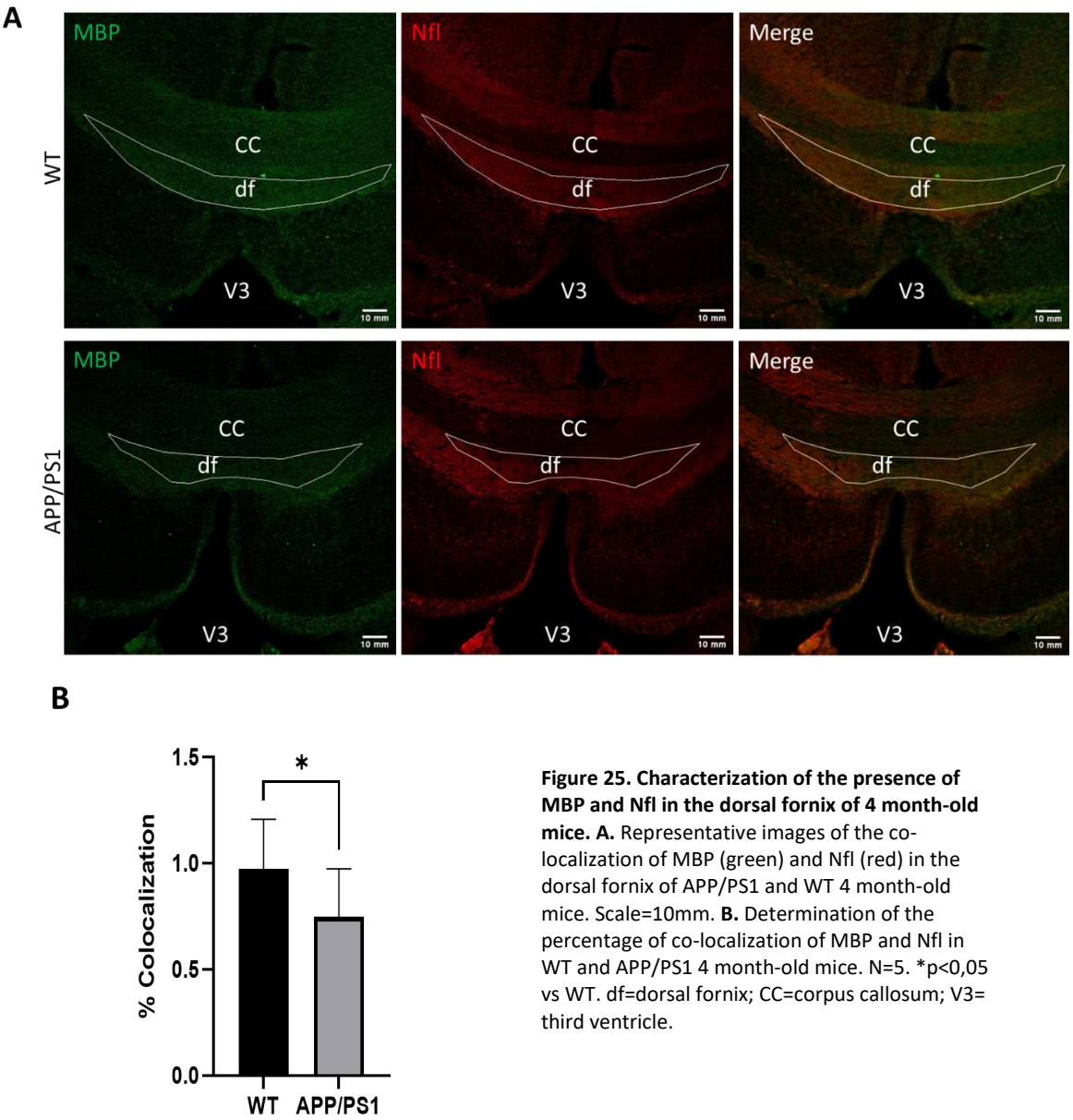

Figure 25. Characterization of the presence of MBP and Nfl in the dorsal fornix of 4 month-old mice. A. Representative images of the co-localization of MBP (green) and Nfl (red) in the dorsal fornix of APP/PS1 and WT 4 month-old mice. Scale=10mm. **B.** Determination of the percentage of co-localization of MBP and Nfl in WT and APP/PS1 4 month-old mice. N=5. *p<0,05 vs WT. df=dorsal fornix; CC=corpus callosum; V3= third ventricle.

MOG levels in 4 month-old mice

In the same manner as previously described, the levels of MOG in the dorsal fornix of 4 month-old control and transgenic mice were determined. Coronal sections were double-stained with anti-MOG antibody and anti-Nfl antibody, and the Hoechst dye was applied to identify and delineate the brain areas. The obtained result was a reduction of MOG levels in the dorsal fornix of 4 month-old WT and APP/PS1 mice (Figure 26).

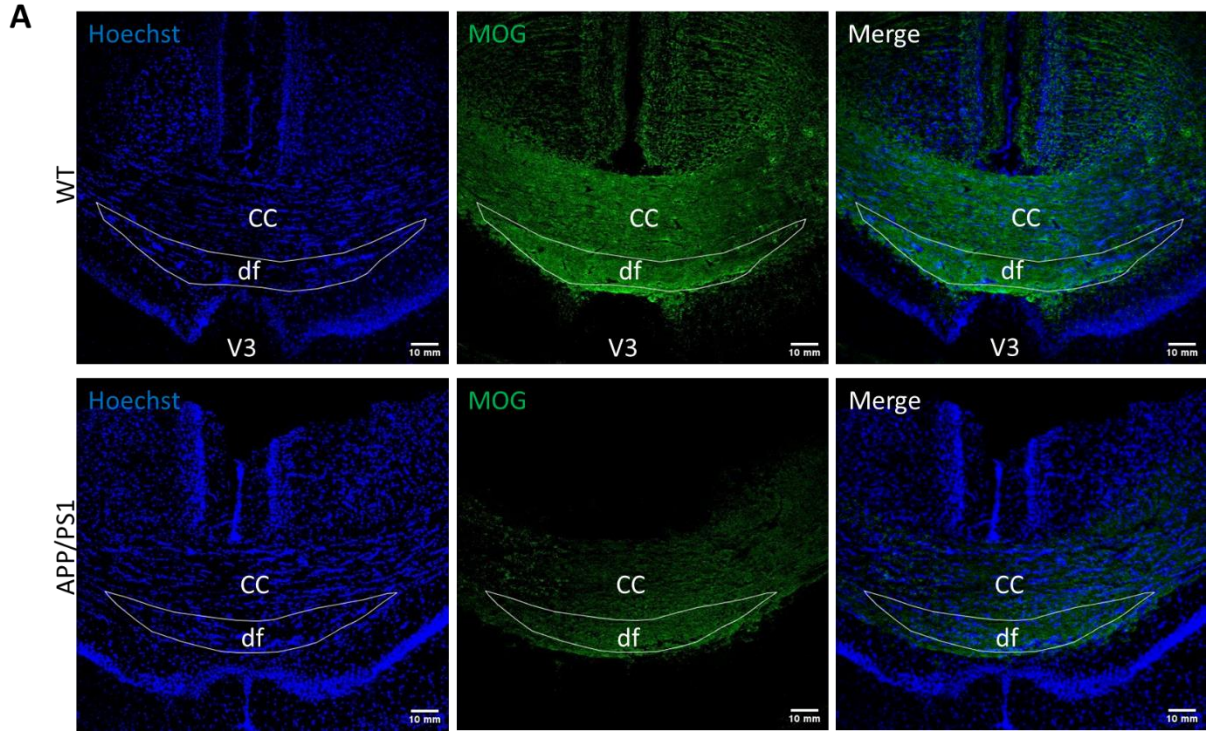

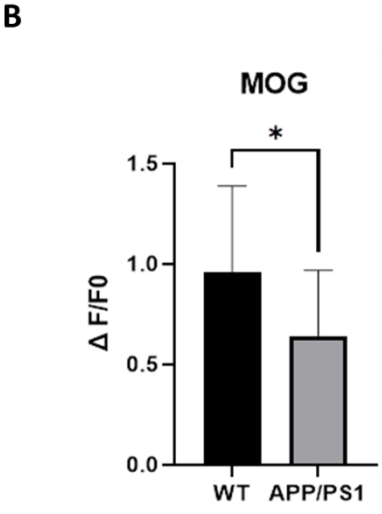

Figure 26. Immunofluorescence determination of MOG levels in the dorsal fornix of 4 month-old mice. A. Representative immunofluorescence images of the dorsal fornix labeling the nuclei with blue (Hoechst) and MOG with green in WT and APP/PS1 4 month-old mice. Scale =10mm. **B.** Quantification of the green fluorescence with respect to the background corresponding to the levels of MOG in WT and APP/PS1 4 month-old mice. N=5. *p<0,05 vs WT. df=dorsal fornix; CC=corpus callosum; V3= third ventricle.

This finding is consistent with the decline in the percentage of MOG colocalization with Nfl in the transgenic mice's dorsal fornix compared to WT, as well as the previously observed result regarding the MBP protein (Figure 27).

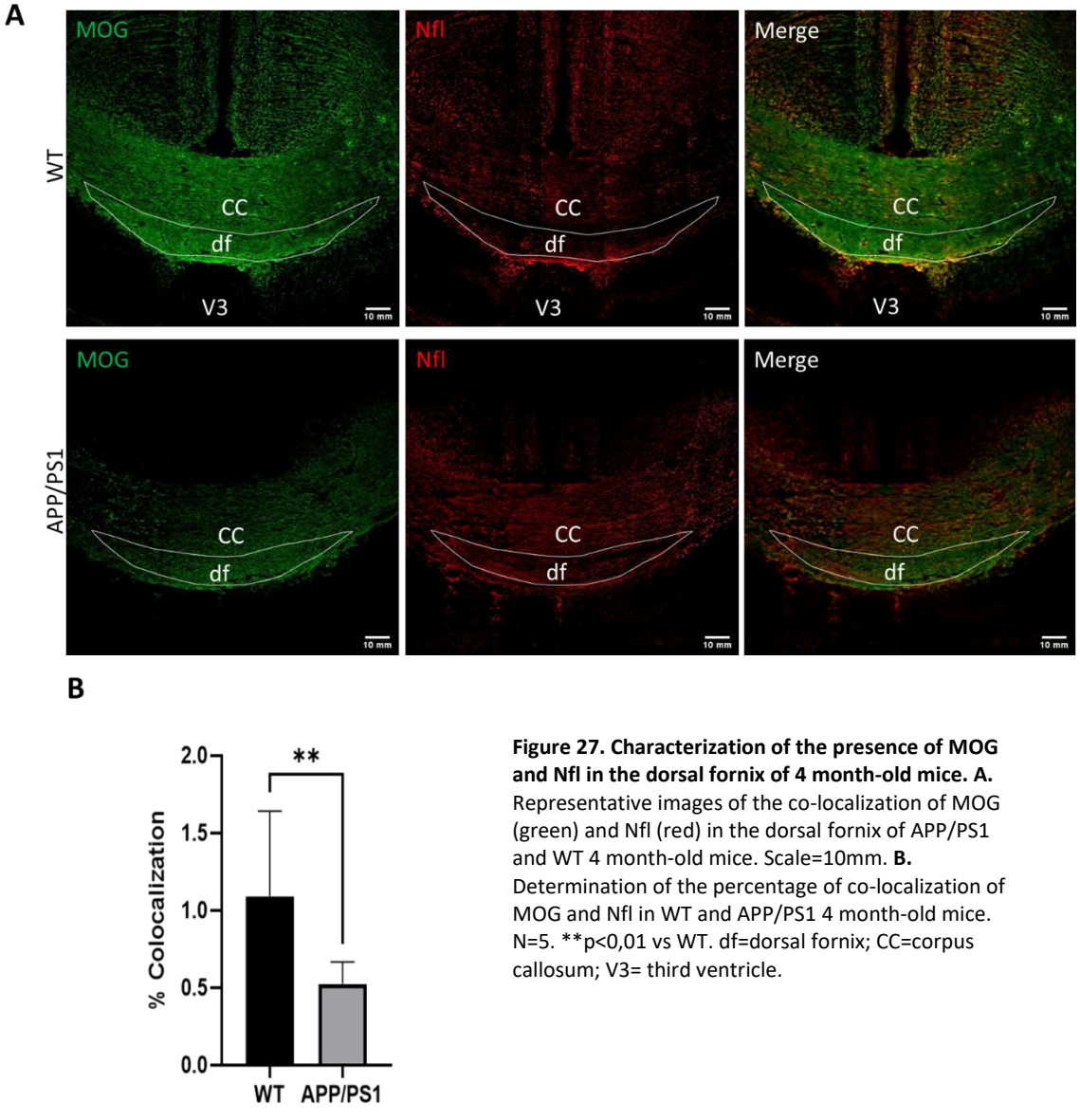

Figure 27. Characterization of the presence of MOG and Nfl in the dorsal fornix of 4 month-old mice. A. Representative images of the co-localization of MOG (green) and Nfl (red) in the dorsal fornix of APP/PS1 and WT 4 month-old mice. Scale=10mm. **B.** Determination of the percentage of co-localization of MOG and Nfl in WT and APP/PS1 4 month-old mice. N=5. **p<0,01 vs WT. df=dorsal fornix; CC=corpus callosum; V3= third ventricle.

MBP levels in 6 month-old mice

Afterwards, in order to investigate whether the myelin degeneration intensifies with age, the same myelin markers were examined on 6 month-old WT and APP/PS1 mice.

The levels of MBP in the dorsal fornix of 6 month-old control and transgenic mice were measured by immunofluorescence assay. Coronal sections from both strains were double-stained with anti-MBP antibody and anti-Nfl antibody. The following representative images and the graph corresponding to the quantification of MBP levels both demonstrate an apparent decline in MBP in the dorsal fornix of 6 month-old APP/PS1 mice when compared to WT (Figure 28).

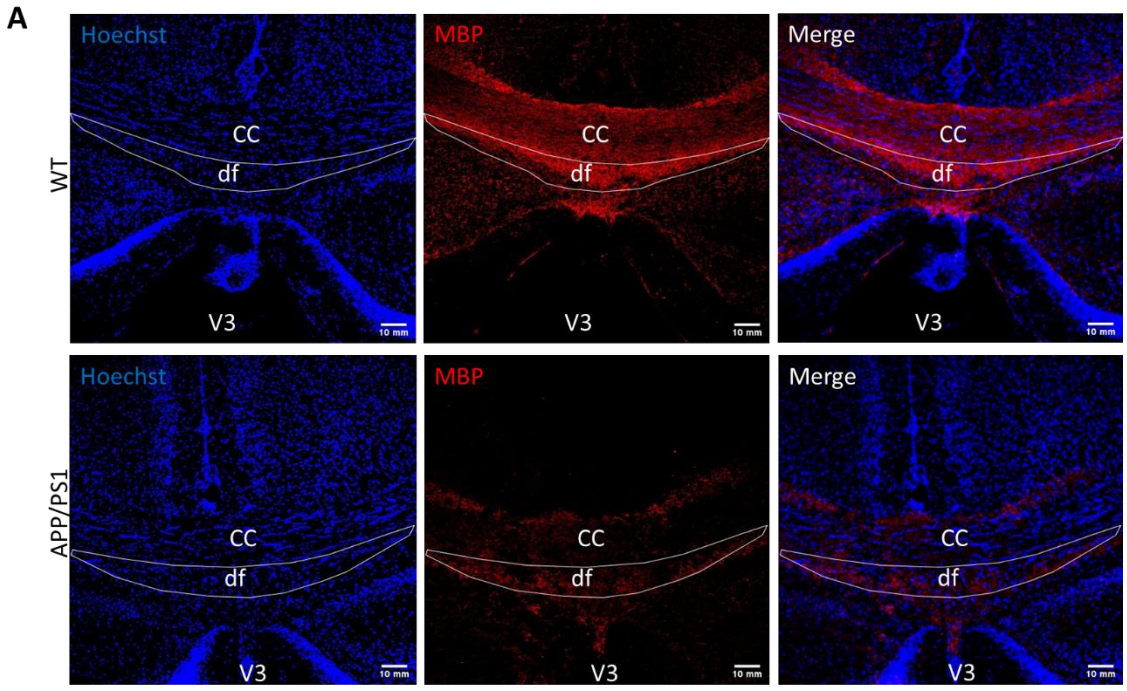

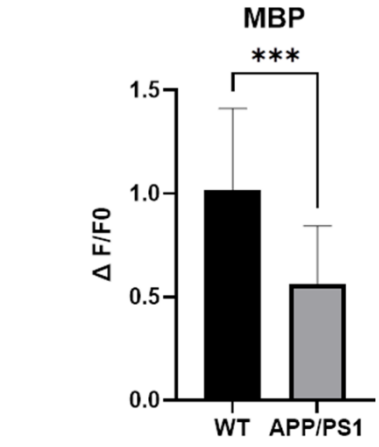

Figure 28. Immunofluorescence determination of MBP levels in the dorsal fornix of 6 month-old mice. A. Representative immunofluorescence images of the dorsal fornix labeling the nuclei with blue (Hoechst) and MBP with red in WT and APP/PS1 6 month-old mice. Scale =10mm. **B.** Quantification of the red fluorescence with respect to the background corresponding to the levels of MBP in WT and APP/PS1 6 month-old mice. N=5. ***p<0,001 vs WT. df=dorsal fornix; CC=corpus callosum; V3= third ventricle.

This result is in accordance with the decline in the percentage of MBP colocalization with Nfl in the dorsal fornix of the transgenic mice compared to WT, as can be observed in the images and the corresponding graph below (Figure 29).

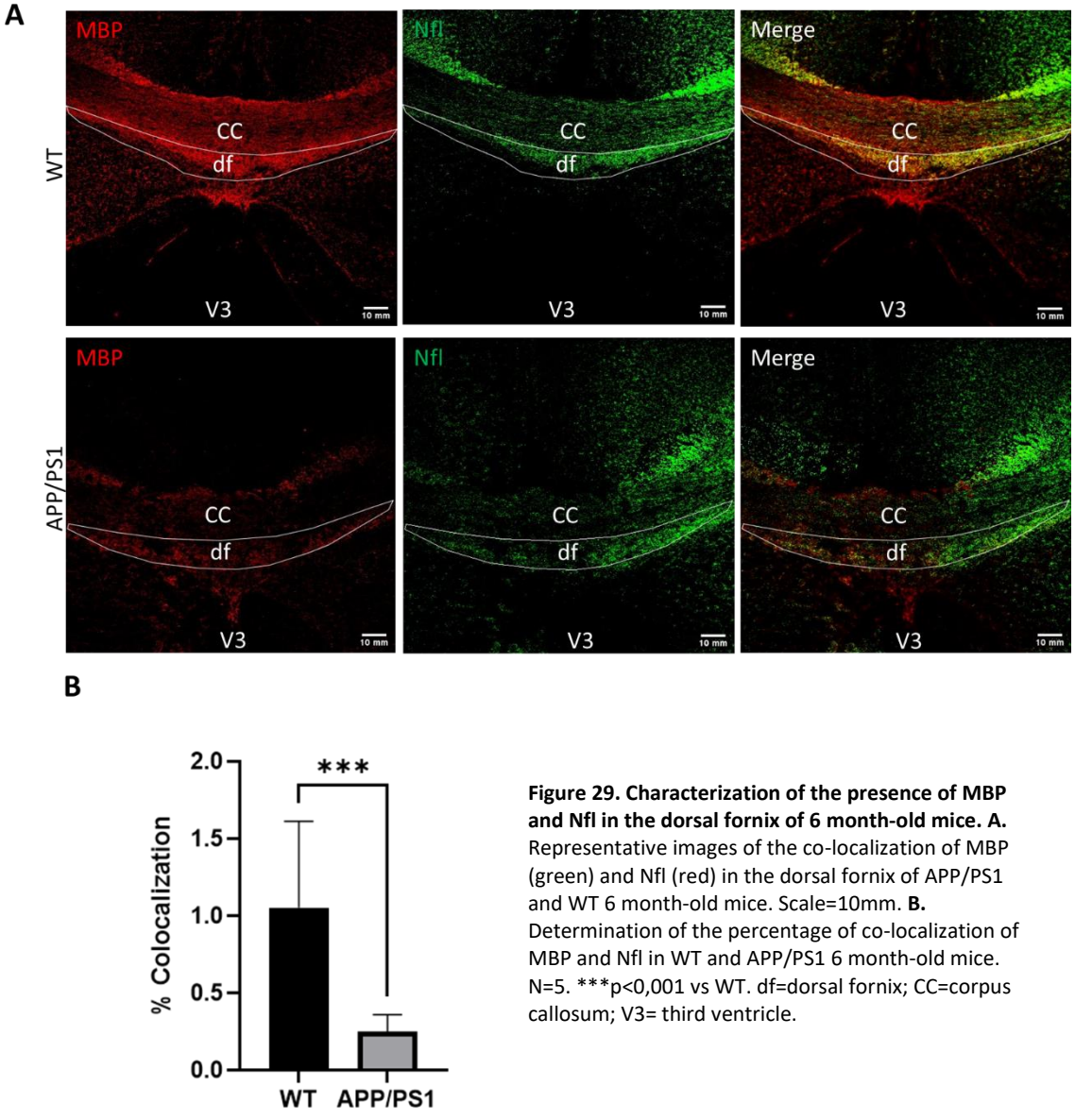

Figure 29. Characterization of the presence of MBP and Nfl in the dorsal fornix of 6 month-old mice. A. Representative images of the co-localization of MBP (green) and Nfl (red) in the dorsal fornix of APP/PS1 and WT 6 month-old mice. Scale=10mm. **B.** Determination of the percentage of co-localization of MBP and Nfl in WT and APP/PS1 6 month-old mice. N=5. ***p<0,001 vs WT. df=dorsal fornix; CC=corpus callosum; V3= third ventricle.

MOG levels in 6 month-old mice

Similarly, the levels of MOG were determined in the dorsal fornix of 6 month-old WT and APP/PS1 mice. Anti-MOG and anti-Nfl were applied to stain coronal sections of both strains. As a result, a significant decrease in MOG levels was observed in the dorsal fornix of 6 month-old WT and APP/PS1 mice (Figure 30).

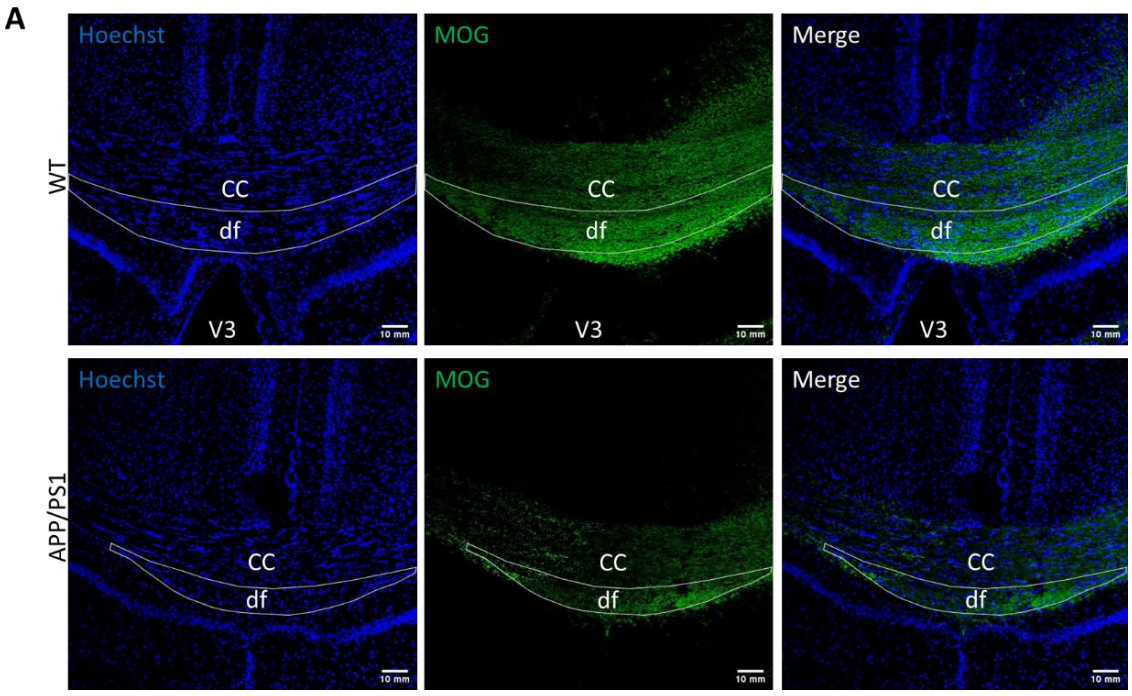

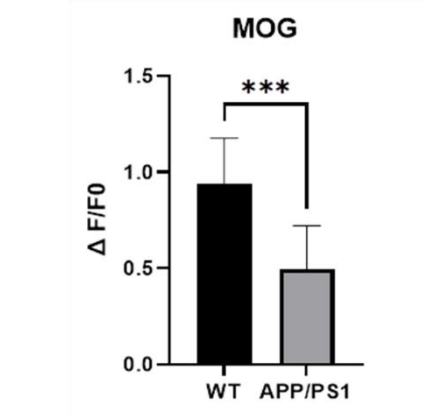

Figure 30. Immunofluorescence determination of MOG levels in the dorsal fornix of 6 month-old mice. A. Representative immunofluorescence images of the dorsal fornix labeling the nuclei with blue (Hoechst) and MOG with green in WT and APP/PS1 6 month-old mice. Scale =10mm. **B.** Quantification of the green fluorescence with respect to the background corresponding to the levels of MOG in WT and APP/PS1 6 month-old mice. N=5. ***p<0,001 vs WT. df=dorsal fornix; CC=corpus callosum; V3= third ventricle.

This is also obvious in the following images and the corresponding graph, that demonstrate a considerable decrease in the percentage of MOG and Nfl colocalization in the dorsal fornix of APP/PS1 mice compared to WT (Figure 31).

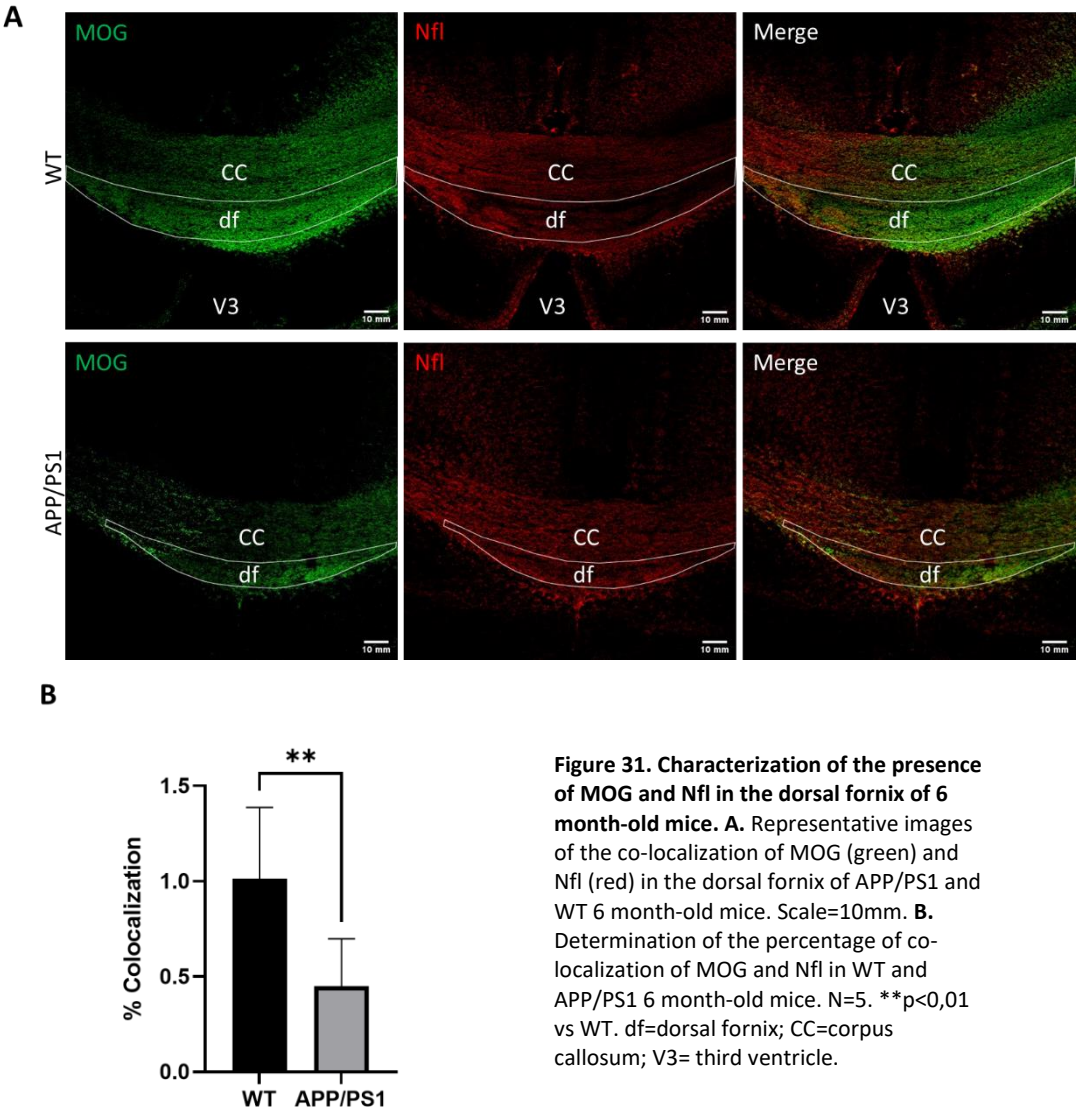

Figure 31. Characterization of the presence of MOG and Nfl in the dorsal fornix of 6 month-old mice. A. Representative images of the co-localization of MOG (green) and Nfl (red) in the dorsal fornix of APP/PS1 and WT 6 month-old mice. Scale=10mm. **B.** Determination of the percentage of co-localization of MOG and Nfl in WT and APP/PS1 6 month-old mice. N=5. **p<0,01 vs WT. df=dorsal fornix; CC=corpus callosum; V3= third ventricle.

Study of oligodendrocyte lineage in the dorsal fornix

Given the above results, it was questioned whether the decrease of myelin in the dorsal fornix of APP/PS1 mice was due to a decrease in the number of oligodendrocyte progenitor cells, or due to their incapacity to differentiate and mature. Consequently, the investigation was conducted to study the oligodendrocyte lineage in the dorsal fornix of young 4 month-old control and transgenic mice. This was achieved through the investigation of two principal oligodendrocyte lineage cell markers, the Oligodendrocyte Transcription Factor 2 (Olig2) and the platelet derived growth factor receptor alpha (PDGFRα). Olig2 is a transcription factor that activates the expression of myelin-associated genes in oligodendrocyte lineage cells and is primarily found in mature oligodendrocytes (OLs). PDGFRα, on the other hand, is abundant in oligodendrocyte progenitor cells (OPCs) and is involved in cell proliferation and differentiation.

PDGFRα in 4 month-old mice

Platelet derived growth factor receptor alpha (PDGFRα) was the first oligodendrocyte lineage cell marker to be studied. The levels of PDGFRα in the dorsal fornix of 4month-old control and transgenic mice were measured by immunofluorescence assay. The tissue was stained with anti-PDGFRα and the Hoechst fluorescent dye was used to mark the cell nuclei. As can be seen below, there was a modest but non-significant increase in PDGFRα levels in the dorsal fornix of APP/PS1 mice when compared to controls (Figure 32).

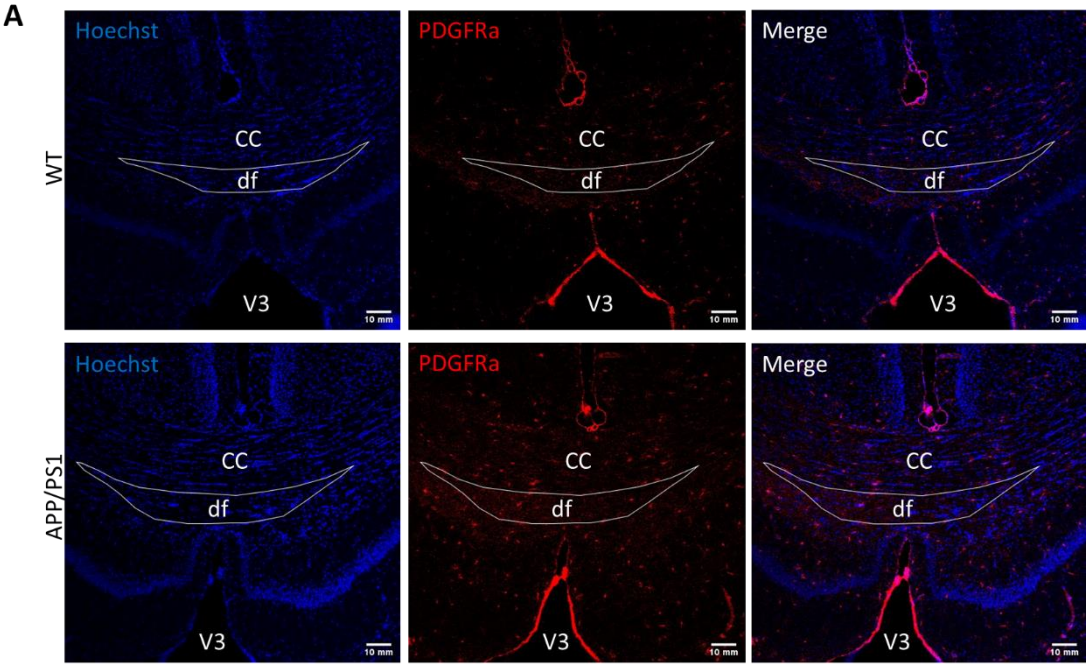

Figure 32. Immunofluorescence determination of PDGFRa levels in the dorsal fornix of 4 month-old mice. A. Representative immunofluorescence images of the dorsal fornix labeling the nuclei with blue (Hoechst) and PDGFRa with red in WT and APP/PS1 4 month-old mice. Scale =10mm. **B.** Quantification of the red fluorescence with respect to the background corresponding to the levels of PDGFRα in WT and APP/PS1 4 mont- old mice. N=5. p>0,05 vs WT. df=dorsal fornix; CC=corpus callosum; V3= third ventricle.

Olig2 in 4 month-old mice

In the same fashion, Olig2 levels were measured in the dorsal fornix of 4 month-old WT and APP/PS1 mice by immunofluorescence assay. Coronal sections were stained with anti-Olig2 and the Hoechst dye was used for cell nuclei detection. Olig2 levels in the dorsal fornix do not show any change in 4 month-old APP/PS1 mice compared to WT mice (Figure 33).

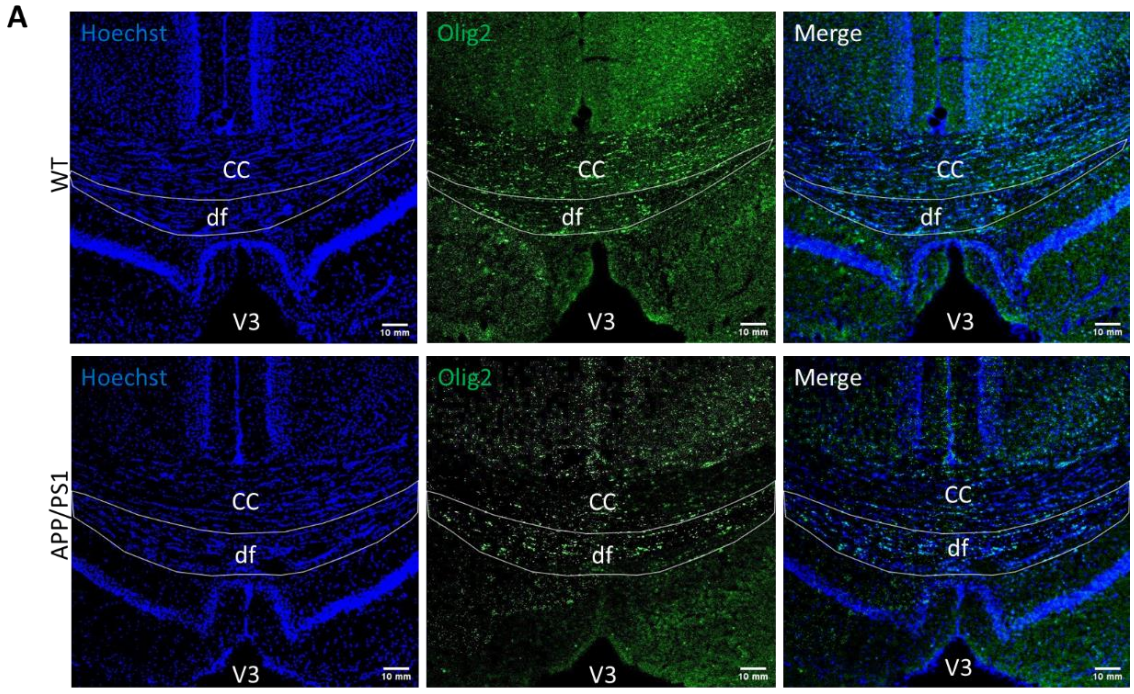

Figure 33. Immunofluorescence determination of Olig2 levels in the dorsal fornix 4 month-old mice. A. Representative immunofluorescence images of the dorsal fornix labeling the nuclei with blue (Hoechst) and Olig2 with green in WT and APP/PS1 4 month-old mice. Scale =10mm. **B.** Quantification of the green fluorescence with respect to the background corresponding to the levels of Olig2 in WT and APP/PS1 4 month-old mice. N=5. p>0,05 vs WT. df=dorsal fornix; CC=corpus callosum; V3= third ventricle.

PDGFRα in 6 month-old mice

Subsequently, 6 month-old WT and APP/PS1 mice were tested for the same markers to see if there was any further disturbance of the oligodendrocyte lineage cells with age.

The levels of PDGFRα were determined in the dorsal fornix of 6 month-old control and transgenic mice by applying immunofluorescence assay. When comparing 6 month-old APP/PS1 mice to WT, PDGFRα demonstrates a noticeable increase in the dorsal fornix of transgenic mice compared to controls, as shown at the representative images and the graph corresponding to the quantification of the PDGFRα levels (Figure 34).

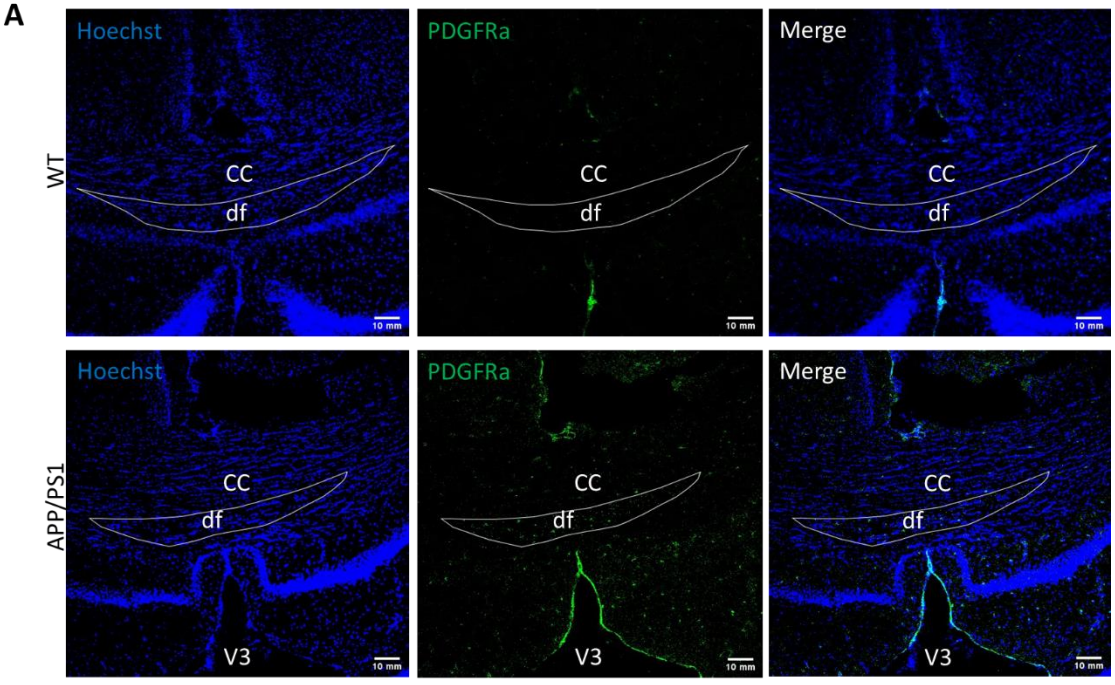

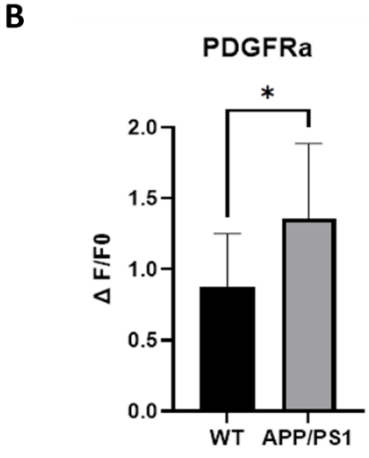

Figure 34. Immunofluorescence determination of PDGFRα levels in the dorsal fornix of 6 month-old mice. A. Representative immunofluorescence images of the dorsal fornix labeling the nuclei with blue (Hoechst) and PDGFRα with green in WT and APP/PS1 6 month-old mice. Scale =10mm. **B.** Quantification of the green fluorescence with respect to the background corresponding to the levels of PDGFRα in WT and APP/PS1 6 month-old mice. N=5. *p<0,05 vs WT. df=dorsal fornix; CC=corpus callosum; V3= third ventricle.

Olig2 in 6 month-old mice

Likewise, the dorsal fornix of 6 month-old WT and APP/PS1 mice was tested for Olig2 levels. Coronal sections of both strains were stained with anti-Olig2. Thus, Olig2 levels in the dorsal fornix of 6 month-old APP/PS1 mice were found to be significantly decreased when compared to WT (Figure 35).

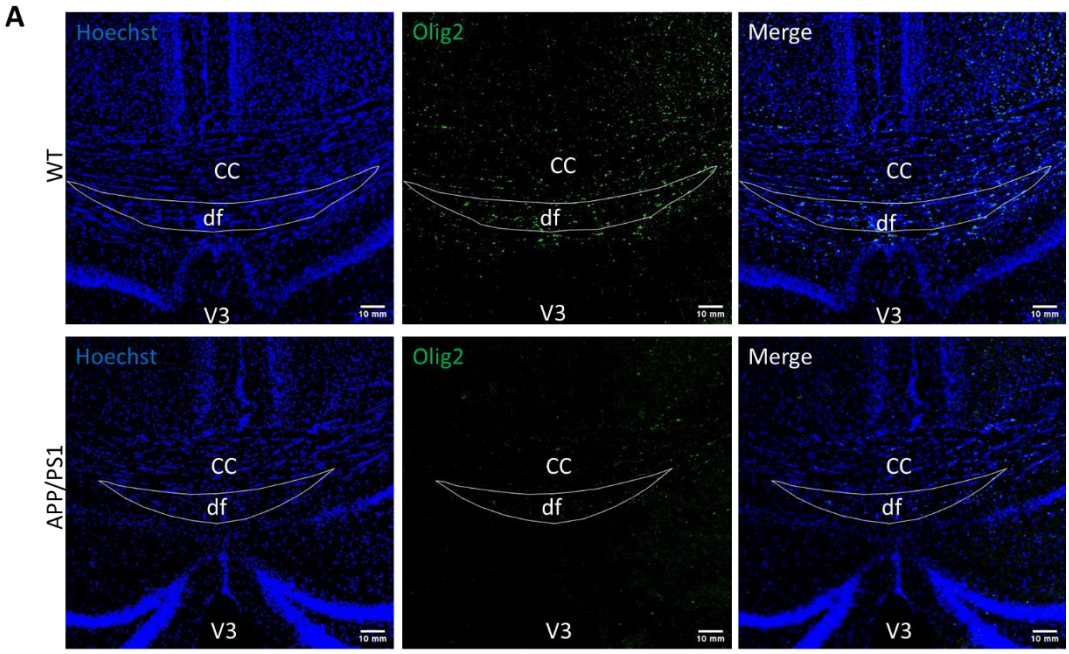

Figure 35. Immunofluorescence determination of Olig2 levels in the dorsal fornix of 6 month-old mice. A. Representative immunofluorescence images of the dorsal fornix labeling the nuclei with blue (Hoechst) and Olig2 with green in WT and APP/PS1 6 month-old mice. Scale =10mm. **B.** Quantification of the green fluorescence with respect to the background corresponding to the levels of Olig2 in WT and APP/PS1 6 month-old mice. N=5. ***p<0,001 vs WT. df=dorsal fornix; CC=corpus callosum; V3= third ventricle.

Determination of myelin components' levels in the hippocampus by Western blot

Following the decrease in myelin components, it was questioned whether these alterations would have an effect on the myelin levels in the hippocampus of APP/PS1 mice. In order to accomplish this, the protein levels of MBP and MOG were measured in the hippocampus via Western blot.

Determination of MBP levels in 4 month-old mice

To begin with, the levels of MBP in the hippocampi of 4 month-old WT and APP/PS1 mice were determined. After the hippocampi were collected and homogenized, 20mg of tissue lysates were used to run the Western blot. The detection of MBP was accomplished with a specific antibody with a predicted band size at 33 kD and β-tubulin was used as a loading control. The anti-MBP antibody was raised against an immunoblot that was predicted to recognize five isoforms of MBP. The predicted molecular weights of isoforms were 18 kD, 17 kD, 14 kD, 21 kD and 13 kD respectively. However, the most tangible observed bands were the ones at 18 kD and 17 kD. It was observed that MBP levels were slightly lower in the hippocampus of transgenic mice compared to controls, as shown below (Figure 36).

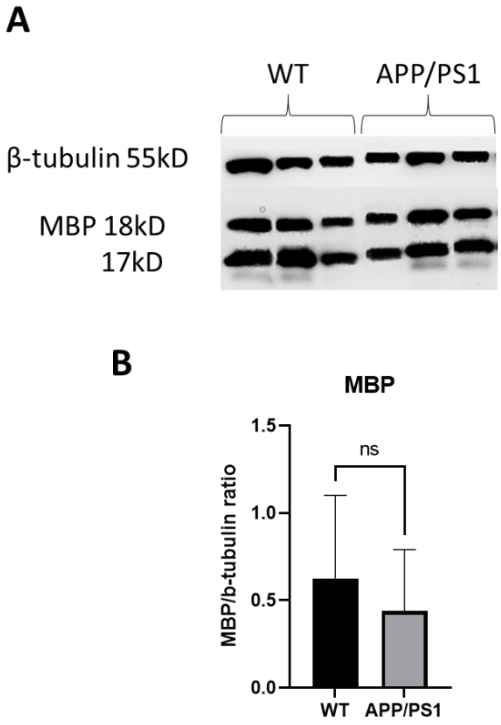

Figure 36. Determination by Western Blot of MBP levels in the hippocampus of 4 month-old mice. A. Representative Western Blot images of MBP and β-tubulin (loading control) in the hippocampus of 4 month-old WT and APP/PS1 mice. **B.** Quantification by densitometry of MBP levels normalized by β-tubulin levels. N=3. $p > 0.05$ vs. WT.

Determination of MOG levels in 4 month-old mice

For the detection of MOG, Western blot was performed using a specific anti-MOG antibody at 1/1000 dilution with predicted and observed band size at 28 kD. When comparing the hippocampus of transgenic mice to controls, it was found that MOG levels remained unchanged, as can been observed in the graph below (Figure 37).

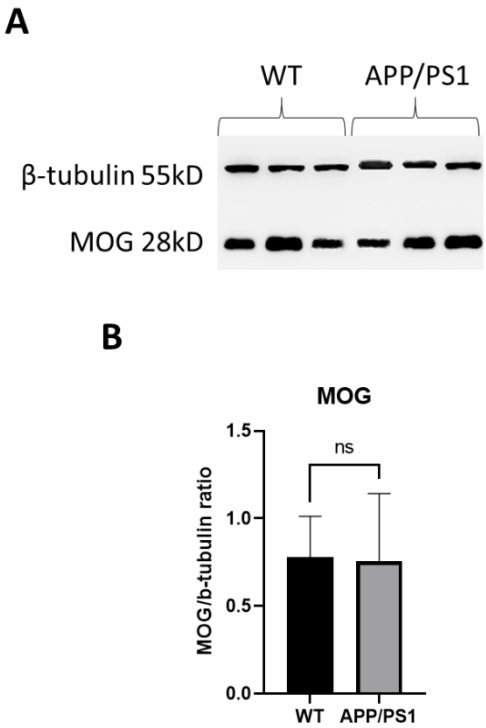

Figure 37. Determination by Western Blot of MOG levels in the hippocampus of 4 month-old mice. A. Representative Western Blot images of MOG and β-tubulin (loading control) in the hippocampus of 4 month-old WT and APP/PS1 mice. **B.** Quantification by densitometry of MOG levels normalized by β-tubulin levels. N=3. $p > 0.05$ vs. WT.

Determination of MBP levels in 6 month-old mice

Following that, the same experiment was applied to 6month-old control and transgenic mice in order to assess the MBP levels in the hippocampus. The same anti-MBP was used and the most noticeable bands were at 18 kD and 17 kD respectively. The obtained results showed a modest decrease of MBP levels in the hippocampus of 6 month-old APP/PS1 mice, but not statistically significant, when compared to WT (Figure 38).

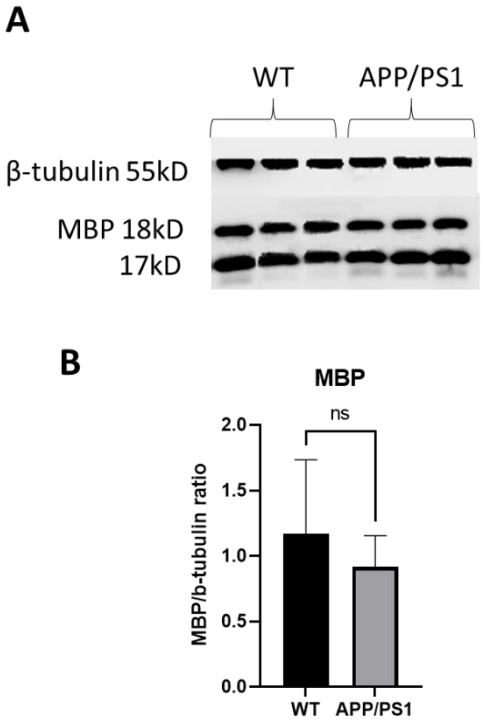

Figure 38. Determination by Western Blot of MBP levels in the hippocampus of 6 month-old mice. A. Representative Western Blot images of MBP and β-tubulin (loading control) in the hippocampus of 6 month-old WT and APP/PS1 mice. **B.** Quantification by densitometry of MBP levels normalized by β-tubulin levels. N=3. $p > 0.05$ vs. WT.

Determination of MOG levels in 6 month-old mice

In the same fashion, the levels of hippocampal MOG were determined by the specific anti-MOG antibody with an apparent molecular mass of 28 kD and b-tubulin with molecular weight of 55kD served as a loading control. The quantification of MOG levels showed a subtle decline in the hippocampi of 6 month-old APP/PS1 mice, compared to WT, although no statistically significant (Figure 39).

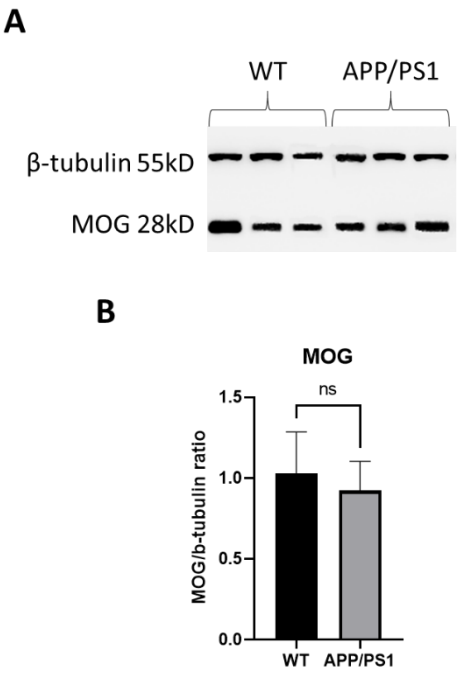

Figure 39. Determination by Western Blot of MOG levels in the hippocampus of 6 month-old mice. A. Representative Western Blot images of MOG and β-tubulin (loading control) in the hippocampus of 6 month-old WT and APP/PS1 mice. **B.** Quantification by densitometry of MOG levels normalized by β-tubulin levels. N=3. $p > 0.05$ vs. WT.

Determination of Oligodendrocyte lineage markers' levels in the hippocampus by Western blot

In light of the previous results regarding the changes in OPCs and OLs levels in the dorsal fornix, it was unclear whether the transgenic mice's hippocampal OPCs and mature OLs were also altered. For this reason, the PDGFRα and Olig2 levels were measured in the hippocampus of control and transgenic by Western blot.

Determination of PDGFRα levels in 4 month-old mice

For the detection of PDGFRα, 20mg of total protein were used in each lane. The monoclonal anti-PDGFRα antibody was used at 1/500 dilution and a band detected at 120kD and b-tubulin was again used as a loading control. As shown below, APP/PS1 mice showed a slight but non-significant decrease in hippocampal PDGFRα levels when compared to WT (Figure 40).

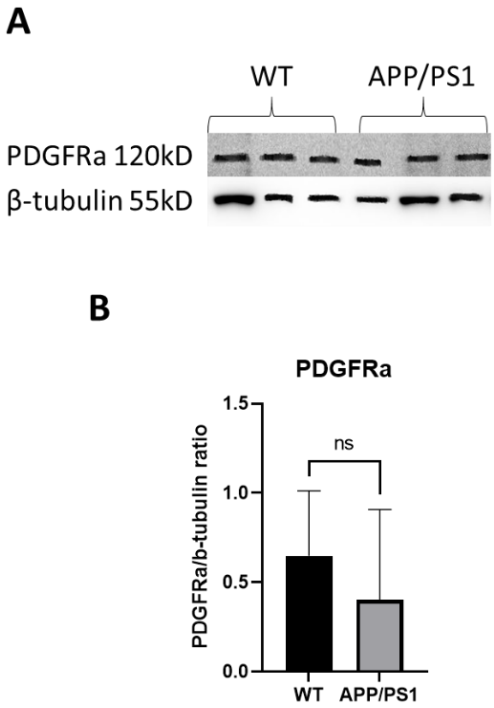

Figure 40. Determination by Western Blot of PDGFRα levels in the hippocampus of 4 month-old mice. A. Representative Western Blot images of PDGFRα and β-tubulin (loading control) in the hippocampus of 4 month-old WT and APP/PS1 mice. **B.** Quantification by densitometry of PDGFRα levels normalized by β-tubulin levels. N=3. $p > 0.05$ vs. WT.

Determination of Olig2 levels in 4 month-old mice

The detection of Olig2 was achieved by employing the polyclonal anti-Olig2 antibody at 1/1000 dilution and calculated molecular weight at 32kD. Likewise, APP/PS1 mice had lower hippocampal Olig2 levels when compares to WT, but these differences were not statistically significant either (Figure 41).

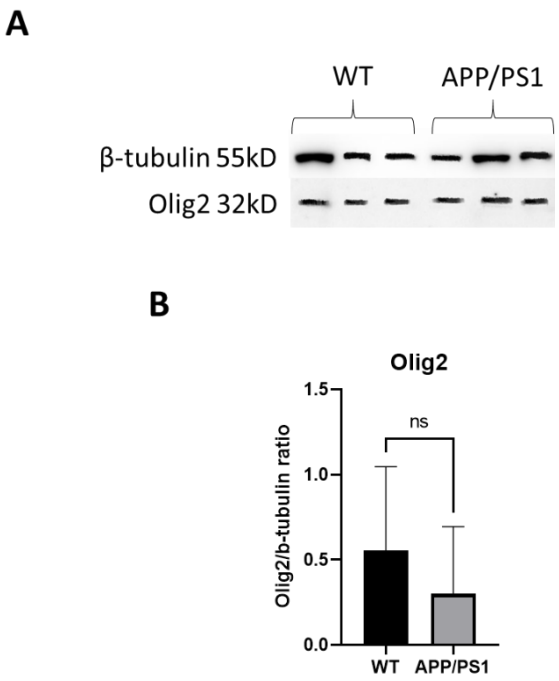

Figure 41. Determination by Western Blot of Olig2 levels in the hippocampus of 4 month-old mice. A. Representative Western Blot images of Olig2 and β-tubulin (loading control) in the hippocampus of 4 month-old WT and APP/PS1 mice. **B.** Quantification by densitometry of Olig2 levels normalized by β-tubulin levels. N=3. $p > 0.05$ vs. WT.

Determination of PDGFRα levels in 6-months-old mice

After that, the same procedure was employed to evaluate the PDGFRα levels in the hippocampus of 6month-old transgenic and control mice. Hippocampal PDGFRα levels were found to further decline in 6 month-old APP/PS1 mice when compared to WT, nonetheless this difference was not statistically significant (Figure 42).

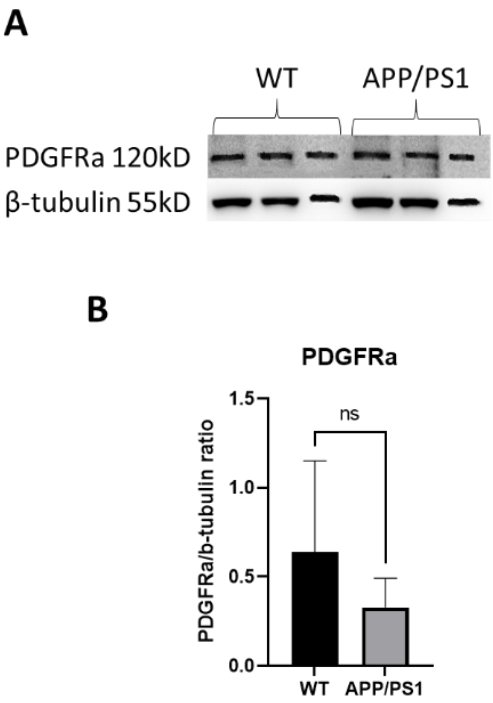

Figure 42. Determination by Western Blot of PDGFRα levels in the hippocampus of 6 month-old mice. A. Representative Western Blot images of PDGFRα and β-tubulin (loading control) in the hippocampus of 6 month-old WT and APP/PS1 mice. **B.** Quantification by densitometry of PDGFRα levels normalized by β-tubulin levels. N=3. $p > 0.05$ vs. WT.

Determination of Olig2 levels in 6 month-old mice

In a similar vein, the quantification of Olig2 levels was assessed in 6 month-old WT and APP/PS1 mice, by using the same polyclonal anti-Olig2 antibody. Regarding the hippocampal Olig2 levels of 6 month-old mice, they were reduced in APP/PS1 mice with respect to WT, albeit not significantly (Figure 43).

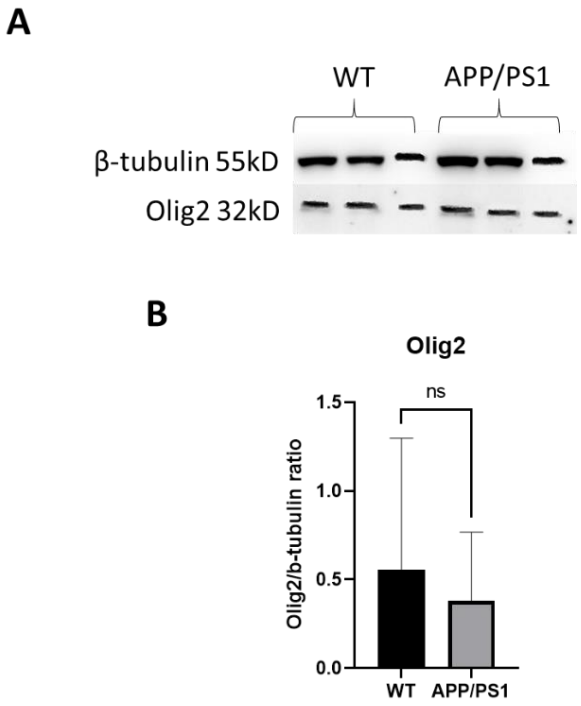

Figure 43. Determination by Western Blot of Olig2 levels in the hippocampus of 6 month-old mice. A. Representative Western Blot images of Olig2 and β-tubulin (loading control) in the hippocampus of 6 month-old WT and APP/PS1 mice. **B.** Quantification by densitometry of Olig2 levels normalized by β-tubulin levels. N=3. $p > 0.05$ vs. WT

Evaluation of the neuroprotective effects of DL-TBOA and QNZ46 in DIV14 cells upon Aβ treatment

The next objective was to shed light on the molecular mechanisms subtending the demyelination already linked to AD. In order to do so, the neurosphere assay was applied. Neural stem progenitor cells (NSPCs) were isolated from the SVZ of P1-3 mice pups, expanded as neurospheres and finally differentiated into neurons, astrocytes and oligodendrocytes. Neurospheres underwent differentiation until DIV14 and pharmacological treatments of 1µM Aβ combined with 10µM DL-TBOA and 10µM QNZ46 were applied on DIV13. In total, four conditions were studied: a) the control cells that received no treatment; b) the Aβ-treated cells; c) the combined Aβ/DL-TBOA-treated cells; and d) the combined Aβ/QNZ46-treated cells.

The concentration of amyloid beta treatment was intended to mimic the early stages of AD, when amyloid deposition is still low. It is known that amyloid beta raises glutamate levels through the inactivation of APC/C-Cdh1. Increased glutamate, linked to APC/C-Cdh1 inactivation, may result in its release from axons, leading to demyelination by activating GluN2C/D-NMDA receptors.

DL-TBOA is a non-transportable competitive blocker of excitatory amino acid transporters that inhibits glutamate absorption, whereas QNZ46 is non-competitive and GluN2C/GluN2D-selective NMDA antagonist that inhibits NMDAR-synaptic plasticity. For this reason, DL-TBOA and QNZ46 were selected as potential therapeutic agents, since they are both known for their neuroprotective properties.

Determination of Nfl levels in DIV14 cells to evaluate the neuroprotective effects of DL-TBOA and QNZ46 upon Aβ treatment

Initially, it was aimed to ascertain whether the neuron population of DIV14 cells was affected upon Aβ treatment combined with DL-TBOA or QNZ46. To do so, immunofluorescence assay was applied to stain cells from each condition with anti-Nfl antibody. The Hoechst fluorescent dye was used to stain the cell nuclei. The ImageJ software was used measure the levels of the neuronal axonal protein Nfl of each condition by immunofluorescence assay. The following result demonstrates that Nfl shows no significant variations across all conditions (Figure 44).

A

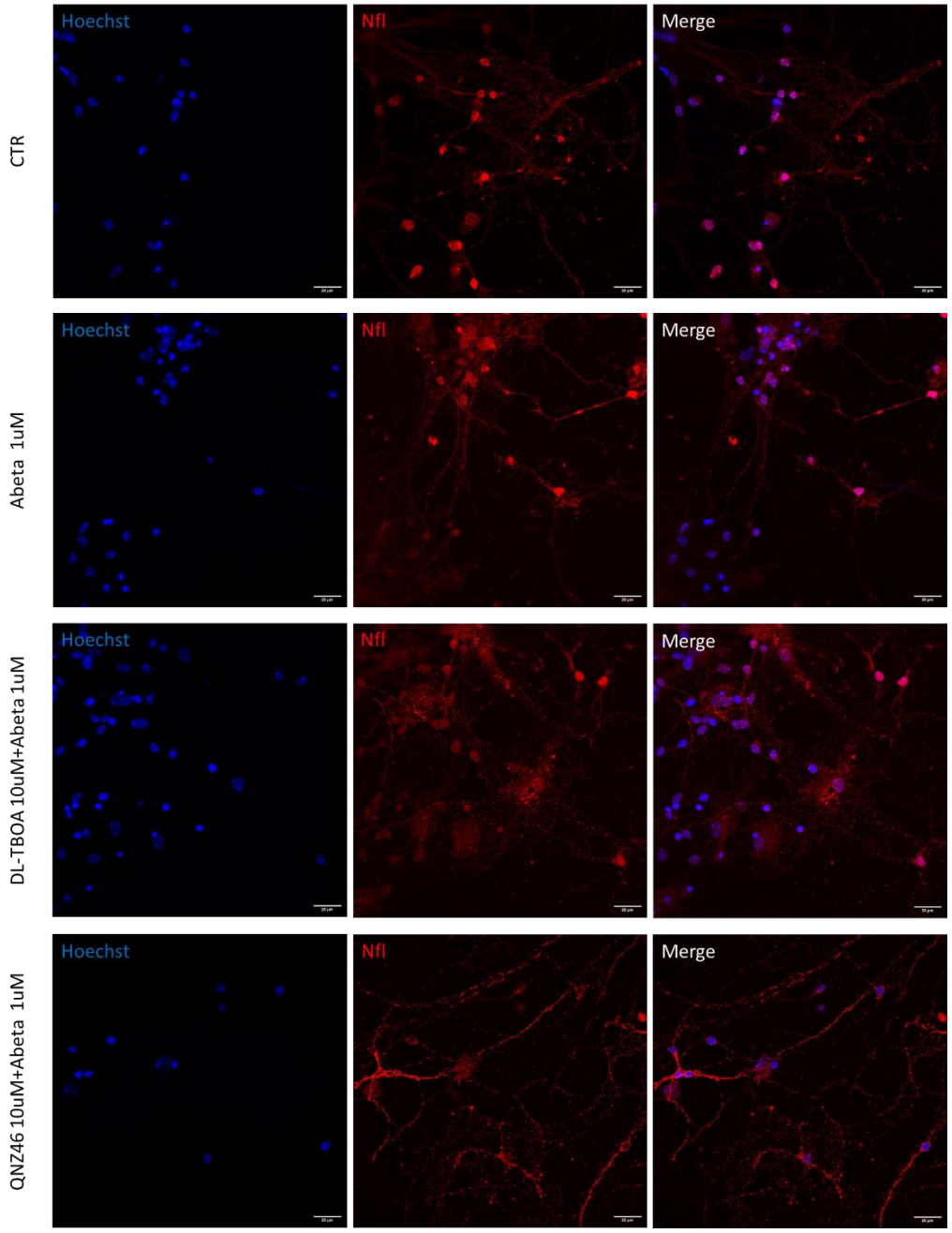
Hoechst
Nfl
Merge
CTR
Abeta 1uM
DL-TBOA 10uM+Abeta 1uM
QNZ46 10uM+Abeta 1uM

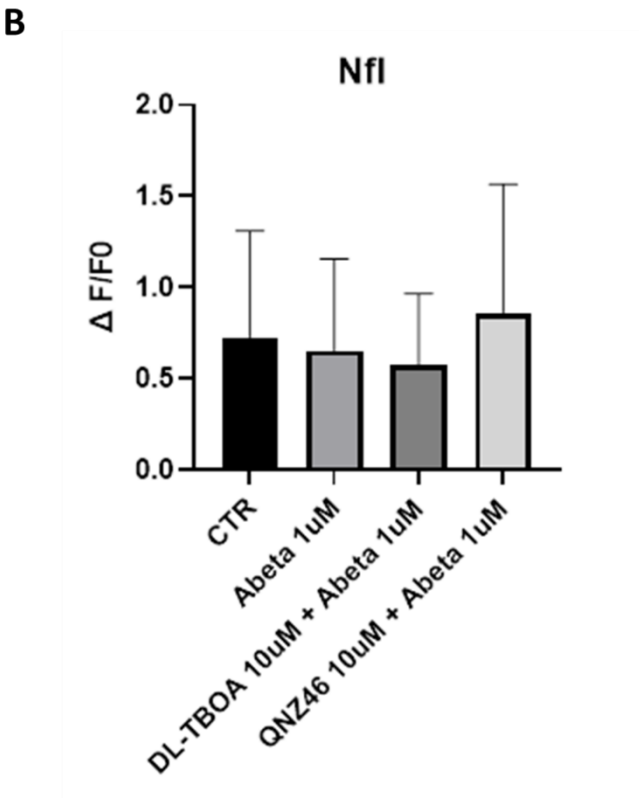

Figure 44. Immunofluorescence determination of Nfl levels in DIV14 cell cultures. A. Representative immunofluorescence images of DIV14 cells labeling the nuclei with blue (Hoechst) and Nfl with red in CTR cells, Abeta-treated cells, combined Abeta/DL-TBOA-treated cells and combined Abeta/QNZ46-treated cells. Scale =20mm. **B.** Quantification of the red fluorescence with respect to the background corresponding to the levels of Nfl in CTR group, Abeta-treated group, combined Abeta/DL-TBOA-treated group and combined Abeta/QNZ46-treated group. N=3. p>0,05 vs CTR. CTR=control untreated cells.

Determination of MBP levels in DIV14 cells to evaluate the neuroprotective effects of DL-TBOA and QNZ46 upon Aβ treatment

Afterwards, the next goal was to investigate whether Aβ treatment induces myelin degeneration and subsequently whether DL-TBOA and QNZ46 ameliorate this effect. This was achieved by labeling the cells from all four conditions with anti-MBP and the Hoechst dye that stains the nuclei. The quantification of MBP levels was determined, using the ImageJ software. A significant decrease in MBP levels was observed in the Aβ-treated group when compared with the control group. This decline in MBP levels was efficiently restored in the Aβ/DL-TBOA group. As for the Aβ/QNZ46 group, it was observed a slight increase in MBP levels when compared with the Aβ-treated group, but again not significant (Figure 45).

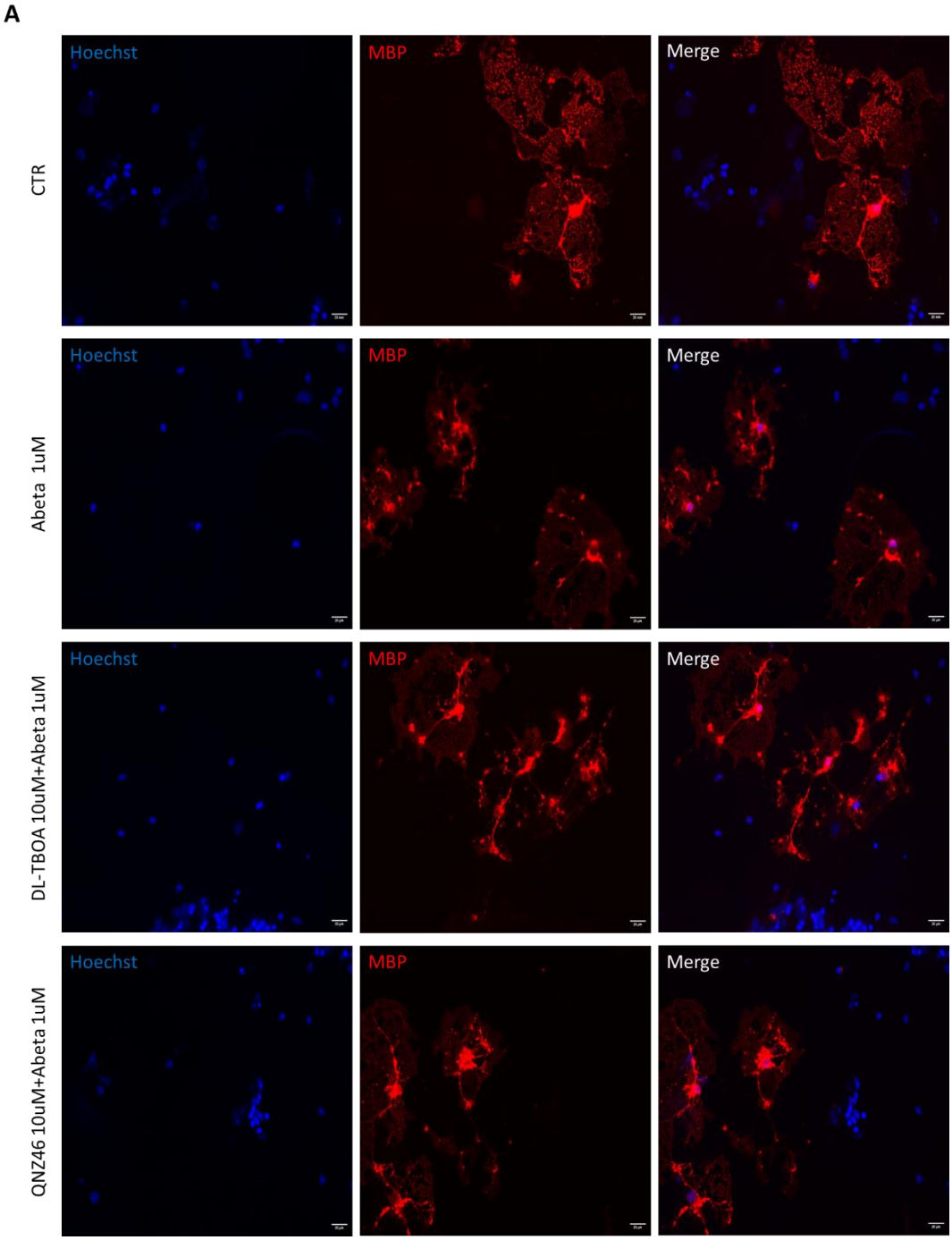
A
Hoechst
MBP
Merge
CTR
Abeta 1uM
DL-TBOA 10uM+Abeta 1uM
QNZ46 10uM+Abeta 1uM

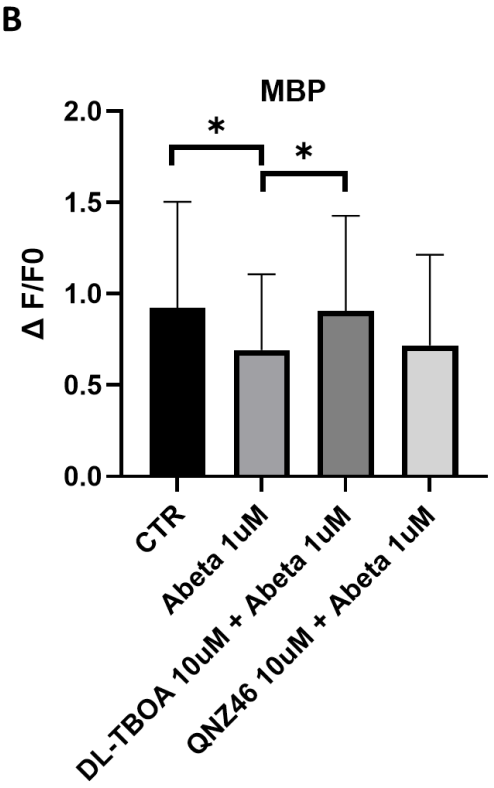

Figure 45. Immunofluorescence determination of MBP levels in DIV14 cell cultures. A. Representative immunofluorescence images of DIV14 cells labeling the nuclei with blue (Hoechst) and MBP with red in CTR cells, Abeta-treated cells, combined Abeta/DL-TBOA-treated cells and combined Abeta/QNZ46-treated cells. Scale =20mm. **B.** Quantification of the red fluorescence with respect to the background corresponding to the levels of MBP in CTR group, Abeta-treated group, combined Abeta/DL-TBOA-treated group and combined Abeta/QNZ46-treated group. N=3. *p<0,05 vs CTR. CTR=control untreated cells.

DISCUSSION

Discussion

Dorsal fornix atrophy is not prominent in young APP/PS1 mice

Although the main lesions in the brain of Alzheimer's patients are senile plaques and neurofibrillary tangles (Cummings, 2008), over the years, alterations in the white matter have been described and may be important in the course of the disease. Our results agree with these conclusions, finding early alterations in the dorsal fornix of AD mice model. Indeed, several studies in recent years suggest that among the early events of late-onset AD are microstructural WM alterations (Delbeuck, Van Der Linden & Collette, 2003; Brier, Thomas & Ances, 2014). The primary sites of microstructural WM abnormalities in AD patients are the parietotemporal regions, the limbic system and certain areas of the corpus callosum (Fellgiebel et al., 2008; Mielke et al., 2009; Zhang et al., 2007; Teipel et al., 2007; Rose et al., 2006; Rose et al., 2006; Lacalle-Aurioles et al., 2016). Studies on animals and *in vivo* humans have shown that the disruption of WM happens early in the AD process (Brun & Englund, 1986; Englund, Brun & Alling, 1988; Bartzokis et al., 2004). An emerging theory suggests that damage to WM tracts is an indication of late-myelinating regions' vulnerability to AD and aging. These WM alterations happen before neuronal deterioration and atrophy become noticeable, making individuals more susceptible to the clinical signs of AD (Bartzokis et al., 2004).

Fornix is one of the WM bundles that has been shown to undergo stable and consistent changes in AD (Oishi & Lyketsos, 2014). Situated on the medial aspects of the cerebral hemispheres, the fornix serves as the hippocampus' principal output tract, and is crucial to the development and maintenance of declarative memories (Thomas, Koumellis & Dineen, 2011). Fornical alterations, including demyelination and axonal loss, have been observed as early as in 1976 (Hopper & Vogel, 1976), and have also been

repeatedly linked to AD (Ringman et al., 2007; Teipel et al., 2007; Mielke et al., 2009; Acosta-Cabronero et al., 2010; Salat et al., 2010; Liu et al., 2011; Douaud et al., 2013). Given its strategic location within the memory circuitry, its identification at preclinical phases of AD disease, and its tendency to precede the structural alterations occurring in the hippocampus, fornix degeneration is very promising as an early AD biomarker (Nowrangi & Rosenberg, 2015; Lacalle-Aurioles & Iturria-Medina, 2023) Nevertheless, no research has yet been conducted specifically on the fornix. For the first time, we have reported on a demyelination specific to the dorsal fornix in transgenic mice as young as 4 months old.

Thus, the objective of this PhD thesis was to determine whether dorsal fornix degeneration is present in young transgenic mice. For this reason, the APP/PS1 double transgenic mouse has been employed as an AD model, which is characterized by the overexpression and excessive processing of the APP protein, resulting in the production of amyloid plaques (Jankowsky et al., 2004; Shen et al., 2018).

In the pathophysiology of AD, neuron loss is a basic and fundamental feature (Coleman & Flood, 1987; Hof, Morrison & Cox, 1990) that begins even in preclinical stages before the neuropathological hallmarks appear (Gómez-Isla et al., 1996). Several brain regions, including the fornix, exhibit a reduction in the total amount of neurons in AD patients (Mountjoy et al., 1983). Fornical atrophy has previously been reported in AD patients (Callen et al., 2001), and lower FA values have been linked to demyelination and degeneration in the fornix WM (Nabizadeh et al., 2022). Studies employing histological, anatomical MRI, or diffusion tensor imaging techniques have also reported fornical atrophy in PDAPP mice (Gonzalez-Lima et al., 2001; Redwine et al., 2003; Song et al., 2004). Furthermore, regional analysis revealed a major effect in the dorsal fornix, where FA was decreased by 20% in CVN-AD mice (Badea et al., 2016). According to another study, plasma Nfl exhibited a negative correlation with FA in the fornix, corpus callosum, and other brain regions of AD patients. This suggests that elevated Nfl

levels in plasma or serum may be an indicator of the degree of atrophy currently present (Nabizadeh et al., 2022).

Firstly, we wanted to assess whether the dorsal fornix of young APP/PS1 transgenic mice endures degeneration. According to our data, there are no discernible variations in Nfl levels in the dorsal fornix between the experimental groups, suggesting that there are comparable numbers of axons. These findings are consistent with previous studies of Delatour and colleagues (2006), where the dorsal fornix diameter was similar in young (10 weeks) APP/PS1 and control animals, though it decreased with age (Delatour et al., 2006). This contrasts with reports from other authors who have demonstrated that in PDAPP mice, the atrophy of the corpus callosum and of the dorsal fornix is described at as young as 3 months old (Gonzalez-Lima et al., 2001; Redwine et al., 2003).

Myelin loss is apparent in the dorsal fornix of young APP/PS1 mice

Our findings indicate a significant decline in MBP and MOG levels in the dorsal fornix of young APP/PS1 mice when compared to WT. In line with our results, Dong et al. (2018) documented early myelin degeneration in APP/PS1 mice at 3–6 months of age; this pathology was noted before observed cognitive impairment at 6 months of age (Dong et al., 2018). Furthermore, in 2-month-old APP/PS1 mice, Wu et al. (2017) found changes in myelin morphology (Wu et al., 2017).

Our research also revealed no significant decrease in MBP and MOG levels in the hippocampi of young APP/PS1 mice. These results corroborate those of other studies that found that myelination is normal until 3–6 months of age in APP/PS1-mice. Defects in myelin integrity and amount were common at 6 months of age in APP/PS1 mice but returned to control levels in 9 month-old mice (Radde et al., 2006; Oddo et al., 2003; Games et al., 1995). This might suggest

that demyelination of the dorsal fornix is an early event that proceeds demyelination of the hippocampus.

Previous histochemical and neuroimaging studies in AD have revealed myelin damage (Dean et al., 2017; Bulk et al., 2018; Mitew et al., 2010; Nasrabady et al., 2010). Prior studies have indicated a reduction in myelin proteins, MBP and CNPase, in AD patients (Roher et al., 2002). As demonstrated by single-cell transcriptomics of myelinating oligodendrocytes (Sjobeck, Haglund & Englund, 2005; Zhan et al., 2014), histochemical staining (Sjobeck, Haglund & Englund, 2005; Zhan et al., 2014; Couttas et al., 2016), and neuroimaging (Bouhrara et al., 2018; Dean et al., 2017; Moscoso et al., 2022), the amount of myelin in the WM of AD patients is decreased. Extensive reductions in WM integrity have been observed in DTI studies of AD and MCI, with the temporal lobes showing the most consistent changes (Chua et al., 2008; Bozzali et al., 2002; Huang, Friedland & Auchus, 2007; Naggara et al., 2006; Xie et al., 2006). Moreover, fornix fractional anisotropy is decreased in AD patients, according to DTI fiber tracking studies (Teipel et al., 2007; Bennett, Huffman & Stark, 2015). Several studies employing DTI and structural MRI demonstrated alterations in parahippocampal WM in aging and MCI subjects (Kalus et al., 2006; Stoub et al., 2006; Rogalski et al., 2009; Wang et al., 2012). Hippocampal atrophy and fornix FA have been found to correlate in AD, which has been observed in normal aging, MCI, and pre-clinical AD (Firbank et al., 2007; Pievani et al., 2010; Lee et al., 2012). Lee and colleagues (2012) reported that in AD, subcortical axonal defects and cortical neuronal damage are probably closely related, perhaps indicating a pathogenic relationship between the two (Lee et al., 2012). Moreover, a recent study found that the precuneus of postmortem AD brains exhibits reduced expression of myelin genes, such as MBP, MAG, MOG, and CNP (Sobue et al., 2021). Sub-regions of the entorhinal cortex and hippocampus of 3xTg-AD mice have been shown to display myelination disruption at the earliest pathological stages (Dong et al., 2018). According to Wu and colleagues (2017), myelination impairments could be identified in the early stages of APP/PS1 mice, suggesting a potential link

between the pathophysiology of AD and myelination development (Wu et al., 2017). Research on multiple sclerosis and aging has long been interested in anti-myelin antibodies, anti-MOG and anti-MBP. Age-related changes to the myelin sheath have been linked to the downregulation of MBP and MOG (Xie et al., 2013). The MBP protein itself has been investigated and could serve as a biomarker for brain tissue damage and neurodegenerative diseases in both serum and cerebrospinal fluid (Barkhof et al., 1992; Katsavos & Anagnostouli, 2013; Zavialova et al., 2017; Kim et al., 2018).

OPCs and OLs exhibit alterations in the dorsal fornix of young APP/PS1 mice

Oligodendrocyte lineage cells are vulnerable to AD pathology. Myelin degradation due to impaired repair of OPCs could possibly be a starting point in AD (Sjobeck, Haglund & Englund, 2005; Roher et al., 2002; Tian et al., 2004; Ihara et al., 2010). According to recent single-cell research, oligodendrocyte changes are a common feature of AD (Chen et al., 2020; Brase et al., 2021). In the postmortem human cortex of AD patients, oligodendrocyte densities were found to be reduced (Nasrabady et al., 2018; Povala et al., 2021). In another study, Nielsen and colleagues (2013) measured the amounts of soluble NG2 in the CSFs of AD patients and the control group. According to their findings, NG2 levels rose with age, and AD patients had lower CSF NG2 levels than non-demented subjects (Nielsen et al., 2013). Furthermore, Olig2-positive cells were found to be lower in the brains of patients with AD (Behrendt et al., 2013).

The idea that oligodendroglia contribute to AD pathogenesis is also supported by studies interpreting oligodendroglial pathology in transgenic mouse models (Schmued et al., 2013; Behrendt et al., 2013). When comparing 12 and 24 month-old APP23 mice to control mice, there was a significant decrease in NG2-glia cells (He & Shen, 2009).

We first assessed the levels of PDGFRα and Olig2 in the dorsal fornix of 4 month-old mice, were we found no observed differences between APP/PS1 and wild-type mice. Then, we repeated the same experiment in 6 month-old mice, where we observed a significant rise in PDGFRα levels in the dorsal fornix of APP/PS1 mice when compared to controls. On the contrary, the levels of Olig2 were significantly reduced in the dorsal fornix of APP/PS1 mice in comparison to WT mice. When assessing the levels of PDGFRα and Olig2 in the hippocampi of APP/PS1 and WT mice we noticed no significant differences among groups. Regarding previous studies, there are contradictory findings regarding the OPCs and OLs populations in transgenic mice.

First, an elevated OPC proliferation was observed in in the WM of 6 month-old APP/PS1 mice (Behrendt et al., 2013), which is in line with our results in the dorsal fornix of 6 month-old APP/PS1 mice but contradict with reduction in OPCs levels in the hippocampus. According to earlier research, OPC exhaustion was observed in the CA1 region of the hippocampus of 6 month-old 3xTg-AD mice (Desai et al., 2009; Desai et al., 2010), which is not consistent with our findings in the hippocampus of APP/PS1 mice. This might be due to the fact that the 3xTg-AD mice bear mutations in three genes that lead to WM disruption in the hippocampus as early as 2 months of age (Desai et al., 2010; Desai et al., 2009). Moreover, DeFlitch et al. (2022) reported that while there is a decline in the OL population, particularly in the DG and CA3 regions, the OPC population in APP/PS1 mice appears to be unchanged when compared to their age-matched littermates (DeFlitch et al., 2022). Interestingly, in the APP/PS1 mice, OPC proliferation and differentiation increased during this particular time window (6–8 months), suggesting that OPC-mediated repair mechanisms may be the cause of improvements in myelin defects (Cai & Xiao, 2015). According to a quantitative analysis conducted in a different study, OPCs actively proliferated in the fornix's white matter, specifically in the vhc and fimbria (Fukushima et al., 2015).

It has been observed that OPCs migrate from the SVZ and differentiate into mature OLs in the adult fornix (Menn et al., 2006). Cellular senescence has now been linked to a number of age-related illnesses, including AD (Bhat et al., 2012). Higher numbers of senescent OPCs and astrocytes may jointly increase the burden of AD pathology and play a major role in LOAD. Taken all these into account, senescent OPCs in the fornix fail to differentiate in mature myelinating OLs contributing to AD pathologies in the early stages and might be a potential mechanism that explains our observations. (Lau, Ramer & Tremblay, 2023).

Aβ-induced glutamate excitotoxity results in myelin loss

According to studies, Aβ oligomers have the ability to bind directly to crucial elements of the glutamatergic synapse, thereby controlling glutamate release at the terminals (Kabogo et al., 2010; Findley et al., 2019). It is believed that the extrasynaptic glutamate levels are augmented by Aβ-induced aberrant glutamate release, leading to hyperstimulation of NMDA receptors and synaptotoxicity in AD (Olajide et al., 2021). According to previous research, inhibitors with EAAT substrate activity can raise extracellular glutamate levels and impair glutamate uptake, which results in neuronal death (Rothstein et al., 1993). Aβ was found to decrease the levels of EAAT1 and EAAT2 in cultured astrocytes (Zumkehr et al., 2015; Huang et al., 2018). In contrast, in another study, Aβ reduced the amount of EAAT2 on the cell surface of cultured astrocytes but had no effect on the overall levels of EAAT1 or EAAT2 (Scimemi et al., 2013). In AD patients' hippocampal CA2-CA3 pyramidal neurons, EAAT3 exhibit abnormal aggregations (Duerson et al., 2009). Studies conducted on animals have produced contradictory results. While Cassano et al. (2012) had reported a decrease in the hippocampal expression of EAAT3 in the 3xTg-AD mice (Cassano et al., 2012), a study by Schallier et al. (2011) revealed

that the hippocampi of AβPP23 AD mice had higher levels of EAAT3 expression (Schallier et al., 2011). Furthermore, as demonstrated, myelinic NMDA GluRs containing GluN2C/D are cytotoxically over-activated in acute ischemic myelin injury due to vesicular glutamate released from axons in the periaxonal space (Doyle et al., 2018). Functional NMDA receptors are expressed by OLs, according to a different study (Káradóttir et al., 2005). Therefore, when extracellular glutamate is elevated in various pathological circumstances, oligodendrocyte NMDA receptors may play a role in the development of WM damage (Volpe, 2001; Stys, 2004; Matute et al., 2001; Dewar, Underhill & Goldberg, 2003).

Research on the pharmacology, physiological, and pathological roles of glutamate transport inhibitors is highly beneficial regarding glutamate excitotoxicity. Blockers of vesicular glutamate release significantly decreased the Ca^{+2}-dependent glutamate release. This demonstrates the relevance of vesicular release to the elevation of glutamate amid ischemia in the WM (Doyle et al., 2018). DL-TBOA is a competitive, non-transportable blocker of EAAT1 and EAAT2, which are found in astrocytes, as well as EAAT3, EAAT4 and EAAT5, which are found in neurons, both post- and presynaptically (Shimamoto et al., 1998; Malik & Willnow, 2019). EAAT2 are also present in the presynaptic area in axon terminals, and EAAT3 are also located in cell soma and dendrites (Malik & Willnow, 2019). DL-TBOA inhibits EAATs with IC_{50} values of 6 µM, 6 µM and 70 µM, for EAAT2, EAAT3 and EAAT1, respectively (Jabaudon et al., 1999). DL-TBOA also inhibits EAAT4 and EAAT5 with K_i values of 4.4 µM and 3.2 µM respectively (Shigeriet al., 2008). TBOA elicited a peak increase in resting glutamate in the adult corpus callosum, suggesting that glutamate regulation in WM is still occurring under physiological conditions via glutamate transport (Doyle et al., 2018). QNZ46 is a non-competitive NMDA antagonist with a high selectivity for GluN2C/D-containing GluRs. According to Doyle et al. (2018), QNZ-46 exhibits unique myelin accumulation and retention, is brain accessible, and possesses the fundamental characteristics of a therapeutically effective medication, indicating exceptional clinical prospects against excitotoxic myelin injury (Doyle et al., 2018).

In the present study, we employed the neurosphere assay technique developed by Soares et al. (2020) to evaluate the excitotoxic consequences of Aβ treatment on the myelin content of DIV14 cells, as well as the potential amelioration upon DL-TBOA and QNZ46 administration. We first observed a significant myelin reduction in Aβ-treated cells when compared to the untreated group. This is further corroborated by earlier research showing that the $A\beta_{1-42}$ oligomer inhibited the formation of myelin sheets at 1 µM *in vitro* (Horiuchi et al., 2012). This phenotype was efficiently alleviated upon combined treatment with 10µM DL-TBOA. This concentration of DL-TBOA blocked specifically the EAAT3, EAAT4 and EAAT5 that are found in neurons, and did not have a similar effect on EAAT1, which require higher concentration (Jabaudon et al., 1999; Shigeriet al., 2008). This would imply that DL-TBOA blocked the glutamate influx inside the neurons. However, DL-TBOA did not affect the glutamate influx inside the astrocytes, which continue to convert glutamate into glutamine, resulting in no further increase of perisynaptic glutamate concentration due to neuron EAAT inhibition. This is in line with findings from previous studies. In one of these studies, DL-TBOA was found to reduce ischemia-evoked glutamate efflux by 42% (Phillis et al., 1994). Furthermore, our findings align with earlier in vivo results of a reversal of Na-dependent glutamate transport (Seki et al., 1999).

Myelin levels were unaltered upon combined treatment with QNZ46 when compared to the Aβ-treated group. These results contradict the claims of Doyle et al. (2018) that the selective negative allosteric modulator QNZ-46 can prevent the cytotoxic over-activation of GluN2C/D-containing myelinic NMDA GluRs (Doyle et al., 2018).

Our results imply that administering a competitive EAAT inhibitor may lessen the glutamate excitotoxicity caused by Aβ (Figure 46). Further research focusing on development of non-substrate inhibitors that impede the reverse glutamate uptake by neurons and

astrocytes may be useful as treatments for neurological disorders marked by glutamate excitotoxicity (Anderson, 2001).

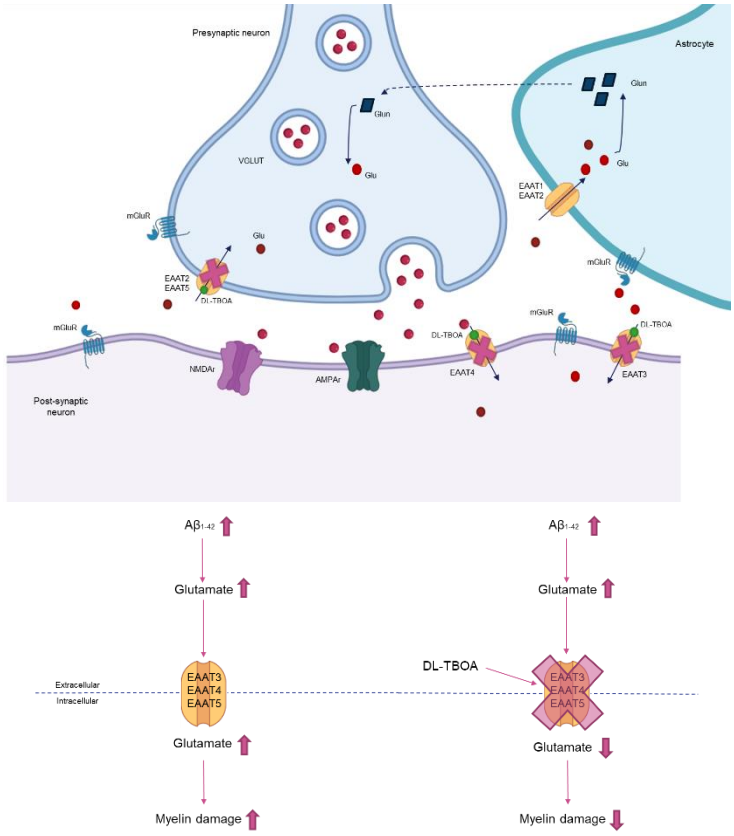

Figure 46. Schematic representation of the proposed mechanism of DL-TBOA EAAT inhibition upon Aβ-induced glutamate excitotoxicity. Designed with BioRender. Glu: glutamate; Gln: glutamine; EAAT: excitatory amino acid transporter; VGLUT: vesicular glutamate transporter; NMDAr: N-methyl-D-aspartate acid receptors; AMPAr: a-amino-3-hydroxy-5-methyl-4-isoxazole propionic acid receptor; mGluR: metabotropic receptor; DL-TBOA: DL-Threo-Beta-Benzyloxyaspartate.

Lastly, our *in vitro* studies revealed that the neuron population was unchained across all conditions. Our results contrast with earlier research conducted by Kim and colleagues (2003). Their findings indicated that even at concentrations as low as 0.6 M, soluble

oligomeric Aβ caused neurotoxicity in CNS neuronal precursor cells (Kim et al., 2003).

In summary, this study elucidates the important role of the fornix at the early stages of AD. Additional research on the fornix, would allow a deeper comprehension of the contribution of forniceal pathologic conditions to neurodegenerative diseases.

CONCLUSIONS

Conclusions

1. The dorsal fornix of young APP/PS1 mice exhibits a significant decline in MBP and MOG levels, which could indicate an early event in myelin loss during AD.

2. Mature OLs are decreasing while OPCs are increasing in the dorsal fornix of young APP/PS1 mice, which could be a response to damage. This could explain the deficits in myelin due to a disruption in remyelination.

3. Nfl levels in the dorsal fornix do not vary across phenotypes and age groups, indicating that changes in the axonal abundance are not detectable at this stage in the dorsal fornix.

4. There are no significant changes in MBP and MOG in the hippocampus of young APP/PS1 mice since the disease has not yet developed to a sufficient degree.

5. The hippocampus of transgenic mice exhibits no alterations in mature OLs and OPCs.

6. Myelin loss is induced by Aβ treatment in neurosphere cultures.

7. Aβ-induced toxicity is efficiently mitigated upon treatment with DL-TBOA in DIV14 cells, implying that EAAT are implicating in the glutamate uptake inside neurons.

8. Aβ treatment has no impact on the neuron population in in vitro studies.

Our final conclusion is that dorsal fornix demyelination is an early event in the progression of AD. More investigation of this area would facilitate a more profound understanding of its significance and implication to memory decline in the course of AD.

RESUMEN

Lista de Abreviaturas

Aβ/ Abeta: beta amiloide

aMCI: deterioro cognitivo leve amnésico

AMPA: ácido a-amino-3-hidroxi-5-metil-4-isoxazol propiónico

AMPAr: receptor del ácido a-amino-3-hidroxi-5-metil-4-isoxazol propiónico

APP/PS1: ratón doble transgénico APPswe/ PSEN1dE9

bFGF: factor básico de crecimiento de fibroblastos

CTR: grupo de control

DIV: día in vitro

df: fórnix dorsal

DL-TBOA: DL-Treo-Beta-Benciloxiaspartato

DTI: imágenes con tensor de difusión

EA: enfermedad de Alzheimer

EAA: aminoácido excitador

EAAT: transportador de aminoácidos excitadores

EGF: factor de crecimiento epidérmico

HBSS: solución salina equilibrada de Hanks

LCR: líquido cefalorraquídeo

MAG: proteína asociada a la mielina

MBP: proteína básica de la mielina

MCI: deterioro cognitivo leve

MOG: glicoproteína mielínica oligodendrocitaria

Nfl: Cadena ligera de neurofilamentos

NG2: antígeno nervioso/glial 2

NMDA: N-metil-D-aspartato ácido

NMDAr: Receptor del ácido N-metil-D-aspartato

Olig2: Factor de transcripción 2 de oligodendrocitos

OL: oligodendrocitos

OPC: células progenitoras de oligodendrocitos

PDGFRα: receptor alfa del factor de crecimiento derivado de plaquetas

PFA: paraformaldehído

QNZ46: ácido 4-[6-metoxi-2-[(1E)-2-(3-nitrofenil) etenil]-4-oxo-3(4H)quinazolinil]benzoico

RM: Resonancia magnética

SFM: medio libre de suero

SNC: sistema nervioso central

SVZ: zona subventricular

WM: materia blanca

WT: cepa salvaje

Sinopsis

La enfermedad de Alzheimer (EA) es una condición neurodegenerativa que dificulta el pensamiento, la memoria y el comportamiento. Dos de las principales anomalías cerebrales relacionadas con la EA son la acumulación de beta-amiloide (Aβ) en agregados fuera de las neuronas y la acumulación de una forma aberrante de la proteína tau dentro de las neuronas. Además, la degeneración de la mielina también se ha documentado ampliamente en pacientes con EA y en modelos animales experimentales. La desmielinización es un evento temprano que surge antes de las patologías tau y Aβ e incluso antes de la atrofia de la materia blanca y gris, y también se ha observado en el fórnix. El fórnix es un fino haz de materia blanca en forma de C formado por fibras mielinizadas, implicado en la memoria episódica. Además, en las fases iniciales de la EA, se ha observado que las anomalías de los oligodendrocitos (OL) sufren alteraciones significativas relacionadas con el deterioro cognitivo. Otro rasgo observado durante la patología de la EA es la liberación excesiva de glutamato en el espacio extracelular por parte de los terminales nerviosos presinápticos, lo que provoca excitotoxicidad al sobreestimular especialmente los receptores NMDA y altera la captación de glutamato por el EAAT. Además, los receptores NMDA funcionales se expresan en la vaina de mielina, lo que podría provocar parcialmente daños en la mielina paranodal en respuesta a niveles elevados de glutamato.

Este trabajo pretende abordar el hecho de que la desmielinización y las alteraciones en las células del linaje oligodendrocitario se producen específicamente en el fórnix dorsal, en ratones transgénicos jóvenes, antes del desarrollo del deterioro cognitivo. Otro objetivo de este estudio, es demostrar que el aumento de glutamato se debe al aumento de Aβ en las neuronas cultivadas. El glutamato podría escaparse de los axones y unirse a los receptores de glutamato NMDA y EAAT, causando daños en la mielina.

Los resultados obtenidos demostraron una disminución significativa de los niveles de componentes de mielina en el fórnix dorsal de los ratones APP/PS1 en comparación con los controles, mientras que los niveles del marcador de neuráxones no se modificaron. Además, se observó un aumento de los niveles de células progenitoras de oligodendrocitos y, al mismo tiempo, una disminución significativa de OL mielinizantes maduras. Simultáneamente, estas alteraciones no se detectaron en sus hipocampos. En los cultivos de neuroesferas, el tratamiento con Aβ produjo una disminución significativa de los niveles de mielina. El co-tratamiento con DL-TBOA, un bloqueante competitivo de EAAT, revirtió eficientemente este descenso. No hubo cambios apreciables en los niveles de mielina en el tratamiento combinado de Aβ con QNZ46, un antagonista no competitivo de NMDA, en comparación con el grupo tratado con Aβ. Además, la población de neuronas no se vio afectada por el tratamiento con Aβ, y no se observaron diferencias notables en ninguna circunstancia.

En conclusión, los ratones APP/PS1 presentan desmielinización del fórnix dorsal acompañada de cambios en las células del linaje oligodendrocitario. En cultivos de neuroesferas, las células tratadas con Aβ también sufren desmielinización, que se revirtió tras el tratamiento con DL-TBOA. Esto implica que la excitotoxicidad por glutamato inducida por Aβ puede ser un mecanismo potencial de degeneración de la mielina.

Introducción

La enfermedad de Alzheimer

La enfermedad de Alzheimer (EA) es un trastorno neurodegenerativo que afecta al pensamiento, la memoria y el comportamiento, lo que provoca dificultades para realizar las actividades cotidianas (Guo et al., 2020). Fue descubierta por el médico alemán Alois Alzheimer en 1907 y se caracteriza por síntomas como confusión mental, dificultad para dormir y deterioro de la memoria (Alzheimer, 1907; Ramirez-Bermudez, 2012). Las anomalías cerebrales asociadas a la EA incluyen la acumulación de placas de beta-amiloide (Aβ) fuera de las neuronas y ovillos de tau dentro de las neuronas, lo que interrumpe la comunicación química y causa problemas cognitivos, de aprendizaje y de funcionamiento diario (Yiannopoulou & Papageorgiou, 2020).

La demencia de Alzheimer suele comenzar con alteraciones leves de la memoria y evolucionar hacia síntomas más graves. La progresión de la enfermedad consta de tres fases principales: preclínica, deterioro cognitivo leve (MCI) y demencia. La identificación precoz de los pacientes con riesgo de desarrollar MCI es posible mediante biomarcadores como la resonancia magnética y la tomografía por emisión de positrones (Porsteinsson et al., 2021).

Las causas y los factores de riesgo son la edad avanzada, la genética y los antecedentes familiares (Silva et al., 2019; Schworer et al., 2024). Más de 55 millones de personas padecen demencia en todo el mundo, el 60% de ellas en países de renta baja y media. En 2050 habrá 139 millones de pacientes, y la enfermedad de Alzheimer representará el 60-70% de los casos (World Alzheimer Report, 2023).

Los tratamientos farmacológicos de la EA están en curso debido a la complejidad de su fisiopatología y a su etiología desconocida (Peng et al., 2023). Se ha descubierto que más de 100 variantes en al

menos 34 genes son patogénicas o modifican el riesgo en la EA (Nystuen et al., 2024). La causa exacta de la EA sigue siendo desconocida, pero la hipótesis de la cascada amiloide es la principal hipótesis a explorar debido a su importancia clínica y a la abundancia de datos experimentales que la apoyan (Hardy & Higgins, 1992; Granzotto & Sensi, 2024).

Linaje de oligodendrocitos y la enfermedad de Alzheimer

Los oligodendrocitos (OL) son, junto con la microglía y la astroglía, uno de los principales tipos de células gliales del sistema nervioso central (SNC) (Kuhn et al., 2019). Se encuentran en diversas regiones, como en la sustancia gris tanto en la sustancia blanca (WM) (Verkhratsky & Butt, 2013). Las células progenitoras de oligodendrocitos (OPC) son la fuente de las OL (Hardy & Reynolds, 1991), cruciales para la producción de mielina (Raine, 1984). Las OPC apoyan la plasticidad del SNC y sirven como fuente endógena de OL (Young, 2013), pueden proliferar, migrar y diferenciarse en OL maduros a lo largo de su vida (Franklin & Ffrench-Constant, 2008).

Las disfunciones de los OL y OPC en la patología de la EA incluyen el deterioro cognitivo en las primeras fases (Zhang et al., 2019), daños en la WM en cerebros postmortem de EA y aberraciones de la WM en pacientes al menos diez años antes de que aparezcan los síntomas clínicos (Scheltens et al., 1995; Gouw et al., 2008; Nasrabady et al., 2018). Los modelos animales de EA han mostrado anomalías en las células del linaje oligodendrocitario, siendo las alteraciones de la WM un indicador clínico precoz en ratones APP/PS1 (Chao et al., 2018; Dong et al., 2018). Se han encontrado OPC senescentes en los cerebros de pacientes con EA y ratones APP/PS1, y sus perfiles de secreción pueden influir en la inflamación, la desmielinización y la disfunción neuronal (Han et al., 2022).

La mielina y la enfermedad de Alzheimer

La mielina, una estructura densa de varias capas, fue descubierta en 1717 por Van Leeuwenhoek y el termino fue utilizado por primera vez en 1854 por Virchow (Kister & Kister, 2023; Boullerne, 2016). Consta de mielina compacta y no compacta (Soldan & Pirko, 2012), con nodos de Ranvier que las segregan a lo largo de axones individuales (Aggarwal et al., 2011). La mielina es un aislante eléctrico eficaz y menos permeable a los iones, lo que influye en su deformación y rigidez (Huxley & Stämpfli, 1949). Su composición lipídica es crucial para la comunicación celular e influye en la maduración, producción e integridad axonal de los oligodendrocitos (Lee et al., 2012).

El daño de la mielina es frecuente en pacientes con EA y en modelos animales experimentales. Las investigaciones muestran una reducción de mielina y lípidos, niveles reducidos de MBP, colesterol más bajo y niveles más altos de péptido Aβ en cerebros con EA (Roher et al., 2002). Recientes métodos de imagen cerebral han mejorado la evaluación de las alteraciones de la mielina en la EA, correlacionándose el deterioro cognitivo en pacientes con EA con cambios en la organización de la mielina (Kavroulakis et al., 2018). La degeneración temprana de la mielina en ratones APP/PS1 precede al deterioro cognitivo a los 6 meses de edad, lo que sugiere que puede estar implicada en la fisiopatología de la EA (Dong et al., 2018).

Glutamato y la enfermedad de Alzheimer

El glutamato, neurotransmisor clave del sistema nervioso, es esencial para la memoria, la potenciación a largo plazo y la plasticidad sináptica (Alix & Domingues, 2011). También puede ser una neurotoxina y contribuir a enfermedades neurológicas (Smith, 2000). La clonación molecular ha identificado varias familias de

proteínas receptoras de glutamato, divididas en receptores ionotrópicos y metabotrópicos (Gregory et al., 2013; Zhou & Danbolt, 2014). El receptor NMDA, un receptor de aminoácidos excitadores (EAA), se ha estudiado ampliamente por su papel en la plasticidad sináptica (Dingledine et al., 1999). Existen cinco transportadores de aminoácidos excitatorios (EAAT) distribuidos en diversas áreas cerebrales y tipos celulares (Lehre et al., 1995; Holmseth et al., 2012). El EAAT3 es el transportador de glutamato más eficiente y se encuentra principalmente en las neuronas postsinápticas (Holmseth et al., 2012), mientras que los EAAT2 están presentes sobre todo en los astrocitos (Schreiner et al., 2014).

El glutamato que es absorbido por la EAAT en los astrocitos desde el líquido extracelular se convierte en glutamina, que es liberada al líquido extracelular, absorbida por las neuronas y convertida de nuevo en glutamato, lo que se conoce como el ciclo glutamina-glutamato. La liberación excesiva de glutamato por los astrocitos y las terminales nerviosas conduce a la excitotoxicidad, sobreestimulando los receptores de glutamato, en particular los receptores NMDA (Hertz, 1979).

La desregulación del glutamato en la EA está influida por la acumulación de proteínas y el estado de agregación, presentes en diferentes etapas del deterioro cognitivo. La excitotoxicidad glutamatérgica es causada por Aβ (Fuchsberger et al., 2016) o tau hiperfosforilada, lo que conduce a la excitabilidad neuronal y la sobreexcitación de receptores de glutamato (Huijbers et al., 2019; 2015). La EA está también relacionada con una deficiente absorción de glutamato (Walton & Dodd, 2006).

Varios modelos animales de EA muestran alteraciones en la señalización del glutamato a medida que progresa la enfermedad, con mecanismos excitotóxicos que causan pérdida de oligodendrocitos y neuronas en respuesta a niveles elevados de glutamato extracelular (Mark et al., 2001; Matute et al., 1997; Lipton & Rosenberg, 1994).

El sistema límbico y la enfermedad de Alzheimer

El sistema límbico, un grupo de regiones cerebrales, es responsable de controlar los procesos viscerales y autonómicos y de apoyar funciones cognitivas como la memoria espacial, el aprendizaje, la motivación y el procesamiento emocional y social (Hariri et al., 2000; Patestas & Gartner, 2006).

El fórnix, un haz de sustancia blanca en forma de C situado en la cara mesial de los hemisferios cerebrales, conecta el hipocampo y otras regiones límbicas (Senova et al. 2020). El fórnix desempeña un papel crucial en la memoria episódica, que se deteriora con el envejecimiento (Head et al., 2008) y es el primer dominio cognitivo afectado por la EA (Salmon & Butters, 1992). La degeneración del fórnix en la patología de la EA es más precisa que la atrofia del hipocampo (Fletcher et al., 2013). La disminución de la anisotropía franccional (FA) en el fórnix es más sensible que los cambios de volumen y/o área en la resonancia magnética estructural en pacientes con EA (Douaud et al., 2013). Las alteraciones del fórnix se han documentado como un biomarcador de la transición de sujetos con MCI cognitivamente normales a amnésicos (Zhuang et al., 2013). La EA temprana está relacionada con la desmielinización del fórnix y una elevada carga de Aβ, lo que acelera el deterioro de la memoria episódica (Rabin et al., 2019).

Objetivos

Los objetivos específicos de este estudio son:

1. Dilucidar la desmielinización del fórnix dorsal en ratones APP/PS1 jóvenes.

2. Detectar alteraciones en las células del linaje oligodendrocitario en el fórnix dorsal de ratones APP/PS1 jóvenes.

3. Determinar si el hipocampo de los ratones transgénicos jóvenes presenta desmielinización u otras anomalías de las OLs.

4. Investigar si la excitotoxicidad por glutamato inducida por Aβ afecta los receptores NMDA y EAAT y posteriormente causa desmielinización en cultivos de neuroesferas.

Material y métodos

Animales de experimentación

Este estudio utiliza ratones transgénicos dobles APPswe/ PSEN1dE9 (APP/PS1) como modelo de la enfermedad de Alzheimer. La cepa C57BL/6J se utilizó como grupo de control. Ambas cepas se obtuvieron de los laboratorios Jackson de Estados Unidos y se establecieron en la UCIM de la Universitat de València. Las crías dobles transgénicas hemicigóticas se obtuvieron mediante cruces y se mantuvieron en condiciones específicas (23±1°C, 60% de humedad, ciclos luz-oscuridad de 12h-12h, dieta ad libitum).

En el proyecto se utilizaron 40 ratones, la mitad para ensayos de inmunofluorescencia y la otra mitad para inmunotransferencia. Todos los procedimientos que requirieron ratones fueron aprobados por la Comisión de Ética en la Investigación Experimental del Vicerrectorado de Investigación de la Universidad de Valencia (ref: 2022 VSC PEA 0123) y de acuerdo con el Real Decreto 53/2013.

Equipamiento

El grupo de investigación de la Dra. Ana Lloret Alcañiz en la Universidad de Valencia utilizó instalaciones y equipos de laboratorio del Departamento de Fisiología, la UCIM y el SCSIE. También utilizaron equipos del Instituto de Medicina Molecular João Lobo Antunes durante la estancia internacional en Lisboa.

Métodos de obtención de muestras

Sacrificio de animales, extracción de tejidos y preparación de homogeneizados

Se realizaron análisis de Western blot en 20 ratones, incluyendo cepas doble transgénicas y de tipo salvaje. Se extrajeron muestras de cerebro, se homogeneizaron y conservaron a -80ºC para su posterior análisis de proteínas. Se utilizaron métodos mecánicos y químicos, con 100 mg de tejido añadidos a 1 mL de tampón de lisis, y homogeneización durante unos segundos.

Fijación y preparación de tejido para inmunofluorescencia

Se utilizaron 20 ratones para el análisis de proteínas y los ensayos de inmunofluorescencia, incluidos transgénicos y salvajes. Se sacrificaron bajo anestesia entre los cuatro y los seis meses de edad y se les administró una inyección intraperitoneal de solución Eutanax. Se realizó una perfusión transcardial de solución salina y paraformaldehído (PFA) al 4%. Los cerebros se posfijaron durante 24 horas en sacarosa 30%. El tejido cerebral se cortó en cortes coronales de 40 µm de grosor. Los cortes se almacenaron en solución de sacarosa 30% para los ensayos de inmunofluorescencia.

Métodos analíticos

Western blotting

Primero se utilizó el método de Lowry para determinar la concentración total de proteínas en las muestras. Se utilizó la técnica Western Blotting para determinar los niveles de diferentes proteínas de interés en el tejido homogeneizado obtenido. En este estudio se utilizaron geles de resolución de poliacrilamida al 15%, 12,5% y 10%.

Se prepararon muestras de proteínas a partir de muestras de tejido homogeneizadas y se incubaron a 95°C durante 5 minutos. Las muestras se cargaron en geles de poliacrilamida y se sometieron a 100 voltios durante 90 minutos. El gel se recogió y se electrotransfirió y la alimentación se ajustó a 240 mA durante 90 minutos.

Para la detección de las proteínas, la membrana se incuba con una solución de bloqueo para una hora, seguida de los anticuerpos primario específicos durante toda la noche. Se retiran los anticuerpos primarios y se realizan tres lavados con TBS-t. A continuación, se incuba la membrana con los anticuerpos secundarios correspondientes. La membrana se expone para la detección por quimioluminiscencia, se revela con el ImageQuantTM LAS 4000. Para normalizar los niveles de proteínas, se determinaron los niveles de β-tubulina en cada membrana como control de carga. Las imágenes de las membranas se analizaron utilizando el software ImageGauge V4.0, que permite la densitometría de las proteínas en cada membrana.

Inmunofluorescencia

En esta tesis se utilizó la técnica de cortes montados en portaobjetos, que consiste en montar cortes de tejido en portaobjetos utilizando un marcador indeleble. Este método permite seleccionar regiones de tejido de interés.

El tampón de citrato de sodio se calentó a 95°C para una revelación eficaz de los antígenos. A continuación, los cortes se lavaron tres veces con PBS-t para eliminar el exceso de sacarosa. El tejido se incubó con la solución de bloqueo por una hora, y luego con los anticuerpos primarios durante toda la noche. Al día siguiente, se incubó con los anticuerpos secundarios. El tejido se lavó tres veces para eliminar el exceso de anticuerpos. El compuesto Hoechst se utilizó para observar los núcleos de las células individuales. Los portaobjetos se cubrieron con cubreobjetos y se almacenaron a 4°C en la oscuridad para su posterior examen con un microscopio confocal.

Ensayo de neuroesferas

El protocolo consistió en aislar las neuronas progenitoras de la SVZ, expandirlas como neuroesferas y dividirlas en neuronas, astrocitos y oligodendrocitos. Se preparó un medio libre de suero (SFM) para la disección y se utilizó un medio de disección HBSS para la microdisección de la zona subventricular (SVZ).

Las crías de ratón fueron eutanasiadas y decapitadas, se expuso la superficie del cráneo y se aisló el cerebro. El cerebro se colocó en una placa de Petri, se diseccionó al microscopio y se retiraron las meninges. Se descartaron el cerebelo y los bulbos olfatorios, y el cerebro se cortó en secciones coronales. Se diseccionó la SVZ y se recogió en un tubo de muestras con una solución de HBSS. Se añadió tripsina-EDTA para disociar el tejido, que se lavó y resuspendió en SFM suplementado con EGF y bFGF. El tejido se disoció

mecánicamente para obtener una solución celular homogénea. Las células se sembraron en placas de Petri y se incubaron durante 6 días para formar neuroesferas primarias. Las neuroesferas se diferenciaron durante 14 días, y se realizó una reposición de medio para suministrar nutrientes y eliminar los productos de desecho. Se aplicaron tratamientos farmacológicos de 1µM de Aβ combinados con 10µM DL-TBOA y 10µM QNZ46 en DIV13 para evaluar su potencial en el alivio de los efectos degenerativos de Aβ.

La fijación celular en DIV14 se realizó con PFA al 4%. El SFM se retiró, se añadieron 500 µL de 4% PFA para 20 minutos y los cubreobjetos se lavaron tres veces con PBS. Los cubreobjetos se almacenaron en PBS y el ensayo inmunocitoquímico se realizó posteriormente.

Microscopía confocal

Se utilizó el microscopio confocal de fluorescencia FV1000 para observar secciones de tejido y capturar fotografías de las regiones de interés. Las imágenes se capturaron y analizaron tras la adquisición.

Análisis de imágenes

Se utilizó el software ImageJ para analizar las imágenes, cuantificando la cantidad de proteína y la intensidad de fluorescencia. Se analizaron tres imágenes por cada animal, determinando el área de interés y la fluorescencia. Los porcentajes de colocalización se determinaron utilizando el plug-in Colocalization Threshold de ImageJ.

Análisis estadístico

El estudio calculó la media y la desviación típica de cada grupo utilizando diversos métodos. La prueba T-Student se utilizó para comparar dos valores de muestras paramétricas, mientras que la prueba ANOVA se aplicó para más. Se utilizó un valor p de 0,05 para validar la hipótesis. La prueba de Levene confirmó la homogeneidad de la varianza entre las muestras.

Resultados

Estudio de la morfología y estructura del fórnix dorsal

El objetivo del estudio era determinar las diferencias estructurales en el fórnix de ratones salvajes (WT) y transgénicos APP/PS1 marcando secciones coronales con la tinción fluorescente Hoechst. Se utilizó el Allen Brain Atlas (Figure 19) para identificar áreas cerebrales en cada sección, como el cuerpo calloso, el tercer ventrículo y el fórnix dorsal.

Se utilizó el software ImageJ para definir el área del fórnix, que no reveló diferencias significativas entre los ratones WT y APP/PS1 en los grupos de edad de 4 y 6 meses (Figures 20 & 21).

Se compararon los niveles de proteína axonal neuronal Nfl en el fórnix de los ratones transgénicos WT y APP/PS1, sin encontrar diferencias significativas en los niveles en los grupos de edad de 4 y 6 meses (Figures 22 & 23).

Estudio de los principales componentes de la mielina en el fórnix dorsal de ratones APP/PS1 y WT

Se examinó si el depósito axonal de mielina estaba alterado en el fórnix dorsal de ratones APP/PS1 jóvenes, de 4 y 6 meses de edad, utilizando ensayos de inmunofluorescencia para analizar los marcadores de mielina MBP y MOG.

Niveles de MBP y MOG en ratones de 4 meses

Las secciones coronales se tiñeron doblemente con anticuerpos anti-MBP y anti-Nfl o con anti-MOG y anti-Nfl, y se utilizó el colorante fluorescente Hoechst para marcar los núcleos celulares. El fórnix dorsal de ratones APP/PS1 de 4 meses de edad mostró una disminución significativa de los niveles de MBP y MOG en comparación con los ratones de tipo salvaje (Figures 24 & 26).

Se encontró una disminución significativa en el porcentaje de colocalización de MBP y Nfl, así como de colocalización de MOG y Nfl en el fórnix dorsal de ratones APP/PS1 comparados con los WT (Figures 25 & 27).

Niveles de MBP y MOG en ratones de 6 meses

Se examinó la degeneración de la mielina en ratones WT y APP/PS1 de 6 meses de edad. El ensayo de inmunofluorescencia mostró un descenso de los niveles de MBP y MOG en el fórnix dorsal de los ratones APP/PS1 en comparación con los ratones WT, lo que indica un aumento de la degeneración de la mielina relacionado con la edad (Figures 28 & 30).

Los ratones transgénicos mostraron una disminución en la colocalización de MBP con Nfl, y en la colocalización de MOG con Nfl en el fórnix dorsal en comparación con los ratones WT (Figures 29 & 31).

Estudio del linaje oligodendrocitario en el fórnix dorsal

Se investigó el linaje oligodendrocitario en el fórnix dorsal de ratones jóvenes de 4 y 6 meses de edad, controles y transgénicos, con el fin de investigar si la disminución de mielina en el fórnix dorsal de los ratones APP/PS1 se debía a una disminución del número de células progenitoras oligodendrocitarias o a su incapacidad para diferenciarse y madurar. Se examinó la presencia de dos marcadores principales, Olig2, que se encuentra principalmente en los oligodendrocitos maduros (OL) y PDGFRα, que abunda en las células progenitoras de oligodendrocitos (OPC).

PDGFRα y Olig 2 en ratones de 4 meses

El ensayo de inmunofluorescencia mostró un aumento modesto, pero no significativo de los niveles de PDGFRα en ratones APP/PS1 de 4 meses de edad en comparación con los controles. Al mismo tiempo, los niveles de Olig2 en el fórnix dorsal de ratones APP/PS1 de 4 meses no muestran cambios significativos en comparación con los ratones WT (Figures 32 & 33).

PDGFRα y Olig2 en ratones de 6 meses

Los resultados mostraron un notable aumento de los niveles de PDGFRα en los ratones transgénicos de 6 meses de edad en comparación con los ratones WT. Por el contrario, los niveles de Olig2 en el fórnix dorsal de los ratones APP/PS1 de 6 meses disminuyeron significativamente en comparación con los ratones WT (Figures 34 & 35).

Determinación de los niveles de componentes de mielina en el hipocampo mediante Western blot

Se examinó el impacto de las alteraciones en los componentes de la mielina en el hipocampo de ratones APP/PS1 mediante la medición por Western blot de los niveles de proteínas MBP y MOG.

Determinación de los niveles de MBP y MOG en ratones de 4 meses

Se examinaron los niveles de MBP y MOG en el hipocampo de ratones WT y APP/PS1 de 4 meses de edad mediante Western blot. Los ratones transgénicos presentaban niveles de MBP ligeramente inferiores a los controles. Los niveles de MOG en el hipocampo de los ratones transgénicos de 4 meses se mantuvieron sin cambios en comparación con los ratones WT (Figures 36 & 37).

Determinación de los niveles de MBP y MOG en ratones de 6 meses

El estudio evaluó los niveles de MBP y MOG en el hipocampo de ratones APP/PS1 de 6 meses de edad, mostrando una disminución modesta pero no estadísticamente significativa en comparación con los WT en ambos casos (Figures 38 & 39).

Determinación de los niveles de marcadores de linaje oligodendrocitario en el hipocampo mediante Western blot

Se midieron los niveles de PDGFRα y Olig2 en el hipocampo de ratones de control y transgénicos para determinar si también se alteraban las OPC y las OL maduras hipocampales.

Determinación de los niveles de PDGFRα y Olig2 en ratones de 4 meses

Los ratones APP/PS1 de 4 meses muestran una ligera disminución de los niveles de PDGFRα en el hipocampo y niveles más bajos de Olig2 en el hipocampo en comparación con los WT, pero estas diferencias no eran estadísticamente significativas (Figures 40 & 41).

Determinación de los niveles de PDGFRα y Olig2 en ratones de 6 meses

Se identificó un pequeño descenso de los niveles de PDGFRα y Olig2 en el hipocampo en ratones transgénicos de 6 meses de edad en comparación con los WT, pero esta diferencia no fue estadísticamente significativa (Figures 42 & 43).

Evaluación de los efectos neuroprotectores de DL-TBOA y QNZ46 en células DIV14 tras el tratamiento con Aβ

El objetivo del estudio era comprender los mecanismos moleculares que subyacen a la desmielinización asociada a la EA mediante el ensayo de neuroesferas. Las neuroesferas se trataron con 1µM de Aβ solo y con tratamientos combinados de 10 µM de DL-TBOA y 10 µM de QNZ46 en DIV13.

Determinación de los niveles de Nfl en células DIV14 para evaluar los efectos neuroprotectores de DL-TBOA y QNZ46 tras el tratamiento con Aβ

El estudio investigó el impacto del tratamiento con Aβ en la abundancia neuronal de células DIV14. Los resultados no mostraron variaciones significativas en la proteína axonal neuronal Nfl en todas las condiciones (Figure 44).

Determinación de los niveles de MBP en células DIV14 para evaluar los efectos neuroprotectores de DL-TBOA y QNZ46 tras el tratamiento con Aβ

El estudio investigó el efecto del tratamiento con Aβ sobre la degeneración de la mielina y los efectos mejoradores de los tratamientos con DL-TBOA y QNZ46. Los resultados mostraron una disminución significativa de los niveles de MBP en las células tratadas con Aβ en comparación con el grupo de control. Este descenso se restableció eficazmente en el grupo Aβ/DL-TBOA. Se observó un ligero pero no significativo aumento de los niveles de

MBP en los grupos Aβ/QNZ46 en comparación con el grupo Aβ (Figure 45).

Discusión

La atrofia del fórnix dorsal no es prominente en ratones APP/PS1 jóvenes

Aunque las principales lesiones en el cerebro de los pacientes con Alzheimer son las placas seniles y los ovillos neurofibrilares (Cummings, 2008), a lo largo de los años se han descrito alteraciones en la sustancia blanca (WM) que pueden ser importantes en el curso de la enfermedad. Nuestros resultados coinciden con estas conclusiones, al encontrar alteraciones tempranas en el fórnix dorsal del modelo de ratón de EA. De hecho, varios estudios realizados en los últimos años sugieren que entre los eventos tempranos de la EA de inicio tardío se encuentran las alteraciones microestructurales de la WM (Delbeuck et al., 2003; Brier et al., 2014). Estudios en animales y en humanos in vivo han demostrado que la alteración de la WM se produce en una fase temprana del proceso de la EA (Brun & Englund, 1986; Englund et al., 1988; Bartzokis et al., 2004). Estas alteraciones de la WM se producen antes de que el deterioro neuronal y la atrofia sean perceptibles, haciendo a los individuos más susceptibles a los signos clínicos de la EA (Bartzokis et al., 2004).

El fórnix es uno de los haces de la WM que ha demostrado sufrir cambios estables y consistentes en la EA (Oishi & Lyketsos, 2014). Situado en la cara medial de los hemisferios cerebrales, el fórnix es el principal tracto de salida del hipocampo y es crucial para el desarrollo y el mantenimiento de los recuerdos declarativos (Thomas et al., 2011). Las alteraciones del fórnix, incluyendo la desmielinización y la pérdida axonal, se han observado ya en 1976 (Hopper & Vogel, 1976), y también se han relacionado repetidamente con la EA (Ringman et al., 2007; Teipel et al., 2007; Mielke et al., 2009; Acosta-Cabronero et al., 2010; Salat et al., 2010; Liu et al., 2011; Douaud et al., 2013). Dada su ubicación estratégica dentro del circuito de la memoria, su identificación en fases

preclínicas de la EA, y su tendencia a preceder a las alteraciones estructurales que se producen en el hipocampo, la degeneración del fórnix es muy prometedora como biomarcador temprano de la EA (Nowrangi & Rosenberg, 2015; Lacalle-Aurioles & Iturria-Medina, 2023) Sin embargo, aún no se ha realizado ninguna investigación específica sobre el fórnix. Por primera vez, hemos informado de una desmielinización específica del fórnix dorsal en ratones transgénicos de tan solo 4 meses de edad.

Así pues, el objetivo de esta tesis doctoral era determinar si la degeneración del fórnix dorsal está presente en ratones APP/PS1 transgénicos jóvenes, que se caracteriza por la sobreexpresión y procesamiento excesivo de la proteína APP (Jankowsky et al., 2004; Shen et al., 2018).

En la fisiopatología de la EA, la pérdida de neuronas es una característica básica y fundamental (Coleman & Flood, 1987; Hof et al., 1990) que comienza incluso en etapas preclínicas antes de que aparezcan los sellos neuropatológicos (Gómez-Isla et al., 1996). La atrofia fornical se ha descrito previamente en pacientes con EA (Callen et al., 2001), y los valores más bajos de FA se han relacionado con la desmielinización y la degeneración en el fornix WM (Nabizadeh et al., 2022). Los estudios que emplean técnicas histológicas, anatómicas de RM o de imágenes con tensor de difusión también han informado de atrofia fornical en ratones PDAPP (Gonzalez-Lima et al., 2001; Redwine et al., 2003; Song et al., 2004). Además, el análisis regional reveló un efecto importante en el fórnix dorsal, donde la FA se redujo en un 20% en los ratones CVN-AD (Badea et al., 2016). Según otro estudio, el Nfl plasmático mostró una correlación negativa con la FA en el fórnix de pacientes con EA. Esto sugiere que los niveles elevados de Nfl en plasma o suero pueden ser un indicador del grado de atrofia actualmente presente (Nabizadeh et al., 2022).

En primer lugar, queríamos evaluar si el fórnix dorsal de ratones transgénicos APP/PS1 jóvenes soporta la degeneración. Según nuestros datos, no hay variaciones perceptibles en los niveles de Nfl en el fórnix dorsal entre los grupos experimentales, lo que sugiere

que hay un número comparable de axones. Estos hallazgos son consistentes con estudios previos de Delatour y colegas (2006), donde el diámetro del fórnix dorsal era similar en animales jóvenes (10 semanas) APP/PS1 y de control, aunque disminuía con la edad (Delatour et al., 2006). Esto contrasta con los informes de otros autores que han demostrado que en ratones PDAPP, la atrofia del fórnix dorsal se describe a una edad tan temprana como los 3 meses (Gonzalez-Lima et al., 2001; Redwine et al., 2003).

La pérdida de mielina es evidente en el fórnix dorsal de ratones APP/PS1 jóvenes

Nuestros hallazgos indican una disminución significativa de los niveles de MBP y MOG en el fórnix dorsal de ratones APP/PS1 jóvenes en comparación con los de tipo salvaje. En consonancia con nuestros resultados, Dong et al. (2018) documentaron una degeneración temprana de la mielina en ratones APP/PS1 a los 3-6 meses de edad; esta patología se observó antes del deterioro cognitivo observado a los 6 meses de edad (Dong et al., 2018). Además, en ratones APP/PS1 de 2 meses de edad, Wu et al. (2017) encontraron cambios en la morfología de la mielina (Wu et al., 2017).

Nuestra investigación tampoco reveló una disminución significativa de los niveles de MBP y MOG en el hipocampo de ratones APP/PS1 jóvenes. Estos resultados corroboran los de otros estudios que hallaron que la mielinización es normal hasta los 3-6 meses de edad en ratones APP/PS1. Los defectos en la integridad y cantidad de mielina eran comunes a los 6 meses de edad en ratones APP/PS1, pero volvían a niveles de control en ratones de 9 meses (Radde et al., 2006; Oddo et al., 2003; Games et al., 1995). Esto podría sugerir que la desmielinización del fórnix dorsal es un acontecimiento temprano que precede a la desmielinización del hipocampo.

Estudios histoquímicos y de neuroimagen previos en la EA han revelado daños en la mielina (Dean et al., 2017; Bulk et al., 2018; Mitew et al., 2010; Nasrabady et al., 2010). Estudios previos han indicado una reducción de las proteínas de la mielina, MBP y CNPasa, en pacientes con EA (Roher et al., 2002). Se han observado amplias reducciones en la integridad de la WM en estudios DTI de EA y MCI, siendo los lóbulos temporales los que muestran los cambios más consistentes (Chua et al., 2008; Bozzali et al., 2002; Huang et al., 2007; Naggara et al., 2006; Xie et al., 2006). Además, la anisotropía fraccional del fórnix está disminuida en pacientes con EA, según estudios de rastreo de fibras DTI (Teipel et al., 2007; Bennett et al., 2015). Varios estudios que emplean DTI y RM estructural demostraron alteraciones en la WM parahipocampal en sujetos con envejecimiento y MCI (Kalus et al., 2006; Stoub et al., 2006; Rogalski et al., 2009; Wang et al., 2012). Se ha descubierto que la atrofia del hipocampo y la FA del fórnix se correlacionan en la EA, lo que se ha observado en el envejecimiento normal, el MCI y la EA preclínica (Firbank et al., 2007; Pievani et al., 2010; Lee et al., 2012). Lee y sus colegas (2012) informaron de que, en la EA, los defectos axonales subcorticales y el daño neuronal cortical están probablemente estrechamente relacionados, lo que quizá indique una relación patogénica entre ambos (Lee et al., 2012). Según Wu y sus colegas (2017), se pudieron identificar alteraciones de la mielinización en las primeras etapas de los ratones APP/PS1, lo que sugiere un posible vínculo entre la fisiopatología de la EA y el desarrollo de la mielinización (Wu et al., 2017). La investigación sobre la esclerosis múltiple y el envejecimiento se ha interesado durante mucho tiempo por los anticuerpos antimielina, anti-MOG y anti-MBP. Los cambios en la vaina de mielina relacionados con la edad se han relacionado con la regulación a la baja de MBP y MOG (Xie et al., 2013). La propia proteína MBP ha sido investigada y podría servir como biomarcador de daño en el tejido cerebral y enfermedades neurodegenerativas tanto en suero como en líquido cefalorraquídeo (Barkhof et al., 1992; Katsavos & Anagnostouli, 2013; Zavialova et al., 2017; Kim et al., 2018).

OPCs y OLs muestran alteraciones en el fórnix dorsal de ratones APP/PS1 jóvenes

Las células del linaje oligodendrocitario son vulnerables a la patología de la EA. La degradación de la mielina debida al deterioro de la reparación de las OPC podría ser un punto de partida en la EA (Sjobeck et al., 2005; Roher et al., 2002; Tian et al., 2004; Ihara et al., 2010). Según recientes investigaciones, los cambios oligodendrocitarios son una característica común de la EA (Chen et al., 2020; Brase et al., 2021). En la corteza humana postmortem de pacientes con EA, se descubrió que las densidades de oligodendrocitos estaban reducidas (Nasrabady et al., 2018; Povala et al., 2021). En otro estudio, Nielsen y sus colegas (2013) midieron las cantidades de NG2 soluble en los LCR de pacientes con EA y del grupo de control. Según sus hallazgos, los niveles de NG2 aumentaron con la edad, y los pacientes con EA tenían niveles más bajos de NG2 en el LCR que los sujetos no dementes (Nielsen et al., 2013). Además, se observó que las células Olig2-positivas eran más bajas en el cerebro de los pacientes con EA (Behrendt et al., 2013).

La idea de que la oligodendroglía contribuye a la patogénesis de la EA también está respaldada por estudios que interpretan la patología oligodendroglial en modelos de ratones transgénicos (Schmued et al., 2013; Behrendt et al., 2013). Al comparar ratones APP23 de 12 y 24 meses con ratones control, se observó una disminución significativa de las células NG2-glia (He & Shen, 2009).

Primero evaluamos los niveles de PDGFRα y Olig2 en el fórnix dorsal de ratones de 4 meses, donde no encontramos diferencias observadas entre los ratones APP/PS1 y los de tipo salvaje. A continuación, repetimos el mismo experimento en ratones de 6 meses, donde observamos un aumento significativo de los niveles de PDGFRα en el fórnix dorsal de los ratones APP/PS1 en comparación con los controles. Por el contrario, los niveles de Olig2 se redujeron significativamente en el fórnix dorsal de los ratones APP/PS1 en comparación con los ratones WT. Al evaluar los niveles

de PDGFRα y Olig2 en el hipocampo de los ratones APP/PS1 y WT no observamos diferencias significativas entre los grupos. Con respecto a estudios anteriores, existen hallazgos contradictorios en cuanto a las poblaciones de OPCs y OLs en ratones transgénicos.

En primer lugar, se observó una elevada proliferación de OPCs en el WM de ratones APP/PS1 de 6 meses de edad (Behrendt et al., 2013), lo que coincide con nuestros resultados en el fórnix dorsal de ratones APP/PS1 de 6 meses de edad, pero contradice la reducción de los niveles de OPCs en el hipocampo. Según investigaciones anteriores, el agotamiento de OPCs se observó en la región CA1 del hipocampo de ratones 3xTg-AD de 6 meses de edad (Desai et al., 2009; Desai et al., 2010), lo que no concuerda con nuestros hallazgos en el hipocampo de ratones APP/PS1. Esto podría deberse al hecho de que los ratones 3xTg-AD portan mutaciones en tres genes que conducen a la alteración de la WM en el hipocampo ya a los 2 meses de edad (Desai et al., 2010; Desai et al., 2009). Además, DeFlitch et al. (2022) informaron de que, si bien hay una disminución en la población de OL, particularmente en las regiones DG y CA3, la población de OPC en ratones APP/PS1 parece no haber cambiado en comparación con sus compañeros de camada de la misma edad (DeFlitch et al., 2022). Curiosamente, en los ratones APP/PS1, la proliferación y diferenciación de OPC aumentó durante esta ventana de tiempo en particular (6-8 meses), lo que sugiere que los mecanismos de reparación mediados por OPC pueden ser la causa de las mejoras en los defectos de mielina (Cai & Xiao, 2015). Según un análisis cuantitativo realizado en un estudio diferente, las OPC proliferaron activamente en la sustancia blanca del fórnix, concretamente en el vhc y la fimbria (Fukushima et al., 2015).

Se ha observado que las OPC migran desde la SVZ y se diferencian en OL maduras en el fórnix adulto (Menn et al. 2006). La senescencia celular se ha relacionado con varias enfermedades relacionadas con la edad, incluida la EA (Bhat et al., 2012). Un mayor número de OPC y astrocitos senescentes puede aumentar conjuntamente la carga de la patología de la EA y desempeñar un papel importante en la LOAD. Teniendo todo esto en cuenta, las OPC senescentes del fórnix

no logran diferenciarse en OL mielinizantes maduras, lo que contribuye a las patologías de la EA en las primeras etapas y podría ser un mecanismo potencial que explique nuestras observaciones. (Lau et al., 2023).

La excitotoxicidad de glutamato inducida por Aβ provoca pérdida de mielina

Según los estudios, los oligómeros de Aβ tienen la capacidad de unirse directamente a elementos cruciales de la sinapsis glutamatérgica, controlando así la liberación de glutamato en los terminales (Kabogo et al., 2010; Findley et al., 2019). Se cree que los niveles de glutamato extrasináptico aumentan por la liberación aberrante de glutamato inducida por Aβ, lo que conduce a la hiperestimulación de los receptores NMDA y a la sinaptotoxicidad en la EA (Olajide et al., 2021). Según investigaciones anteriores, los inhibidores de la actividad del sustrato EAAT pueden elevar los niveles de glutamato extracelular y perjudicar la captación de glutamato, lo que provoca la muerte neuronal (Rothstein et al., 1993). Se observó que Aβ disminuía los niveles de EAAT1 y EAAT2 en astrocitos cultivados (Zumkehr et al., 2015; Huang et al., 2018). Por el contrario, en otro estudio, Aβ redujo la cantidad de EAAT2 en la superficie celular de astrocitos cultivados, pero no tuvo ningún efecto sobre los niveles generales de EAAT1 o EAAT2 (Scimemi et al., 2013). En las neuronas piramidales CA2-CA3 del hipocampo de pacientes con EA, EAAT3 presenta agregaciones anormales (Duerson et al., 2009). Los estudios realizados en animales han arrojado resultados contradictorios. Mientras que Cassano et al. (2012) habían informado de una disminución de la expresión hipocampal de EAAT3 en los ratones 3xTg-AD (Cassano et al., 2012), un estudio de Schallier et al. (2011) reveló que los hipocampos de los ratones AβPP23 AD presentaban mayores niveles de expresión de EAAT3 (Schallier et al., 2011). Además, como se ha demostrado, los GluR NMDA mielínicos que contienen GluN2C/D se sobreactivan

citotóxicamente en la lesión isquémica aguda de la mielina debido al glutamato vesicular liberado de los axones en el espacio periaxonal (Doyle et al., 2018). Los receptores NMDA funcionales son expresados por los OL, según un estudio diferente (Káradóttir, et al., 2005). Por lo tanto, cuando el glutamato extracelular se eleva en diversas circunstancias patológicas, los receptores NMDA de los oligodendrocitos pueden desempeñar un papel en el desarrollo de daños en la WM (Volpe, 2001; Stys, 2004; Matute et al., 2001; Dewar, et al., 2003).

La investigación en farmacología, funciones fisiológicas y patológicas de los inhibidores del transporte de glutamato es muy beneficiosa en relación con la excitotoxicidad del glutamato. Los bloqueantes de la liberación vesicular de glutamato disminuyeron significativamente la liberación de glutamato dependiente de Ca^{+2}. Esto demuestra la relevancia de la liberación vesicular en la elevación de la excitotoxicidad por glutamato. Esto demuestra la relevancia de la liberación vesicular para la elevación de glutamato en medio de la isquemia en el WM (Doyle et al., 2018). El DL-TBOA es un bloqueante competitivo no transportable de EAAT1 y EAAT2, que se encuentran en los astrocitos, así como de EAAT3, EAAT4 y EAAT5, que se encuentran en las neuronas, tanto post- como presinápticamente (Shimamoto et al., 1998; Malik & Willnow, 2019). Los EAAT2 también están presentes en la zona presináptica en los terminales de los axones, y los EAAT3 también se localizan en el soma celular y en las dendritas (Malik & Willnow, 2019). El DL-TBOA inhibe las EAAT con valores IC_{50} de 6 µM, 6 µM y 70 µM, para EAAT2, EAAT3 y EAAT1, respectivamente (Jabaudon et al., 1999). DL-TBOA también inhibe EAAT4 y EAAT5 con valores de K_i de 4,4 µM y 3,2 µM respectivamente (Shigeriet al., 2008). El TBOA provocó un aumento máximo del glutamato en reposo en el cuerpo calloso adulto, lo que sugiere que la regulación del glutamato en la WM sigue ocurriendo en condiciones fisiológicas a través del transporte de glutamato (Doyle et al., 2018). QNZ46 es un antagonista NMDA no competitivo con una alta selectividad para los GluR que contienen GluN2C/D. Según Doyle et al. (2018), QNZ-46 exhibe una acumulación y retención de mielina únicas, es accesible al cerebro y posee las

características fundamentales de un medicamento terapéuticamente eficaz, lo que indica perspectivas clínicas excepcionales contra la lesión excitotóxica de la mielina (Doyle et al., 2018).

En el presente estudio, empleamos la técnica de ensayo de neuroesferas desarrollada por Soares et al. (2020) para evaluar las consecuencias excitotóxicas del tratamiento con Aβ en el contenido de mielina de las células DIV14, así como la posible mejora tras la administración de DL-TBOA y QNZ46. En primer lugar, observamos una reducción significativa de la mielina en las células tratadas con Aβ en comparación con el grupo no tratado. Esto se ve corroborado por investigaciones anteriores que muestran que el oligómero $A\beta_{1-42}$ inhibe la formación de láminas de mielina a 1 µM in vitro (Horiuchi et al., 2012). Este fenotipo se alivió eficazmente con el tratamiento combinado con 10µM de DL-TBOA. Esta concentración de DL-TBOA bloqueó específicamente las EAAT3, EAAT4 y EAAT5 que se encuentran en las neuronas, y no tuvo un efecto similar sobre la EAAT1, que requiere una concentración mayor (Jabaudon et al., 1999; Shigeriet al., 2008). Esto implicaría que la DL-TBOA bloqueó la afluencia de glutamato en el interior de las neuronas. Sin embargo, la DL-TBOA no afectó a la afluencia de glutamato en el interior de los astrocitos, que siguen convirtiendo el glutamato en glutamina, por lo que la concentración perisináptica de glutamato no siguió aumentando debido a la inhibición de la EAAT neuronal. Esto coincide con los resultados de estudios anteriores. En uno de estos estudios, se observó que la DL-TBOA reducía el flujo de glutamato provocado por la isquemia en un 42% (Phillis et al., 1994). Además, nuestros hallazgos coinciden con resultados anteriores in vivo de una inversión del transporte de glutamato dependiente del Na (Seki et al., 1999).

Los niveles de mielina no se vieron alterados tras el tratamiento combinado con QNZ46 en comparación con el grupo tratado con Aβ. Estos resultados contradicen las afirmaciones de Doyle et al. (2018) de que el modulador alostérico negativo selectivo QNZ-46 puede

prevenir la sobreactivación citotóxica de los NMDA GluR mielínicos que contienen GluN2C/D (Doyle et al., 2018).

Nuestros resultados implican que la administración de un inhibidor competitivo de EAAT puede disminuir la excitotoxicidad del glutamato causada por Aβ (Figura 46). Otras investigaciones centradas en el desarrollo de inhibidores no sustratos que impidan la captación inversa de glutamato por neuronas y astrocitos pueden ser útiles como tratamientos para trastornos neurológicos marcados por la excitotoxicidad del glutamato (Anderson, 2001).

Por último, nuestros estudios *in vitro* revelaron que la población de neuronas estaba desencadenada en todas las condiciones. Nuestros resultados contrastan con investigaciones anteriores realizadas por Kim y colegas (2003). Sus hallazgos indicaron que incluso a concentraciones tan bajas como 0,6 M, el Aβ oligomérico soluble causaba neurotoxicidad en las células precursoras neuronales del SNC (Kim et al., 2003).

En resumen, este estudio dilucida el importante papel del fórnix en las primeras fases de la EA. Investigaciones adicionales sobre el fórnix, permitirían una comprensión más profunda de la contribución de las condiciones patológicas forniceales a las enfermedades neurodegenerativas.

Conclusiones

1. El fórnix dorsal de ratones APP/PS1 jóvenes muestra un descenso significativo en los niveles de MBP y MOG.

2. Los OL maduros disminuyen mientras que los OPC aumentan en el fórnix dorsal de ratones APP/PS1 jóvenes.

3. Los niveles de Nfl en el fórnix dorsal no varían entre fenotipos y grupos de edad.

4. Hay una disminución modesta pero no estadísticamente significativa de MBP y MOG en el hipocampo de ratones APP/PS1 jóvenes ya que la enfermedad aún no se ha desarrollado lo suficiente.

5. El hipocampo de los ratones transgénicos muestra una ligera reducción de OLs y OPCs maduros.

6. La pérdida de mielina es inducida por el tratamiento con Abeta en cultivos de neuroesferas.

7. La excitotoxicidad por glutamato inducida por Abeta es parcialmente mitigada por el tratamiento con DL-TBOA en células DIV14.

8. El tratamiento con Abeta no tiene impacto en la población neuronal en estudios *in vitro*.

Nuestra conclusión final es que la desmielinización del fórnix dorsal es un acontecimiento temprano en la progresión de la EA. Una mayor investigación de esta área facilitaría una comprensión más profunda de su importancia e implicación en el deterioro de la memoria en el curso de la EA.

REFERENCES

References

2023 Alzheimer's disease facts and figures. (2023). *Alzheimer's & Dementia*, *19*(4), 1598–1695. https://doi.org/10.1002/alz.13016

2024 Alzheimer's disease facts and figures. (2024). *Alzheimer's & Dementia*. https://doi.org/10.1002/alz.13809

Acosta-Cabronero, J., Williams, G. B., Pengas, G., & Nestor, P. J. (2009). Absolute diffusivities define the landscape of white matter degeneration in Alzheimer's disease. *Brain*, *133*(2), 529–539. https://doi.org/10.1093/brain/awp257

Agarwal, M., Alam, M. R., Haider, M. K., Malik, M. Z., & Kim, D. K. (2020). Alzheimer's Disease: An Overview of Major Hypotheses and Therapeutic Options in Nanotechnology. *Nanomaterials*, *11*(1), 59. https://doi.org/10.3390/nano11010059

Aggarwal, S., Yurlova, L., & Simons, M. (2011). Central nervous system myelin: structure, synthesis and assembly. *Trends in Cell Biology*, *21*(10), 585–593. https://doi.org/10.1016/j.tcb.2011.06.004

Aggleton, J., Vann, S., Oswald, C., & Good, M. (2000). Identifying cortical inputs to the rat hippocampus that subserve allocentric spatial processes: A simple problem with a complex answer. *Hippocampus*, *10*(4), 466–474. https://doi.org/10.1002/1098-1063(2000)10:4

Ali, Z., & Bhaskar, S. B. (2016). Basic statistical tools in research and data analysis. *Indian Journal of Anaesthesia/Indian Journal of Anaesthesia*, *60*(9), 662. https://doi.org/10.4103/0019-5049.190623

Alix, J. J., & De Jesus Domingues, A. M. (2011). White matter synapses: Form, function, and dysfunction. *Neurology*, *76*(4), 397–404. https://doi.org/10.1212/wnl.0b013e3182088273

Alty, J., Goldberg, L. R., Roccati, E., Lawler, K., Bai, Q., Huang, G., Bindoff, A. D., Li, R., Wang, X., St George, R. J., Rudd, K., Bartlett, L., Collins, J. M., Aiyede, M., Fernando, N., Bhagwat, A., Giffard, J., Salmon, K., McDonald, S., . . . Vickers, J. C. (2024). Development of a smartphone screening test for preclinical Alzheimer's disease and validation across the

dementia continuum. *BMC Neurology*, *24*(1). https://doi.org/10.1186/s12883-024-03609-z

Alzheimer, A. (1907). Über eine eigenartige Erkrankung der Hirnrinde. *Psychiatrie Und Psychisch-Gerichtliche Medizin*, *64*, 146–148.

Alzheimer, A. (1911). über eigenartige Krankheitsfälle des späteren Alters. *Zeitschrift Für Die Gesamte Neurologie Und Psychiatrie*, *4*(1), 356–385. https://doi.org/10.1007/bf02866241

Alzheimer's Disease International. (2023). World Alzheimer Report 2023: Reducing dementia risk: never too early, never too late. In *https://www.alzint.org/*. Retrieved May 30, 2024, from https://www.alzint.org/resource/world-alzheimer-report-2023/

Anderson, C. M., Bridges, R. J., Chamberlin, A. R., Shimamoto, K., Yasuda-Kamatani, Y., & Swanson, R. A. (2001). Differing effects of substrate and non-substrate transport inhibitors on glutamate uptake reversal. *Journal of Neurochemistry*, *79*(6), 1207–1216. https://doi.org/10.1046/j.1471-4159.2001.00668.x

Arnett, H. A., Mason, J., Marino, M., Suzuki, K., Matsushima, G. K., & Ting, J. P. Y. (2001). TNFα promotes proliferation of oligodendrocyte progenitors and remyelination. *Nature Neuroscience*, *4*(11), 1116–1122. https://doi.org/10.1038/nn738

Arriza, J. L., Eliasof, S., Kavanaugh, M. P., & Amara, S. G. (1997). Excitatory amino acid transporter 5, a retinal glutamate transporter coupled to a chloride conductance. Proceedings of the National Academy of Sciences of the United States of America, 94(8), 4155–4160. https://doi.org/10.1073/pnas.94.8.4155

Arsenault, D., Julien, C., Tremblay, C., & Calon, F. (2011). DHA Improves Cognition and Prevents Dysfunction of Entorhinal Cortex Neurons in 3xTg-AD Mice. *PloS One*, *6*(2), e17397. https://doi.org/10.1371/journal.pone.0017397

Attwell, D. (2000). Brain Uptake of Glutamate: Food for Thought. *the Journal of Nutrition/the Journal of Nutrition*, *130*(4), 1023S-1025S. https://doi.org/10.1093/jn/130.4.1023s

Augustine, G. J., Burns, M. E., DeBello, W. M., Pettit, D. L., & Schweizer, F. E. (1996). Exocytosis: Proteins and

Perturbations. *Annual Review of Pharmacology and Toxicology*, *36*(1), 659–701. https://doi.org/10.1146/annurev.pa.36.040196.003303

Baerwald, K. D., & Popko, B. (1998). Developing and mature oligodendrocytes respond differently to the immune cytokine interferon-gamma. *Journal of Neuroscience Research*, *52*(2), 230–239. https://doi.org/10.1002/(sici)1097-4547(19980415)52:2

Bagaria, J., Bagyinszky, E., & An, S. S. A. (2022). Genetics, Functions, and Clinical Impact of Presenilin-1 (PSEN1) Gene. *International Journal of Molecular Sciences*, *23*(18), 10970. https://doi.org/10.3390/ijms231810970

Baltan, S., Besancon, E. F., Mbow, B., Ye, Z., Hamner, M. A., & Ransom, B. R. (2008). White Matter Vulnerability to Ischemic Injury Increases with Age Because of Enhanced Excitotoxicity. *the Journal of Neuroscience/the Journal of Neuroscience*, *28*(6), 1479–1489. https://doi.org/10.1523/jneurosci.5137-07.2008

Bangen, K. J., Delano-Wood, L., Deoni, S. C. L., Clark, A. L., Evangelista, N. D., Hoffman, S. N., Sorg, S. F., Holmqvist, S.,

Osuna, J., Weigand, A. J., Jak, A. J., Bondi, M. W., & Lamar, M. (2021). Decreased myelin content of the fornix predicts poorer memory performance beyond vascular risk, hippocampal volume, and fractional anisotropy in nondemented older adults. *Brain Imaging and Behavior*, *15*(5), 2563–2571. https://doi.org/10.1007/s11682-021-00458-z

Barage, S. H., & Sonawane, K. D. (2015). Amyloid cascade hypothesis: Pathogenesis and therapeutic strategies in Alzheimer's disease. *Neuropeptides*, *52*, 1–18. https://doi.org/10.1016/j.npep.2015.06.008

Barber, R. C. (2012). The Genetics of Alzheimer's Disease. *Scientifica*, *2012*, 1–14. https://doi.org/10.6064/2012/246210

Barkhof, F., Frequin, S. T., Hommes, O. R., Lamers, K., Van Geel, W., & Valk, J. (1992). A correlative triad of gadolinium-DTPA MRI, EDSS, and CSF-MBP in relapsing multiple sclerosis patients treated with high-dose intravenous methylprednisolone. *Neurology*, *42*(1), 63. https://doi.org/10.1212/wnl.42.1.63

Baron, W., Decker, L., Colognato, H., & Ffrench-Constant, C. (2003). Regulation of Integrin Growth Factor Interactions in Oligodendrocytes by Lipid Raft Microdomains. *CB/Current Biology*, *13*(2), 151–155. https://doi.org/10.1016/s0960-9822(02)01437-9

Bartzokis, G. (2004). Age-related myelin breakdown: a developmental model of cognitive decline and Alzheimer's disease. *Neurobiology of Aging*, *25*(1), 5–18. https://doi.org/10.1016/j.neurobiolaging.2003.03.001

Bartzokis, G., Sultzer, D., Lu, P. H., Nuechterlein, K. H., Mintz, J., & Cummings, J. L. (2004). Heterogeneous age-related breakdown of white matter structural integrity: implications for cortical "disconnection" in aging and Alzheimer's disease. *Neurobiology of Aging*, *25*(7), 843–851. https://doi.org/10.1016/j.neurobiolaging.2003.09.005

Behrendt, G., Baer, K., Buffo, A., Curtis, M. A., Faull, R. L., Rees, M. I., Götz, M., & Dimou, L. (2012). Dynamic changes in myelin aberrations and oligodendrocyte generation in chronic amyloidosis in mice and men. *GLIA*, *61*(2), 273–286. https://doi.org/10.1002/glia.22432

Beirowski, B. (2013). Concepts for regulation of axon integrity by enwrapping glia. *Frontiers in Cellular Neuroscience*, *7*. https://doi.org/10.3389/fncel.2013.00256

Bennett, I. J., Huffman, D. J., & Stark, C. E. (2014). Limbic Tract Integrity Contributes to Pattern Separation Performance Across the Lifespan. *Cerebral Cortex*, *25*(9), 2988–2999. https://doi.org/10.1093/cercor/bhu093

Bergles, D. E., Roberts, J. D. B., Somogyi, P., & Jahr, C. E. (2000). Glutamatergic synapses on oligodendrocyte precursor cells in the hippocampus. *Nature*, *405*(6783), 187–191. https://doi.org/10.1038/35012083

Bertram, L., Lill, C. M., & Tanzi, R. E. (2010). The Genetics of Alzheimer Disease: Back to the Future. *Neuron*, *68*(2), 270–281. https://doi.org/10.1016/j.neuron.2010.10.013

Bhat, R., Crowe, E. P., Bitto, A., Moh, M., Katsetos, C. D., Garcia, F. U., Johnson, F. B., Trojanowski, J. Q., Sell, C., & Torres, C. (2012). Astrocyte Senescence as a Component of Alzheimer's Disease. *PloS One*, *7*(9), e45069. https://doi.org/10.1371/journal.pone.0045069

BIOGEN INC. (2021). Aducanumab (aducanumab-avwa; AduhelmTM). U.S. Food and Drug Administration. (n.d.). In *https://www.accessdata.fda.gov/scripts/cder/daf/index.cfm?event=BasicSearch.process*.

Birnbaumer, L., Campbell, K. P., Catterall, W. A., Harpold, M. M., Hofmann, F., Horne, W. A., Mori, Y., Schwartz, A., Snutch, T. P., Tanabe, T., & Tsien, R. W. (1994). The naming of voltage-gated calcium channels. *Neuron*, *13*(3), 505–506. https://doi.org/10.1016/0896-6273(94)90021-3

Bonaccorso, C., Micale, N., Ettari, R., Grasso, S., & Zappala, M. (2011). Glutamate Binding-Site Ligands of NMDA Receptors. *Current Medicinal Chemistry*, *18*(36), 5483–5506. https://doi.org/10.2174/092986711798347225

Bonora, M., De Marchi, E., Patergnani, S., Suski, J. M., Celsi, F., Bononi, A., Giorgi, C., Marchi, S., Rimessi, A., Duszyński, J., Pozzan, T., Wieckowski, M. R., & Pinton, P. (2014). Tumor necrosis factor-α impairs oligodendroglial differentiation through a mitochondria-dependent process. *Cell Death and Differentiation*, *21*(8), 1198–1208. https://doi.org/10.1038/cdd.2014.35

Bouhrara, M., Reiter, D. A., Bergeron, C. M., Zukley, L. M., Ferrucci, L., Resnick, S. M., & Spencer, R. G. (2018). Evidence of demyelination in mild cognitive impairment and dementia using a direct and specific magnetic resonance imaging measure of myelin content. *Alzheimer's & Dementia*, *14*(8), 998–1004. https://doi.org/10.1016/j.jalz.2018.03.007

Boullerne, A. I. (2016). The history of myelin. *Experimental Neurology*, *283*, 431–445. https://doi.org/10.1016/j.expneurol.2016.06.005

Bouvier, M., Szatkowski, M., Amato, A., & Attwell, D. (1992). The glial cell glutamate uptake carrier countertransports pH-changing anions. *Nature*, *360*(6403), 471–474. https://doi.org/10.1038/360471a0

Bozoki, A. C., Korolev, I. O., Davis, N. C., Hoisington, L. A., & Berger, K. L. (2011). Disruption of limbic white matter pathways in mild cognitive impairment and Alzheimer's disease: A DTI/FDG-PET Study. *Human Brain Mapping*, *33*(8), 1792–1802. https://doi.org/10.1002/hbm.21320

Bozzali, M. (2002). White matter damage in Alzheimer's disease assessed in vivo using diffusion tensor magnetic resonance

imaging. *Journal of Neurology, Neurosurgery and Psychiatry*, *72*(6), 742–746. https://doi.org/10.1136/jnnp.72.6.742

Braak, H., & Braak, E. (1996). Development of Alzheimer-related neurofibrillary changes in the neocortex inversely recapitulates cortical myelogenesis. *Acta Neuropathologica*, *92*(2), 197–201. https://doi.org/10.1007/s004010050508

Brand-Schieber, E., & Werner, P. (2003). AMPA/kainate receptors in mouse spinal cord cell-specific display of receptor subunits by oligodendrocytes and astrocytes and at the nodes of Ranvier. *GLIA*, *42*(1), 12–24. https://doi.org/10.1002/glia.10136

Brase, L., You, S. F., Albanus, R. D., Del-Aguila, J. L., Dai, Y., Novotny, B. C., Soriano-Tarraga, C., Dykstra, T., Fernandez, M. V., Budde, J. P., Bergmann, K., Morris, J. C., Bateman, R. J., Perrin, R. J., McDade, E., Xiong, C., Goate, A., Farlow, M., Chhatwal, J. P., . . . Harari, O. (2021). A landscape of the genetic and cellular heterogeneity in Alzheimer disease. *medRxiv (Cold Spring Harbor Laboratory)*. https://doi.org/10.1101/2021.11.30.21267072

Brier, M. R., Thomas, J. B., & Ances, B. M. (2014). Network Dysfunction in Alzheimer's Disease: Refining the Disconnection Hypothesis. *Brain Connectivity*, *4*(5), 299–311. https://doi.org/10.1089/brain.2014.0236

Broca, P. P. (1890). Anatomie compare des circonvolutions cérébrales. In Masson (Ed.), *Extrait de la "Revue d'Anthropologie"* (2nd ed., Vol. 1, pp. 85–498). Elsevier.

Brun, A., & Englund, E. (1986). A white matter disorder in dementia of the Alzheimer type: A pathoanatomical study. *Annals of Neurology*, *19*(3), 253–262. https://doi.org/10.1002/ana.410190306

Bryant, M. R., Marta, C. B., Kim, F. S., & Bansal, R. (2008). Phosphorylation and lipid raft association of fibroblast growth factor receptor-2 in oligodendrocytes. *GLIA*, *57*(9), 935–946. https://doi.org/10.1002/glia.20818

Bulk, M., Abdelmoula, W. M., Nabuurs, R. J., Van Der Graaf, L. M., Mulders, C. W., Mulder, A. A., Jost, C. R., Koster, A. J., Van Buchem, M. A., Natté, R., Dijkstra, J., & Van Der Weerd, L. (2018). Postmortem MRI and histology demonstrate differential iron accumulation and cortical myelin

organization in early- and late-onset Alzheimer's disease. *Neurobiology of Aging*, *62*, 231–242. https://doi.org/10.1016/j.neurobiolaging.2017.10.017

Caballero, M. N. A., Suárez-Calvet, M., Duering, M., Franzmeier, N., Benzinger, T., Fagan, A. M., Bateman, R. J., Jack, C. R., Levin, J., Dichgans, M., Jucker, M., Karch, C., Masters, C. L., Morris, J. C., Weiner, M., Rossor, M., Fox, N. C., Lee, J. H., Salloway, S., . . . Ewers, M. (2018). White matter diffusion alterations precede symptom onset in autosomal dominant Alzheimer's disease. *Brain*, *141*(10), 3065–3080. https://doi.org/10.1093/brain/awy229

Cáceres, C., Heusser, B., Garnham, A., & Moczko, E. (2023). The Major Hypotheses of Alzheimer's Disease: Related Nanotechnology-Based Approaches for Its Diagnosis and Treatment. *Cells*, *12*(23), 2669. https://doi.org/10.3390/cells12232669

Cai, Z., & Xiao, M. (2015). Oligodendrocytes and Alzheimer's disease. *International Journal of Neuroscience*, *126*(2), 97–104. https://doi.org/10.3109/00207454.2015.1025778

Callen, D., Black, S., Gao, F., Caldwell, C., & Szalai, J. (2001). Beyond the hippocampus: MRI volumetry confirms widespread limbic atrophy in AD. *Neurology*, *57*(9), 1669–1674. https://doi.org/10.1212/wnl.57.9.1669

Cameron, A. S., & Archibald, Y. M. (1981). Verbal memory deficit after left fornix removal: a case report. *International Journal of Neuroscience*, *201*(12).

Camillo, G. (1886). Sulla fina anatomia degli organi centrali del sistema nervoso. In *Internet Archive*. URLIGO HOEPLI EDITORE LIBRAIO. https://archive.org/details/b21978724/mode/2up

Canu, E., Agosta, F., Spinelli, E. G., Magnani, G., Marcone, A., Scola, E., Falautano, M., Comi, G., Falini, A., & Filippi, M. (2013). White matter microstructural damage in Alzheimer's disease at different ages of onset. *Neurobiology of Aging*, *34*(10), 2331–2340. https://doi.org/10.1016/j.neurobiolaging.2013.03.026

Cassano, T., Serviddio, G., Gaetani, S., Romano, A., Dipasquale, P., Cianci, S., Bellanti, F., Laconca, L., Romano, A. D., Padalino, I., LaFerla, F. M., Nicoletti, F., Cuomo, V., & Vendemiale, G.

(2012). Glutamatergic alterations and mitochondrial impairment in a murine model of Alzheimer disease. Neurobiology of Aging, 33(6), 1121.e1-1121.e12. https://doi.org/10.1016/j.neurobiolaging.2011.09.021

Catani, M., Dell'Acqua, F., & De Schotten, M. T. (2013). A revised limbic system model for memory, emotion and behaviour. *Neuroscience & Biobehavioral Reviews/Neuroscience and Biobehavioral Reviews*, *37*(8), 1724–1737. https://doi.org/10.1016/j.neubiorev.2013.07.001

Chao, F. L., Zhang, L., Zhang, Y., Zhou, C. N., Jiang, L., Xiao, Q., Luo, Y. M., Lv, F. L., He, Q., & Tang, Y. (2018). Running exercise protects against myelin breakdown in the absence of neurogenesis in the hippocampus of AD mice. *Brain Research*, *1684*, 50–59. https://doi.org/10.1016/j.brainres.2018.01.007

Chao, L. L., DeCarli, C., Kriger, S., Truran, D., Zhang, Y., Laxamana, J., Villeneuve, S., Jagust, W. J., Sanossian, N., Mack, W. J., Chui, H. C., & Weiner, M. W. (2013). Associations between White Matter Hyperintensities and β Amyloid on Integrity of Projection, Association, and Limbic Fiber Tracts Measured

with Diffusion Tensor MRI. *PloS One*, *8*(6), e65175. https://doi.org/10.1371/journal.pone.0065175

Chaudhry, F. A., Lehre, K. P., Van Lookeren Campagne, M., Ottersen, O. P., Danbolt, N. C., & Storm-Mathisen, J. (1995). Glutamate transporters in glial plasma membranes: Highly differentiated localizations revealed by quantitative ultrastructural immunocytochemistry. Neuron, 15(3), 711–720. https://doi.org/10.1016/0896-6273(95)90158-2

Chen, J. F., Liu, K., Hu, B., Li, R. R., Xin, W., Chen, H., Wang, F., Chen, L., Li, R. X., Ren, S. Y., Xiao, L., Chan, J. R., & Mei, F. (2021). Enhancing myelin renewal reverses cognitive dysfunction in a murine model of Alzheimer's disease. *Neuron*, *109*(14), 2292-2307.e5. https://doi.org/10.1016/j.neuron.2021.05.012

Chen, W. T., Lu, A., Craessaerts, K., Pavie, B., Frigerio, C. S., Corthout, N., Qian, X., Laláková, J., Kühnemund, M., Voytyuk, I., Wolfs, L., Mancuso, R., Salta, E., Balusu, S., Snellinx, A., Munck, S., Jurek, A., Navarro, J. F., Saido, T. C., . . . De Strooper, B. (2020). Spatial Transcriptomics and In Situ Sequencing to

Study Alzheimer's Disease. *Cell*, *182*(4), 976-991.e19. https://doi.org/10.1016/j.cell.2020.06.038

Choi, D., Maulucci-Gedde, M., & Kriegstein, A. (1987). Glutamate neurotoxicity in cortical cell culture. *the Journal of Neuroscience/the Journal of Neuroscience*, *7*(2), 357–368. https://doi.org/10.1523/jneurosci.07-02-00357.1987

Chua, T. C., Wen, W., Slavin, M. J., & Sachdev, P. S. (2008). Diffusion tensor imaging in mild cognitive impairment and Alzheimer's disease: a review. *Current Opinion in Neurology*, *21*(1), 83–92. https://doi.org/10.1097/wco.0b013e3282f4594b

Ciurea, V. A., Covache-Busuioc, R. A., Mohan, A. G., Costin, H. P., & Voicu, V. (2023). Alzheimer's disease: 120 years of research and progress. *Journal of Medicine and Life*, *16*(2), 173–177. https://doi.org/10.25122/jml-2022-0111

Clements, J. D., Lester, R. a. J., Tong, G., Jahr, C. E., & Westbrook, G. L. (1992). The Time Course of Glutamate in the Synaptic Cleft. *Science*, *258*(5087), 1498–1501. https://doi.org/10.1126/science.1359647

Coleman, P. D., & Flood, D. G. (1987). Neuron numbers and dendritic extent in normal aging and Alzheimer's disease. *Neurobiology of Aging*, *8*(6), 521–545. https://doi.org/10.1016/0197-4580(87)90127-8

Conti, F. (1999). Neuronal and Glial Localization of NR1 and NR2A/B Subunits of the NMDA Receptor in the Human Cerebral Cortex. *Cerebral Cortex*, *9*(2), 110–120. https://doi.org/10.1093/cercor/9.2.110

Copenhaver, B. R., Rabin, L. A., Saykin, A. J., Roth, R. M., Wishart, H. A., Flashman, L. A., Santulli, R. B., McHugh, T. L., & Mamourian, A. C. (2006). The fornix and mammillary bodies in older adults with Alzheimer's disease, mild cognitive impairment, and cognitive complaints: A volumetric MRI study. *Psychiatry Research. Neuroimaging*, *147*(2–3), 93–103. https://doi.org/10.1016/j.pscychresns.2006.01.015

Cousin, M. A., & Robinson, P. J. (1999). Mechanisms of Synaptic Vesicle Recycling Illuminated by Fluorescent Dyes. *Journal of Neurochemistry*, *73*(6), 2227–2239. https://doi.org/10.1046/j.1471-4159.1999.0732227.x

Couttas, T. A., Kain, N., Suchowerska, A. K., Quek, L. E., Turner, N., Fath, T., Garner, B., & Don, A. S. (2016). Loss of ceramide synthase 2 activity, necessary for myelin biosynthesis, precedes tau pathology in the cortical pathogenesis of Alzheimer's disease. *Neurobiology of Aging*, *43*, 89–100. https://doi.org/10.1016/j.neurobiolaging.2016.03.027

Crescenzi, R., DeBrosse, C., Nanga, R. P. R., Byrne, M. D., Krishnamoorthy, G., D'Aquilla, K., Nath, H., Morales, K. H., Iba, M., Hariharan, H., Lee, V. M. Y., Detre, J. A., & Reddy, R. (2017). Longitudinal imaging reveals subhippocampal dynamics in glutamate levels associated with histopathologic events in a mouse model of tauopathy and healthy mice. *Hippocampus*, *27*(3), 285–302. https://doi.org/10.1002/hipo.22693

Cummings, J. (2008). The Black Book of Alzheimer's Disease. *Primary Psychiatry*, *15*(2), 66–76.

Curtis, D. R., Phillis, J. W., & Watkins, J. C. (1959). Chemical Excitation of Spinal Neurones. *Nature*, *183*(4661), 611–612. https://doi.org/10.1038/183611a0

Curtis, D. R., Phillis, J. W., & Watkins, J. C. (1960). The chemical excitation of spinal neurones by certain acidic amino acids. *Journal of Physiology*, *150*(3), 656–682. https://doi.org/10.1113/jphysiol.1960.sp006410

Da Silva, S. V., Haberl, M. G., Zhang, P., Bethge, P., Lemos, C., Gonçalves, N., Gorlewicz, A., Malezieux, M., Gonçalves, F. Q., Grosjean, N., Blanchet, C., Frick, A., Nägerl, U. V., Cunha, R. A., & Mulle, C. (2016). Early synaptic deficits in the APP/PS1 mouse model of Alzheimer's disease involve neuronal adenosine A2A receptors. *Nature Communications*, *7*(1). https://doi.org/10.1038/ncomms11915

Dahm, R. (2006). Alzheimer's discovery. *CB/Current Biology*, *16*(21), R906–R910. https://doi.org/10.1016/j.cub.2006.09.056

Danbolt, N. C. (2001). Glutamate uptake. *Progress in Neurobiology*, *65*(1), 1–105. https://doi.org/10.1016/s0301-0082(00)00067-8

Danbolt, N., Storm-Mathisen, J., & Kanner, B. (1992). An [Na+ + K+]coupled l-glutamate transporter purified from rat brain

is located in glial cell processes. Neuroscience, 51(2), 295–310. https://doi.org/10.1016/0306-4522(92)90316-t

Danysz, W., & Parsons, C. G. (2012). Alzheimer's disease, β-amyloid, glutamate, NMDA receptors and memantine – searching for the connections. *British Journal of Pharmacology*, *167*(2), 324–352. https://doi.org/10.1111/j.1476-5381.2012.02057.x

Dawson, M. (2003). NG2-expressing glial progenitor cells: an abundant and widespread population of cycling cells in the adult rat CNS. *Molecular and Cellular Neurosciences*, *24*(2), 476–488. https://doi.org/10.1016/s1044-7431(03)00210-0

De Strooper, B., & Karran, E. (2016). The Cellular Phase of Alzheimer's Disease. *Cell*, *164*(4), 603–615. https://doi.org/10.1016/j.cell.2015.12.056

Dean, D. C., Hurley, S. A., Kecskemeti, S. R., O'Grady, J. P., Canda, C., Davenport-Sis, N. J., Carlsson, C. M., Zetterberg, H., Blennow, K., Asthana, S., Sager, M. A., Johnson, S. C., Alexander, A. L., & Bendlin, B. B. (2017). Association of Amyloid Pathology With Myelin Alteration in Preclinical

Alzheimer Disease. *JAMA Neurology*, *74*(1), 41. https://doi.org/10.1001/jamaneurol.2016.3232

DeFlitch, L., Gonzalez-Fernandez, E., Crawley, I., & Kang, S. H. (2022). Age and Alzheimer's Disease-Related Oligodendrocyte Changes in Hippocampal Subregions. *Frontiers in Cellular Neuroscience*, *16*. https://doi.org/10.3389/fncel.2022.847097

Dehnes, Y., Chaudhry, F. A., Ullensvang, K., Lehre, K. P., Storm-Mathisen, J., & Danbolt, N. C. (1998). The Glutamate Transporter EAAT4 in Rat Cerebellar Purkinje Cells: A Glutamate-Gated Chloride Channel Concentrated near the Synapse in Parts of the Dendritic Membrane Facing Astroglia. the Journal of Neuroscience/the Journal of Neuroscience, 18(10), 3606–3619. https://doi.org/10.1523/jneurosci.18-10-03606.1998

Deiters, O. (1865). Untersuchungen über Gehirn und Rückenmark des Menschen und der Säugethiere. In *Internet Archive*. https://archive.org/details/untersuchungen00deit/mode/2up

Del Río Hortega, P. (1921). La glía de escasas radiaciones (oligodendroglía). *Real Sociedad Española De Historia Natural*, *21*, 63–92.

Del Río-Hortega, P. (1920). Estudios Sobre la Neuroglia. La Microglía Y Su Transformación en Células en Bastoncito Y Cuerpos Gránulo-adiposos. In *Google Books*.

Del Río-Hortega, P. (1933). Arte y artificio de la ciencia histológica. *Residencia Revista De La Residencia De Estudiantes*, *IV* (6), 191–206.

Delatour, B., Guégan, M., Volk, A., & Dhenain, M. (2006). In vivo MRI and histological evaluation of brain atrophy in APP/PS1 transgenic mice. *Neurobiology of Aging*, *27*(6), 835–847. https://doi.org/10.1016/j.neurobiolaging.2005.04.011

Delbeuck, X. (2003). Alzheimer's disease as a disconnection syndrome? *Neuropsychology Review*, *13*(2), 79–92. https://doi.org/10.1023/a:1023832305702

Demeter, S., Rosene, D. L., & Van Hoesen, G. W. (1985). Interhemispheric pathways of the hippocampal formation, presubiculum, and entorhinal and posterior parahippocampal cortices in the rhesus monkey: The

structure and organization of the hippocampal commissures. *Journal of Comparative Neurology*, *233*(1), 30–47. https://doi.org/10.1002/cne.902330104

Desai, M. K., Mastrangelo, M. A., Ryan, D. A., Sudol, K. L., Narrow, W. C., & Bowers, W. J. (2010). Early Oligodendrocyte/Myelin Pathology in Alzheimer's Disease Mice Constitutes a Novel Therapeutic Target. *the American Journal of Pathology*, *177*(3), 1422–1435. https://doi.org/10.2353/ajpath.2010.100087

Desai, M. K., Sudol, K. L., Janelsins, M. C., Mastrangelo, M. A., Frazer, M. E., & Bowers, W. J. (2008). Triple-transgenic Alzheimer's disease mice exhibit region-specific abnormalities in brain myelination patterns prior to appearance of amyloid and tau pathology. *GLIA*, *57*(1), 54–65. https://doi.org/10.1002/glia.20734

Dewar, D., Underhill, S. M., & Goldberg, M. P. (2003). Oligodendrocytes and Ischemic Brain Injury. *Journal of Cerebral Blood Flow and Metabolism*, *23*(3), 263–274. https://doi.org/10.1097/01.wcb.0000053472.41007.f9

Dingledine, R., Borges, K., Bowie, D., & Traynelis, S. F. (1999). The glutamate receptor ion channels. *Pharmacological Reviews*, *51*, 7–61. https://pubmed.ncbi.nlm.nih.gov/10049997/

Dong, Y. X., Zhang, H. Y., Li, H. Y., Liu, P. H., Sui, Y., & Sun, X. H. (2018). Association between Alzheimer's disease pathogenesis and early demyelination and oligodendrocyte dysfunction. *Neural Regeneration Research/Neural Regeneration Research*, *13*(5), 908. https://doi.org/10.4103/1673-5374.232486

Douaud, G., Menke, R. a. L., Gass, A., Monsch, A. U., Rao, A., Whitcher, B., Zamboni, G., Matthews, P. M., Sollberger, M., & Smith, S. (2013). Brain Microstructure Reveals Early Abnormalities more than Two Years prior to Clinical Progression from Mild Cognitive Impairment to Alzheimer's Disease. *the Journal of Neuroscience/the Journal of Neuroscience*, *33*(5), 2147–2155. https://doi.org/10.1523/jneurosci.4437-12.2013

Douet, V., & Chang, L. (2015). Fornix as an imaging marker for episodic memory deficits in healthy aging and in various

neurological disorders. *Frontiers in Aging Neuroscience*, *6*. https://doi.org/10.3389/fnagi.2014.00343

Doyle, S., Hansen, D. B., Vella, J., Bond, P., Harper, G., Zammit, C., Valentino, M., & Fern, R. (2018). Vesicular glutamate release from central axons contributes to myelin damage. *Nature Communications*, *9*(1). https://doi.org/10.1038/s41467-018-03427-1

Duerson, K., Woltjer, R. L., Mookherjee, P., Leverenz, J. B., Montine, T. J., Bird, T. D., Pow, D. V., Rauen, T., & Cook, D. G. (2009). Detergent-Insoluble EAAC1/EAAT3 Aberrantly Accumulates in Hippocampal Neurons of Alzheimer's Disease Patients. Brain Pathology, 19(2), 267–278. https://doi.org/10.1111/j.1750-3639.2008.00186.x

EISAI INC. (2023). Lecanemab (lecanemab-irmb; LEQEMBITM). U.S. Food and Drug Administration. (n.d.). In *https://www.accessdata.fda.gov/scripts/cder/daf/index.cfm?event=overview.process&ApplNo=761269*.

Elliott, A. D. (2019). Confocal Microscopy: Principles and Modern Practices. *Current Protocols in Cytometry*, *92*(1). https://doi.org/10.1002/cpcy.68

Emery, B., & Dugas, J. C. (2013). Purification of Oligodendrocyte Lineage Cells from Mouse Cortices by Immunopanning. *Cold Spring Harbor Protocols*, *2013*(9), pdb.prot073973. https://doi.org/10.1101/pdb.prot073973

Englund, E., Brun, A., & Alling, C. (1988). WHITE MATTER CHANGES IN DEMENTIA OF ALZHEIMER'S TYPE. *Brain*, *111*(6), 1425–1439. https://doi.org/10.1093/brain/111.6.1425

Epstein, F. H., Lipton, S. A., & Rosenberg, P. A. (1994). Excitatory Amino Acids as a Final Common Pathway for Neurologic Disorders. *New England Journal of Medicine/the New England Journal of Medicine*, *330*(9), 613–622. https://doi.org/10.1056/nejm199403033300907

Erecińska, M., & Silver, I. A. (1990). Metabolism and role of glutamate in mammalian brain. *Progress in Neurobiology*, *35*(4), 245–296. https://doi.org/10.1016/0301-0082(90)90013-7

Fairman, W. A., & Amara, S. G. (1999). Functional diversity of excitatory amino acid transporters: ion channel and transport modes. *American Journal of Physiology. Renal Physiology. /American Journal of Physiology. Renal*

Physiology, *277*(4), F481–F486. https://doi.org/10.1152/ajprenal.1999.277.4.f481

Fairman, W. A., Vandenberg, R. J., Arriza, J. L., Kavanaught, M. P., & Amara, S. G. (1995). An excitatory amino-acid transporter with properties of a ligand-gated chloride channel. Nature, 375(6532), 599–603. https://doi.org/10.1038/375599a0

Fedele, E. (2023). Anti-Amyloid Therapies for Alzheimer's Disease and the Amyloid Cascade Hypothesis. *International Journal of Molecular Sciences*, *24*(19), 14499. https://doi.org/10.3390/ijms241914499

Fellgiebel, A., Schermuly, I., Gerhard, A., Keller, I., Albrecht, J., Weibrich, C., Müller, M. J., & Stoeter, P. (2008). Functional relevant loss of long association fibre tracts integrity in early Alzheimer's disease. *Neuropsychologia*, *46*(6), 1698–1706. https://doi.org/10.1016/j.neuropsychologia.2007.12.010

Findley, C. A., Bartke, A., Hascup, K. N., & Hascup, E. R. (2019). Amyloid Beta-Related Alterations to Glutamate Signaling Dynamics During Alzheimer's Disease Progression. *ASN Neuro*, *11*, 175909141985554. https://doi.org/10.1177/1759091419855541

Firbank, M. J., Blamire, A. M., Krishnan, M. S., Teodorczuk, A., English, P., Gholkar, A., Harrison, R. M., & O'Brien, J. T. (2007). Diffusion tensor imaging in dementia with Lewy bodies and Alzheimer's disease. *Psychiatry Research. Neuroimaging*, *155*(2), 135–145. https://doi.org/10.1016/j.pscychresns.2007.01.001

Fletcher, E., Raman, M., Huebner, P., Liu, A., Mungas, D., Carmichael, O., & DeCarli, C. (2013). Loss of Fornix White Matter Volume as a Predictor of Cognitive Impairment in Cognitively Normal Elderly Individuals. *JAMA Neurology*, *70*(11), 1389. https://doi.org/10.1001/jamaneurol.2013.3263

Fogarty, M., Richardson, W. D., & Kessaris, N. (2005). A subset of oligodendrocytes generated from radial glia in the dorsal spinal cord. *Development*, *132*(8), 1951–1959. https://doi.org/10.1242/dev.01777

Fonnum, F. (1984). Glutamate: A Neurotransmitter in Mammalian Brain. *Journal of Neurochemistry*, *42*(1), 1–11. https://doi.org/10.1111/j.1471-4159.1984.tb09689.x

Forsythe, I. D., & Barnes-Davies, M. (1997). Synaptic transmission: Well-placed modulators. *CB/Current Biology*, *7*(6), R362–R365. https://doi.org/10.1016/s0960-9822(06)00175-8

Franklin, R. J. M., & Ffrench-Constant, C. (2008). Remyelination in the CNS: from biology to therapy. *Nature Reviews. Neuroscience*, *9*(11), 839–855. https://doi.org/10.1038/nrn2480

Fu, Y., Sun, W., Shi, Y., Shi, R., & Cheng, J. X. (2009). Glutamate Excitotoxicity Inflicts Paranodal Myelin Splitting and Retraction. *PloS One*, *4*(8), e6705. https://doi.org/10.1371/journal.pone.0006705

Fuchsberger, T., Martínez-Bellver, S., Giraldo, E., Teruel-Martí, V., Lloret, A., & Viña, J. (2016). Aβ Induces Excitotoxicity Mediated by APC/C-Cdh1 Depletion That Can Be Prevented by Glutaminase Inhibition Promoting Neuronal Survival. Scientific Reports, 6(1). https://doi.org/10.1038/srep31158

Fujikawa, D. G. (2005). Prolonged seizures and cellular injury: Understanding the connection. *Epilepsy & Behavior*, *7*, 3–11. https://doi.org/10.1016/j.yebeh.2005.08.003

Fukushima, S., Nishikawa, K., Furube, E., Muneoka, S., Ono, K., Takebayashi, H., & Miyata, S. (2015). Oligodendrogenesis in the fornix of adult mouse brain; the effect of LPS-induced inflammatory stimulation. *Brain Research*, *1627*, 52–69. https://doi.org/10.1016/j.brainres.2015.09.011

Furness, D., Dehnes, Y., Akhtar, A., Rossi, D., Hamann, M., Grutle, N., Gundersen, V., Holmseth, S., Lehre, K., Ullensvang, K., Wojewodzic, M., Zhou, Y., Attwell, D., & Danbolt, N. (2008). A quantitative assessment of glutamate uptake into hippocampal synaptic terminals and astrocytes: New insights into a neuronal role for excitatory amino acid transporter 2 (EAAT2). Neuroscience, 157(1), 80–94. https://doi.org/10.1016/j.neuroscience.2008.08.043

Gaffan, E. A., Gaffan, D., & Hodges, J. R. (1991). AMNESIA FOLLOWING DAMAGE TO THE LEFT FORNIX AND TO OTHER SITES: A COMPARATIVE STUDY. *Brain*, *114*(3), 1297–1313. https://doi.org/10.1093/brain/114.3.1297

Gagliardi, R. J. (2000). Neuroprotection, excitotoxicicity and nmda antagonists. *Arquivos De Neuro-Psiquiatria*, *58*(2B), 583–588. https://doi.org/10.1590/s0004-282x2000000300030

Gameiro, A., Braams, S., Rauen, T., & Grewer, C. (2011). The Discovery of Slowness: Low-Capacity Transport and Slow Anion Channel Gating by the Glutamate Transporter EAAT5. Biophysical Journal, 100(11), 2623–2632. https://doi.org/10.1016/j.bpj.2011.04.034

Games, D., Adams, D., Alessandrini, R., Barbour, R., Borthelette, P., Blackwell, C., Carr, T., Clemens, J., Donaldson, T., Gillespie, F., Guido, T., Hagopian, S., Johnson-Wood, K., Khan, K., Lee, M., Leibowitz, P., Lieberburg, I., Little, S., Masliah, E., . . . Zhao, J. (1995). Alzheimer-type neuropathology in transgenic mice overexpressing V717F β-amyloid precursor protein. *Nature*, *373*(6514), 523–527. https://doi.org/10.1038/373523a0

Gao, F., Gao, K., He, C., Liu, M., Wan, H., & Wang, P. (2019). Multi-site dynamic recording for Aβ oligomers-induced Alzheimer's disease in vitro based on neuronal network chip. *Biosensors & Bioelectronics/Biosensors & Bioelectronics (Online)*, *133*, 183–191. https://doi.org/10.1016/j.bios.2019.03.025

Gardinier, M. V., Amiguet, P., Linington, C., & Matthieu, J. (1992). Myelin/oligodendrocyte glycoprotein is a unique member of the immunoglobulin superfamily. *Journal of Neuroscience Research*, *33*(1), 177–187. https://doi.org/10.1002/jnr.490330123

Geha, S., Pallud, J., Junier, M. P., Devaux, B., Leonard, N., Chassoux, F., Chneiweiss, H., Daumas-Duport, C., & Varlet, P. (2010). NG2+/Olig2+ Cells are the Major Cycle-Related Cell Population of the Adult Human Normal Brain. *Brain Pathology*, *20*(2), 399–411. https://doi.org/10.1111/j.1750-3639.2009.00295.x

Ghatak, S., Dolatabadi, N., Trudler, D., Zhang, X., Wu, Y., Mohata, M., Ambasudhan, R., Talantova, M., & Lipton, S. A. (2019). Mechanisms of hyperexcitability in Alzheimer's disease hiPSC-derived neurons and cerebral organoids vs isogenic controls. *eLife*, *8*. https://doi.org/10.7554/elife.50333

Gibson, E. M., Purger, D., Mount, C. W., Goldstein, A. K., Lin, G. L., Wood, L. S., Inema, I., Miller, S. E., Bieri, G., Zuchero, J. B., Barres, B. A., Woo, P. J., Vogel, H., & Monje, M. (2014). Neuronal Activity Promotes Oligodendrogenesis and

Adaptive Myelination in the Mammalian Brain. *Science*, *344*(6183). https://doi.org/10.1126/science.1252304

Gloor, P., Salanova, V., Olivier, A., & Quesney, L. F. (1993). The human dorsal hippocampal commissure. *Brain*, *116*(5), 1249–1273. https://doi.org/10.1093/brain/116.5.1249

Gold, B. T., Powell, D. K., Andersen, A. H., & Smith, C. D. (2010). Alterations in multiple measures of white matter integrity in normal women at high risk for Alzheimer's disease. *NeuroImage*, *52*(4), 1487–1494. https://doi.org/10.1016/j.neuroimage.2010.05.036

Gómez-Isla, T., Price, J. L., McKeel, D. W., Morris, J. C., Growdon, J. H., & Hyman, B. T. (1996). Profound Loss of Layer II Entorhinal Cortex Neurons Occurs in Very Mild Alzheimer's Disease. *the Journal of Neuroscience/the Journal of Neuroscience*, *16*(14), 4491–4500. https://doi.org/10.1523/jneurosci.16-14-04491.1996

Gonda, X. (2012). Basic Pharmacology of NMDA Receptors. *Current Pharmaceutical Design*, *18*(12), 1558–1567. https://doi.org/10.2174/138161212799958521

Gonzalez-Lima, F., Berndt, J. D., Valla, J. E., Games, D., & Reiman, E. M. (2001). Reduced corpus callosum, fornix and hippocampus in PDAPP transgenic mouse model of Alzheimer's disease. *NeuroReport/Neuroreport*, *12*(11), 2375–2379. https://doi.org/10.1097/00001756-200108080-00018

Gouw, A. A., Seewann, A., Vrenken, H., Van Der Flier, W. M., Rozemuller, J. M., Barkhof, F., Scheltens, P., & Geurts, J. J. G. (2008). Heterogeneity of white matter hyperintensities in Alzheimer's disease: post-mortem quantitative MRI and neuropathology. *Brain*, *131*(12), 3286–3298. https://doi.org/10.1093/brain/awn265

Granzotto, A., & Sensi, S. L. (2024). Once upon a time, the Amyloid Cascade Hypothesis. *Ageing Research Reviews*, *93*, 102161. https://doi.org/10.1016/j.arr.2023.102161

Gregersen, R., Christensen, T., Lehrmann, E., Diemer, N., & Finsen, B. (2001). Focal cerebral ischemia induces increased myelin basic protein and growth-associated protein-43 gene transcription in peri-infarct areas in the rat brain.

Experimental Brain Research, *138*(3), 384–392. https://doi.org/10.1007/s002210100715

Gregory, K. J., Noetzel, M. J., & Niswender, C. M. (2013). Pharmacology of Metabotropic Glutamate Receptor Allosteric Modulators. In *Progress in molecular biology and translational science* (pp. 61–121). https://doi.org/10.1016/b978-0-12-394587-7.00002-6

Grewer, C., Watzke, N., Wiessner, M., & Rauen, T. (2000). Glutamate translocation of the neuronal glutamate transporter EAAC1 occurs within milliseconds. Proceedings of the National Academy of Sciences of the United States of America, 97(17), 9706–9711. https://doi.org/10.1073/pnas.160170397

Groves, A. K., Barnett, S. C., Franklin, R. J. M., Crang, A. J., Mayer, M., Blakemore, W. F., & Noble, M. (1993). Repair of demyelinated lesions by transplantation of purified 0-2A progenitor cells. *Nature*, *362*(6419), 453–455. https://doi.org/10.1038/362453a0

Guo, T., Zhang, D., Zeng, Y., Huang, T. Y., Xu, H., & Zhao, Y. (2020). Molecular and cellular mechanisms underlying the

pathogenesis of Alzheimer's disease. *Molecular Neurodegeneration*, *15*(1). https://doi.org/10.1186/s13024-020-00391-7

Haass, C., & Selkoe, D. J. (2007). Soluble protein oligomers in neurodegeneration: lessons from the Alzheimer's amyloid β-peptide. *Nature Reviews. Molecular Cell Biology*, *8*(2), 101–112. https://doi.org/10.1038/nrm2101

Han, S., Gim, Y., Jang, E. H., & Hur, E. M. (2022). Functions and dysfunctions of oligodendrocytes in neurodegenerative diseases. *Frontiers in Cellular Neuroscience*, *16*. https://doi.org/10.3389/fncel.2022.1083159

Harayama, T., & Riezman, H. (2018). Understanding the diversity of membrane lipid composition. *Nature Reviews. Molecular Cell Biology*, *19*(5), 281–296. https://doi.org/10.1038/nrm.2017.138

Hardy, J. A., & Higgins, G. A. (1992). Alzheimer's Disease: The Amyloid Cascade Hypothesis. *Science*, *256*(5054), 184–185. https://doi.org/10.1126/science.1566067

Hardy, R., & Reynolds, R. (1991). Proliferation and differentiation potential of rat forebrain oligodendroglial progenitors both

in vitro and in vivo. *Development*, *111*(4), 1061–1080. https://doi.org/10.1242/dev.111.4.1061

Hariri, A. R., Bookheimer, S. Y., & Mazziotta, J. C. (2000). Modulating emotional responses. *NeuroReport/Neuroreport*, *11*(1), 43–48. https://doi.org/10.1097/00001756-200001170-00009

Hartline, D. K. (2008). What is myelin? *Neuron Glia Biology*, *4*(2), 153–163. https://doi.org/10.1017/s1740925x09990263

Hascup, K. N., & Hascup, E. R. (2015). Altered Neurotransmission Prior to Cognitive Decline in AβPP/PS1 Mice, a Model of Alzheimer's Disease. *Journal of Alzheimer's Disease*, *44*(3), 771–776. https://doi.org/10.3233/jad-142160

Hascup, K. N., Findley, C. A., Britz, J., Esperant-Hilaire, N., Broderick, S. O., Delfino, K., Tischkau, S., Bartke, A., & Hascup, E. R. (2020). Riluzole attenuates glutamatergic tone and cognitive decline in AβPP/PS1 mice. *Journal of Neurochemistry*, *156*(4), 513–523. https://doi.org/10.1111/jnc.15224

Hascup, K. N., Findley, C. A., Sime, L. N., & Hascup, E. R. (2020). Hippocampal alterations in glutamatergic signaling during

amyloid progression in AβPP/PS1 mice. *Scientific Reports*, *10*(1). https://doi.org/10.1038/s41598-020-71587-6

Hattori, T., Sato, R., Aoki, S., Yuasa, T., & Mizusawa, H. (2011). Different Patterns of Fornix Damage in Idiopathic Normal Pressure Hydrocephalus and Alzheimer Disease. *American Journal of Neuroradiology*, *33*(2), 274–279. https://doi.org/10.3174/ajnr.a2780

Hayashi, T. (1954). EFFECTS OF SODIUM GLUTAMATE ON THE NERVOUS SYSTEM. *Keio Journal of Medicine*, *3*(4), 183–192. https://doi.org/10.2302/kjm.3.183

He, P., & Shen, Y. (2009). Interruption of β-Catenin Signaling Reduces Neurogenesis in Alzheimer's Disease. *the Journal of Neuroscience/the Journal of Neuroscience*, *29*(20), 6545–6557. https://doi.org/10.1523/jneurosci.0421-09.2009

Head, D., Rodrigue, K. M., Kennedy, K. M., & Raz, N. (2008). Neuroanatomical and cognitive mediators of age-related differences in episodic memory. *Neuropsychology*, *22*(4), 491–507. https://doi.org/10.1037/0894-4105.22.4.491

Heimer, L., & Van Hoesen, G. W. (2006). The limbic lobe and its output channels: Implications for emotional functions and

adaptive behavior. *Neuroscience & Biobehavioral Reviews/Neuroscience and Biobehavioral Reviews*, *30*(2), 126–147. https://doi.org/10.1016/j.neubiorev.2005.06.006

Hertz, L. (1979). Functional interactions between neurons and astrocytes I. Turnover and metabolism of putative amino acid transmitters. *Progress in Neurobiology*, *13*(3), 277–323. https://doi.org/10.1016/0301-0082(79)90018-2

Hirschfeld, L. R., Risacher, S. L., Nho, K., & Saykin, A. J. (2022). Myelin repair in Alzheimer's disease: a review of biological pathways and potential therapeutics. *Translational Neurodegeneration*, *11*(1). https://doi.org/10.1186/s40035-022-00321-1

Hodges, J. R., & Carpenter, K. (1991). Anterograde amnesia with fornix damage following removal of IIIrd ventricle colloid cyst. *Journal of Neurology, Neurosurgery and Psychiatry*, *54*(7), 633–638. https://doi.org/10.1136/jnnp.54.7.633

Hof, P. R., Morrison, J. H., & Cox, K. (1990). Quantitative analysis of a vulnerable subset of pyramidal neurons in Alzheimer's disease: I. Superior frontal and inferior temporal cortex.

Journal of Comparative Neurology, *301*(1), 44–54. https://doi.org/10.1002/cne.903010105

Holmseth, S., Dehnes, Y., Huang, Y. H., Follin-Arbelet, V. V., Grutle, N. J., Mylonakou, M. N., Plachez, C., Zhou, Y., Furness, D. N., Bergles, D. E., Lehre, K. P., & Danbolt, N. C. (2012). The Density of EAAC1 (EAAT3) Glutamate Transporters Expressed by Neurons in the Mammalian CNS. the Journal of Neuroscience/the Journal of Neuroscience, 32(17), 6000–6013. https://doi.org/10.1523/jneurosci.5347-11.2012

Hopper, M. W., & Vogel, F. S. (1976). The limbic system in Alzheimer's disease. A neuropathologic investigation. *PubMed*, *85*(1), 1–20. https://pubmed.ncbi.nlm.nih.gov/135514

Horiuchi, M., Maezawa, I., Itoh, A., Wakayama, K., Jin, L. W., Itoh, T., & DeCarli, C. (2012). Amyloid β1–42 oligomer inhibits myelin sheet formation in vitro. *Neurobiology of Aging*, *33*(3), 499–509. https://doi.org/10.1016/j.neurobiolaging.2010.05.007

Huang, H., Fan, X., Weiner, M., Martin-Cook, K., Xiao, G., Davis, J., Devous, M., Rosenberg, R., & Diaz-Arrastia, R. (2012). Distinctive disruption patterns of white matter tracts in

Alzheimer's disease with full diffusion tensor characterization. *Neurobiology of Aging*, *33*(9), 2029–2045. https://doi.org/10.1016/j.neurobiolaging.2011.06.027

Huang, J., Friedland, R., & Auchus, A. (2007). Diffusion Tensor Imaging of Normal-Appearing White Matter in Mild Cognitive Impairment and Early Alzheimer Disease: Preliminary Evidence of Axonal Degeneration in the Temporal Lobe. *American Journal of Neuroradiology*, *28*(10), 1943–1948. https://doi.org/10.3174/ajnr.a0700

Huang, S., Tong, H., Lei, M., Zhou, M., Guo, W., Li, G., Tang, X., Li, Z., Mo, M., Zhang, X., Chen, X., Cen, L., Wei, L., Xiao, Y., Li, K., Huang, Q., Yang, X., Liu, W., Zhang, L., . . . Xu, P. (2018). Astrocytic glutamatergic transporters are involved in Aβ-induced synaptic dysfunction. Brain Research, 1678, 129–137. https://doi.org/10.1016/j.brainres.2017.10.011

Hughes, E. G., Kang, S. H., Fukaya, M., & Bergles, D. E. (2013). Oligodendrocyte progenitors balance growth with self-repulsion to achieve homeostasis in the adult brain. *Nature Neuroscience*, *16*(6), 668–676. https://doi.org/10.1038/nn.3390

Huijbers, W., Mormino, E. C., Schultz, A. P., Wigman, S., Ward, A. M., Larvie, M., Amariglio, R. E., Marshall, G. A., Rentz, D. M., Johnson, K. A., & Sperling, R. A. (2015). Amyloid-β deposition in mild cognitive impairment is associated with increased hippocampal activity, atrophy and clinical progression. *Brain*, *138*(4), 1023–1035. https://doi.org/10.1093/brain/awv007

Huijbers, W., Schultz, A. P., Papp, K. V., LaPoint, M. R., Hanseeuw, B., Chhatwal, J. P., Hedden, T., Johnson, K. A., & Sperling, R. A. (2018). Tau Accumulation in Clinically Normal Older Adults Is Associated with Hippocampal Hyperactivity. *the Journal of Neuroscience/the Journal of Neuroscience*, *39*(3), 548–556. https://doi.org/10.1523/jneurosci.1397-18.2018

Hunsberger, H. C., Rudy, C. C., Batten, S. R., Gerhardt, G. A., & Reed, M. N. (2014). P301L tau expression affects glutamate release and clearance in the hippocampal trisynaptic pathway. *Journal of Neurochemistry*, *132*(2), 169–182. https://doi.org/10.1111/jnc.12967

Hunsberger, H. C., Weitzner, D. S., Rudy, C. C., Hickman, J. E., Libell, E. M., Speer, R. R., Gerhardt, G. A., & Reed, M. N. (2015).

Riluzole rescues glutamate alterations, cognitive deficits, and tau pathology associated with P301L tau expression. *Journal of Neurochemistry*, *135*(2), 381–394. https://doi.org/10.1111/jnc.13230

Huxley, A. F., & Stämpeli, R. (1949). Evidence for saltatory conduction in peripheral myelinated nerve fibres. *Journal of Physiology*, *108*(3), 315–339. https://doi.org/10.1113/jphysiol.1949.sp004335

Hynd, M. (2004). Glutamate-mediated excitotoxicity and neurodegeneration in Alzheimer's disease. *Neurochemistry International*, *45*(5), 583–595. https://doi.org/10.1016/j.neuint.2004.03.007

Ihara, M., Polvikoski, T. M., Hall, R., Slade, J. Y., Perry, R. H., Oakley, A. E., Englund, E., O'Brien, J. T., Ince, P. G., & Kalaria, R. N. (2010). Quantification of myelin loss in frontal lobe white matter in vascular dementia, Alzheimer's disease, and dementia with Lewy bodies. *Acta Neuropathologica*, *119*(5), 579–589. https://doi.org/10.1007/s00401-009-0635-8

Jabaudon, D., Shimamoto, K., Yasuda-Kamatani, Y., Scanziani, M., Gähwiler, B. H., & Gerber, U. (1999). Inhibition of uptake

unmasks rapid extracellular turnover of glutamate of nonvesicular origin. Proceedings of the National Academy of Sciences of the United States of America, 96(15), 8733–8738. https://doi.org/10.1073/pnas.96.15.8733

Jackman, N., Ishii, A., & Bansal, R. (2009). Oligodendrocyte Development and Myelin Biogenesis: Parsing Out the Roles of Glycosphingolipids. *Physiology*, *24*(5), 290–297. https://doi.org/10.1152/physiol.00016.2009

Jakovcevski, I., Filipovic, R., Mo, Z., Rakic, S., & Zecevic, N. (2009). Oligodendrocyte development and the onset of myelination in the human fetal brain. *Frontiers in Neuroanatomy*, *3*. https://doi.org/10.3389/neuro.05.005.2009

Jankowsky, J. L., Fadale, D. J., Anderson, J., Xu, G. M., Gonzales, V., Jenkins, N. A., Copeland, N. G., Lee, M. K., Younkin, L. H., Wagner, S. L., Younkin, S. G., & Borchelt, D. R. (2003). Mutant presenilins specifically elevate the levels of the 42 residue β-amyloid peptide in vivo: evidence for augmentation of a 42-specific γ secretase. *Human Molecular Genetics Online/Human Molecular Genetics*, *13*(2), 159–170. https://doi.org/10.1093/hmg/ddh019

Jiao, Y., Sun, Z., Lee, T., Fusco, F. R., Kimble, T. D., Meade, C. A., Cuthbertson, S., & Reiner, A. (1999). A simple and sensitive antigen retrieval method for free-floating and slide-mounted tissue sections. *Journal of Neuroscience Methods*, *93*(2), 149–162. https://doi.org/10.1016/s0165-0270(99)00142-9

Johannes, L., & Galli, T. (1998). Exocytosis: SNAREs drum up! *European Journal of Neuroscience/EJN. European Journal of Neuroscience*, *10*(2), 415–422. https://doi.org/10.1046/j.1460-9568.1998.00081.x

Kabir, M. T., Uddin, M. S., Setu, J. R., Ashraf, G. M., Bin-Jumah, M. N., & Abdel-Daim, M. M. (2020). Exploring the Role of PSEN Mutations in the Pathogenesis of Alzheimer's Disease. *Neurotoxicity Research/Neurotoxicity Resarch*, *38*(4), 833–849. https://doi.org/10.1007/s12640-020-00232-x

Kabogo, D., Rauw, G., Amritraj, A., Baker, G., & Kar, S. (2010). β-Amyloid-related peptides potentiate K+-evoked glutamate release from adult rat hippocampal slices. *Neurobiology of Aging*, *31*(7), 1164–1172. https://doi.org/10.1016/j.neurobiolaging.2008.08.009

Kalus, P., Slotboom, J., Gallinat, J., Mahlberg, R., Cattapan-Ludewig, K., Wiest, R., Nyffeler, T., Buri, C., Federspiel, A., Kunz, D., Schroth, G., & Kiefer, C. (2006). Examining the gateway to the limbic system with diffusion tensor imaging: The perforant pathway in dementia. *NeuroImage*, *30*(3), 713–720. https://doi.org/10.1016/j.neuroimage.2005.10.035

Kanai, Y., & Hediger, M. A. (1992). Primary structure and functional characterization of a high-affinity glutamate transporter. Nature, 360(6403), 467–471. https://doi.org/10.1038/360467a0

Kang, Z., Wang, C., Zepp, J., Wu, L., Sun, K., Zhao, J., Chandrasekharan, U., DiCorleto, P. E., Trapp, B. D., Ransohoff, R. M., & Li, X. (2013). Act1 mediates IL-17–induced EAE pathogenesis selectively in NG2+ glial cells. *Nature Neuroscience*, *16*(10), 1401–1408. https://doi.org/10.1038/nn.3505

Kantarci, K., Senjem, M., Avula, R., Zhang, B., Samikoglu, A., Weigand, S., Przybelski, S., Edmonson, H., Vemuri, P., Knopman, D., Boeve, B., Ivnik, R., Smith, G., Petersen, R., & Jack, C. (2011). Diffusion tensor imaging and cognitive

function in older adults with no dementia. *Neurology*, *77*(1), 26–34. https://doi.org/10.1212/wnl.0b013e31822313dc

Káradóttir, R., Cavelier, P., Bergersen, L. H., & Attwell, D. (2005). NMDA receptors are expressed in oligodendrocytes and activated in ischaemia. *Nature*, *438*(7071), 1162–1166. https://doi.org/10.1038/nature04302

Katsavos, S., & Anagnostouli, M. (2013). Biomarkers in Multiple Sclerosis: An Up-to-Date Overview. *Multiple Sclerosis International*, *2013*, 1–20. https://doi.org/10.1155/2013/340508

Kavroulakis, E., Simos, P. G., Kalaitzakis, G., Maris, T. G., Karageorgou, D., Zaganas, I., Panagiotakis, S., Basta, M., Vgontzas, A., & Papadaki, E. (2017). Myelin content changes in probable Alzheimer's disease and mild cognitive impairment: Associations with age and severity of neuropsychiatric impairment. *Journal of Magnetic Resonance Imaging*, *47*(5), 1359–1372. https://doi.org/10.1002/jmri.25849

Kaya, I., Jennische, E., Lange, S., Baykal, A. T., Malmberg, P., & Fletcher, J. S. (2020). Brain region-specific amyloid plaque-

associated myelin lipid loss, APOE deposition and disruption of the myelin sheath in familial Alzheimer's disease mice. *Journal of Neurochemistry*, *154*(1), 84–98. https://doi.org/10.1111/jnc.14999

Kerever, A., Kamagata, K., Yokosawa, S., Otake, Y., Ochi, H., Yamada, T., Hori, M., Kamiya, K., Nishikori, A., Aoki, S., & Arikawa-Hirasawa, E. (2015). See-through Brains and Diffusion Tensor MRI Clarified Fiber Connections: A Preliminary Microstructural Study in a Mouse with Callosal Agenesis. *Magnetic Resonance in Medical Sciences*, *14*(2), 159–162. https://doi.org/10.2463/mrms.2014-0142

Kessaris, N., Fogarty, M., Iannarelli, P., Grist, M., Wegner, M., & Richardson, W. D. (2005). Competing waves of oligodendrocytes in the forebrain and postnatal elimination of an embryonic lineage. *Nature Neuroscience*, *9*(2), 173–179. https://doi.org/10.1038/nn1620

Kim, H. J., Tsao, J. W., & Stanfill, A. G. (2018). The current state of biomarkers of mild traumatic brain injury. *JCI Insight*, *3*(1). https://doi.org/10.1172/jci.insight.97105

Kim, H., Chae, S., Lee, D., Chromy, B., Lee, S. C., Park, Y., Klein, W. L., Krafft, G. A., & Hong, S. (2002). Selective neuronal degeneration induced by soluble oligomeric amyloid beta-protein. *the FASEB Journal*, *17*(1), 118–120. https://doi.org/10.1096/fj.01-0987fje

Kirby, L., & Castelo-Branco, G. (2021). Crossing boundaries: Interplay between the immune system and oligodendrocyte lineage cells. *Seminars in Cell & Developmental Biology*, *116*, 45–52. https://doi.org/10.1016/j.semcdb.2020.10.013

Kister, A., & Kister, I. (2023). Overview of myelin, major myelin lipids, and myelin-associated proteins. *Frontiers in Chemistry*, *10*. https://doi.org/10.3389/fchem.2022.1041961

Koh, J. Y., & Choi, D. W. (1987). Effect of anticonvulsant drugs on glutamate neurotoxicity in cortical cell culture. *Neurology*, *37*(2), 319. https://doi.org/10.1212/wnl.37.2.319

Krämer, E. M., Klein, C., Koch, T., Boytinck, M., & Trotter, J. (1999). Compartmentation of Fyn Kinase with Glycosylphosphatidylinositol-anchored Molecules in Oligodendrocytes Facilitates Kinase Activation during Myelination. *Journal of Biological Chemistry/˜the œJournal*

of Biological Chemistry, *274*(41), 29042–29049. https://doi.org/10.1074/jbc.274.41.29042

Krebs, H. A. (1935). Metabolism of amino-acids. *Biochemical Journal. Cellular Aspects*, *29*(8), 1951–1969. https://doi.org/10.1042/bj0291951

Kuhn, S., Gritti, L., Crooks, D., & Dombrowski, Y. (2019). Oligodendrocytes in Development, Myelin Generation and Beyond. *Cells*, *8*(11), 1424. https://doi.org/10.3390/cells8111424

Kurien, B. T., & Scofield, R. H. (2015). Western Blotting: An Introduction. In *Methods in molecular biology* (pp. 17–30). https://doi.org/10.1007/978-1-4939-2694-7_5

Kurkinen, M., Fułek, M., Fułek, K., Beszłej, J. A., Kurpas, D., & Leszek, J. (2023). The Amyloid Cascade Hypothesis in Alzheimer's Disease: Should We Change Our Thinking? *Biomolecules*, *13*(3), 453. https://doi.org/10.3390/biom13030453

Lacalle-Aurioles, M., & Iturria-Medina, Y. (2023). Fornix degeneration in risk factors of Alzheimer's disease, possible trigger of cognitive decline. *Cerebral Circulation, Cognition*

and Behavior, *4*, 100158. https://doi.org/10.1016/j.cccb.2023.100158

Lacalle-Aurioles, M., Navas-Sánchez, F. J., Alemán-Gómez, Y., Olazarán, J., Guzmán-De-Villoria, J. A., Cruz-Orduña, I., Mateos-Pérez, J. M., & Desco, M. (2016). The Disconnection Hypothesis in Alzheimer's Disease Studied Through Multimodal Magnetic Resonance Imaging: Structural, Perfusion, and Diffusion Tensor Imaging. *Journal of Alzheimer's Disease*, *50*(4), 1051–1064. https://doi.org/10.3233/jad-150288

Lang, J. (1992). Topographic Anatomy of Preformed Intracranial Spaces. In *Acta neurochirurgica. Supplementum* (pp. 1–10). https://doi.org/10.1007/978-3-7091-6687-1_1

Lappe-Siefke, C., Goebbels, S., Gravel, M., Nicksch, E., Lee, J., Braun, P. E., Griffiths, I. R., & Nave, K. A. (2003). Disruption of Cnp1 uncouples oligodendroglial functions in axonal support and myelination. *Nature Genetics*, *33*(3), 366–374. https://doi.org/10.1038/ng1095

Lau, V., Ramer, L., & Tremblay, M. V. (2023). An aging, pathology burden, and glial senescence build-up hypothesis for late

onset Alzheimer's disease. *Nature Communications*, *14*(1). https://doi.org/10.1038/s41467-023-37304-3

Lee, D. Y., Fletcher, E., Carmichael, O. T., Singh, B., Mungas, D. M., Reed, B. R., Martinez, O., Buonocore, M. H., Persianinova, M., & DeCarli, C. (2012). Sub-Regional Hippocampal Injury is Associated with Fornix Degeneration in Alzheimer's Disease. *Frontiers in Aging Neuroscience*, *4*. https://doi.org/10.3389/fnagi.2012.00001

Lee, S., Viqar, F., Zimmerman, M. E., Narkhede, A., Tosto, G., Benzinger, T. L., Marcus, D. S., Fagan, A. M., Goate, A., Fox, N. C., Cairns, N. J., Holtzman, D. M., Buckles, V., Ghetti, B., McDade, E., Martins, R. N., Saykin, A. J., Masters, C. L., Ringman, J. M., . . . Brickman, A. M. (2016). White matter hyperintensities are a core feature of Alzheimer's disease: Evidence from the dominantly inherited Alzheimer network. *Annals of Neurology*, *79*(6), 929–939. https://doi.org/10.1002/ana.24647

Lee, Y., Morrison, B. M., Li, Y., Lengacher, S., Farah, M. H., Hoffman, P. N., Liu, Y., Tsingalia, A., Jin, L., Zhang, P. W., Pellerin, L., Magistretti, P. J., & Rothstein, J. D. (2012). Oligodendroglia

metabolically support axons and contribute to neurodegeneration. *Nature*, *487*(7408), 443–448. https://doi.org/10.1038/nature11314

Lehre, K., Levy, L., Ottersen, O., Storm-Mathisen, J., & Danbolt, N. (1995). Differential expression of two glial glutamate transporters in the rat brain: quantitative and immunocytochemical observations. ˜the œJournal of Neuroscience/˜the œJournal of Neuroscience, 15(3), 1835–1853. https://doi.org/10.1523/jneurosci.15-03-01835.1995

Lerma, J., & Marques, J. M. (2013). Kainate Receptors in Health and Disease. *Neuron*, *80*(2), 292–311. https://doi.org/10.1016/j.neuron.2013.09.045

Levene, H. (1961). *Robust tests for equality of variances*. 279–292. https://ci.nii.ac.jp/naid/10007628681

Levy, L. M., Warr, O., & Attwell, D. (1998). Stoichiometry of the Glial Glutamate Transporter GLT-1 Expressed Inducibly in a Chinese Hamster Ovary Cell Line Selected for Low Endogenous Na+-Dependent Glutamate Uptake. *the Journal of Neuroscience/the Journal of Neuroscience*, *18*(23), 9620–9628. https://doi.org/10.1523/jneurosci.18-23-09620.1998

Li, Z., Zhang, Z., Ren, Y., Wang, Y., Fang, J., Yue, H., Ma, S., & Guan, F. (2021). Aging and age-related diseases: from mechanisms to therapeutic strategies. *Biogerontology*, *22*(2), 165–187. https://doi.org/10.1007/s10522-021-09910-5

Liu, P. P., Xie, Y., Meng, X. Y., & Kang, J. S. (2019). History and progress of hypotheses and clinical trials for Alzheimer's disease. *Signal Transduction and Targeted Therapy*, *4*(1). https://doi.org/10.1038/s41392-019-0063-8

Liu, Y., Spulber, G., Lehtimäki, K. K., Könönen, M., Hallikainen, I., Gröhn, H., Kivipelto, M., Hallikainen, M., Vanninen, R., & Soininen, H. (2011). Diffusion tensor imaging and Tract-Based Spatial Statistics in Alzheimer's disease and mild cognitive impairment. *Neurobiology of Aging*, *32*(9), 1558–1571. https://doi.org/10.1016/j.neurobiolaging.2009.10.006

Livingston, G., Huntley, J., Sommerlad, A., Ames, D., Ballard, C., Banerjee, S., Brayne, C., Burns, A., Cohen-Mansfield, J., Cooper, C., Costafreda, S. G., Dias, A., Fox, N., Gitlin, L. N., Howard, R., Kales, H. C., Kivimäki, M., Larson, E. B., Ogunniyi, A., . . . Mukadam, N. (2020). Dementia prevention,

intervention, and care: 2020 report of the Lancet Commission. *Lancet*, *396*(10248), 413–446. https://doi.org/10.1016/s0140-6736(20)30367-6

Lok, K., Zhao, H., Shen, H., Wang, Z., Gao, X., Zhao, W., & Yin, M. (2013). Characterization of the APP/PS1 mouse model of Alzheimer's disease in senescence accelerated background. *Neuroscience Letters*, *557*, 84–89. https://doi.org/10.1016/j.neulet.2013.10.051

López-Muguruza, E., & Matute, C. (2023). Alterations of Oligodendrocyte and Myelin Energy Metabolism in Multiple Sclerosis. *International Journal of Molecular Sciences*, *24*(16), 12912. https://doi.org/10.3390/ijms241612912

Lorenzini, L., Fernandez, M., Baldassarro, V. A., Bighinati, A., Giuliani, A., Calzà, L., & Giardino, L. (2020). White Matter and Neuroprotection in Alzheimer's Dementia. *Molecules/Molecules Online/Molecules Annual*, *25*(3), 503. https://doi.org/10.3390/molecules25030503

Magaki, S., Hojat, S. A., Wei, B., So, A., & Yong, W. H. (2018). An Introduction to the Performance of Immunohistochemistry.

In *Methods in molecular biology* (pp. 289–298). https://doi.org/10.1007/978-1-4939-8935-5_25

Maitre, M., Jeltsch-David, H., Okechukwu, N. G., Klein, C., Patte-Mensah, C., & Mensah-Nyagan, A. G. (2023). Myelin in Alzheimer's disease: culprit or bystander? *Acta Neuropathologica Communications*, *11*(1). https://doi.org/10.1186/s40478-023-01554-5

Malik, N., & Willnow, N. (2019). Excitatory Amino Acid Transporters in Physiology and Disorders of the Central Nervous System. International Journal of Molecular Sciences, 20(22), 5671. https://doi.org/10.3390/ijms20225671

Mark, L. P., Prost, R. W., Ulmer, J. L., Smith, M. M., Daniels, D. L., Strottmann, J. M., Brown, W. D., & Hacein-Bey, L. (2001). *Pictorial review of glutamate excitotoxicity: fundamental concepts for neuroimaging. 22*(10), 1813–1824. http://www.ajnr.org/content/22/10/1813.full.pdf

Martinez-Hernandez, A., Bell, K. P., & Norenberg, M. D. (1977). Glutamine Synthetase: Glial Localization in Brain. *Science*, *195*(4284), 1356–1358. https://doi.org/10.1126/science.14400

Matute, C. (2006). Oligodendrocyte NMDA receptors: a novel therapeutic target. *Trends in Molecular Medicine*, *12*(7), 289–292. https://doi.org/10.1016/j.molmed.2006.05.004

Matute, C., Alberdi, E., Domercq, M., Pérez-Cerdá, F., Pérez-SamartíN, A., & Sánchez-Gómez, M. V. (2001). The link between excitotoxic oligodendroglial death and demyelinating diseases. *Trends in Neurosciences*, *24*(4), 224–230. https://doi.org/10.1016/s0166-2236(00)01746-x

Matute, C., Sánchez-Gómez, M. V., Martínez-Millán, L., & Miledi, R. (1997). Glutamate receptor-mediated toxicity in optic nerve oligodendrocytes. *Proceedings of the National Academy of Sciences of the United States of America*, *94*(16), 8830–8835. https://doi.org/10.1073/pnas.94.16.8830

Mcdonald, J. W., Althomsons, S. P., Hyrc, K. L., Choi, D. W., & Goldberg, M. P. (1998). Oligodendrocytes from forebrain are highly vulnerable to AMPA/kainate receptor-mediated excitotoxicity. *Nature Medicine*, *4*(3), 291–297. https://doi.org/10.1038/nm0398-291

McMackin, D., Cockburn, J., Anslow, P., & Gaffan, D. (1995). Correlation of fornix damage with memory impairment in six

cases of colloid cyst removal. *Acta Neurochirurgica*, *135*(1–2), 12–18. https://doi.org/10.1007/bf02307408

Meldrum, B. S. (2000). Glutamate as a Neurotransmitter in the Brain: Review of Physiology and Pathology. *the Journal of Nutrition/the Journal of Nutrition*, *130*(4), 1007S-1015S. https://doi.org/10.1093/jn/130.4.1007s

Menichella, D. M., Majdan, M., Awatramani, R., Goodenough, D. A., Sirkowski, E., Scherer, S. S., & Paul, D. L. (2006). Genetic and Physiological Evidence That Oligodendrocyte Gap Junctions Contribute to Spatial Buffering of Potassium Released during Neuronal Activity. *the Journal of Neuroscience/the Journal of Neuroscience*, *26*(43), 10984–10991. https://doi.org/10.1523/jneurosci.0304-06.2006

Menn, B., Garcia-Verdugo, J. M., Yaschine, C., Gonzalez-Perez, O., Rowitch, D., & Alvarez-Buylla, A. (2006). Origin of Oligodendrocytes in the Subventricular Zone of the Adult Brain. *the Journal of Neuroscience/the Journal of Neuroscience*, *26*(30), 7907–7918. https://doi.org/10.1523/jneurosci.1299-06.2006

Metzler-Baddeley, C., Hunt, S., Jones, D. K., Leemans, A., Aggleton, J. P., & O'Sullivan, M. J. (2012). Temporal association tracts and the breakdown of episodic memory in mild cognitive impairment. *Neurology*, *79*(23), 2233–2240. https://doi.org/10.1212/wnl.0b013e31827689e8

Metzler-Baddeley, C., Jones, D. K., Belaroussi, B., Aggleton, J. P., & O'Sullivan, M. J. (2011). Frontotemporal Connections in Episodic Memory and Aging: A Diffusion MRI Tractography Study. *the Journal of Neuroscience/the Journal of Neuroscience*, *31*(37), 13236–13245. https://doi.org/10.1523/jneurosci.2317-11.2011

Micu, I., Jiang, Q., Coderre, E., Ridsdale, A., Zhang, L., Woulfe, J., Yin, X., Trapp, B. D., McRory, J. E., Rehak, R., Zamponi, G. W., Wang, W., & Stys, P. K. (2005). NMDA receptors mediate calcium accumulation in myelin during chemical ischaemia. *Nature*, *439*(7079), 988–992. https://doi.org/10.1038/nature04474

Mielke, M. M., Okonkwo, O. C., Oishi, K., Mori, S., Tighe, S., Miller, M. I., Ceritoglu, C., Brown, T., Albert, M., & Lyketsos, C. G. (2012a). Fornix integrity and hippocampal volume predict

memory decline and progression to Alzheimer's disease. *Alzheimer's & Dementia*, *8*(2), 105–113. https://doi.org/10.1016/j.jalz.2011.05.2416

Mielke, M. M., Okonkwo, O. C., Oishi, K., Mori, S., Tighe, S., Miller, M. I., Ceritoglu, C., Brown, T., Albert, M., & Lyketsos, C. G. (2012b). Fornix integrity and hippocampal volume predict memory decline and progression to Alzheimer's disease. *Alzheimer's & Dementia*, *8*(2), 105–113. https://doi.org/10.1016/j.jalz.2011.05.2416

Mielke, M., Kozauer, N., Chan, K., George, M., Toroney, J., Zerrate, M., Bandeen-Roche, K., Wang, M. C., vanZijl, P., & Pekar, J. (2009). Regionally-specific diffusion tensor imaging in mild cognitive impairment and Alzheimer's disease. *NeuroImage*, *46*(1), 47–55. https://doi.org/10.1016/j.neuroimage.2009.01.054

Mierzwa, A. J., Marion, C. M., Sullivan, G. M., McDaniel, D. P., & Armstrong, R. C. (2015). Components of Myelin Damage and Repair in the Progression of White Matter Pathology After Mild Traumatic Brain Injury. *Journal of Neuropathology and*

Experimental Neurology, *74*(3), 218–232. https://doi.org/10.1097/nen.0000000000000165

Mim, C., Balani, P., Rauen, T., & Grewer, C. (2005). The Glutamate Transporter Subtypes EAAT4 and EAATs 1-3 Transport Glutamate with Dramatically Different Kinetics and Voltage Dependence but Share a Common Uptake Mechanism. the Journal of General Physiology/the Journal of General Physiology, 126(6), 571–589. https://doi.org/10.1085/jgp.200509365

Mitew, S., Kirkcaldie, M. T. K., Halliday, G. M., Shepherd, C. E., Vickers, J. C., & Dickson, T. C. (2010). Focal demyelination in Alzheimer's disease and transgenic mouse models. *Acta Neuropathologica*, *119*(5), 567–577. https://doi.org/10.1007/s00401-010-0657-2

Mody, I. (1995). NMDA receptor-dependent excitotoxicity: the role of intracellular Ca2+ release. *Trends in Pharmacological Sciences*, *16*(10), 356–359. https://doi.org/10.1016/s0165-6147(00)89070-7

Mookherjee, P., Green, P. S., Watson, G. S., Marques, M. A., Tanaka, K., Meeker, K. D., Meabon, J. S., Li, N., Zhu, P., Olson, V. G.,

& Cook, D. G. (2011). GLT-1 Loss Accelerates Cognitive Deficit Onset in an Alzheimer's Disease Animal Model. Journal of Alzheimer's Disease, 26(3), 447–455. https://doi.org/10.3233/jad-2011-110503

Morell, P., & Quarles, R. H. (1999). *Characteristic Composition of Myelin*. https://www.ncbi.nlm.nih.gov/books/NBK28221/

Morelli, A., Ravera, S., & Panfoli, I. (2011). Hypothesis of an Energetic Function for Myelin. *Cell Biochemistry and Biophysics*, *61*(1), 179–187. https://doi.org/10.1007/s12013-011-9174-8

Mori, S., & Aggarwal, M. (2014). In vivo magnetic resonance imaging of the human limbic white matter. *Frontiers in Aging Neuroscience*, *6*. https://doi.org/10.3389/fnagi.2014.00321

Mortamais, M., Reynes, C., Brickman, A. M., Provenzano, F. A., Muraskin, J. S., Portet, F., Berr, C., Touchon, J., Bonafé, A., Bars, E. L., Maller, J. J., Meslin, C., Sabatier, R., Ritchie, K., & Artero, S. (2013). Spatial Distribution of Cerebral White Matter Lesions Predicts Progression to Mild Cognitive Impairment and Dementia. *PloS One*, *8*(2), e56972. https://doi.org/10.1371/journal.pone.0056972

Moscoso, A., Silva-Rodríguez, J., Aldrey, J. M., Cortés, J., Pías-Peleteiro, J. M., Ruibal, L., & Aguiar, P. (2021). 18F-florbetapir PET as a marker of myelin integrity across the Alzheimer's disease spectrum. *European Journal of Nuclear Medicine and Molecular Imaging*, *49*(4), 1242–1253. https://doi.org/10.1007/s00259-021-05493-y

Mountjoy, C., Roth, M., Evans, N., & Evans, H. (1983). Cortical neuronal counts in normal elderly controls and demented patients. *Neurobiology of Aging*, *4*(1), 1–11. https://doi.org/10.1016/0197-4580(83)90048-9

Nabizadeh, F., Balabandian, M., Rostami, M. R., Kankam, S. B., Ranjbaran, F., & Pourhamzeh, M. (2022). Plasma neurofilament light levels correlate with white matter damage prior to Alzheimer's disease: results from ADNI. *Aging Clinical and Experimental Research*, *34*(10), 2363–2372. https://doi.org/10.1007/s40520-022-02095-y

Nagao, S., Kwak, S., & Kanazawa, I. (1997). Correspondence. Neuroscience, 78(4), 929–933. https://doi.org/10.1016/s0306-4522(97)00021-3

Naggara, O., Oppenheim, C., Rieu, D., Raoux, N., Rodrigo, S., Barba, G. D., & Meder, J. F. (2006). Diffusion tensor imaging in early Alzheimer's disease. *Psychiatry Research. Neuroimaging*, *146*(3), 243–249. https://doi.org/10.1016/j.pscychresns.2006.01.005

Nakano, I. (1998). The limbic system: An outline and brief history of its concept. *Neuropathology*, *18*(2), 211–214. https://doi.org/10.1111/j.1440-1789.1998.tb00102.x

Nardini, E., Hogan, R., Flamier, A., & Bernier, G. (2021). Alzheimer's disease: a tale of two diseases? *Neural Regeneration Research/Neural Regeneration Research*, *16*(10), 1958. https://doi.org/10.4103/1673-5374.308070

Narine, M., & Colognato, H. (2022). Current Insights Into Oligodendrocyte Metabolism and Its Power to Sculpt the Myelin Landscape. *Frontiers in Cellular Neuroscience*, *16*. https://doi.org/10.3389/fncel.2022.892968

Nasrabady, S. E., Rizvi, B., Goldman, J. E., & Brickman, A. M. (2018). White matter changes in Alzheimer's disease: a focus on myelin and oligodendrocytes. *Acta Neuropathologica*

Communications, *6*(1). https://doi.org/10.1186/s40478-018-0515-3

Nauta, W. J. H. (1958). HIPPOCAMPAL PROJECTIONS AND RELATED NEURAL PATHWAYS TO THE MID-BRAIN IN THE CAT. *Brain*, *81*(3), 319–340. https://doi.org/10.1093/brain/81.3.319

Nave, K. A. (2010). Myelination and the trophic support of long axons. *Nature Reviews. Neuroscience*, *11*(4), 275–283. https://doi.org/10.1038/nrn2797

Nicoletti, F., Bockaert, J., Collingridge, G., Conn, P., Ferraguti, F., Schoepp, D., Wroblewski, J., & Pin, J. (2011). Metabotropic glutamate receptors: From the workbench to the bedside. *Neuropharmacology*, *60*(7–8), 1017–1041. https://doi.org/10.1016/j.neuropharm.2010.10.022

Nielsen, H. M., Ek, D., Avdic, U., Orbjörn, C., Hansson, O., Veerhuis, R., Rozemuller, A. J., Brun, A., Minthon, L., & Wennström, M. (2013). NG2 cells, a new trail for Alzheimer's disease mechanisms? *Acta Neuropathologica Communications*, *1*(1). https://doi.org/10.1186/2051-5960-1-7

Nishiyama, A. (2007). Polydendrocytes: NG2 Cells with Many Roles in Development and Repair of the CNS. *Neuroscientist*, *13*(1), 62–76. https://doi.org/10.1177/1073858406295586

Nishiyama, A., Boshans, L., Goncalves, C. M., Wegrzyn, J., & Patel, K. D. (2016). Lineage, fate, and fate potential of NG2-glia. *Brain Research*, *1638*, 116–128. https://doi.org/10.1016/j.brainres.2015.08.013

Nishiyama, A., Komitova, M., Suzuki, R., & Zhu, X. (2009). Polydendrocytes (NG2 cells): multifunctional cells with lineage plasticity. *Nature Reviews. Neuroscience*, *10*(1), 9–22. https://doi.org/10.1038/nrn2495

Nishiyama, A., Lin, X. H., Giese, N., Heldin, C. H., & Stallcup, W. (1996). Co-localization of NG2 proteoglycan and PDGF α-receptor on O2A progenitor cells in the developing rat brain. *Journal of Neuroscience Research*, *43*(3), 299–314. https://doi.org/10.1002/(sici)1097-4547(19960201)43:3

Niswender, C. M., & Conn, P. J. (2010). Metabotropic Glutamate Receptors: Physiology, Pharmacology, and Disease. *Annual Review of Pharmacology and Toxicology*, *50*(1), 295–322.

https://doi.org/10.1146/annurev.pharmtox.011008.145533

Norris, C. M., Blalock, E. M., Thibault, O., Brewer, L. D., Clodfelter, G. V., Porter, N. M., & Landfield, P. W. (2006). Electrophysiological Mechanisms of Delayed Excitotoxicity: Positive Feedback Loop Between NMDA Receptor Current and Depolarization-Mediated Glutamate Release. Journal of Neurophysiology, 96(5), 2488–2500. https://doi.org/10.1152/jn.00593.2005

Nowrangi, M. A., & Rosenberg, P. B. (2015). The Fornix in Mild Cognitive Impairment and Alzheimer's Disease. *Frontiers in Aging Neuroscience*, *7*. https://doi.org/10.3389/fnagi.2015.00001

Nowrangi, M. A., Lyketsos, C. G., Leoutsakos, J. S., Oishi, K., Albert, M., Mori, S., & Mielke, M. M. (2012). Longitudinal, region-specific course of diffusion tensor imaging measures in mild cognitive impairment and Alzheimer's disease. *Alzheimer's & Dementia*, *9*(5), 519–528. https://doi.org/10.1016/j.jalz.2012.05.2186

Nystuen, K. L., McNamee, S. M., Akula, M., Holton, K. M., DeAngelis, M. M., & Haider, N. B. (2024). Alzheimer's Disease: Models and Molecular Mechanisms Informing Disease and Treatments. *Bioengineering*, *11*(1), 45. https://doi.org/10.3390/bioengineering11010045

Obrenovitch, T. P., & Urenjak, J. (1997). Altered glutamatergic transmission in neurological disorders: From high extracellular glutamate to excessive synaptic efficacy. *Progress in Neurobiology*, *51*(1), 39–87. https://doi.org/10.1016/s0301-0082(96)00049-4

Oddo, S., Caccamo, A., Shepherd, J. D., Murphy, M., Golde, T. E., Kayed, R., Metherate, R., Mattson, M. P., Akbari, Y., & LaFerla, F. M. (2003). Triple-Transgenic Model of Alzheimer's Disease with Plaques and Tangles. *Neuron*, *39*(3), 409–421. https://doi.org/10.1016/s0896-6273(03)00434-3

Oishi, K., & Lyketsos, C. G. (2014). Alzheimere's disease and the fornix. *Frontiers in Aging Neuroscience*, *6*. https://doi.org/10.3389/fnagi.2014.00241

Oishi, K., Mielke, M. M., Albert, M., Lyketsos, C. G., & Mori, S. (2011). The Fornix Sign: A Potential Sign for Alzheimer's Disease Based on Diffusion Tensor Imaging. *Journal of Neuroimaging*, *22*(4), 365–374. https://doi.org/10.1111/j.1552-6569.2011.00633.x

Olajide, O. J., Gbadamosi, I. T., Yawson, E. O., Arogundade, T., Lewu, F. S., Ogunrinola, K. Y., Adigun, O. O., Bamisi, O., Lambe, E., Arietarhire, L. O., Oluyomi, O. O., Idowu, O. K., Kareem, R., Asogwa, N. T., & Adeniyi, P. A. (2021). Hippocampal Degeneration and Behavioral Impairment During Alzheimer-Like Pathogenesis Involves Glutamate Excitotoxicity. *Journal of Molecular Neuroscience*, *71*(6), 1205–1220. https://doi.org/10.1007/s12031-020-01747-w

Orobets, K. S., & Karamyshev, A. L. (2023). Amyloid Precursor Protein and Alzheimer's Disease. *International Journal of Molecular Sciences*, *24*(19), 14794. https://doi.org/10.3390/ijms241914794

Ota, M., Sato, N., Kimura, Y., Shigemoto, Y., Kunugi, H., & Matsuda, H. (2019). Changes of Myelin Organization in Patients with Alzheimer's Disease Shown by q-Space Myelin Map Imaging.

Dementia and Geriatric Cognitive Disorders. Extra, *9*(1), 24–33. https://doi.org/10.1159/000493937

Ottersen, O. P., Laake, J. H., Reichelt, W., Haug, F. M., & Torp, R. (1996). Ischemic disruption of glutamate homeostasis in brain: quantitative immunocytochemical analyses. *Journal of Chemical Neuroanatomy*, *12*(1), 1–14. https://doi.org/10.1016/s0891-0618(96)00178-0

Ozdogmus, O., Cavdar, S., Ersoy, Y., Ercan, F., & Uzun, I. (2009). A preliminary study, using electron and light-microscopic methods, of axon numbers in the fornix in autopsies of patients with temporal lobe epilepsy. *Anatomical Science International*, *84*(1–2), 2–6. https://doi.org/10.1007/s12565-008-0001-2

Pandurangan, K., Jayakumar, J., Savoia, S., Nanda, R., Lata, S., Kumar, E. H., S, S., Vasudevan, S., Srinivasan, C., Joseph, J., Sivaprakasam, M., & Verma, R. (2024). Systematic development of immunohistochemistry protocol for large cryosections-specific to non-perfused fetal brain. *Journal of Neuroscience Methods*, *405*, 110085. https://doi.org/10.1016/j.jneumeth.2024.110085

Papez, J. W. (1937). A proposed mechanism of emotion. *The Journal of Neuropsychiatry and Clinical Neurosciences*, *7*, 103–112.

Papuć, E., Kurys-Denis, E., Krupski, W., Tatara, M., & Rejdak, K. (2015). Can Antibodies Against Glial Derived Antigens be Early Biomarkers of Hippocampal Demyelination and Memory Loss in Alzheimer's Disease? *Journal of Alzheimer's Disease*, *48*(1), 115–121. https://doi.org/10.3233/jad-150309

Parnetti, L., Chipi, E., Salvadori, N., D'Andrea, K., & Eusebi, P. (2019). Prevalence and risk of progression of preclinical Alzheimer's disease stages: a systematic review and meta-analysis. *Alzheimer's Research & Therapy*, *11*(1). https://doi.org/10.1186/s13195-018-0459-7

Patestas, M. A., & Gartner, L. P. (2006). Limbic system. In *A Text book of Neuroanatomy* (pp. 344–359). Blackwell.

Paxinos, G., & Watson, C. (2013). *The Rat Brain in Stereotaxic Coordinates*. Academic Press.

Pelvig, D., Pakkenberg, H., Stark, A., & Pakkenberg, B. (2008). Neocortical glial cell numbers in human brains.

Neurobiology of Aging, *29*(11), 1754–1762. https://doi.org/10.1016/j.neurobiolaging.2007.04.013

Peng, Y., Jin, H., Xue, Y. H., Chen, Q., Yao, S. Y., Du, M. Q., & Liu, S. (2023). Current and future therapeutic strategies for Alzheimer's disease: an overview of drug development bottlenecks. *Frontiers in Aging Neuroscience*, *15*. https://doi.org/10.3389/fnagi.2023.1206572

Petralia, R., Rubio, M., & Wenthold, R. (1999). Cellular and subcellular distribution of glutamate receptors. In P. Jonas & H. Monyer (Eds.), *Ionotropic glutamate receptors in the CNS* (pp. 143–171). Springer.

Phillis, J., Smith-Barbour, M., Perkins, L., & O'Regan, M. (1994). Characterization of glutamate, aspartate, and GABA release from ischemic rat cerebral cortex. *Brain Research Bulletin*, *34*(5), 457–466. https://doi.org/10.1016/0361-9230(94)90019-1

Pievani, M., Agosta, F., Pagani, E., Canu, E., Sala, S., Absinta, M., Geroldi, C., Ganzola, R., Frisoni, G. B., & Filippi, M. (2010). Assessment of white matter tract damage in mild cognitive impairment and Alzheimer's disease. *Human Brain*

Mapping, *31*(12), 1862–1875. https://doi.org/10.1002/hbm.20978

Pihlajamaki, M., Jauhiainen, A., & Soininen, H. (2009). Structural and Functional MRI in Mild Cognitive Impairment. *Current Alzheimer Research*, *6*(2), 179–185. https://doi.org/10.2174/156720509787602898

Pines, G., Danbolt, N. C., Bjørås, M., Zhang, Y., Bendahan, A., Eide, L., Koepsell, H., Storm-Mathisen, J., Seeberg, E., & Kanner, B. I. (1992). Cloning and expression of a rat brain L-glutamate transporter. Nature, 360(6403), 464–467. https://doi.org/10.1038/360464a0

Poitelon, Y., Kopec, A. M., & Belin, S. (2020). Myelin Fat Facts: An Overview of Lipids and Fatty Acid Metabolism. *Cells*, *9*(4), 812. https://doi.org/10.3390/cells9040812

Porsteinsson, A., Isaacson, R., Knox, S., Sabbagh, M., & Rubino, I. (2021). Diagnosis of Early Alzheimer's Disease: Clinical Practice in 2021. *the Journal of Prevention of Alzheimer's Disease/JPAD*, 1–16. https://doi.org/10.14283/jpad.2021.23

Povala, G., Bellaver, B., De Bastiani, M. A., Brum, W. S., Ferreira, P. C. L., Bieger, A., Pascoal, T. A., Benedet, A. L., Souza, D. O., Araujo, R. M., Zatt, B., Rosa-Neto, P., Zimmer, E. R., & Author_Id, N. (2021). Soluble amyloid-beta isoforms predict downstream Alzheimer's disease pathology. *Cell & Bioscience*, *11*(1). https://doi.org/10.1186/s13578-021-00712-3

Prince, M., Bryce, R., Albanese, E., Wimo, A., Ribeiro, W., & Ferri, C. P. (2013). The global prevalence of dementia: A systematic review and metaanalysis. *Alzheimer's & Dementia*, *9*(1), 63. https://doi.org/10.1016/j.jalz.2012.11.007

Pringle, N. P., & Richardson, W. D. (1993). A singularity of PDGF alpha-receptor expression in the dorsoventral axis of the neural tube may define the origin of the oligodendrocyte lineage. *Development*, *117*(2), 525–533. https://doi.org/10.1242/dev.117.2.525

Pringle, N. P., Mudhar, H. S., Collarini, E. J., & Richardson, W. D. (1992). PDGF receptors in the rat CNS: during late neurogenesis, PDGF alpha-receptor expression appears to be restricted to glial cells of the oligodendrocyte lineage.

Development, *115*(2), 535–551. https://doi.org/10.1242/dev.115.2.535

Privat, A., Jacque, C., Bourre, J., Dupouey, P., & Baumann, N. (1979). Absence of the major dense line in myelin of the mutant mouse 'shiverer.' *Neuroscience Letters*, *12*(1), 107–112. https://doi.org/10.1016/0304-3940(79)91489-7

Qian, A., & Johnson, J. W. (2002). Channel gating of NMDA receptors. *Physiology & Behavior*, *77*(4–5), 577–582. https://doi.org/10.1016/s0031-9384(02)00906-x

Quarles, R. H. (2006). Myelin-associated glycoprotein (MAG): past, present and beyond. Journal of Neurochemistry, 100(6), 1431–1448. https://doi.org/10.1111/j.1471-4159.2006.04319.x

Rabin, J. S., Perea, R. D., Buckley, R. F., Johnson, K. A., Sperling, R. A., & Hedden, T. (2019). Synergism between fornix microstructure and beta amyloid accelerates memory decline in clinically normal older adults. *Neurobiology of Aging*, *81*, 38–46. https://doi.org/10.1016/j.neurobiolaging.2019.05.005

Rabin, J. S., Perea, R. D., Buckley, R. F., Neal, T. E., Buckner, R. L., Johnson, K. A., Sperling, R. A., & Hedden, T. (2018). Global White Matter Diffusion Characteristics Predict Longitudinal Cognitive Change Independently of Amyloid Status in Clinically Normal Older Adults. *Cerebral Cortex*, *29*(3), 1251–1262. https://doi.org/10.1093/cercor/bhy031

Racine, A. M., Adluru, N., Alexander, A. L., Christian, B. T., Okonkwo, O. C., Oh, J., Cleary, C. A., Birdsill, A., Hillmer, A. T., Murali, D., Barnhart, T. E., Gallagher, C. L., Carlsson, C. M., Rowley, H. A., Dowling, N. M., Asthana, S., Sager, M. A., Bendlin, B. B., & Johnson, S. C. (2014). Associations between white matter microstructure and amyloid burden in preclinical Alzheimer's disease: A multimodal imaging investigation. *NeuroImage. Clinical*, *4*, 604–614. https://doi.org/10.1016/j.nicl.2014.02.001

Radde, R., Bolmont, T., Kaeser, S. A., Coomaraswamy, J., Lindau, D., Stoltze, L., Calhoun, M. E., Jäggi, F., Wolburg, H., Gengler, S., Haass, C., Ghetti, B., Czech, C., Hölscher, C., Mathews, P. M., & Jucker, M. (2006). Aβ42-driven cerebral amyloidosis in transgenic mice reveals early and robust pathology. *EMBO*

Reports, *7*(9), 940–946. https://doi.org/10.1038/sj.embor.7400784

Raff, M. C., Miller, R. H., & Noble, M. (1983). A glial progenitor cell that develops in vitro into an astrocyte or an oligodendrocyte depending on culture medium. *Nature*, *303*(5916), 390–396. https://doi.org/10.1038/303390a0

Raine, C. S. (1984). The Neuropathology of Myelin Diseases. In *Springer eBooks* (pp. 259–310). https://doi.org/10.1007/978-1-4757-1830-0_8

Ramirez-Bermudez, J. (2012). Alzheimer's Disease: Critical Notes on the History of a Medical Concept. *Archives of Medical Research*, *43*(8), 595–599. https://doi.org/10.1016/j.arcmed.2012.11.008

Rasband, M. N., & Peles, E. (2020). Mechanisms of node of Ranvier assembly. *Nature Reviews. Neuroscience*, *22*(1), 7–20. https://doi.org/10.1038/s41583-020-00406-8

Redwine, J. M., Kosofsky, B., Jacobs, R. E., Games, D., Reilly, J. F., Morrison, J. H., Young, W. G., & Bloom, F. E. (2003). Dentate gyrus volume is reduced before onset of plaque formation in PDAPP mice: A magnetic resonance microscopy and

stereologic analysis. *Proceedings of the National Academy of Sciences of the United States of America*, *100*(3), 1381–1386. https://doi.org/10.1073/pnas.242746599

Rego, A., & De Almeida, L. (2005). Molecular Targets and Therapeutic Strategies in Huntingtons Disease. *Current Drug Targets. CNS & Neurological Disorders*, *4*(4), 361–381. https://doi.org/10.2174/1568007054546081

Reisberg, B., Franssen, E. H., Souren, L. E., Auer, S. R., Akram, I., & Kenowsky, S. (2002). Evidence and mechanisms of retrogenesis in Alzheimer's and other dementias: Management and treatment import. *American Journal of Alzheimer's Disease and Other Dementias*, *17*(4), 202–212. https://doi.org/10.1177/153331750201700411

Reitz, C., Rogaeva, E., & Beecham, G. W. (2020). Late-onset vs nonmendelian early-onset Alzheimer disease. *Neurology. Genetics*, *6*(5). https://doi.org/10.1212/nxg.0000000000000512

Reynolds, B. A., & Weiss, S. (1992). Generation of Neurons and Astrocytes from Isolated Cells of the Adult Mammalian

Central Nervous System. *Science*, *255*(5052), 1707–1710. https://doi.org/10.1126/science.1553558

Richardson, W. D., Kessaris, N., & Pringle, N. (2006). Oligodendrocyte wars. *Nature Reviews. Neuroscience*, *7*(1), 11–18. https://doi.org/10.1038/nrn1826

Richardson, W. D., Young, K. M., Tripathi, R. B., & McKenzie, I. (2011). NG2-glia as Multipotent Neural Stem Cells: Fact or Fantasy? *Neuron*, *70*(4), 661–673. https://doi.org/10.1016/j.neuron.2011.05.013

Ringman, J. M., O'Neill, J., Geschwind, D., Medina, L., Apostolova, L. G., Rodriguez, Y., Schaffer, B., Varpetian, A., Tseng, B., Ortiz, F., Fitten, J., Cummings, J. L., & Bartzokis, G. (2007). Diffusion tensor imaging in preclinical and presymptomatic carriers of familial Alzheimer's disease mutations. *Brain*, *130*(7), 1767–1776. https://doi.org/10.1093/brain/awm102

Rivers, L. E., Young, K. M., Rizzi, M., Jamen, F., Psachoulia, K., Wade, A., Kessaris, N., & Richardson, W. D. (2008). PDGFRA/NG2 glia generate myelinating oligodendrocytes and piriform projection neurons in adult mice. *Nature Neuroscience*, *11*(12), 1392–1401. https://doi.org/10.1038/nn.2220

Robertson, W. F. (1899). On a new method of obtaining a black reaction in certain tissue-elements of the central nervous system (platinum method). *Scottish Medical Journal*, *4*(23).

Robertson, W. F. (1900a). A microscopic demonstration of the normal and pathological histology of mesoglia cells. *The Journal of Mental Science*, *46*, 733–752.

Robertson, W. F. (1900b). *A text-book of pathology in relation to mental diseases*. William F. Clay.

Rodriguez-Rodriguez, P., Almeida, A., & Bolaños, J. P. (2013). Brain energy metabolism in glutamate-receptor activation and excitotoxicity: Role for APC/C-Cdh1 in the balance glycolysis/pentose phosphate pathway. Neurochemistry International, 62(5), 750–756. https://doi.org/10.1016/j.neuint.2013.02.005

Rogalski, E. J., Murphy, C. M., deToledo-Morrell, L., Shah, R. C., Moseley, M. E., Bammer, R., & Stebbins, G. T. (2009). Changes in parahippocampal white matter integrity in amnestic mild cognitive impairment: a diffusion tensor imaging study. *DOAJ (DOAJ: Directory of Open Access Journals)*. https://doi.org/10.3233/ben-2009-0235

Rogawski, M. A. (2013). AMPA receptors as a molecular target in epilepsy therapy. *Acta Neurologica Scandinavica*, *127*, 9–18. https://doi.org/10.1111/ane.12099

Roher, A. E., Weiss, N., Kokjohn, T. A., Kuo, Y. M., Kalback, W., Anthony, J., Watson, D., Luehrs, D. C., Sue, L., Walker, D., Emmerling, M., Goux, W., & Beach, T. (2002). Increased Aβ Peptides and Reduced Cholesterol and Myelin Proteins Characterize White Matter Degeneration in Alzheimer's Disease. *Biochemistry*, *41*(37), 11080–11090. https://doi.org/10.1021/bi026173d

Rose, S. E., Chen, F., Chalk, J., Zelaya, F., Strugnel, W., Benson, M., Semple, J., & Doddrell, D. (2000). Loss of connectivity in Alzheimer's disease: an evaluation of white matter tract integrity with colour coded MR diffusion tensor imaging. *Journal of Neurology, Neurosurgery and Psychiatry*, *69*(4), 528–530. https://doi.org/10.1136/jnnp.69.4.528

Rose, S. E., McMahon, K., Janke, A., O'Dowd, B., De Zubicaray, G., Strudwick, M., & Chalk, J. (2006). Diffusion indices on magnetic resonance imaging and neuropsychological performance in amnestic mild cognitive impairment. *Journal*

of Neurology, Neurosurgery and Psychiatry, *77*(10), 1122–1128. https://doi.org/10.1136/jnnp.2005.074336

Rosene, D. L., & Van Hoesen, G. (1987). The Hippocampal Formation of the Primate Brain: A review of Some Comparative Aspects of Cytoarchitecture and Connections. In E. G. Jones & A. Peters (Eds.), *Cerebral Cortex: Further Aspects of Cortical Function, Including Hippocampus* (Vol. 6). Plenum Press.

Rothstein, J. D., Dykes-Hoberg, M., Pardo, C. A., Bristol, L. A., Jin, L., Kuncl, R. W., Kanai, Y., Hediger, M. A., Wang, Y., Schielke, J. P., & Welty, D. F. (1996). Knockout of Glutamate Transporters Reveals a Major Role for Astroglial Transport in Excitotoxicity and Clearance of Glutamate. *Neuron*, *16*(3), 675–686. https://doi.org/10.1016/s0896-6273(00)80086-0

Rothstein, J. D., Jin, L., Dykes-Hoberg, M., & Kuncl, R. W. (1993). Chronic inhibition of glutamate uptake produces a model of slow neurotoxicity. *Proceedings of the National Academy of Sciences of the United States of America*, *90*(14), 6591–6595. https://doi.org/10.1073/pnas.90.14.6591

Sabia, S., Fayosse, A., Dumurgier, J., Van Hees, V. T., Paquet, C., Sommerlad, A., Kivimäki, M., Dugravot, A., & Singh-Manoux,

A. (2021). Association of sleep duration in middle and old age with incidence of dementia. *Nature Communications*, *12*(1). https://doi.org/10.1038/s41467-021-22354-2

Salat, D., Tuch, D., Van Der Kouwe, A., Greve, D., Pappu, V., Lee, S., Hevelone, N., Zaleta, A., Growdon, J., Corkin, S., Fischl, B., & Rosas, H. (2010). White matter pathology isolates the hippocampal formation in Alzheimer's disease. *Neurobiology of Aging*, *31*(2), 244–256. https://doi.org/10.1016/j.neurobiolaging.2008.03.013

Salmon, D. P., & Butters, N. (1992). Neuropsychological assessment of dementia in the elderly. In R. Katzman & J. W. Rowe (Eds.), *Principles of geriatric neurology* (pp. 144–163).

Salter, M. G., & Fern, R. (2005). NMDA receptors are expressed in developing oligodendrocyte processes and mediate injury. *Nature*, *438*(7071), 1167–1171. https://doi.org/10.1038/nature04301

Salzer, J., & Zalc, B. (2016). Myelination. *CB/Current Biology*, *26*(20), R971–R975. https://doi.org/10.1016/j.cub.2016.07.074

Sánchez, I., Hassinger, L., Paskevich, P. A., Shine, H. D., & Nixon, R. A. (1996). Oligodendroglia Regulate the Regional Expansion of

Axon Caliber and Local Accumulation of Neurofilaments during Development Independently of Myelin Formation. *the Journal of Neuroscience/the Journal of Neuroscience*, *16*(16), 5095–5105. https://doi.org/10.1523/jneurosci.16-16-05095.1996

Santangelo, R. M., Acker, T. M., Zimmerman, S. S., Katzman, B. M., Strong, K. L., Traynelis, S. F., & Liotta, D. C. (2012). Novel NMDA receptor modulators: an update. *Expert Opinion on Therapeutic Patents*, *22*(11), 1337–1352. https://doi.org/10.1517/13543776.2012.728587

Sasaguri, H., Nilsson, P., Hashimoto, S., Nagata, K., Saito, T., De Strooper, B., Hardy, J., Vassar, R., Winblad, B., & Saido, T. C. (2017). APP mouse models for Alzheimer's disease preclinical studies. *EMBO Journal*, *36*(17), 2473–2487. https://doi.org/10.15252/embj.201797397

Saunders, R. C., & Aggleton, J. P. (2007). Origin and topography of fibers contributing to the fornix in macaque monkeys. *Hippocampus*, *17*(5), 396–411. https://doi.org/10.1002/hipo.20276

SchäBitz, W. R., Li, F., & Fisher, M. (2000). The N -Methyl- d -Aspartate Antagonist CNS 1102 Protects Cerebral Gray and White Matter From Ischemic Injury Following Temporary Focal Ischemia in Rats. *Stroke*, *31*(7), 1709–1714. https://doi.org/10.1161/01.str.31.7.1709

Schallier, A., Smolders, I., Van Dam, D., Loyens, E., De Deyn, P. P., Michotte, A., Michotte, Y., & Massie, A. (2011). Region- and Age-Specific Changes in Glutamate Transport in the AβPP23 Mouse Model for Alzheimer's Disease. Journal of Alzheimer's Disease, 24(2), 287–300. https://doi.org/10.3233/jad-2011-101005

Scheltens, P., Barkhof, F., Leys, D., Wolters, E. C., Ravid, R., & Kamphorst, W. (1995). Histopathologic correlates of white matter changes on MRI in Alzheimer's disease and normal aging. *Neurology*, *45*(5), 883–888. https://doi.org/10.1212/wnl.45.5.883

Schmued, L. C., Raymick, J., Paule, M. G., Dumas, M., & Sarkar, S. (2013). Characterization of Myelin Pathology in the Hippocampal Complex of a Transgenic Mouse Model of

Alzheimer's Disease. *Current Alzheimer Research*, *10*(1), 30–37. https://doi.org/10.2174/1567205011310010005

Schreiner, A. E., Durry, S., Aida, T., Stock, M. C., Rüther, U., Tanaka, K., Rose, C. R., & Kafitz, K. W. (2013). Laminar and subcellular heterogeneity of GLAST and GLT-1 immunoreactivity in the developing postnatal mouse hippocampus. Journal of Comparative Neurology, 522(1), 204–224. https://doi.org/10.1002/cne.23450

Schworer, E. K., Handen, B. L., Petersen, M., O'Bryant, S., Peven, J. C., Tudorascu, D. L., Lee, L., Krinsky-McHale, S. J., Hom, C. L., Clare, I. C. H., Christian, B. T., Schupf, N., Lee, J. H., Head, E., Mapstone, M., Lott, I., Ances, B. M., Zaman, S., Brickman, A. M., . . . Hartley, S. L. (2024). Cognitive and functional performance and plasma biomarkers of early Alzheimer's disease in Down syndrome. *Alzheimer's & Dementia. Diagnosis, Assessment & Disease Monitoring*, *16*(2). https://doi.org/10.1002/dad2.12582

Scimemi, A., Meabon, J. S., Woltjer, R. L., Sullivan, J. M., Diamond, J. S., & Cook, D. G. (2013). Amyloid-β1–42Slows Clearance of Synaptically Released Glutamate by Mislocalizing Astrocytic

GLT-1. the Journal of Neuroscience/the Journal of Neuroscience, 33(12), 5312–5318. https://doi.org/10.1523/jneurosci.5274-12.2013

Seki, Y., Feustel, P. J., Keller, R. W., Tranmer, B. I., & Kimelberg, H. K. (1999). Inhibition of Ischemia-Induced Glutamate Release in Rat Striatum by Dihydrokinate and an Anion Channel Blocker. *Stroke*, *30*(2), 433–440. https://doi.org/10.1161/01.str.30.2.433

Senova, S., Fomenko, A., Gondard, E., & Lozano, A. M. (2020). Anatomy and function of the fornix in the context of its potential as a therapeutic target. *Journal of Neurology, Neurosurgery and Psychiatry*, *91*(5), 547–559. https://doi.org/10.1136/jnnp-2019-322375

Shelton, M. K., & McCarthy, K. D. (1999). Mature hippocampal astrocytes exhibit functional metabotropic and ionotropic glutamate receptors in situ. *GLIA*, *26*(1), 1–11. https://doi.org/10.1002/(sici)1098-1136(199903)26:1

Shen, Z., Lei, J., Li, X., Wang, Z., Bao, X., & Wang, R. (2018). Multifaceted assessment of the APP/PS1 mouse model for Alzheimer's disease: Applying MRS, DTI, and ASL. *Brain*

Research, *1698*, 114–120. https://doi.org/10.1016/j.brainres.2018.08.001

Shigeri, Y., Shimamoto, K., Yasuda-Kamatani, Y., Seal, R. P., Yumoto, N., Nakajima, T., & Amara, S. G. (2001). Effects of threo-β-hydroxyaspartate derivatives on excitatory amino acid transporters (EAAT4 and EAAT5). Journal of Neurochemistry, 79(2), 297–302. https://doi.org/10.1046/j.1471-4159.2001.00588.x

Shimamoto, K., Lebrun, B., Yasuda-Kamatani, Y., Sakaitani, M., Shigeri, Y., Yumoto, N., & Nakajima, T. (1998). dl-threo-β-Benzyloxyaspartate, A Potent Blocker of Excitatory Amino Acid Transporters. *Molecular Pharmacology*, *53*(2), 195–201. https://doi.org/10.1124/mol.53.2.195

Silva, M. V. F., De Mello Gomide Loures, C., Alves, L. C. V., De Souza, L. C., Borges, K. B. G., & Carvalho, M. D. G. (2019). Alzheimer's disease: risk factors and potentially protective measures. *Journal of Biomedical Science*, *26*(1). https://doi.org/10.1186/s12929-019-0524-y

Simpson, J. E., Fernando, M. S., Clark, L., Ince, P. G., Matthews, F., Forster, G., O'Brien, J. T., Barber, R., Kalaria, R. N., Brayne,

C., Shaw, P. J., Lewis, C. E., & Wharton, S. B. (2007). White matter lesions in an unselected cohort of the elderly: astrocytic, microglial and oligodendrocyte precursor cell responses. *Neuropathology & Applied Neurobiology/Neuropathology and Applied Neurobiology*, *33*(4), 410–419. https://doi.org/10.1111/j.1365-2990.2007.00828.x

Sjöbeck, M., Haglund, M., & Englund, E. (2005). Decreasing myelin density reflected increasing white matter pathology in Alzheimer's disease—a neuropathological study. *International Journal of Geriatric Psychiatry*, *20*(10), 919–926. https://doi.org/10.1002/gps.1384

Sjöbeck, M., Haglund, M., & Englund, E. (2006). White matter mapping in Alzheimer's disease: A neuropathological study. *Neurobiology of Aging*, *27*(5), 673–680. https://doi.org/10.1016/j.neurobiolaging.2005.03.007

Skoff, R. P., Bessert, D. A., Barks, J. D., Song, D., Cerghet, M., & Silverstein, F. S. (2001). Hypoxic–ischemic injury results in acute disruption of myelin gene expression and death of oligodendroglial precursors in neonatal mice. *International*

Journal of Developmental Neuroscience, *19*(2), 197–208. https://doi.org/10.1016/s0736-5748(00)00075-7

Small, D. H., & Cappai, R. (2006). Alois Alzheimer and Alzheimer's disease: a centennial perspective. *Journal of Neurochemistry*, *99*(3), 708–710. https://doi.org/10.1111/j.1471-4159.2006.04212.x

Smith, C. D., Malcein, M., Meurer, K., Schmitt, F. A., Markesbery, W. R., & Pettigrew, L. C. (1999). MRI Temporal Lobe Volume Measures and Neuropsychologic Function in Alzheimer's Disease. *Journal of Neuroimaging*, *9*(1), 2–9. https://doi.org/10.1111/jon1999912

Smith, K. J., Blakemore, W. F., & Mcdonald, W. I. (1979). Central remyelination restores secure conduction. *Nature*, *280*(5721), 395–396. https://doi.org/10.1038/280395a0

Smith, Q. R. (2000). Transport of Glutamate and Other Amino Acids at the Blood-Brain Barrier. *the Journal of Nutrition/the Journal of Nutrition*, *130*(4), 1016S-1022S. https://doi.org/10.1093/jn/130.4.1016s

Soares, R., Ribeiro, F. F., Lourenço, D. M., Rodrigues, R. S., Moreira, J. B., Sebastião, A. M., Morais, V. A., & Xapelli, S. (2020).

Isolation and Expansion of Neurospheres from Postnatal (P1-3) Mouse Neurogenic Niches. *Journal of Visualized Experiments*, *159*. https://doi.org/10.3791/60822

Soldán, M., & Pirko, I. (2012). Biogenesis and Significance of Central Nervous System Myelin. *Seminars in Neurology*, *32*(01), 009–014. https://doi.org/10.1055/s-0032-1306381

Song, S. K., Kim, J. H., Lin, S. J., Brendza, R. P., & Holtzman, D. M. (2004). Diffusion tensor imaging detects age-dependent white matter changes in a transgenic mouse model with amyloid deposition. *Neurobiology of Disease*, *15*(3), 640–647. https://doi.org/10.1016/j.nbd.2003.12.003

Squire, L. R., & Zola-Morgan, S. (1991). The Medial Temporal Lobe Memory System. *Science*, *253*(5026), 1380–1386. https://doi.org/10.1126/science.1896849

Stadelmann, C., Timmler, S., Barrantes-Freer, A., & Simons, M. (2019). Myelin in the Central Nervous System: Structure, Function, and Pathology. *Physiological Reviews*, *99*(3), 1381–1431. https://doi.org/10.1152/physrev.00031.2018

Stallcup, W. B. (1981). The NG2 antigen, a putative lineage marker: Immunofluorescent localization in primary cultures of rat

brain. *Developmental Biology*, *83*(1), 154–165. https://doi.org/10.1016/s0012-1606(81)80018-8

Steinhäuser, C., & Gallo, V. (1996). News on glutamate receptors in glial cells. *Trends in Neurosciences*, *19*(8), 339–345. https://doi.org/10.1016/0166-2236(96)10043-6

Stern, J. R., Eggleston, L. V., Hems, R., & Krebs, H. A. (1949). Accumulation of glutamic acid in isolated brain tissue. *Biochemical Journal. Cellular Aspects*, *44*(4), 410–418. https://doi.org/10.1042/bj0440410

Storck, T., Schulte, S., Hofmann, K., & Stoffel, W. (1992). Structure, expression, and functional analysis of a Na(+)-dependent glutamate/aspartate transporter from rat brain. Proceedings of the National Academy of Sciences of the United States of America, 89(22), 10955–10959. https://doi.org/10.1073/pnas.89.22.10955

Stoub, T. R., deToledo-Morrell, L., Stebbins, G. T., Leurgans, S., Bennett, D. A., & Shah, R. C. (2006). Hippocampal disconnection contributes to memory dysfunction in individuals at risk for Alzheimer's disease. *Proceedings of the National Academy of Sciences of the United States of*

America, *103*(26), 10041–10045. https://doi.org/10.1073/pnas.0603414103

Strange, B. A., Witter, M. P., Lein, E. S., & Moser, E. I. (2014). Functional organization of the hippocampal longitudinal axis. *Nature Reviews. Neuroscience*, *15*(10), 655–669. https://doi.org/10.1038/nrn3785

Stricker, N. H., Schweinsburg, B. C., Delano-Wood, L., Wierenga, C. E., Bangen, K. J., Haaland, K. Y., Frank, L. R., Salmon, D. P., & Bondi, M. W. (2009). Decreased white matter integrity in late-myelinating fiber pathways in Alzheimer's disease supports retrogenesis. *NeuroImage*, *45*(1), 10–16. https://doi.org/10.1016/j.neuroimage.2008.11.027

Stys, P. (2004). White Matter Injury Mechanisms. *Current Molecular Medicine*, *4*(2), 113–130. https://doi.org/10.2174/1566524043479220

Südhof, T. C. (1995). The synaptic vesicle cycle: a cascade of protein–protein interactions. *Nature*, *375*(6533), 645–653. https://doi.org/10.1038/375645a0

Sun, S. W., Song, S. K., Harms, M. P., Lin, S. J., Holtzman, D. M., Merchant, K. M., & Kotyk, J. J. (2005). Detection of age-

dependent brain injury in a mouse model of brain amyloidosis associated with Alzheimer's disease using magnetic resonance diffusion tensor imaging. *Experimental Neurology*, *191*(1), 77–85. https://doi.org/10.1016/j.expneurol.2004.09.006

Sun, Y., Islam, S., Michikawa, M., & Zou, K. (2024). Presenilin: A Multi-Functional Molecule in the Pathogenesis of Alzheimer's Disease and Other Neurodegenerative Diseases. *International Journal of Molecular Sciences*, *25*(3), 1757. https://doi.org/10.3390/ijms25031757

Swanson, L. (2014). *Neuroanatomical Terminology: A Lexicon of Classical Origins and Historical Foundations*. Oxford University Press.

Tannenberg, R., Scott, H., Westphalen, R., & Dodd, P. (2004). The Identification and Characterization of Excitotoxic Nerve-endings in Alzheimer Disease. *Current Alzheimer Research*, *1*(1), 11–25. https://doi.org/10.2174/1567205043480591

Tapiero, H., Mathé, G., Couvreur, P., & Tew, K. (2002). II. Glutamine and glutamate. *Biomedicine & Pharmacotherapy*, *56*(9), 446–457. https://doi.org/10.1016/s0753-3322(02)00285-8

Teipel, S. J., Grothe, M., Lista, S., Toschi, N., Garaci, F. G., & Hampel, H. (2013). Relevance of Magnetic Resonance Imaging for Early Detection and Diagnosis of Alzheimer Disease. *Medical Clinics of North America/the Medical Clinics of North America*, *97*(3), 399–424. https://doi.org/10.1016/j.mcna.2012.12.013

Teipel, S. J., Stahl, R., Dietrich, O., Schoenberg, S. O., Perneczky, R., Bokde, A. L., Reiser, M. F., Möller, H. J., & Hampel, H. (2007). Multivariate network analysis of fiber tract integrity in Alzheimer's disease. *NeuroImage*, *34*(3), 985–995. https://doi.org/10.1016/j.neuroimage.2006.07.047

Teixeira, A. L., Rocha, N. P., & Gatchel, J. (2023). Behavioral or neuropsychiatric symptoms of Alzheimer's disease: from psychopathology to pharmacological management. *Arquivos De Neuro-Psiquiatria*, *81*(12), 1152–1162. https://doi.org/10.1055/s-0043-1777774

The Hippocampus in Clinical Neuroscience. (2014). In *Monographs in clinical neuroscience/Frontiers of neurology and neuroscience/Monographs in neural sciences*. https://doi.org/10.1159/isbn.978-3-318-02568-2

Thomas, A. G., Koumellis, P., & Dineen, R. A. (2011). The Fornix in Health and Disease: An Imaging Review. *Radiographics*, *31*(4), 1107–1121. https://doi.org/10.1148/rg.314105729

Tian, J., Shi, J., Bailey, K., & Mann, D. M. A. (2003). Relationships between arteriosclerosis, cerebral amyloid angiopathy and myelin loss from cerebral cortical white matter in Alzheimer's disease. *Neuropathology & Applied Neurobiology/Neuropathology and Applied Neurobiology*, *30*(1), 46–56. https://doi.org/10.1046/j.0305-1846.2003.00510.x

Timsit, S., Martinez, S., Allinquant, B., Peyron, F., Puelles, L., & Zalc, B. (1995). Oligodendrocytes originate in a restricted zone of the embryonic ventral neural tube defined by DM-20 mRNA expression. *the Journal of Neuroscience/the Journal of Neuroscience*, *15*(2), 1012–1024. https://doi.org/10.1523/jneurosci.15-02-01012.1995

Traynelis, S. F., Wollmuth, L. P., McBain, C. J., Menniti, F. S., Vance, K. M., Ogden, K. K., Hansen, K. B., Yuan, H., Myers, S. J., & Dingledine, R. (2010). Glutamate Receptor Ion Channels: Structure, Regulation, and Function. *Pharmacological*

Reviews, *62*(3), 405–496. https://doi.org/10.1124/pr.109.002451

Tse, K., Cheng, A., Ma, F., & Herrup, K. (2018). DNA damage-associated oligodendrocyte degeneration precedes amyloid pathology and contributes to Alzheimer's disease and dementia. *Alzheimer's & Dementia*, *14*(5), 664–679. https://doi.org/10.1016/j.jalz.2017.11.010

Tsivilis, D., Vann, S. D., Denby, C., Roberts, N., Mayes, A. R., Montaldi, D., & Aggleton, J. P. (2008). A disproportionate role for the fornix and mammillary bodies in recall versus recognition memory. *Nature Neuroscience*, *11*(7), 834–842. https://doi.org/10.1038/nn.2149

Tucker, D. M., Roeltgen, D. P., Tully, R., Hartmann, J., & Boxell, C. (1988). Memory Dysfunction Following Unilateral Transection of the Fornix: A Hippocampal Disconnection Syndrome. *Cortex*, *24*(3), 465–472. https://doi.org/10.1016/s0010-9452(88)80010-8

Tzschentke, T. M. (2002). Glutamatergic mechanisms in different disease states: overview and therapeutical implications - An

introduction. *Amino Acids*, *23*(1–3), 147–152. https://doi.org/10.1007/s00726-001-0120-8

Vallstedt, A., Klos, J. M., & Ericson, J. (2005). Multiple Dorsoventral Origins of Oligodendrocyte Generation in the Spinal Cord and Hindbrain. *Neuron*, *45*(1), 55–67. https://doi.org/10.1016/j.neuron.2004.12.026

Van Den Berg, C. J., & Garfinkel, D. (1971). A simulation study of brain compartments. Metabolism of glutamate and related substances in mouse brain. *Biochemical Journal. Cellular Aspects*, *123*(2), 211–218. https://doi.org/10.1042/bj1230211

Verkhratsky, A., & Butt, A. (2013). *Glial Physiology and Pathophysiology*. https://doi.org/10.1002/9781118402061

Verkhratsky, A., Ho, M. S., Zorec, R., & Parpura, V. (2019). The Concept of Neuroglia. In *Advances in experimental medicine and biology* (pp. 1–13). https://doi.org/10.1007/978-981-13-9913-8_1

Vernadakis, A. (1996). GLIA-NEURON INTERCOMMUNICATIONS AND SYNAPTIC PLASTICITY. *Progress in Neurobiology*, *49*(3), 185–214. https://doi.org/10.1016/s0301-0082(96)00012-3

Virchow, R. (1856). Gesammelte Abhandlungen zur Wissenschaftlichen Medicin. In *Internet Archive*. https://archive.org/details/b21462161/mode/2up

Virchow, R. (1859). Die Cellularpathologie in ihrer Begründung auf physiologische und pathologische Gewebelehre. In *Internet Archive*. https://archive.org/details/diecellularpatho00virc/mode/2up

Volpe, J. J. (2001). Neurobiology of Periventricular Leukomalacia in the Premature Infant. *Pediatric Research*, *50*(5), 553–562. https://doi.org/10.1203/00006450-200111000-00003

Von Bartheld, C. S., Bahney, J., & Herculano-Houzel, S. (2016). The search for true numbers of neurons and glial cells in the human brain: A review of 150 years of cell counting. *Journal of Comparative Neurology*, *524*(18), 3865–3895. https://doi.org/10.1002/cne.24040

Wadiche, J. I., Arriza, J. L., Amara, S. G., & Kavanaugh, M. P. (1995). Kinetics of a human glutamate transporter. Neuron, 14(5), 1019–1027. https://doi.org/10.1016/0896-6273(95)90340-2

Wadiche, J. I., & Kavanaugh, M. P. (1998). Macroscopic and Microscopic Properties of a Cloned Glutamate Transporter/Chloride Channel. ˜the œJournal of Neuroscience/˜the œJournal of Neuroscience, 18(19), 7650–7661. https://doi.org/10.1523/jneurosci.18-19-07650.1998

Wallin, A., Gottfries, C. G., Karlsson, I., & Svennerholm, L. (1989). Decreased myelin lipids in Alzheimer's disease and vascular dementia. *Acta Neurologica Scandinavica*, *80*(4), 319–323. https://doi.org/10.1111/j.1600-0404.1989.tb03886.x

Walton, H., & Dodd, P. (2007). Glutamate–glutamine cycling in Alzheimer's disease. Neurochemistry International, 50(7–8), 1052–1066. https://doi.org/10.1016/j.neuint.2006.10.007

Wang, C., Stebbins, G. T., Medina, D. A., Shah, R. C., Bammer, R., Moseley, M. E., & deToledo-Morrell, L. (2012). Atrophy and dysfunction of parahippocampal white matter in mild Alzheimer's disease. *Neurobiology of Aging*, *33*(1), 43–52. https://doi.org/10.1016/j.neurobiolaging.2010.01.020

Warf, B., Fok-Seang, J., & Miller, R. (1991). Evidence for the ventral origin of oligodendrocyte precursors in the rat spinal cord.

the Journal of Neuroscience/the Journal of Neuroscience, *11*(8), 2477–2488. https://doi.org/10.1523/jneurosci.11-08-02477.1991

Wenthold, R. J., & Roche, K. W. (1998). Chapter 10 The organization and regulation of non-NMDA receptors in neurons. In *Progress in brain research* (pp. 133–152). https://doi.org/10.1016/s0079-6123(08)60435-5

Wersinger, E., Schwab, Y., Sahel, J., Rendon, A., Pow, D. V., Picaud, S., & Roux, M. J. (2006). The glutamate transporter EAAT5 works as a presynaptic receptor in mouse rod bipolar cells. Journal of Physiology, 577(1), 221–234. https://doi.org/10.1113/jphysiol.2006.118281

Westergaard, N., Sonnewald, U., & Schousboe, A. (1995). Metabolic Trafficking between Neurons and Astrocytes: The Glutamate/Glutamine Cycle Revisited. *Developmental Neuroscience*, *17*(4), 203–211. https://doi.org/10.1159/000111288

Windebank, A., Wood, P., Bunge, R., & Dyck, P. (1985). Myelination determines the caliber of dorsal root ganglion neurons in culture. *the Journal of Neuroscience/the Journal of*

Neuroscience, *5*(6), 1563–1569. https://doi.org/10.1523/jneurosci.05-06-01563.1985

Won, S. J., Kim, D. Y., & Gwag, B. J. (2002). Cellular and Molecular Pathways of Ischemic Neuronal Death. *BMB Reports*, *35*(1), 67–86. https://doi.org/10.5483/bmbrep.2002.35.1.067

World Health Organization (WHO). (2023). Dementia. In *https://www.who.int/*. Retrieved May 30, 2024, from https://www.who.int/news-room/fact-sheets/detail/dementia

Wu, Y., Ma, Y., Liu, Z., Geng, Q., Chen, Z., & Zhang, Y. (2017). Alterations of myelin morphology and oligodendrocyte development in early stage of Alzheimer's disease mouse model. *Neuroscience Letters*, *642*, 102–106. https://doi.org/10.1016/j.neulet.2017.02.007

Wyss, J. M., Swanson, L. W., & Cowan, W. M. (1980). The organization of the fimbria, dorsal fornix and ventral hippocampal commissure in the rat. *Anatomy and Embryology*, *158*(3), 303–316. https://doi.org/10.1007/bf00301819

Xiao, X., Liu, H., Liu, X., Zhang, W., Zhang, S., & Jiao, B. (2021). APP, PSEN1, and PSEN2 Variants in Alzheimer's Disease: Systematic Re-evaluation According to ACMG Guidelines. *Frontiers in Aging Neuroscience*, *13*. https://doi.org/10.3389/fnagi.2021.695808

Xie, F., Zhang, J. C., Fu, H., & Chen, J. (2013). Age-related decline of myelin proteins is highly correlated with activation of astrocytes and microglia in the rat CNS. *International Journal of Molecular Medicine*, *32*(5), 1021–1028. https://doi.org/10.3892/ijmm.2013.1486

Xie, S., Xiao, J. X., Gong, G. L., Zang, Y. F., Wang, Y. H., Wu, H. K., & Jiang, X. X. (2006). Voxel-based detection of white matter abnormalities in mild Alzheimer disease. *Neurology*, *66*(12), 1845–1849. https://doi.org/10.1212/01.wnl.0000219625.77625.aa

Yamada, K., Watanabe, M., Shibata, T., Tanaka, K., Wada, K., & Inoue, Y. (1996). EAAT4 is a post-synaptic glutamate transporter at Purkinje cell synapses. NeuroReport/Neuroreport, 7(12), 2013–2017. https://doi.org/10.1097/00001756-199608120-00032

Yang, P. C., & Mahmood, T. (2012). Western blot: Technique, theory, and trouble shooting. *North American Journal of Medical Sciences*, *4*(9), 429. https://doi.org/10.4103/1947-2714.100998

Yang, Y., Bagyinszky, E., & An, S. S. A. (2023). Presenilin-1 (PSEN1) Mutations: Clinical Phenotypes beyond Alzheimer's Disease. *International Journal of Molecular Sciences*, *24*(9), 8417. https://doi.org/10.3390/ijms24098417

Yi, J. H., & Hazell, A. S. (2006). Excitotoxic mechanisms and the role of astrocytic glutamate transporters in traumatic brain injury. *Neurochemistry International*, *48*(5), 394–403. https://doi.org/10.1016/j.neuint.2005.12.001

Yiannopoulou, K. G., & Papageorgiou, S. G. (2020). Current and Future Treatments in Alzheimer Disease: An Update. *Journal of Central Nervous System Disease*, *12*, 117957352090739. https://doi.org/10.1177/1179573520907397

Young, K. M., Psachoulia, K., Tripathi, R. B., Dunn, S. J., Cossell, L., Attwell, D., Tohyama, K., & Richardson, W. D. (2013). Oligodendrocyte Dynamics in the Healthy Adult CNS:

Evidence for Myelin Remodeling. *Neuron*, *77*(5), 873–885. https://doi.org/10.1016/j.neuron.2013.01.006

Zavialova, M., Shevchenko, V., Nikolaev, E., & Zgoda, V. (2017). Is myelin basic protein a potential biomarker of brain cancer? *European Journal of Mass Spectrometry*, *23*(4), 192–196. https://doi.org/10.1177/1469066717719810

Zeller, N. K., Hunkeler, M. J., Campagnoni, A. T., Sprague, J., & Lazzarini, R. A. (1984). Characterization of mouse myelin basic protein messenger RNAs with a myelin basic protein cDNA clone. *Proceedings of the National Academy of Sciences of the United States of America*, *81*(1), 18–22. https://doi.org/10.1073/pnas.81.1.18

Zhan, X., Jickling, G. C., Ander, B. P., Liu, D., Stamova, B., Cox, C., Jin, L. W., DeCarli, C., & Sharp, F. R. (2014). Myelin Injury and Degraded Myelin Vesicles in Alzheimer's Disease. *Current Alzheimer Research*, *11*(3), 232–238. https://doi.org/10.2174/1567205011666140131120922

Zhang, P., Kishimoto, Y., Grammatikakis, I., Gottimukkala, K., Cutler, R. G., Zhang, S., Abdelmohsen, K., Bohr, V. A., Sen, J. M., Gorospe, M., & Mattson, M. P. (2019). Senolytic therapy

alleviates Aβ-associated oligodendrocyte progenitor cell senescence and cognitive deficits in an Alzheimer's disease model. *Nature Neuroscience*, *22*(5), 719–728. https://doi.org/10.1038/s41593-019-0372-9

Zhang, Y., Schuff, N., Jahng, G. H., Bayne, W., Mori, S., Schad, L., Mueller, S., Du, A. T., Kramer, J. H., Yaffe, K., Chui, H., Jagust, W. J., Miller, B. L., & Weiner, M. W. (2007). Diffusion tensor imaging of cingulum fibers in mild cognitive impairment and Alzheimer disease. *Neurology*, *68*(1), 13–19. https://doi.org/10.1212/01.wnl.0000250326.77323.01

Zhou, Y., & Danbolt, N. C. (2014). Glutamate as a neurotransmitter in the healthy brain. *Journal of Neural Transmission*, *121*(8), 799–817. https://doi.org/10.1007/s00702-014-1180-8

Zhuang, L., Sachdev, P. S., Trollor, J. N., Reppermund, S., Kochan, N. A., Brodaty, H., & Wen, W. (2013). Microstructural White Matter Changes, Not Hippocampal Atrophy, Detect Early Amnestic Mild Cognitive Impairment. *PloS One*, *8*(3), e58887. https://doi.org/10.1371/journal.pone.0058887

Zhuang, L., Wen, W., Zhu, W., Trollor, J., Kochan, N., Crawford, J., Reppermund, S., Brodaty, H., & Sachdev, P. (2010). White

matter integrity in mild cognitive impairment: A tract-based spatial statistics study. *NeuroImage*, *53*(1), 16–25. https://doi.org/10.1016/j.neuroimage.2010.05.068

Zumkehr, J., Rodriguez-Ortiz, C. J., Cheng, D., Kieu, Z., Wai, T., Hawkins, C., Kilian, J., Lim, S. L., Medeiros, R., & Kitazawa, M. (2015). Ceftriaxone ameliorates tau pathology and cognitive decline via restoration of glial glutamate transporter in a mouse model of Alzheimer's disease. Neurobiology of Aging, 36(7), 2260–2271. https://doi.org/10.1016/j.neurobiolaging.2015.04.005